Photocatalytic Electron Transfer and Energy Transfer Cycloadditions of Phenols

By

Travis Ryan Blum

A dissertation submitted in partial fulfillment

of the requirements for the degree of

Doctor of Philosophy

(Chemistry)

at the

UNIVERSITY OF WISCONSIN–MADISON

2016

Date of final oral examination: 01/04/2016

The dissertation is approved by the following members of the Final Oral Committee:

Tehshik P. Yoon, Professor, Chemistry

Shannon S. Stahl, Professor, Chemistry

Laura L. Kiessling, Professor, Chemistry

Samuel H. Gellman, Professor, Chemistry

Randall H. Goldsmith, Assistant Professor, Chemistry

Photocatalytic Electron Transfer and Energy Transfer Cycloadditions of Phenols

By

Travis Ryan Blum

Under the supervision of Professor Tehshik P. Yoon
at the University of Wisconsin–Madison

Abstract

Despite the explosion of interest in the field of photocatalysis during the most recent decade, there exist several limitations in the suite of methods applied to organic synthesis. This document describes efforts to improve two underdeveloped areas in photocatalysis using phenols as a versatile motif to control both redox and Lewis acid coordination chemistries. Initial research centered on the rich oxidation chemistry of phenols as a proving ground for the development of a photocatalytic platform for performing oxidation of organic molecules. This enabled the development of a robust method for the synthesis of 2,3-dihydrobenxofurans through an oxidative [3+2] cycloaddition of phenols and alkenes using ammonium persulfate as a cheap and environmentally benign oxidant. In addition to generating a wide variety of novel benzofurans, this method also provided a means for the rapid synthesis of two natural products. Preliminary work extending this platform to enolate oxidation has demonstrated promising results. In addition, a novel Lewis acid-coupled energy transfer [2+2] cycloaddition of 2'-hydroxychalcones has been discovered, which is believed to represent the first example of Lewis-acid catalyzed energy transfer in synthetic photochemistry. Our initial observations have enabled the development of a highly enantioselective [2+2] cycloaddition, which gives access to a wide array of stereochemically enriched vinyl and aryl substituted cyclobutanes.

Acknowledgements

If you (the reader) will grant a short indulgence, the single author listed on this document belies the hands that have contributed to its development and execution both directly and indirectly. These individuals have earned a great deal more than the recognition they receive here, but I hope to take a moment to convey my genuine gratitude.

I feel tremendously fortunate to count myself among the students of Professor Tehshik Yoon, who has deftly guided my development as a scientist and researcher. His creativity, perspective, and gift for communication have shaped my approach to science and advising in numerous ways. I value highly the institutions he has constructed within his laboratory to expose his students to new ideas and approaches to chemistry, especially those that lie outside of his own expertise. I appreciate his tolerance of my petulance, his support for my bad ideas, his willingness to indulge my curiosities, and his forgiveness of my mistakes, of which there are far too many.

I also owe an immense debt of gratitude to my committee members Prof. Shannon Stahl, Prof. Laura Kiessling, Prof. Samuel Gellman, and Prof. Randy Goldsmith. I have had the privilege of interacting with all of them throughout my graduate career through literature seminars, departmental committees, and supergroup meetings. These have been influential experiences, and I am grateful for the time, feedback, and grey matter all of them have contributed to my education.

The Yoon group represents an exceptional place to conduct research, due in no small part to the personable, intelligent, and motivated scientists it contains. I have been particularly grateful for my interactions with many of them, beginning with Kevin Williamson and Kaz Skubi. They remain among the most thoughtful, intelligent, and self-critical scientists I know, and have provided a constant source of companionship and intellectual challenge through my graduate career. My office colleagues Dr. Dani Schultz, Dr. Laura Ruiz Espelt, Dr. Megan Cismesia, Dr. Juana Du, Shane Lies, and Iain McPherson have enriched my graduate experience beyond

measure. I have also been fortunate to work directly with a number of scientists on the research presented in this thesis, and wish to thank Sarah Nordeen, Spencer Scholz, and Dr. Zachary Miller for their help, guidance, patience, and good humor as we moved science forward.

I count myself lucky to have participated in a graduate internship at Merck Research Labs during my graduate career, which proved valuable in gaining context, perspective, and technical skills in the field of biocatalysis. This program dramatically shaped my career trajectory, and I am indebted to those who made it possible and worthwhile. Chief among these individuals were my supervisor Dr. Erika Milczek, and her colleagues Dr. Jeffrey Moore and Dr. Matt Truppo. Their collective enthusiasm, candor, patience, and vision made my time at Merck a formative experience.

Finally, it is unquestionably necessary for me to thank those in my family whose support and understanding have given me the freedom to fully apply myself to research for the last half-decade. My parents Edward and Mary Blum, and my brothers Trevor and Tory have made the most of my infrequent visits, and I cherish the time I have been able to spend in their company. I have also been fortunate to spend the last several years studying in the same city with my twin brother Tyler, who has provided an invaluable source of companionship and good humor during my graduate career. He will forever have my gratitude. Finally, my constant and unfailing partner Nitasha Bennett has provided no shortage of support, perspective, challenge, and guidance throughout our journey together. She has shaped both my personal and professional character in countless ways, and I cannot overstate the joy she has brought to this chapter of my life.

Table of Contents

List of Figures

Chapter 1

Chapter 4

List of Tables

Chapter 2

Chapter 4

Chapter 1. Cooperative strategies for controlling photocatalytic energy transfer processes in organic synthesis

1.1 Introduction

1.1.1 Introduction to Photocatalyis

As methods for the synthesis of organic molecules become more advanced, science has come to harness novel reagents and energy sources to drive reactivity. The field of photochemistry in particular has led to tremendous advances in the generation and use of electronically excited species derived from the collection of light energy. Photoexcitation serves as a unique way to access reactive species, and has been used extensively to promote novel modes of reactivity. In particular, light has proven uniquely capable of facilitating several classes of transformations, such as those needed to make highly strained ring systems. While poweful, traditional photochemistry has not been applied in organic synthesis to a level commensurate with its potential value.

The limited applications of photochemistry primarily stem from the intrinsic properties of organic molecules. Generally, organic molecules interact only weakly with light, and most organic chromophores absorb only short wavelength (high energy) light. The combination of these factors can limit the selectivity of photoreactions, and hinder their application in synthesis. Photocatalysis has been instrumental in providing considerable generality and synthetic power to the field of synthetic photochemistry by enabling the intrinsic photochemical properties of a molecule to be decoupled from its absorption characteristics. Irradiation of a rapidly expanding set of catalytic small molecule chromophores (hereafter referred to as photocatalysts) converts light energy into chemical potential that can be transferred to a substrate *via* several mechanisms. With this advance, it has become possible to efficiently access a wide array of open shell radicals, radical ions, and electronically excited species that are often inefficiently generated or are not obtainable through direct excitation.[1]

Recently, it has become recognized that photocatalysis can readily interface with other strategies to direct, enhance, or modify reactivity. Thus, it has become common to couple photocatalysis with other substoichiometric or non-consumable reagents that redirect substrates toward new pathways by regulating the generation, reactivity, or character of the desired organic intermediates. This concept has proven immensely powerful, since the activation of molecules using light represents an orthogonal approach to thermal chemical activation, and provides additional opportunities to achieve selective reactivity. While a number of powerful methods have been developed to co-catalytically generate and utilize photoinduced electron transfer (PET) strategies in organic synthesis,[1] this review will focus instead on the cooperative strategies for controlling reactivity in energy transfer (ET) photocatalysis.

To warrant inclusion in this discussion, chemistry must include both a molecular photocatalyst (a sub-stoichiometric, non-substrate, small molecule chromophore that is not consumed or modified by the transformation), and a second non-consumed reagent or catalyst that modifies, controls, or otherwise impacts the reactivity and selectivity of an organic transformation. For the purposes of this discussion, tethered and bifunctional catalysts will also be considered, since the principles of catalysis and selectivity are generally conserved in these examples. Processes which are driven by direct substrate irradiation have been included in numerous prior reviews, and will not be covered here.[2] Because one of the major goals of this review is to illuminate the considerations that influence photocatalytic activity and stability in the presence of other reactive species, reactions must be performed in a single step. Multistep, single pot reactions that utilize multiple catalysts will not feature here. This discussion will also be limited to molecular photocatalysts of homogeneous (well-defined) composition, and only to examples that are applied to organic chemistry (organic synthesis). This excludes a discussion of semiconductor photocatalysis, which has been reviewed recently,[3] and will not cover co-catalytic strategies for small-molecule activation and energy conversion. Because of the polydisperse

nature of micelles, vesicles, and membranes, these forms of confined media will not be covered in this review.[4]

Because photocatalysis represents a powerful strategy for enabling organic synthesis, several excellent reviews on organic photocatalysis have been published, including those highlighting carbon-carbon bond formation,[5] and natural product synthesis.[6] Additionally, several subfields of photocatalysis have been the subject of recent attention, including visible-light photoredox catalysis[1] and co-catalysis,[7] and the related field of asymmetric photochemistry.[8] Additionally, while relevant examples will be discussed herein, supramolecular catalysis has also been extensively reviewed.[9]

1.1.2 Energy Transfer

In contrast to photoinduced electron transfer, where radical ions are the products of interaction with the catalyst photoexcited state, energy transfer produces neutral, electronically excited species as a result of photosensitization. This sensitization process can occur through several mechanisms, but the most common in organic chemistry is Dexter energy transfer. This process can be conceptualized as a concerted electron exchange between the triplet excited state photocatalyst and the ground state of the substrate to generate a ground state photocatalyst and a triplet substrate molecule (Figure 1). In order for this process to take place with high efficiency, the transfer of energy from the sensitizer (photocatalyst) to the substrate sould be therodynamically favorable, and thus the relative energies of the S_0 and T_1 states (also referred to

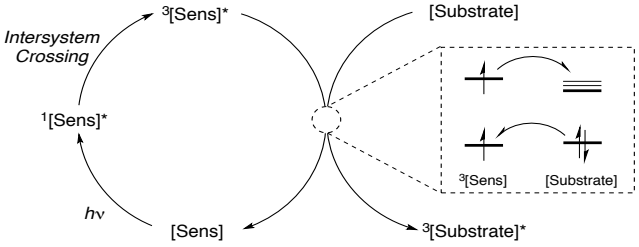

Figure 1.1: General schematic for Dexter energy transfer.

as the S_0-T_1 gap, or the "triplet energy," E_T) for both photocatalyst and substrate are key considerations in the efficiency of energy transfer. This has led to the practice of matching triplet energies to facilitate a high probability of electron exchange between photocatalyst and substrate. While useful for predicting whether energy transfer is energetically feasible, well-matched triplet energies do not always ensure fast or efficient energy transfer between two species.

Because of the unique electronic nature of photoexcited intermediates, it is not surprising that they have often have divergent reactivity patterns from the ground-state, open shell species produced in PET, and they can generate highly complex and strained structures. Sensitization often provides more efficient access to these species, as it allows for direct production of a particular reactive state without requiring direct irradiation of the substrate chromophore. In addition to providing more efficient access to a desired state, photosensitization also has practical benefits. Many of the canonical photosensitizers used for triplet energy transfer undergo both efficient intersystem crossing, both in terms of quantum yield and in terms of energetics. This often means that triplet sensitization can be performed under longer wavelength, lower energy irradiation than unsensitized photochemistry.

This chapter will highlight the use of energy transfer processes that facilitate organic synthesis using cooperative strategies to dictate reactivity or selectivity. It is worth noting that many examples presented below employ the photocatalytic generation of singlet oxygen ($^1O_2$) as the key sensitization process. The reactivity of singlet oxygen has been extensively reviewed and will not be covered here.[10] However, the ready availability of dioxygen, the divergent reactivity profile between the ground state triplet ($^3O_2$) and the excited singlet ($^1O_2$), and the valuable reactions that can be performed (hetero-cycloadditions, C–H functionalizations, etc,) *via* singlet oxygen all serve to promote its use in this field of chemistry. As sensitization strategies continue

to mature, their application to the photosensitization of organic substates presents an attractive and underexplored area of research, with many potential uses.

1.2 Cooperativity in Supramolecular and Templated Photocatalysis

Because of the transient lifetimes of the intermediates, and the difficulty inherent in controlling their generation and reactivity, a number of supramolecular strategies for controlling these reactions have been used for both the study and application of energy transfer. While often used as stoichiometric controllers, supramolecular cavities and templating agents that modify the energetics of photocatalyzed reactions have historically been the most powerful methods to control excited state behaviors. Additionally, because of their unique nature and functional behavior, they often allow for a high degree of synergy between photocatalyst and supramolecular scaffold, promoting a wide array of selective chemistries with diverse applications.

1.2.1 Zeolites

Zeolite supramolecular structures exist both naturally and as synthetic variants, and have long been used as catalysts in a number of chemical fields. These scaffolds were among the first used to probe supramolecular control of photochemical processes. The anionic nature of these aluminosilicate materials affords them the ability to exchange alkali metal ions with other cationic species in a medium, or to sequester organic molecules from solution within the extensive micropourous framework of the material. Their rigid structure also makes them ideal for studying photochemical processes in isolation, and the potential for shape-selective reactions of electronically excited molecules. While this review seeks to summarize the effects of zeolites on photocatalyzed energy transfer processes, there exist a number of reviews on the subject of selective photochemistry within these structures that cover the extensive research on directly excited substrates.[11]

One of the earliest uses for zeolites in photochemistry has leveraged their ability to sequester organic species within the porous framework to drive product selectivity through shape selection in sensitized alkene isomerization reactions.[12] In solution, benzophenone sensitizers promote the isomerization of stilbenes to typically afford a 2:1 mixture of alkene isomers at the photostationary state, enriched in *cis*-stilbene. However, because of is larger diameter, *cis*-stilbene cannot diffuse into silicalite pores, while *trans*-stilbene can. Thus, carrying out the same isomerization in the presence of silicalite affords a >9:1 mixture of isomers favoring *trans*-stilbene due to the ability of the zeolite to preferentially sequester the *trans*-isomer away from the active sensitizer. The opposite isomerization has also been demonstrated in principle by immobilizing a protonated 4-aminobenzophenone sensitizer (**1.1**) within HMOR zeolite channels. This prevents sensitization of *cis*-stilbene, which is isolated in solution, and allows for exclusive sensitization of the *trans* isomer. Using this strategy, fast trans-cis isomerization has been observed, but the reaction fails to reach complete conversion due to deactivation of the immoblilized photosensitizer.[13]

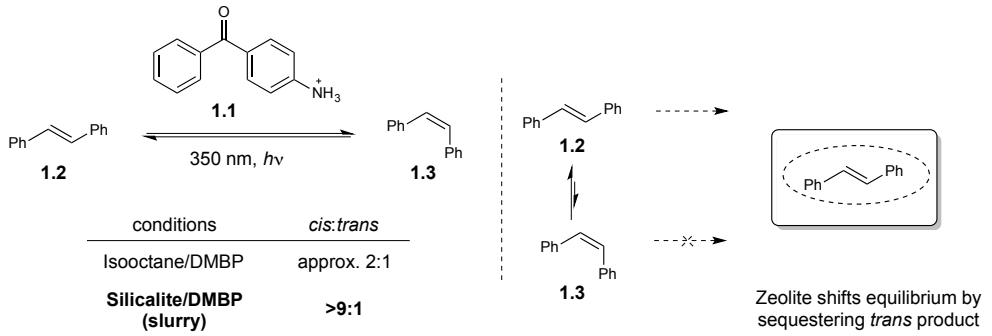

Figure 1.2: Photosensitized cis-trans isomerization of stilbenes facilitated by silicalite

While thermodynamically uphill isomerizations can afford valuable products, more traditional photosensitized bond forming processes have also been extensively studied using zeolite materials. Among these reactions have been photooxidation reactions using $^1O_2$ by the Schenk ene reaction, as well as [2+2] and [4+2] cycloadditions of alkenes and dienes. In seminal work from the lab of Fox,[14] it was shown that inorganic $Ru(bpy)_3^{2+}$ (**1.8**) cations could be

immobilized within the zeolite supercage structure, and efficiently generate $^1O_2$ for the oxygenation of methylcyclohexene (Figure 1.3A). Unfortunately, the zeolite-immobilized sensitizer did not afford distinct selectivity from homogeneous (solution phase) photooxygenation of alkenes. However, pioneering work from the lab of Ramamurthy[15] using thionin (**1.9**) as a sensitizer immobilized within a Faujasite (NaY) zeolite network demonstrated the ability of zeolite scaffolds to dramatically alter selectivity in encapsulated photoreactions. In contrast to photooxygenation in homogeneous solution, the zeolite-supported sensitizer demonstrated a high degree of selectivity in the oxygenation of several classes of alkenes, including both cyclic and acyclic systems (Figure 1.3B).

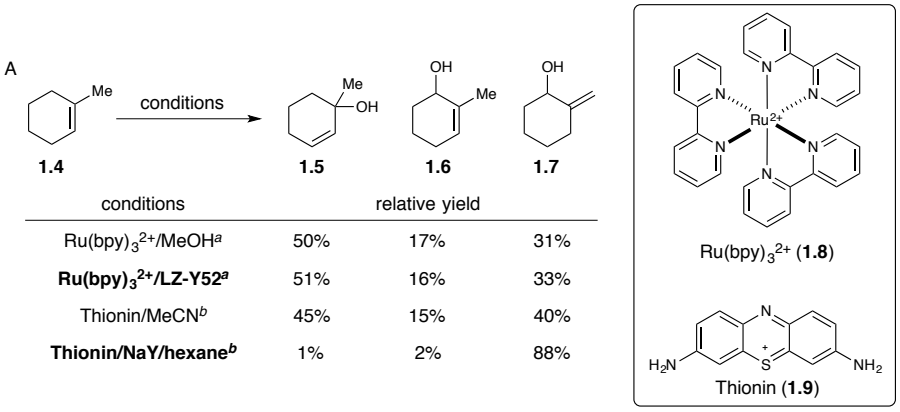

conditions	relative yield		
Ru(bpy)$_3^{2+}$/MeOH[a]	50%	17%	31%
Ru(bpy)$_3^{2+}$/LZ-Y52[a]	51%	16%	33%
Thionin/MeCN[b]	45%	15%	40%
Thionin/NaY/hexane[b]	1%	2%	88%

conditions	relative yield		
Thionin/MeCN	6%	45%	48%
Thionin/NaY/hexane	100%	0%	0%

conditions	relative yield	
Thionin/MeCN	46%	54%
Thionin/NaY/hexane	100%	0%

Figure 1.3: (A) Photosensitized oxidation of methylcyclohexene. (B) NaY-mediated selectivity in alkene photooxidation.

Extensive study of the mechanism in this and similar transformations (*vide infra*) has yet to afford a single factor for controlling the selectivity in intrazeolite photooxygenations. Substrate steric parameters, the ability to bind cations, and the cationic character of the zeolite host itself have all been shown to influence both reactivity and selectivity within the zeolite.[16] Collective experimental and computational efforts have resulted in a composite model for selectivity which invokes coordination of alkali cations to the substrate alkene through cation-π interactions, and subsequent attack by singlet oxygen to generate the perepoxide **1.18**. Cationic coordination in this species is suggested to alter the "*cis* effect" selectivity of the intrazeolite ene reaction by biasing the terminal oxygen of the perepoxide toward the less substituted side of the alkene (**1.18** versus **1.19**). In addition, the cation is thought to influence the charge distribution on the two carbon atoms of the perepoxide (promoting Markovnikov selectivity), and influence the conformation of the allylic substituents through the supramolecular cage, though these effects can be highly dependent on the nature of the alkene substituents. Additional effects, including other susbtrate cation-π interactions (such as pendant aryl rings) or Lewis acid-base interactions (alcohols and carbonyls) can also influence the binding and conformation of the zeolite-alkene complex, and thereby influence both regio- and stereoselectivity in the resulting ene reaction.

The use of a dye-exchanged zeolite to promote the photooxygenation of alkenes has been studied extensively since its discovery. In addition to the lab of Ramamurthy, the groups of

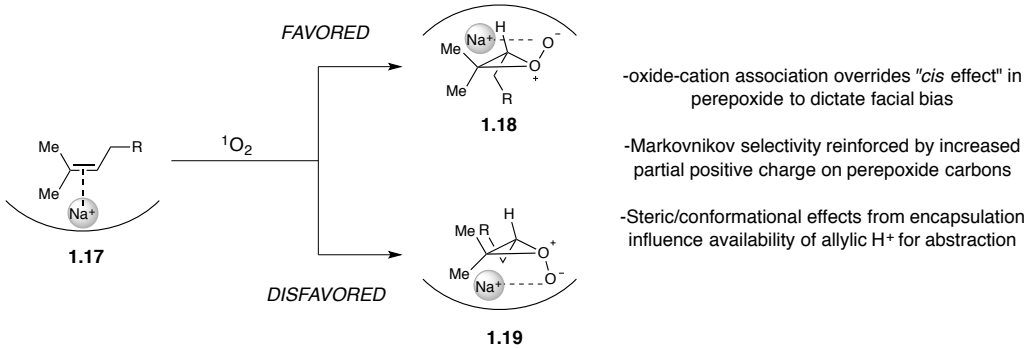

Figure 1.4: Proposed model for zeolite-induced selectivity in alkene photooxygenation

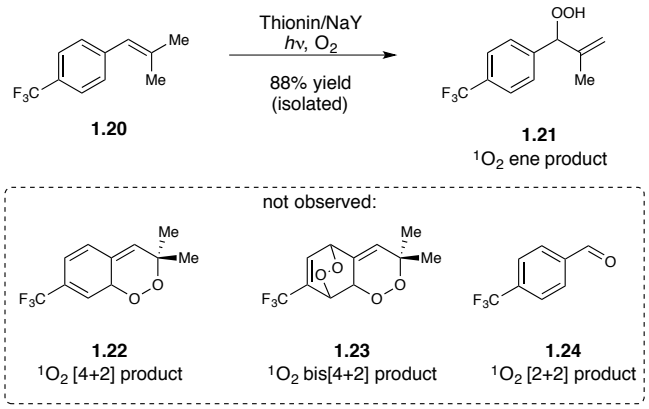

Figure 1.5: Selective photooxidation of styrenes with thionin/NaY cooperative system

Clennan and Stratakis have made major contributions to the application of this strategy in organic synthesis. Stratakis and coworkers were able to demonstrate the selective oxidation of β-dialkyl styrenes such as **1.20** in thionin-supported zeolites.[17] When performed in solution, photooxygenation of **1.20** affords a complex mixture of ene (**1.21**), [4+2] (**1.22**), bis[4+2] (**1.23**), and [2+2] (**1.24**) products in 1–3 h. However, when carried out in NaY, the photooxygenation reaches full conversion within 5 min, and is exclusively selective for the ene product (**1.21**). Milligram scale reactions and isolations were performed for **1.21**, affording the pure hydroperoxide in 88% yield. Subsequent work has demonstrated that the substitution of the aromatic ring of the substrate styrene can have subtle effects on the regiochemistry of proton abstraction (*cis* vs. *trans* methyl groups) within the zeolite architecture.[18]

The lab of Clennan has also demonstrated a more scalable method for carrying out photooxygenation with methylene blue-exchanged zeolites by using polyfluorinated solvents.[19] In contrast to the hydrocarbon solvents typically used for photooxidation of alkenes in zeolites, perfluorohexane has several advantages: (1) It has no reactivity within the zeolite cavity, (2) it extends the lifetime of $^1O_2$ and allows the photoexcited species to sample more space within the zeolite network, and (3) organic compounds become less soluble in the fluorous solvent, and their diffusion into the zeolite become a more favorable process. Using this method, preparative-scale

(up to 500 mg) photooxidations of aliphatic alkenes can be performed, with yields and selectivities that meet or exceed those of standard hydrocarbon slurries.

In addition to the above examples, Tung and coworkers have also established the ability of dye exchanged pentasil zeolites (ZSM-5) to influence reactivity in the Schenk ene reaction.[20] While the selectivities are not generally as high as in LiY/NaY zeolites, the more contrained environment of pentasil zeolites provides a complementary mode of selectivity induction, and displays a distinct product distribution from both solution phase oxidation and from thionin-NaY oxidation.

Beyond the Schenk ene reaction, pentasil zeolites have also been used to control selectivity in $^1O_2$ [4+2] cycloadditions. In contrast to the above examples, which used an immobilized dye, work from the lab of Tung used solvated dyes to act on dienes pre-immobilized within the ZSM-5 pore network.[21] The adsorbed dienes show exclusive selectivity for [4+2] cycloaddition, whereas in homogeneous isooctane solution a broad product distribution is observed (Figure 1.7). The authors suggest that this effect arises to the long lifetime of $^1O_2$ in nonpolar solution relative to other reactive oxygen species generated by electron transfer quenching of the photosensitizers

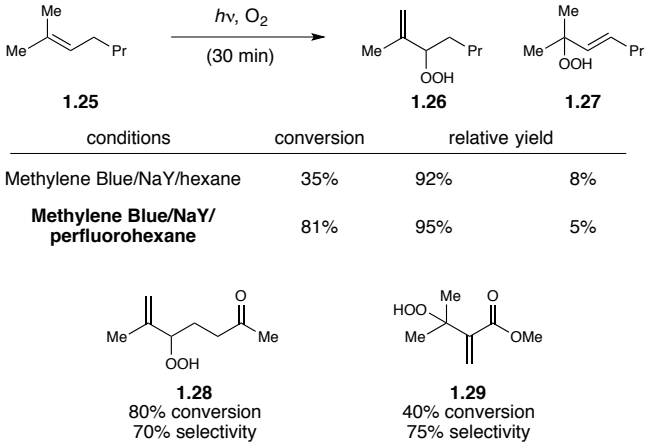

Figure 1.6: Scalable photooxidation of alkenes using perfluorohexane solvent

1.32 and **1.33**. In solution, products arising from both electron transfer and energy transfer are observed, but when the substrate is sequestered within ZSM-5, only $^1O_2$ has a lifetime long enough to diffuse into the zeolite pores to undergo reaction with the diene.

Because of the utility of performing selective oxidation, there have been extensive studies exploring the factors that control intrazeolite photooxygenation of alkenes. The effect of both

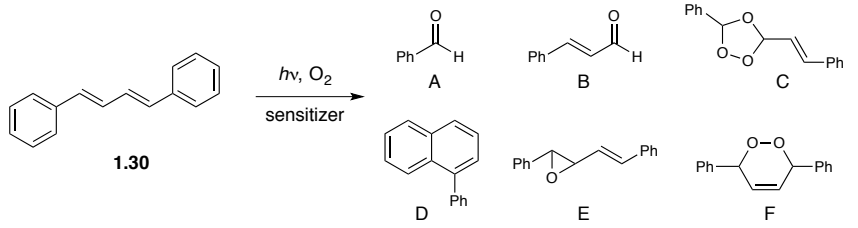

conditions	conversion	relative yield A	B	C	D	E	F
DCA, PTE	96%	73%	73%	16%	4%	4%	3%
DCA, PTE, ZSM-5 immobilized substrate	**100%**	**0%**	**0%**	**0%**	**0%**	**0%**	**100%**

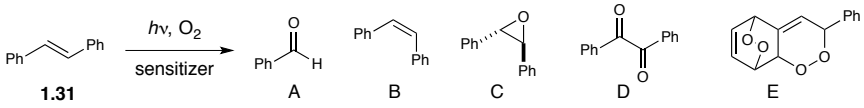

conditions	conversion	relative yield A	B	C	D	E
DCA, PTE	100%	48%	12%	28%	12%	12%
DCA, PTE, ZSM-5 immobilized substrate	**100%**	**100%**	**0%**	**0%**	**0%**	**0%**
HA, PTE	100%	3%	0%	0%	0%	97%
HA, PTE, ZSM-5 immobilized substrate	**100%**	**100%**	**0%**	**0%**	**0%**	**0%**

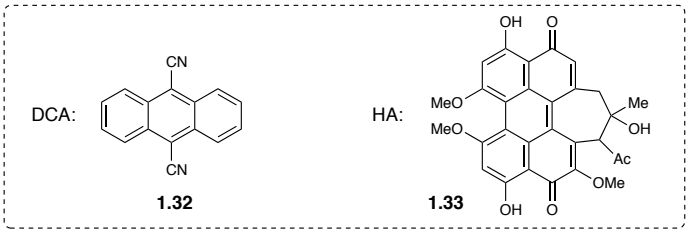

Figure 1.7: Mechanism-selective photooxidation of conjugated alkenes using ZSM-5 zeolites

proximal and remote functional groups on the selectivity of oxidation has been probed with polar functional groups (Lewis acid-base interactions),[22] remote aryl groups (cation-π interactions),[23] and allylic alcohols.[24] Additional work on regio- and chemoselectivity in dienes,[25] cyclic alkenes,[26] electron deficient alkenes,[16a] has also been performed. Co-adsorbed chiral guests, such as (+)-ephedrine·HCl, have demonstrated the ability to influence absolute stereocontrol in these reactions, affording modest enantioselectivities (up to 15% ee).[27] Exploratory work on [2+2] cycloadditions of photogenerated singlet oxygen with chiral enecarbamates within zeolites has also been performed, demonstrating a profound effect of encapsulation on the selective production of enantioenriched methyldesoxybenzoin.[28] While these collectively represent impressive examples of the ability to bias the intrinsic reactivity of alkenes, these reports have largely been limited to fundamental studies, and their application in practical synthesis has been underexplored. Additionally, several of the above hydroperoxide products are subject to overoxidation within the zeolite architecture, and thus while their selective reactivity remains promising, practical hurdles persist in their synthetic implementation.

Finally, the oxidation of sulfides to sulfoxides and sulfones by singlet oxygen has also been explored in methylene blue-exchanged NaY zeolites.[29] Interestingly, solution phase photosensitized oxidation of sulfide **1.38** yields almost exclusively Pummerer rearrangement

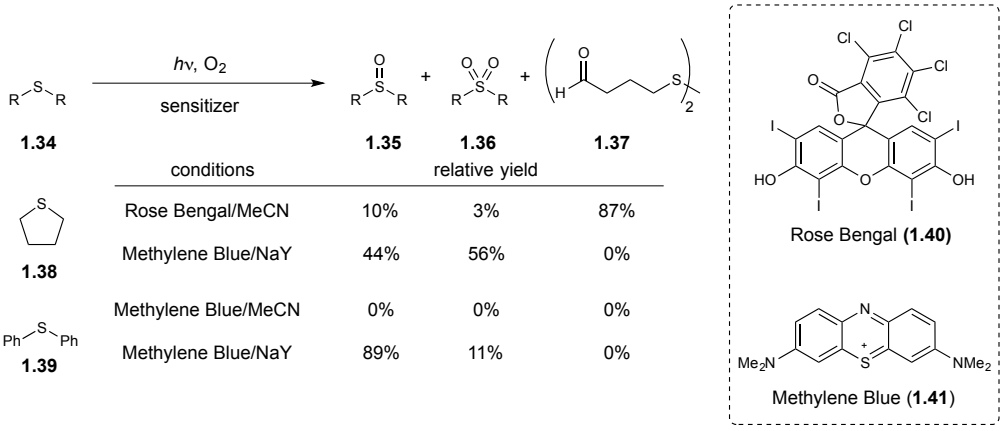

Figure 1.8: Zeolite-promoted sulfide oxidation

products (**1.37**), with low yields of sulfur oxygenation products (**1.35** and **1.36**). However, within the highly charged environment of the zeolite, the Pummerer rearrangement is completely suppressed, giving exclusive formation of sulfoxide and sulfone products with a ratio dependent on the concentration of the substrate within the zeolite. This is due primarily to the ability of the reactive persulfoxide intermediate to act as an O-atom transfer reagent, facilitating the oxidation of both substrate, as well as the oxidation of the product sulfoxide (**1.36**) to afford sulfone (**1.37**). Notably, the zeolite can faciliatate the oxidation of susbtrates that are inert under solution-phase photooxidation conditions, such as diphenylsulfide **1.39**.

As the above examples illustrate, zeolites offer a powerful platform for tuning the reactivity of electronically excited molecules through supramolecular interactions. However, it should not be surprising that this ability to alter the mechanism and shape selectivity of organic chemistry reactions is not universal. Numerous examples exist of immobilized substrates or sensitizers which do not significantly alter selectivity from solution-phase behavior.[14,30] In these instances, a number of confounding effects, including the rate of diffusion or exchange within the zeolite pores, the size and shape of the pores themselves, the hydration or protonation state of the zeolite, and the nature of the alkali cations within the framework (Li, Na, K, Cs, Rb) can all have effects on the photochemistry that takes place within the structure. These complex effects, combined with the rigid and difficult to tune structure of zeolite, have prevented approaches to fine tuning this chemistry from evolving beyond empirical optimization, and highlight areas for investigation as this field moves forward.

1.2.2 Cavitands and Molecular Containers

In contrast to the rigid structure of zeolites, molecular containers have offered photochemists an alternative strategy for controlling primary photocatalytic proceses with soluble

synthetic scaffolds. While structurally different from zeolites, their role in controlling photochemistry remains the same: to stabilize or sequester reactive species in a manner that facilitates selective chemistry.

1.2.2.1 Cyclodextrins

As one of the canonical supramolecular scaffolds for molecular recognition, cyclodextrins have a rich history in organic photochemistry.[31] These cyclic carbohydrates create a hydrophobic pocket into which many organic molecules fit, allowing for selective reactions of electronically excited states.

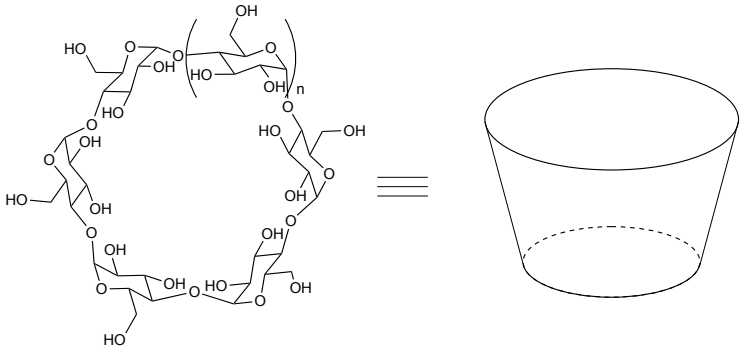

Figure 1.9: General structure of cyclodextrins

Notably, work from the lab of Kuroda demonstrated that modified cyclodextrins could be appended to metal porphyrins to control the selectivity of sensitized photooxygenation in Linoleic acid.[32] In aqueous solution with water-soluble porphyrin **1.43**, there exists no regioselectivity between the double bonds of linoleic acid in the singlet oxygen sensitized ene reaction. However, under conditions favoring preassociation within the cyclodextrin-modified sensitizer **1.44**, a dramatic shift in selectivity is observed, with preferential attack at the $\Delta^{12,13}$ alkene over the $\Delta^{9,10}$ alkene (Figure 1.10).

Weber and coworkers later employed a similar strategy to alter selectivity in the regio- and setereoselective sensitized photooxygenation of pinene.[33] However the use of a metalloporphyrin scaffold also affords a number of products accessible by autooxidation processes. It should also be noted that an extensive collection of fundamental work on the photosensitized isomerization

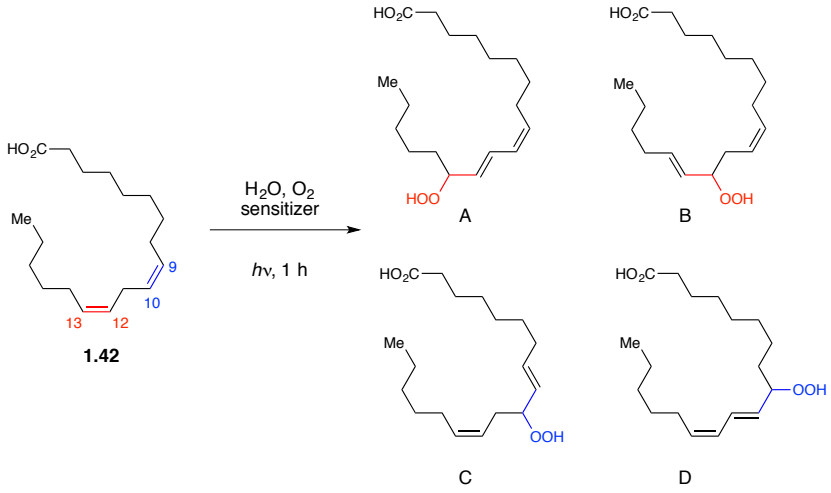

sensitizer	yield	$\Delta^{13,12}$ oxidation (A/B)	$\Delta^{9,10}$ oxidation (C/D)
Porphyrin **1.43**	12%	50% (40/10)	50% (11/40)
β-Cyclodextrin sandwich porphyrin 1.44	**14%**	**82% (51/31)**	**18% (11/7)**

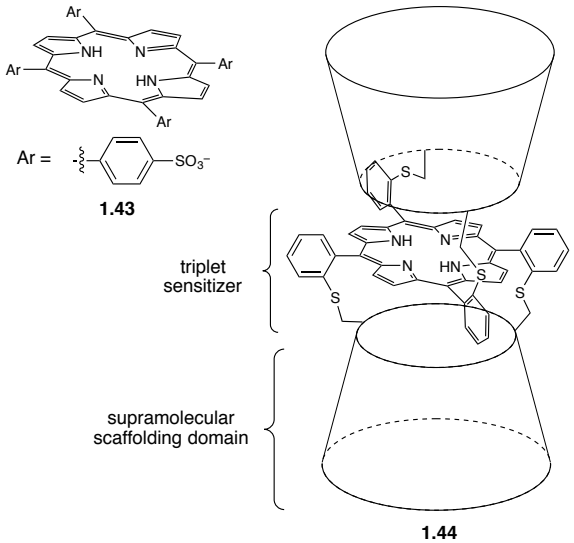

Figure 1.10: Supramolecular photooxygenation of unsaturated fatty acids

of cyclooctene has been carried out by the lab of Inoue in modified cyclodextrin cavities, but this has not yet been realized in synthetic methods, and will not be extensively discussed here. For leading references, the reader is directed to several articles on the subject.[34]

1.2.2.2 Self-Assembled Scaffolds

While cyclodextrins offer one of the most accessible and well-studied supramolecular scaffolds for photochemistry, several other molecular containers have been utilized to modify selectivity in photocatalytic reactions of organic molecules. Among these alternatives is the water-soluble cavitand octa acid (OA, Figure 1.11). Work from the lab of Ramamurthy in 2007 demonstrated this capability in the sensitized photooxygenation of cyclic alkenes sequestered in octa acid.[35] Whereas in solution the sensitized Schenk ene reaction affords a mixture of three different hydroperoxides, when encapsulated, the reaction is almost completely selective for production of the tertiary hydroperoxide using both water soluble and encapsulated triplet sensitizers (Figure 1.12). Interestingly, this product distribution is complementary to that observed within zeolites (see Figure 1.3). This ability to bias the selectivity of triplet pathways has also been extended to the encapsulated dimerization of acenaphthylene, which demonstrates a modified product mixture upon encapsulated senstitization due to the spacial constraints within the octa acid cavity.[36] Other reports have also examined the ability of octa acid to bias the

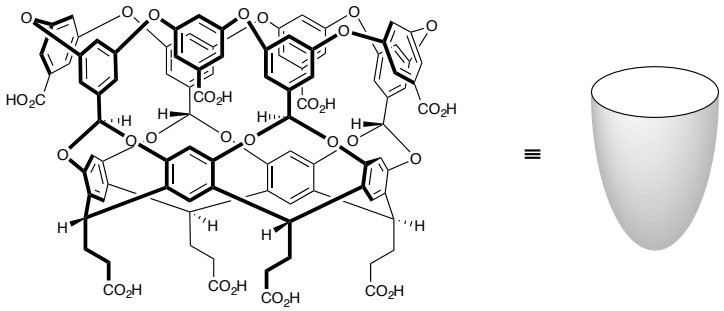

Figure 1.11: Molecular structure and representation of the water-soluble cavity octa acid (OA).

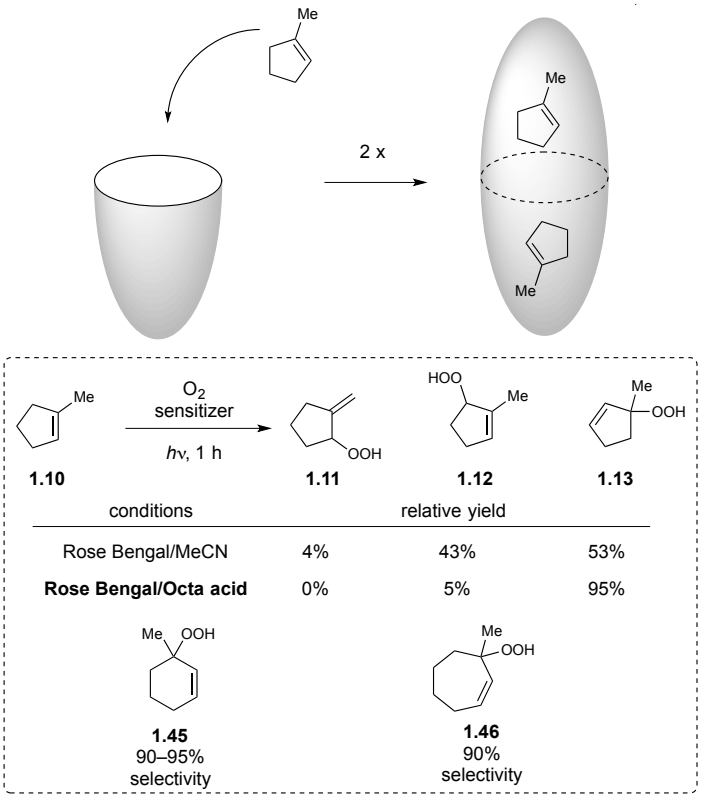

Figure 1.12: Sensitized photooxidation of alkenes encapsulated in octa acid

photostationary state of triplet sensitized olefin *cis-trans* isomerizations, however this work remains in development.[37]

Other self-assembled scaffolds have been applied to sensitized photochemistry, including Pd-nanocages (Figure 1.12).[38] Ramamurthy and coworkers have also studied the dimerization of acenaphthylene in these molecular vessels as well. In solution, acenaphthylene undergoes [2+2] dimerization to afford both *syn* and *anti* isomers, with the *syn* product arising through a singlet manifold, and the *anti* product through the triplet manifold. This is supported by a reversal in product selectivity upon triplet sensitization (Figure 1.13). However, once encapsulated within a Pd-nanocage, the special limitations within the capsule prevent the formation of the *anti* isomer, and lead to exclusive formation of the *syn* dimer under triplet sensitization (Figure 1.13).

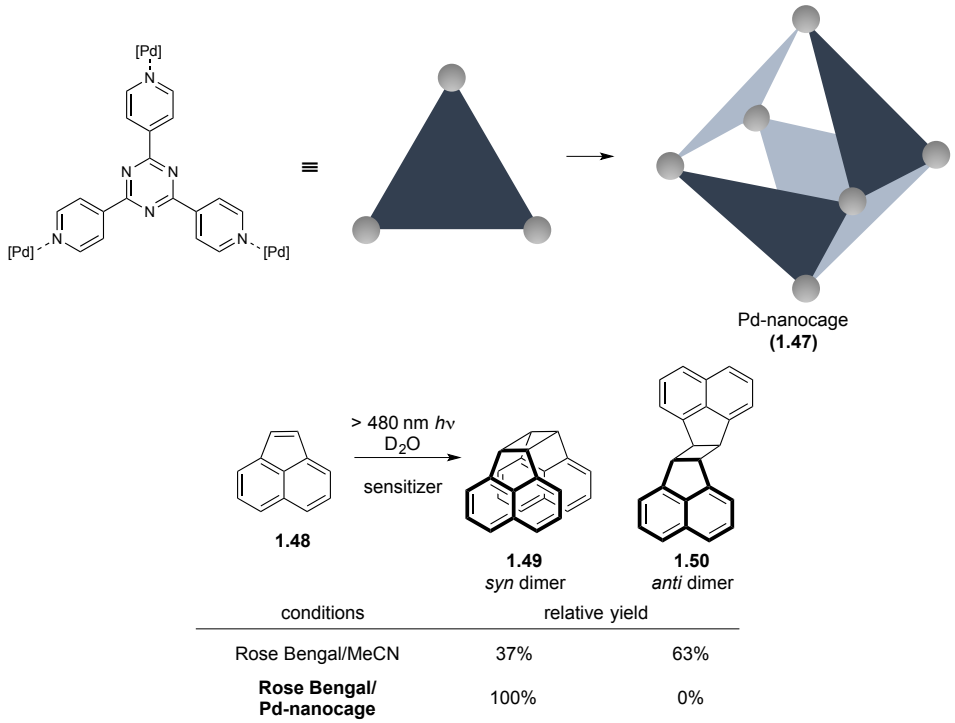

Figure 1.13: Supramolecular control over selectivity in acenaphthalene dimerization dictated by Pd-nanocages

Additional investigations on the effects of supramolecular scaffolding in excited state photochemistry have been explored by the lab of Shimizu using photoactive bis-urea hosts (**1.51**) that self-assemble into columnar nanotubes.[39] When certain guest molecules (**1.52**, **1.55**) were adsorbed into this framework and exposed to UV irradiation in aerated solvent, highly selective generation of allylic and benzylic alcohols was observed. The authors acknowledge a complex mechanism, but suggest that both a persistent radical and singlet oxygen are involved in the

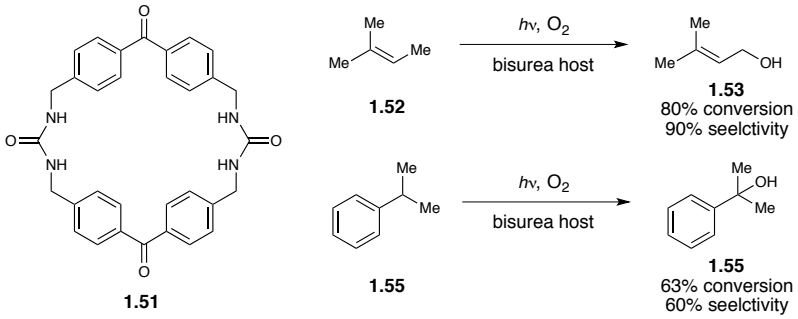

Figure 1.14: Selective photooxidation of allylic and benzylic C–H bonds in self-assembled photoactive nanotubes

selective oxidation. Interestingly, the observed selectivity is completely distinct from homogenous and other encapsulated photooxidations, suggesting that these bis-urea hosts offer a unique platform for photochemical oxidations.

1.2.2.3 Dendrimers

Other well-defined soft material scaffolds have proven to be useful for controlling photochemical reactivity in electronically excited states. Seminal work from the lab of Fréchet showed that photoactive benzophenone catalysts could be elaborated with dendrimeric branches to arrive at amphiphilic sensitizers that are active singlet oxygen sensitizers.[40] It was demonstrated that these macromolecular scaffolds provide a notable rate acceleration for the [4+2] cycloaddition of cyclopentadiene and $^1O_2$ to afford oxygenated cyclopentenes (**1.59**, Figure 1.15). The authors suggest that dendrimeric scaffolds likely improve reactivity by increasing the local concentration of both singlet oxygen and cyclopentadiene within the nonpolar dendrimer core, while sequestering the more polar diol product in the methanolic solvent. This scaffold has been modified and elaborated for the sensitization of singlet oxygen to oxidize both phenols,[41] and sulfides,[42] as well as for the sensitization of diazo- compounds to produce triplet carbenes.[43] While notable proof of concept studies are listed above, several dendrimeric sensitizer platforms require additional study to achieve distinct reactivities and selectivities beyond standard homogeneous triplet sensitization.

While previous work focused mostly on the synthesis and characterization of covalently modified dendrimeric sensitizers, more recent work from the labs of Han and Li has demonstrated that dendrimeric scaffolds can also alter reactivity through noncovalent interactions by influencing the localization of reactants.[44] This strategy is conceptually similar to several examples of zeolite sumpramolecular catalysis discussed previously.[20] In aqueous solution, DCA sensitized oxidation of **1.30** proceeded primarily through an electron transfer ($O_2^{\bullet -}$) mechanism

to afford complex mixtures of products (Figure 1.16). However, using water soluble acid-terminated dendrimers, the authors showed that sequestering the substrate alkene and DCA sensitizer separately facilitates selective formation of energy transfer ($^1O_2$) derived products. Again, this is attributed to the longer lifetime of singlet oxygen in aqueous media than superoxide and other charge-transfer species. This extended lifetime means that only singlet oxygen is capable of diffusing between the dendrimeric microreactors to achieve the desired

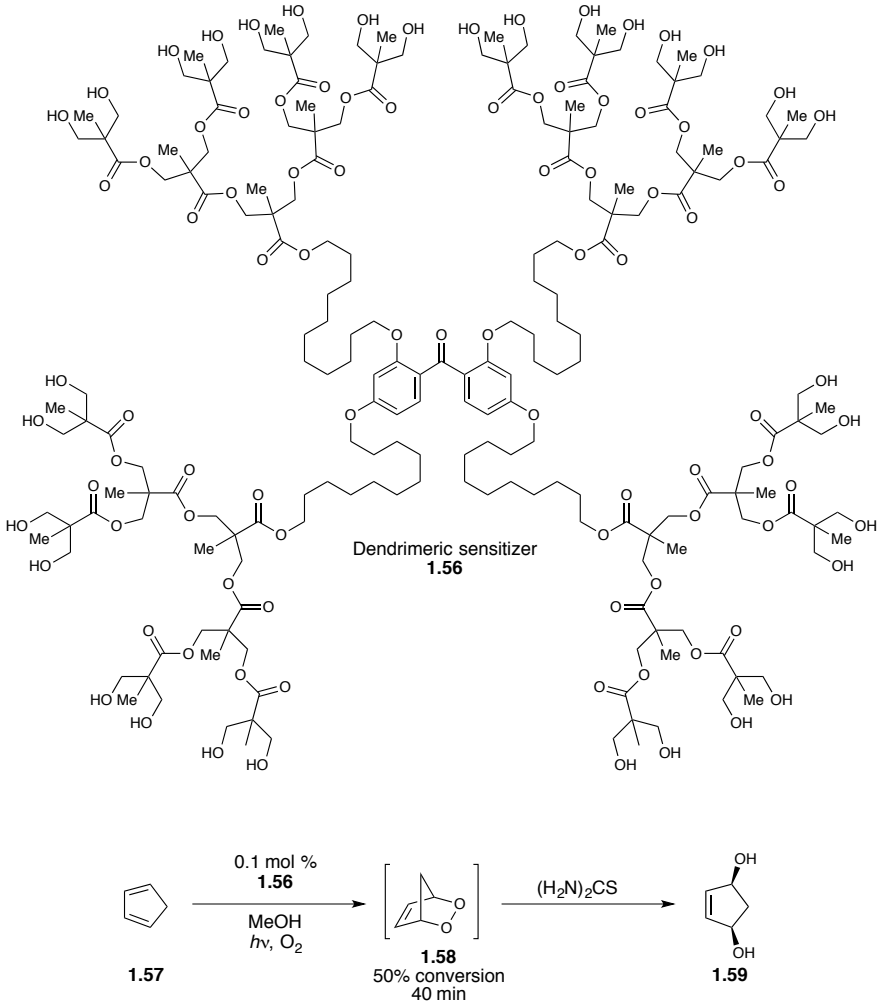

Figure 1.15: Dendrimer-modified photozensitizer for the photosensitized oxyfunctionalization of cyclopentadiene

photooxygenation, allowing this supramolecular strategy to select for a very specific reactivity manifold.

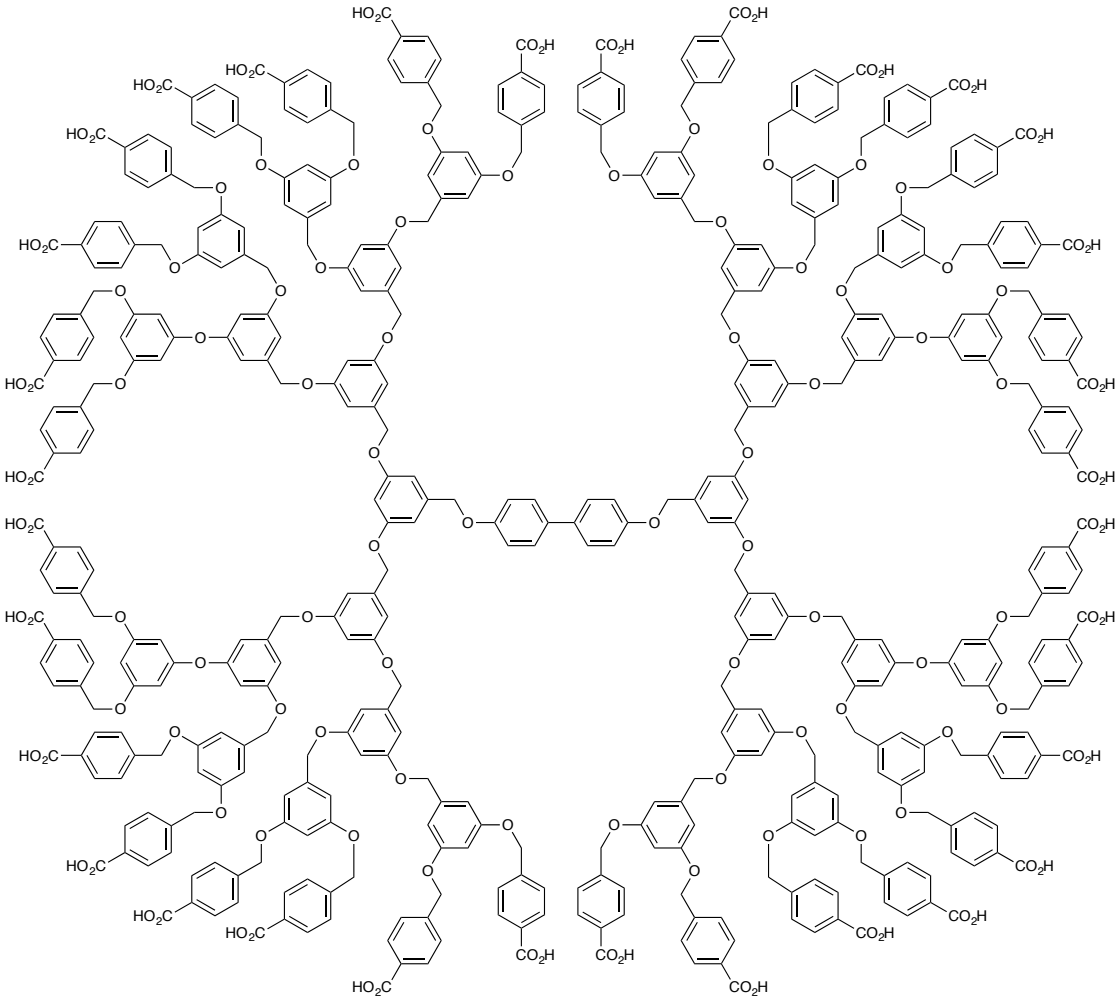

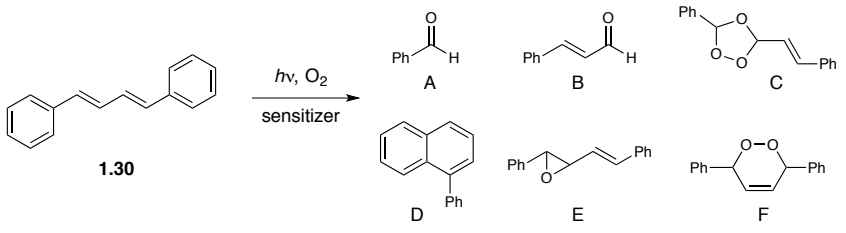

		relative yield					
conditions	conversion	A	B	C	D	E	F
DCA, MeCN	96%	84%	84%	1%	5%	0%	10%
DCA, 1.59	**100%**	**0%**	**0%**	**0%**	**0%**	**0%**	**100%**

Figure 1.16: Dendrimer-controlled energy-transfer photooxidiation

Additional work on photooxidation of organic molecules in vesicles and micelles,[45] polymers,[46] and nafion membranes[47] has also been performed, though the highly disperse molecular architecture of these species precludes them from our discussion here. However, the field of supramolecular photochemistry remains an active and fruitful area of discovery, and translating the fundamental insights gained from this field into synthetic advances remains an immediate goal for this community.

1.2.3 Templated Photoreactions

Scaffolding and templating reagents have also been used as control elements in primary photocatalytic processes, often as part of bifunctional catalysts which control reactivity through non-colvalent interactions. While traditionally much smaller than zeolites or molecular containers, these systems typically benefit from greater synthetic accessibility, which enables a significant amount of tunability in their structure and function.

A conceptually similar example to much of supramolecular catalysis is exemplified by the asymmetric [4+2] cycloaddition of singlet oxygen with pyridones reported by the lab of Bach.[48] In this work, a templating agent derived from Kemp's triacid (**1.63**) engages in a complementary hydrogen bonding interaction with the substrate lactam, generating chiral complex **1.64** (Figure 1.17). This interaction then dictates facial selectivity in the addition of singlet oxygen (generated by a tetraphenylporphyrin catalyst) to the pyridone (intermediate **1.61**), which is then isolated as **1.62** after an acid-promoted Kornblum–DeLaMare rearrangement. With this method, a number of oxidized pyridones are accessible in good yield and good enantiomeric excess (**1.65**–**1.67**).

While a useful scaffold for controlling asymmetric photochemical reactions of lactams, the templating agent **1.63** imbues no kinetic advantage to the cycloaddition chemistry of substrate **1.60**. In this sense, it acts exclusively as a non-covalent chiral controller, and must be used in

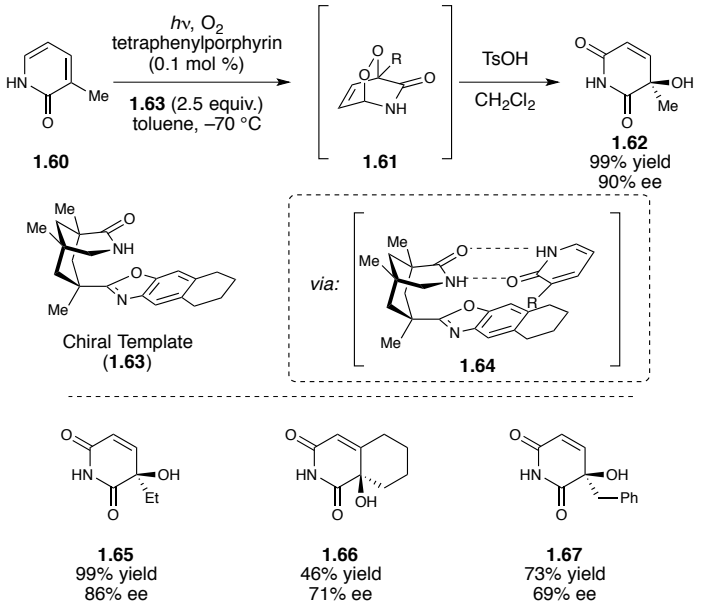

Figure 1.17: Enantioselective photooxidation of dihydropyridones using a chiral templating agent.

superstoichiometric quantities to achieve synthetically useful enantioselectivities. To combat this, one of the most successful strategies leveraged in enantioselective photochemistry has involved modifying chiral templating agents to create chiral energy transfer sensitizers, thereby creating photocatalysts with desireable reactivity by combining dual functions into a single species. This creates the opportunity for enantiocontrol in photosensitized transformations by allowing intramolecular energy transfer pathways (for bound substrates) to outcompete intermolecular (unbound substrate) pathways. This idea was first probed in a synthetic context by Krische,[49] whose seminal work established the feasibility of performing enantioselective [2+2] photocycloadditions of quinolones (**1.68**) with a triplet sensitizer linked to a molecular recognition element (**1.68**), albeit in low enantioselectivity (20% ee, Figure 1.18).

This work was eventually built upon by Bach, who used a chiral xanthone derived from Kemp's triacid (**1.71**) to catalyze a similar [2+2] quinolone photocycloaddtion with loadings as low as 10 mol%.[50] Subsequent work from the lab of Bach has demonstrated several salient features of this system (see Figure 1.19). The efficiency with which the templating catalyst absorbs

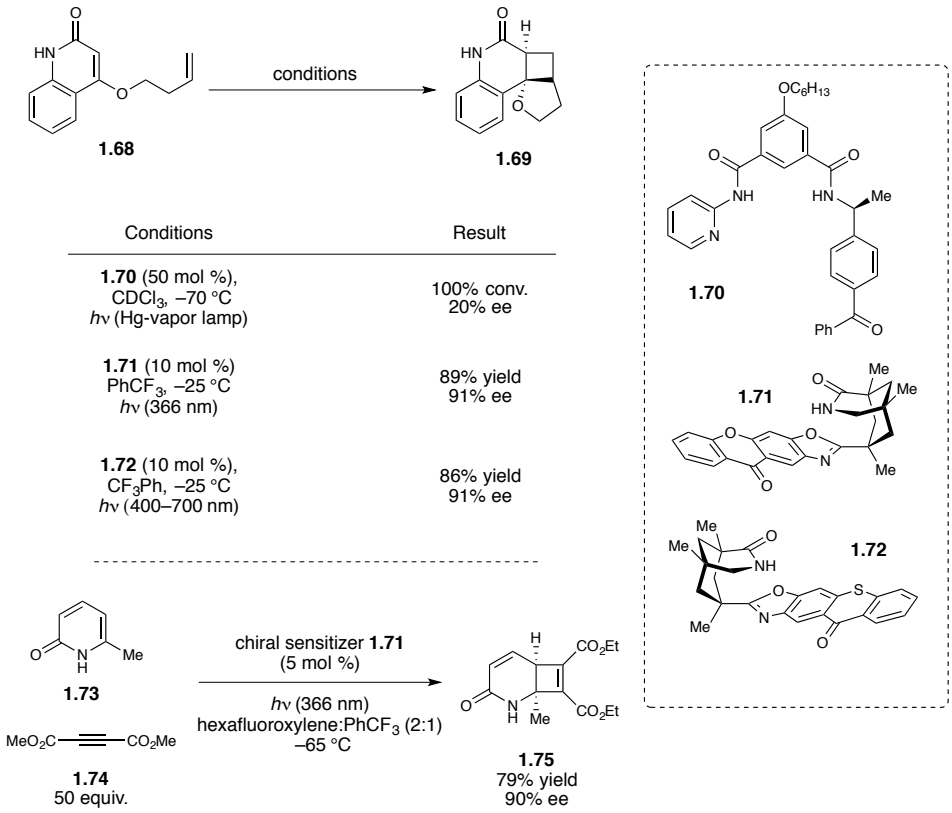

Figure 1.18: Asymmetric [2+2] photocycloadditions with sensitizing templates

the incident photons (366 nm) is important for high enantioselectivity in this transformation. By effectively blocking direct excitation of the substrate, it becomes possible to prevent an unsensitized background reaction in the absence of the chiral template. Indeed, substrates that possess increased absorbance at the wavelength used to excite the templating catalyst show decreased enantioselectivities.[51] Additionally, the length and structure of the alkene tether has a profound influence on the enantioselectivity of the reaction. Observations made in the course of the study suggest that sluggish [2+2] cycloaddition in alternate substrates can allow for competitive template dissociation after sensitization, thereby suppressing product enantioselectivity.[51]

The combination of a molecular recognition element and a triplet sensitizer has also been extended to the cycloadditions of 2-pyridones, with great success (Figure 1.18, **1.73** to **1.74**),[52] and

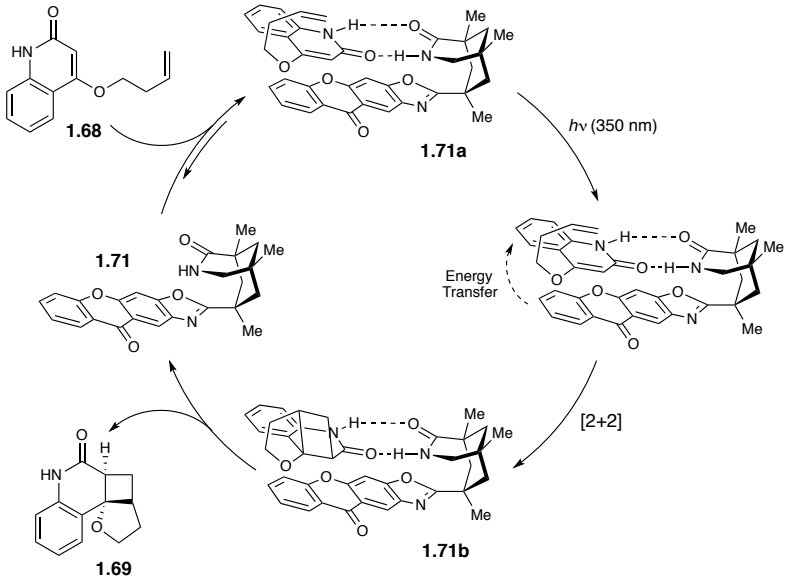

Figure 1.19: Proposed mechanism for the templated [2+2] photocycloaddition using chiral sensitizer 1.171.

the triplet sensitizer component of the template has proven tunable. The replacement of the xanthone moiety with a thioxanthone (**1.72**) affords a triplet sensitizer with efficient absorption in the visible spectrum, while maintaining a high enough triplet energy to undergo efficient energy transfer in the substrate·template complex.[53]

1.3 Molecular Co-catalysis

As the generation of photoexcited intermediates has become better understood, the methods for harnessing their reactivity have evolved. While powerful in their own right, supramolecular strategies can appear cumbersome to the practicing organic chemist, and efforts have been made to leverage small-molecule systems to achieve selective energy transfer co-catalysis. Templated and bifunctional platforms have begun to offer a practical solution, but remain a specialized strategy for specific sets of substrates and cycloadditions. Co-catalytic platforms in photocatalysis have emerged that control and expand the accessible chemistry of photoexcited intermediates through interactions with transition metals and transient

intermediates generated through organocatalysis, phase-transfer catalysis, and Brønsted acid catalysis.

1.3.1 Transition Metal Co-catalysis

Transition metal co-catalysis in primary photocatalytic processes was originally shown to function through indirect interactions with the electronically excited species in solution. This entails transition metal activation of ground state products generated through triplet photosensitization.

This strategy was first demonstrated by the lab of Adam, who used tetraphenylporphyrin as a singlet oxygen sensitizer to generate allylic hydroperoxides. These were subsequently intercepted by a Ti(IV) alkoxide catalyst, which catalyzes O-atom transfer to the double bond to generate α-epoxy alcohols (Figure 1.20).[54] The scope for this transformation is remarkably broad,

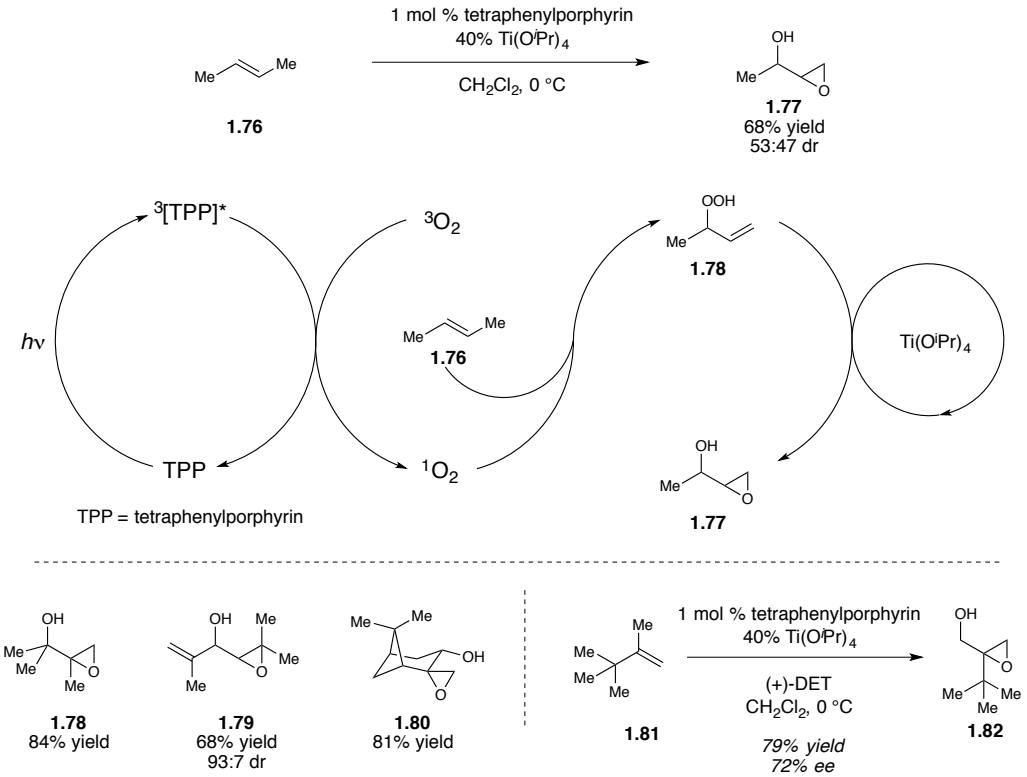

Figure 1.20: Co-catalytic allylic oxidation-epoxidation of alkenes

and the primary competing reactions are reduction of the allylic hydroperoxide for electron deficient substrates for which the epoxidation step is slow. Additionally, the authors demonstrate that the use of (+)-diethyl tartrate as a chiral ligand in the epoxidation generates enantioenriched products in good yields and moderate enantioselectivities (Figure 1.20).

Using a similar strategy to that of Adam and coworkers, the lab of Campestrini recently demonstrated a similar transformation using $Mo(CO)_6$ as a catalyst.[55] However, because the molybdenum catalyst consumes two equivalents of hydroperoxide for each epoxide formed, a maximum theoretical yield of only 50% is possible for each olefin substrate. Nevertheless, yields of up to 38% (77% of theoretical maximum) were obtained under the optimized conditions.

In addition to epoxidation chemistry, singlet oxygen sensitization has also been shown to enable olefin dihydroxylation chemistry through a multi-catalytic cascade process developed by Krief and coworkers.[56] In searching for alternative oxidants to replace potassium ferricyanide in the Sharpless asymmetric dihydroxylation reaction, it was found that selenoxides can facilitate

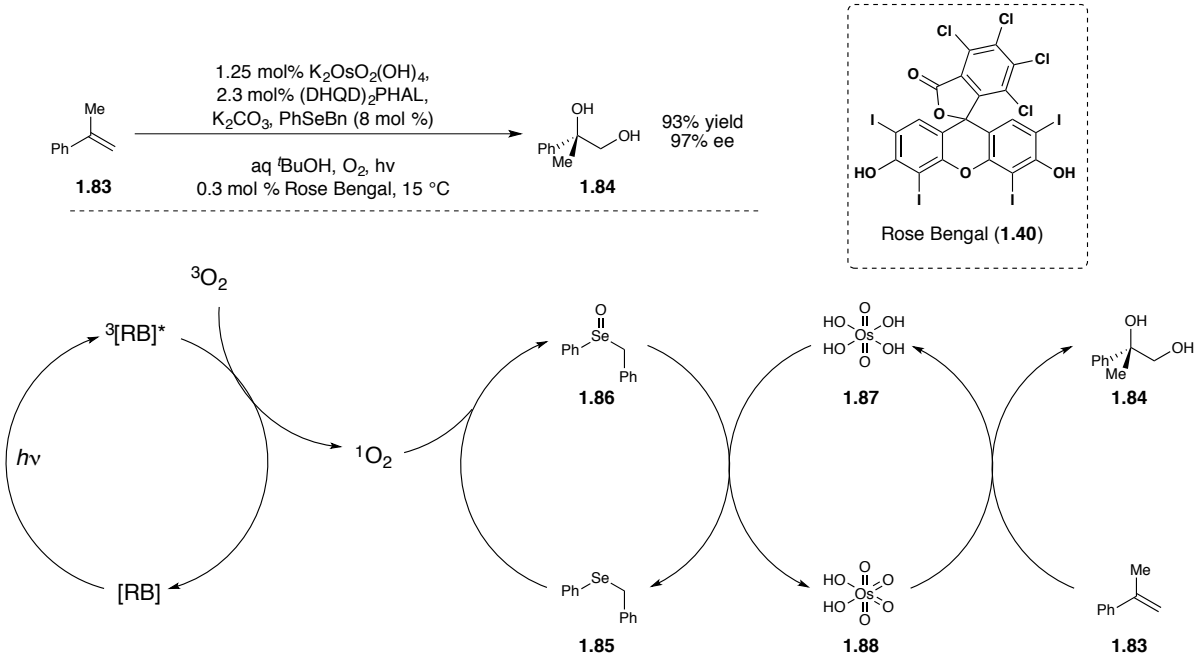

Figure 1.21: Sensitization in the aerobic asymmetric dihydroxylation of alkenes

the oxidation of Os(VI) to Os(VIII).[57] Having already developed a method for the aerobic generation of selenoxides by triplet sensitization of singlet oxygen,[58] Krief and coworkers recognized that an appropriately optimized cascade process could be used to facilitate catalytic aerobic dihydroxylation. Thus, using rose bengal (**1.40**) as a singlet oxygen sensitizer, benzyl phenyl selenide as a catalytic redox mediator, and 0.40 mol % $K_2OsO_2(OH)_2$ as a catalyst, high yields and ee's were obtained in the dihydroxylation of styrene derivatives (Figure 1.21).

A fundamentally different strategy for activation of reactive intermediates in primary photocatalytic processes is to perform energy transfer from the photocatalyst excited state to a reactive intermediate generated *in situ*. This has been proposed in recent work from the lab of Kobayashi, in the photocatalyzed Ullman coupling of carbazoles with aryl iodides.[59] Under the optimized conditions, the authors favor an energy transfer mechanism in which the photoexcited $Ir(ppy)_3$ photocatalyst undergoes energy transfer to a Cu(I)-carbazolide species (**1.94**), which then facilitates a single-electron reduction of the substrate aryl iodide (**1.90**) to drive the desired coupling. While intriguing, this mechanism requires additional validation before it can be extensively generalized. Nevertheless, this reaction functions well for a variety of aryl iodides, and a handful of carbazoles (Figure 1.22), building on prior work from the labs of Fu and Peters on photoinduced Ullman couplings without an exogenous photosensitizer.[60]

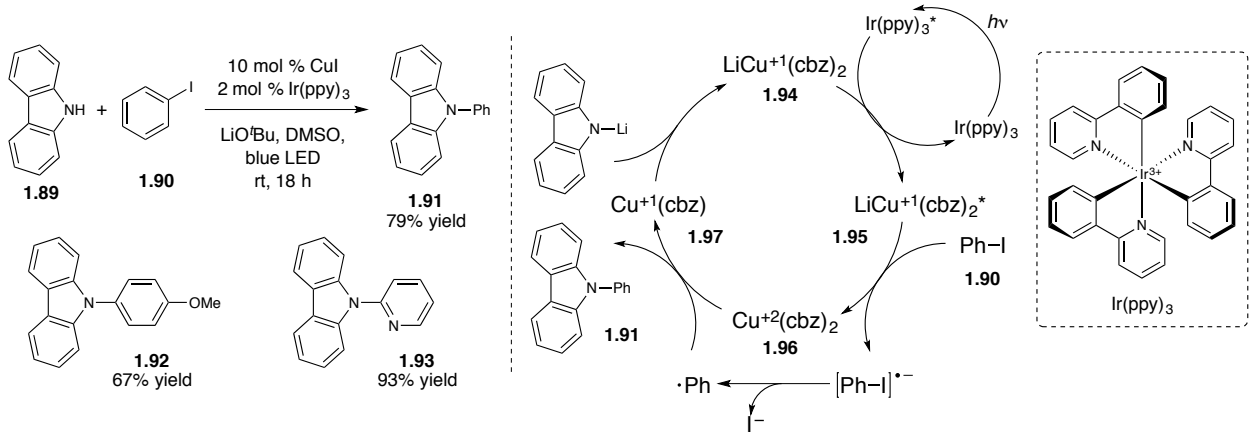

Figure 1.22: Iridium-Copper(I) co-catalyzed Ullmann coupling of carbazoles

1.3.2 Organic Co-catalysis

Several examples exist of the combination of primary photocatalytic processes with three separate modes of organocatalytic activation: amine catalysis, phase transfer catalysis, and Brønsted acid catalysis. These strategies all function by catalyzing downstream chemical reactions after photosensitization, and not by promoting sensitization itself. Because of the diverse, synthetically tractable nature of many of these catalysts, this area has profound implications for enantioselective catalysis in primary photochemistry.

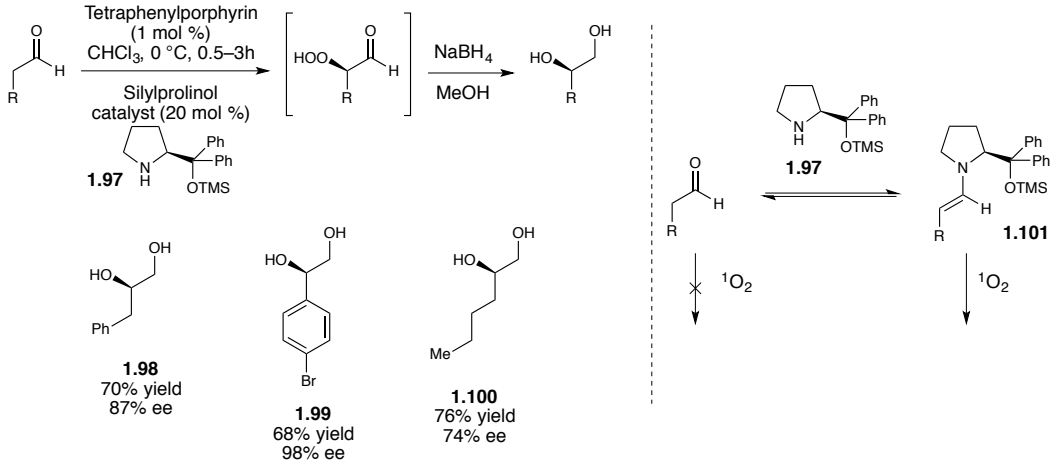

Figure 1.23: Photooxidation of aldehydes by tetraphenylporphyrin-enamine co-catalysis

Catalysis by amines has been known since original seminal work from the lab of Shioiri, who demonstrated that excess (–)-nicotine could enable the enantioselective oxygenation of indoles.[61] Unfortunately, the mechanism of activation or enantioinduction was never elucidated, but more recent work from the lab of Córdova has explored amino acid catalysis as a means to achieve enantioselective photooxygenation of aldehydes and ketones.[62] Recognizing the rapid relative reactivity of enamines relative to ketones and aldehydes with singlet oxygen, Córdova and coworkers identified first natural amino acids, and then diarylprolinol derivatives which afford moderate yields and selectivities in the synthesis of diols and α-oxycarbonyl compounds (Figure 1.23) in the presence of a catalytic singlet oxygen photosensitizer (tetraphenylporphyrin). A

number of cyclic and acyclic ketones and aldehydes are tolerated, with reported results as high as 71% yield and 98% ee (Figure 1.23).

The original proposed mechanism from Córdova and coworkers invokes nucleophilic attack of the electron rich enamine onto $^1O_2$ as an electrophilic radical oxidant (Figure 1.23). Subsequent H-atom abstraction affords the hydroperoxyl species, which is reduced to the alcohol during workup. Minimal evidence to support this scheme was offered in the original publications. However, recent work from the lab of Gryko has demonstrated the formation of trace $^1O_2$-derived oxidative byproducts by GC-MS that support the key intermediacy of both enamine and singlet oxygen in this system.[63]

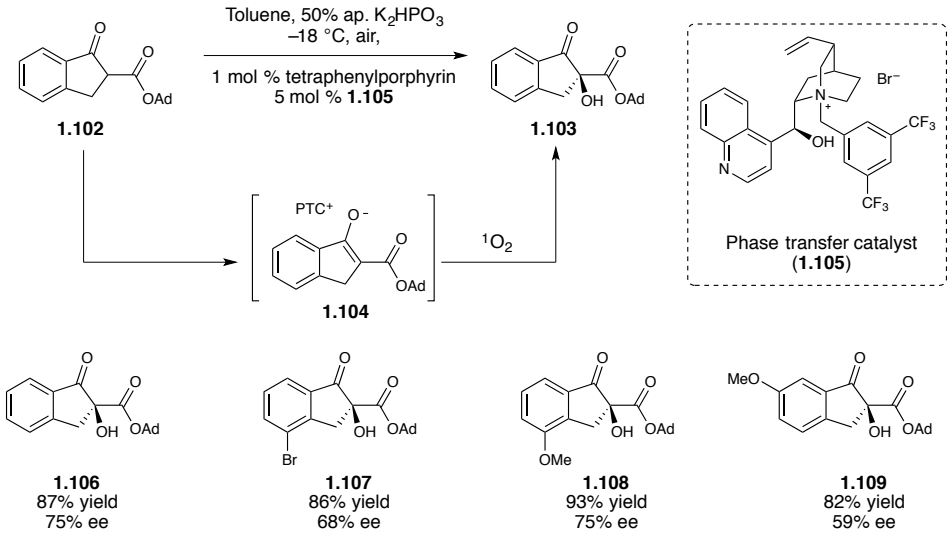

Figure 1.24: Asymmetric photooxidation of *β*-ketoester enolates by cooperative phase-transfer catalysis.

In addition to amine catalysis, phase transfer catalysis has also been used to control selectivity in the oxidation of carbonyl compounds *via* enolate chemistry. Because of the dramatically shortened lifetime of singlet oxygen in water relative to aprotic solvents, energy transfer reactivity can sometimes be preferentially carried out in organic media. Recognizing this, Meng and coworkers used an established cinchona alkaloid family of chiral phase transfer catalysts to transport indanone *β*-ketoester enolates into an organic phase to facilitate

enantioselective α-photooxygenation in a co-catalytic manifold.[64] Using tetraphenylporphyrin as a singlet oxygen sensitizer, and cinchona alkaloid **1.105** as a phase-transfer catalyst, α-hydroxy-β-ketoesters (**1.103**) could be synthesized in excellent yields and moderate-to-good enantioselectivities. Support for the intermediacy of singlet oxygen was obtained using the singlet oxygen trap DABCO (1,4-diazabicyclo[2.2.2]octane),[65] which reduced reactivity. The reaction did, however, proceed efficiently in the presence of *p*-benzoquinone, a well-established trap of superoxide ($O_2^{\bullet -}$).[66]

1.3.3 Brønsted Acid Co-Catalysis

Brønsted acid co-catalysts have been used in in two different platforms to control and promote reactivity using photocatalysis, through both direct, and indirect co-catalysis. Konig and coworkers have suggested that co-catalytic Brønsted acids can alter selectivities in the photochemical decomposition of azides to perform intermolecular C–H amidation reactions of heteroaromatic substrates.[67] This is proposed to occur through photocatalytic activation of benzoyl azides (**1.110**) using $Ru(bpy)_3Cl_2$ as a triplet sensitizer, which liberates dinitrogen to generate a free nitrene (**1.116**). Under neutral reaction conditions this intermediate undergoes Curtius rearrangement to a phenyl isocyanate, or performs C–H abstraction to yield benzamide. However, under the strongly acidic reaction conditions, the proposed reactive nitrene intermediate becomes protonated, which minimizes these side reactions, and promotes electrophilic attack onto electron rich aromatic systems to afford C–H amination products (Figure 1.25, **1.113**–**1.115**, **1.119**–**1.120**). This reaction is shown to operate on a number of heterocyclic systems in good yields, functionalizing the most electron rich position of the aromatic ring, consistent with the electrophilic nature of the putative protonated nitrene intermediate.

Additional work has recently been reported by the group of Hanson, who have demonstrated that excited state proton transfer chemistry can be sensitized using transition metal

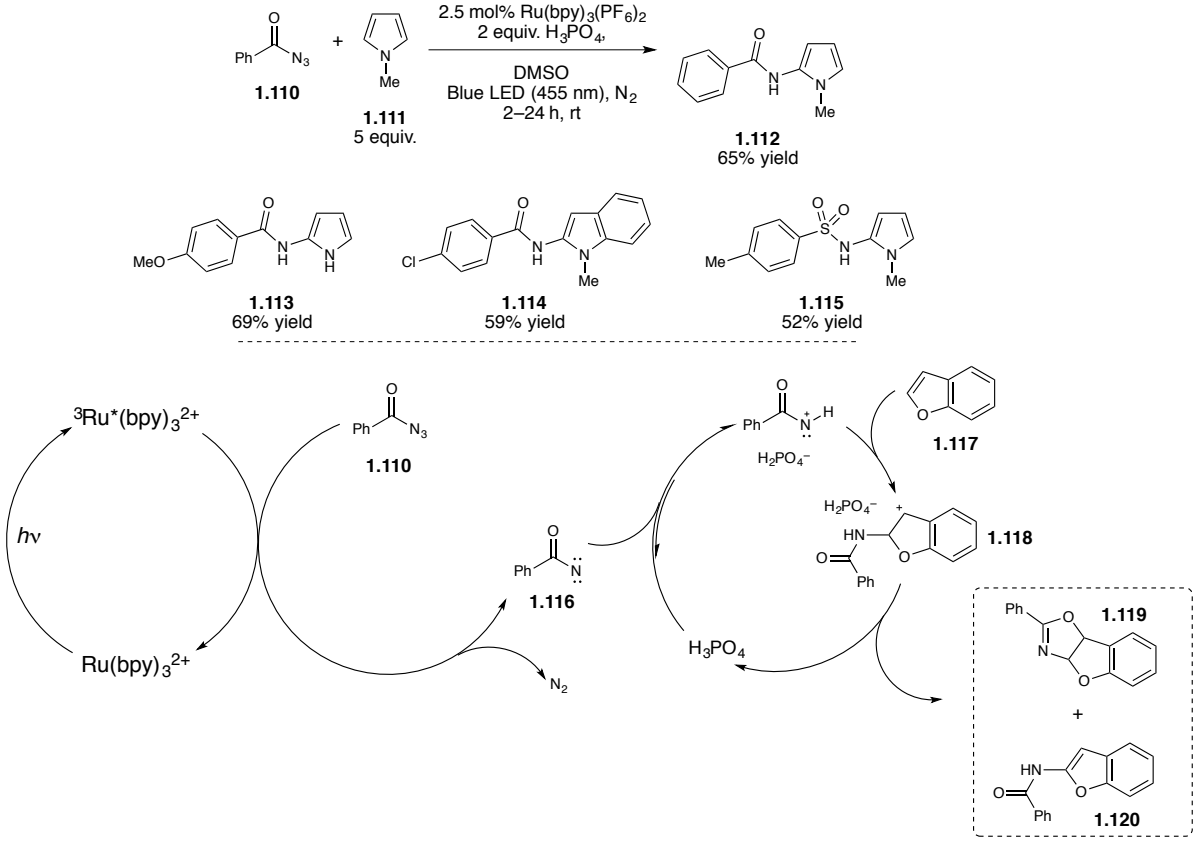

Figure 1.25: Synthetic scope and proposed mechanism for the C–H amination of electron rich arenes by benzoyl and sulfonyl azides

chromophores.[68] The authors propose that photoexcitation of naphthol derivatives increases the acidity of the phenolic proton, and enables the protonation and deprotection of silylenol ethers. While direct irradiation of appropriate naphthols in the ultraviolet range provides efficient reactivity, the authors show that longer wavelengths of light can be used through energy transfer sensitization by the cyclometallated iridium(III) complex **1.128**. Thus, energy transfer from the photoexcited metal complex to the napthol co-catalyst alters the acidity of the phenolic proton, leading to protonation and decomposition of the starting silylenol ether to the corresponding ketone product.

Collectively, the field of co-catalytic primary photocatalysis has yielded several informative and clever applications of excited state energy transfer chemistry, and reveals a photochemical landscape that contains great potential but is underdeveloped relative to its

ground state relatives. As photocatalysis continues to grow as a powerful strategy for generating reactive species, further exploration of this area promises to afford new and exciting applications of photochemistry in synthesis.

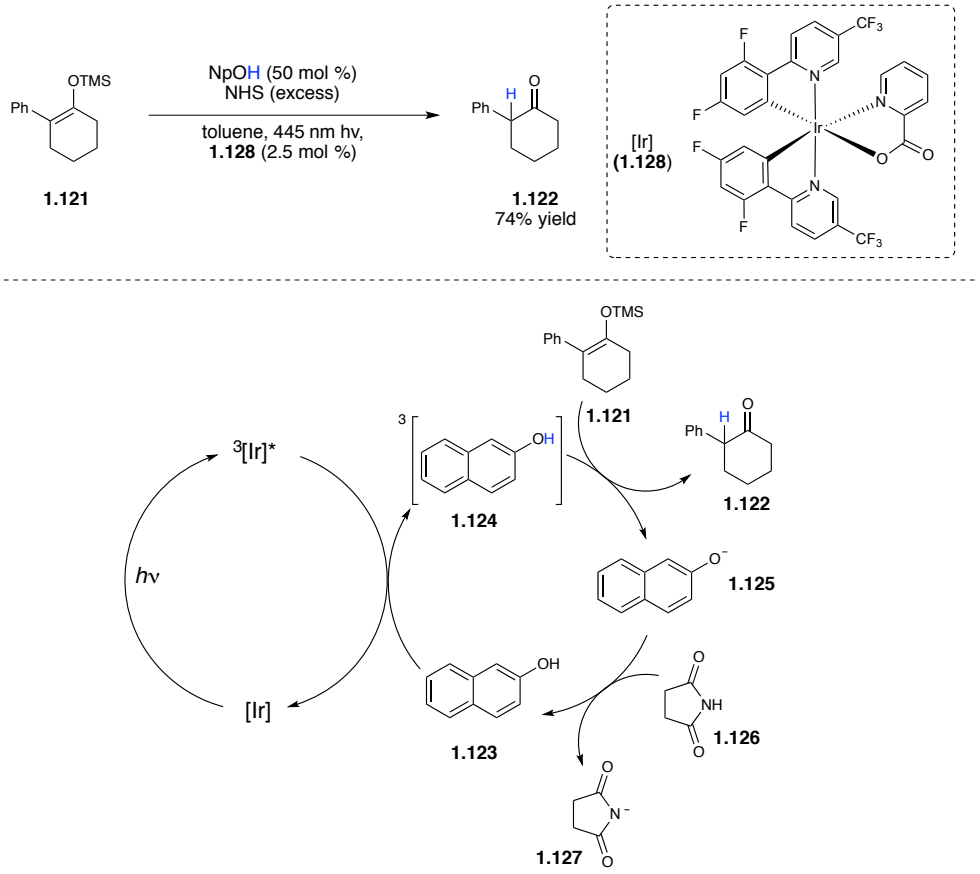

Figure 1.26: Co-catalytic excited state proton transfer (ESPT) for the acidic deprotection of silylenol ethers.

1.4 Concluding Remarks

While the last decade has seen a resurgence in the application of photochemistry to organic synthesis, due primarily to the introduction of robust, tunable catalysts that efficiently absorb visible light, the field of co-catalysis in organic photochemistry has a rich and storied history which has not been contextualized to date. While the use of photocatalysts in

photoinduced electron transfer chemistry continues to be the most broadly applied strategy for employing photochemistry today, primary photochemical processes also benefit from the cooperativity between photocatalysis and exogenous controllers of excited state reactivity. This idea has proliferated rapidly in modern photochemical synthesis, and has expanded the number of species that can be selectively generated and harnessed through cooperative control of reactivity. These cooperative strategies are among the most promising and attractive means for enhancing photochemical capabilities in organic synthesis.

1.5 References

[1] (a) Narayanam, J. M. R.; Stephenson, C. R. J. "Visible light photoredox catalysis: applications in organic synthesis." *Chem. Soc. Rev.* **2011**, *40*, 102–113. (b) Tucker, J. W.; Stephenson, C. R. J. "Shining light on photoredox catalysis: Theory and synthetic applications." *J. Org. Chem.* **2012**, *77*, 1617–1622. (c) Xuan, J.; Xiao, W.-J. "Visible-Light Photoredox Catalysis." *Angew. Chem. Int. Ed.* **2012**, *51*, 6828–6838. (d) Reckenthäler, M.; Griesbeck, A. G. "Photoredox Catalysis for Organic Syntheses." *Adv. Synth. Catal.* **2013**, *355*, 2727–2744. (e) Schultz, D. M.; Yoon, T. P. "Solar Synthesis: Prospects in Visible Light Photocatalysis." *Science* **2014**, *343*, 1239176-1–1239176-8. (f) Prier, C. K.; Rankic, D. A.; MacMillan, D. W. C. "Visible Light Photoredox Catalysis with Transition Metal Complexes: Applications in Organic Synthesis." *Chem. Rev.* **2013**, *113*, 5322–5363.

[2] Bach, T.; Hehn, J.P. "Photochemical reactions as key steps in natural product synthesis." *Angew. Chem. Int. Ed.* **2011**, *50*, 1000–1046.

[3] (a) Fox, M. A.; Dulay, M. T. "Heterogeneous photocatalysis." *Chem. Rev.* **1993**, *93*, 341–357. (b) Shiraishi, Y.; Hirai, T. "Selective organic transformations on titanium oxide-based photocatalysts." *J. Photochem. Photobiol., C.* **2008**, *9*, 157–170. (c) Kisch, H. "Semiconductor Photocatalysis-Mechanistic and Synthetic Aspects." *Angew. Chem. Int. Ed.* **2013**, *52*, 812–847. (d) Zou, X.; Tao, Z.; Asefa, T. "Semiconductor and Plasmonic Photocatalysis for Selective Organic Transformations." *Curr. Org. Chem.* **2013**, *17*, 1274–1287.

[4] Maldotti, A.; Molinari, A.; Amadelli, R. "Photocatalysis with Organized Systems for the Oxofunctionalization of Hydrocarbons by O2." *Chem. Rev.* **2002**, *102*, 3811–3836.

[5] (a) Fagnoni, M.; Dondi, D.; Ravelli, D.; Albini, A. "Photocatalysis for the formation of the C–C bond." *Chem. Rev.* **2007**, *107*, 2725–2756. (b) Hoffmann, N. "Efficient photochemical electron transfer sensitization of homogeneous organic reactions." *J. Photochem. Photobiol., C.* **2008**, *9*, 43–60.

[6] (a) Hoffmann, N. "Photochemical reactions as key steps in organic synthesis." *Chem. Rev.* **2008**, *108*, 1052–1103. (b) Beatty, J. W.; Stephenson, C. R. J. "Amine Functionalization via Oxidative Photoredox Catalysis: Methodology Development and Complex Molecule Synthesis." *Acc. Chem. Res.* **2015**, *48*, 1474–1484.

[7] Hopkinson, M. N.; Sahoo, B.; Li, J.-L.; Glorius, F. "Dual Catalysis Sees the Light: Combining Photoredox with Organo-, Acid, and Transition-Metal Catalysis." *Chem. Eur. J.* **2014**, *20*, 3874–3886.

[8] (a) Rau, H. "Asymmetric photochemistry in solution." *Chem. Rev.* **1983**, *83*, 535–547. (b) Inoue, Y. "Asymmetric photochemical reactions in solution." *Chem. Rev.* **1992**, *92*, 741–770. (c) Brimioulle, R.; Lenhart, D.; Maturi, M. M.; Bach, T. "Enantioselective Catalysis of Photochemical Reactions." *Angew. Chem. Int. Ed.* **2015**, *54*, 3872–3890. (d) Meggers, E. "Asymmetric catalysis activated by visible light." *Chem. Commun.* **2015**, *51*, 3290–3301.

[9] (a) Vallavoju, N.; Sivaguru, J. "Supramolecular photocatalysis: combining confinement and non-covalent interactions to control light initiated reactions." *Chem. Soc. Rev.* **2014**, *43*, 4084–4101. (b) Bibal, B.; Mongin, C.; Bassani, D.M. "Template effects and supramolecular control of photoreactions in solution." *Chem. Soc. Rev.* **2014**, *43*, 4179–4198. (c) Ramamurthy, V.; Mondal, B. "Supramolecular photochemistry concepts highlighted with select examples." *J. Photochem. Photobiol. C: Photochem. Rev.* **2015**, *23*, 68–102. (d) Yang, C.; Inoue, Y. "Supramolecular photochirogenesis." *Chem. Soc. Rev.* **2014**, *43*, 4123–4143. (e) Svoboda, J.; Konig, B. "Templated photochemistry: Toward catalysts enhancing the efficiency and selectivity of photoreactions in homogenous solutions." *Chem. Rev.* **2006**, *106*, 5413–5430. (f) Ramamurthy, V.; Gupta, S. "Supramolecular photochemistry: from molecular crystals to water-soluble capsules." *Chem. Soc. Rev.* **2015**, *44*, 119–135.

[10] (a) Alberti, M.; Orfanopoulos, M." Recent Mechanistic Insights in the Singlet Oxygen Ene Reaction." *Synlett*, **2010**, *7*, 999–1026. (b) Clennan, E.L. "New Mechanistic and Synthetic Aspects of Singlet Oxygen Chemistry." *Tetrahedron* **2000**, *56*, 9151–9179.

[11] (a) Joy, A.; Ramamurthy, V. "Chiral photochemistry within zeolites." *Chem. Eur. J.* **2000**, *6*, 1287–1293. (b) Ramamurthy, V.; Shailaja, J.; Kaanumalle, L.S.; Chandrasekhar, J. "Controlling chemistry with cations: photochemistry within zeolites." *Chem. Comm.* **2003**, 1987–1999. (c) Corma, A.; Garcia, H. "Zeolite-based phtosocatalysts." *Chem. Comm.* **2004**, 1443–1459. (d) Ramamurthy, V. "Controlling photochemical reactions via confinement: zeolites." *J. Photochem. Photobiol. C* **2000**, *1*, 145–166.

[12] Gessner, F.; Olea, A.; Lobaugh, J.H.; Johnston, L.J.; Scaiano, J.C. "Intrazeolite Photochemistry. 5. Use of Zeolites in the Control of Photostationary Ratios in Sensicized Cis-Trans Isomerizations." *J. Org. Chem.* **1989**. *54*, 259–261.

[13] Baldovi, M.V.; Corma, A.; Garcia, H.; Marti, V. "Shape selective Photosensitized Isomerization of Stilbene Using a Benzophenone Incorporated Within Acid Zeolites." *Tet. Lett.* **1994**, *35*, 9447–9450.

[14] Pettit, T.L.; Fox, M.A. "Photoassisted Oxygenation of Olefins: An Exchanged Zeolite as a Heterogeneous Photosensitizer." *J. Phys. Chem.* **1986**, *90*, 1353–1354.

[15] (a) Li, X.; Ramamurthy, V. "Selective oxidation of olefins within organic dye cation-exchanged zeolites." *J. Am. Chem. Soc.* **1996**, *118*, 10666–10667. (b) Robbins, R.J.; Ramamurthy, V. "Generation and reactivity of singlet oxygen within zeolites: remarkable control of hydroperoxidation of alkenes." *Chem. Comm.* **1997**, 1071–1072.

[16] (a) Clennan, E.L.; Sram, J.P.; Pace, A.; Vincer, K.; White, S. "Intrazeolite Photooxidations of Electron-Poor Alkenes." *J. Org. Chem.* **2002**, *67*, 3975–3978. (b) Clennan, E.L.; Sram, J.P. "Photochemical Reactions in the Interior of a Zeolite. Part 5: The Origin of the Zeolite Induced Regioselectivity in the Singlet Oxygen Ene Reaction." *Tetrahedron* **2000**, *56*, 6945–6950. (c) Stratakis, M.; Froudakis, G. "Site specificity in the photooxidation of some trisubstituted alkenes in thionin-supported zeolite Na-Y. On the role of the alkali metal cation." *Org Lett.* **2000**, *2*, 1369–1372. (d) Kaanumalle, L.S.; Shailaja, J.; Robbins, R.J.; Ramamurthy, V. "Cation controlled singlet oxygen mediated oxidation of olefins within zeolites." *J. Photochem. Photobiol. A: Chem.* **2002**, *153*, 55–65.

[17] Statakis, m.; Kosmas, G. "Enhanced diastereoselectivity of an ene hydroperoxidation reaction by confinement within zeolite Na-Y; a stereoisotopic study." *Tet. Lett.* **2001**, *42*, 6007–6009.

[18] Stratakis, M.; Rabalakos, C.; Mpourmpakis, G.; Froudakis, G.E. "Ene Hydroperoxidation of Isobutenylarenes within Dye-Exchanged Zeolite Na-Y: Control of Site Selectivity by Cation-Arene Interactions." *J. Org. Chem.* **2003**, *68*, 2839–2843.

[19] Pace, A.; Clennan, E.L. "A new experimental protocol for intrazeolite photooxidations. The first product-based estimate of an upper limit for the intrazeolite singlet oxygen lifetime." *J. Am. Chem. Soc.* **2002**, *124*, 11236–11237.

[20] Chen, Y-Z.; Wu, L-Z.; Zhang, L-P.; Tung, C-H. "Confined space-controlled hydroperoxidation of trisubstituted alkenes adsorbed on pentasil zeolites." *J. Org. Chem.* **2005**, *70*, 4676–4681.

[21] Ting, S-H.; Wang, H.; Ying, Y-M. "Photosensitized oxidation of alkenes adsorbed on pentasil zeolites." *J. Am. Chem. Soc.* **1998**, *120*, 5179–5186.

[22] Stratakis, M.; Sofikiti, N.; Baskakis, C.; Raptis, C. "Dye-sensitized intrazeolite photooxygenation of 4-substituted cyclohexenes. Remote substituent effects in regioselectivity and diastereoselectivity." *Tet. Lett.* **2004**, *45*, 5433–5436.

[23] Stratakis, M.' Raptis, C.; Sofikiti, N.; Tsangarakis, C.; Kosmas, G.; Zaravinos, I-P.; Kalaitzakis, D.; Stavroulakis, D.; Baskakis, C.; Stathoulopoulou. A. "Intrazeolite photooxygenation of chiral alkenes. Control of facial selectivity by confinement and cation–π interactions." *Tetrahedron* **2006**, *62*, 10623–10632.

[24] Clennan, E.L.; Zhang, D.; Singleton, J. "A comparison of intrazeolite and solution singlet oxygen Ene reactions of allylic alcohols." *Photochem. & Photobiol.* **2006**, *82*, 1226–1232.

[25] Stratakis, M.; Sofikiti, N. "Intrazeolite photo-oxygenation of (R)-(–)-α-phellandrene." *J. Chem. Res. (S)* **2002**, 374–375.

[26] Shailaja, J.; Sivaguru, J.; Robbins, R.J.; Ramamurthy, V.; Sunoj, R.B.; Chandrasekhar, J. "Singlet Oxygen Mediated Oxidation of Olefins within Zeolites: Selectivity and Complexities." *Tetrahedron*, **2000**, *56*, 6927–6943.

[27] Joy, A.; Robbins, R.J.; Pitchumani, K.; Ramamurthy, V. "Asymmetrically modified zeolite as a medium for enantioselective photoreactions: Reactions from spin forbidden excited states." *Tet. Lett.* **1997**, *38*, 8825–8828.

[28] Sivaguru, J.; Saito, H.; Solomon, M.R.; Kaanumalle, L.S.; Poon, T.; Jockusch, S.; Adam, W.; Ramamurthy, V.; Inoue, Y. Turro, N. J. "Control of Chirality by Cations in Confined Spaces : Photooxidation of Enecarbamates Inside Zeolite Supercages Control of Chirality by Cations in Confined Spaces : Photooxidation of Enecarbamates Inside Zeolite Supercages." *Photochem. & Photobiol.* **2006**, 82, 123–131.

[29] (a) Zhou, W.; Clennan, E.L. "Organic Reactions in Zeolites. 1. Photooxidations of Sulfides in Methylene Blue Doped Zeolite Y." *J. Am. Chem. Soc.* **1999**, *121*, 2915–2916. (b) Clennan, E.L.; Zhou, W.; Chan, J. "Mechanistic Organic Chemistry in a Microreactor. Zeolite-Controlled Photooxidations of Organic Sulfides." *J. Org. Chem.* **2002**, 67*, 9368–9378*

[30] (a) Pitchumani, K.; Gamlin, J.N.; Ramamurthy, V.; Sheffer, J.R. "Triplet–triplet energy transfer between organic molecules trapped in zeolites." *Chem. Comm.* **1996**, 2049–2050. (b) Pitchumani, K.; Warrier, M.; Sheffer, J.R.; Ramamurthy, V. "Novel approaches towards the generation of excited triplets of organic guest molecules with zeolites." *Chem. Comm.* **1998**, 1197–1198.

[31] (a) Bortolus, P.; Grabner, G.; Kohler, G.; Monti, S. "Photochemistry of Cyclodextrin Host-Guest Complexes." *Coord. Chem. Rev.* **1993**, *125*, 261–268. (b) Bortolus, P. Monti, S. "Photochemistry in Cyclodextrin Cavities." *Adv. Photochem.* **196**, *21*, 1–133. (c) Ramamurthy, V.; Eaton, D.F. "Photochemistry and photophysics within cyclodextrin cavities." *Acc. Chem. Res.* **1988**, *21*, 300–306.

[32] Kuroda, Y.; Sera, T.; Ogoshi, H. "Regioselectivities and Stereoselectivities of Singlet Oxygen Generated by Cyclodextrin Sandwiched Porphyrin Sensitization. Lipoxygenase-like Activity." *J. Am. Chem. Soc.* **1991**, *113*, 2793–2794.

[33] Weber, L.; Imiolczyk, I.; Haufe, G.; Rehorek, D.; Hennig, H. "Photocatalytic enantiodiscriminating oxygenation with cyclodextrin-linked porphyrins and molecular oxygen." *J. Chem. Soc., Chem. Comm.* **1992**, 301–303.

[34] For selected examples, see: (a) Fukuhara, G.; Mori, T.; Wada, T.; Inoue, Y. "Entropy-controlled supramolecular photochirogenesis: Enantiodifferentiating Z-E photoisomerization of cyclooctene included and sensitized by permethylated 6-o-modified β-cyclodextrins." *J. Org. Chem.* **2006**, *71*, 8233–8243. (b) Inoue, Y.; Wada, T.; Suguhara, N.; Yamamoto, K.; Kimura, K.; Tong, L-H.; Gao, X-M.; Hou, Z-J.; Liu, Y. "Supramolecular photochirogenesis. 2. Enantiodifferentiating photoisomerization of cyclooctene included and sensitized by 6-O-modified cyclodextrins." *J. Org. Chem.* **2000**, *65*, 8041–8050. (and references therein).

[35] Natarajan, A.; Kaanumalle, L.S.; Jockusch, S.; Gibb, C.L.D.; Gibb, B.C.; Turro, N.J.; Ramaburthy, V. "Controlling Photoreactions with Restricted Spaces and Weak Intermolecular Forces: Exquisite Selectivity during Oxidation of Olefins by Singlet Oxygen." *J. Am. Chem. Soc.* **2007**, *129*, 4132–4133.

[36] Kaanumalle, L.S.; Ramamurthy, V. "Photodimerization of acenaphthylene within a nanocapsule: excited state lifetime dependent dimer selectivity." *Chem. Comm.* **2007**, 1062–1064.

[37] Samanta, S.R; Parthasarathy, A.; Ramamurthy, V. "Supramolecular control during triplet sensitized geometric isomerization of stilbenes encapsulated in a water soluble organic capsule." *Photochem. & Photobiol. Sci.* **2012**, *11*, 1652–1660.

[38] Karthikeyan, S.; Ramamurthy, V. "Self-assembled coordination cage as a reaction vessel: Triplet sensitized [2+2] photodimerization of acenaphthylene, and [4+4] photodimerization of 9-anthraldehyde." *Tet. Lett.* **2005**, *26*, 4495–4498.

[39] Greer, M.F.; Walla, M.D.; Solntsev, K.M.; Strassert, C.A.; Shimizu, L.S. "Self-assembled benzophenone bis-urea macrocycles facilitate selective oxidations by singlet oxygen." *J. Org. Chem.* **2013**, *78*, 5568–5578.

[40] Hecht, S.; Frechet, J.M.J. "Light-Driven Catalysis within Dendrimers: Designing Amphiphilic Singlet Oxygen Sensitizers." *J. Am. Chem. Soc.* **2001**, *123*, 6959–6960.

[41] Shiraishi, Y.; Koizumi, H.; Hirai, T. "Photosensitized Oxygenation of Sulfides within an Amphiphilic Dendrimer Containins a Benzophenone Core." *J. Phys. Chem. B* **2005**, *109*. 8580–8586.

[42] Shiraishi, Y.; Kimata, Y.; Koizumi, H.; Hirai, T. "Temperature-controlled photooxygenation with polymer nanocapsules encapsulating an organic photosensitizer." *Langmuir* **2008**, *9832–9836*.

[43] Pastor-Perez, L.; Barriau, E.; Frey, H.; Perez-Prieto, J.; Stiriba, S-E. "Photocatalysis within hyperbranched polyethers with a benzophenone core." *J. Org. Chem.* **2008**, *73*, 4680–4683.

[44] Yuan, Z.; Zheng, S.; Zeng, Y.; Chen, J.; Han, Y.; Li, Y.; Li, Y. "Photosensitized oxidation of alkenes with dendrimers as microreactors: controllable selectivity between energy and electron transfer pathway." *New J. Chem.* **2010**, *34*, 718–722.

[45] (a) Li, H.R.; Wu, L.Z.; Tung, C.H. "Vesicle controlled selectivity in photosensitized oxidation of olefins." *Chem. Comm.* **2000**, 1085–1086. (b) Li, H-R.; Wu, L-Z.; Tung, C-H. "Reactions of singlet oxygen with olefins and sterically hindered amine in mixed surfactant vesicles." *J. Am. Chem. Soc.* **2000**, *122*, 2446–2451. (c) Pattabiraman, M.; Kaanumalle, L.S.; Ramamurthy, V. "Photoproduct selectivity in reactions involving singlet and triplet excited states within bile salt micelles." *Langmuir*, **2006**, *2185–2192*.

[46] (a) Polo, E.; Amadelli, R.; Carassiti, V.; Maldotti, A. "Entrapping of iron(III) porphyrins in a polystyrene matrix and their photocatalytic activity in oxidation reactions by molecular oxygen." *Inorg. Chim. Acta* **1991**, *192*, 1–3. (b) Arumugam, S.; Vutukuri, D.R.; Thayumanavan, S.; Ramamurthy, V. "A styrene based water soluble polymer as a reaction medium for photodimerization of aromatic hydrocarbons in water." *J. Photochem. Photobiol. A.* **2007**, *185*, 168–171.

[47] Tung, C-H.; Guan, J-Q. "Remarkable product selectivity in photosensitized oxidation of alkenes within nafion membranes." *J. Am. Chem. Soc.* **1998**, *120*, 11874–11879.

[48] Wiegand, C.; Herdtweck, E.; Bach, T. "Enantioselectivity in visible light-induced, singlet oxygen [2+4] cycloaddition reactions (type II photooxygenations) of 2-pyridones." *Chem. Comm.* **2012**, *48*, 10195–10197.

[49] Cauble, D.F.; Lynch, V.; Krische, M.J. "Studies on the enantioselective catalysis of photochemically promoted transformations: "Sensitizing receptors" as chiral catalysts." *J. Org. Chem.* **2003**, *68*, 15–21.

[50] (a) Muller, C.; Bauer, A.; Bach, T. "Light-Driven Enantioselective Organocatalysis." *Angew. Chem. Int. Ed.* **2009**, *48*, 6640–6642. (b) Maturi, M.M.; Wenninger, M.; Alonso, R.; Bauer, A.; Pothig, A.; Riedle, E.; Bach, T. "Intramolecular [2+2] photocycloaddition of 3- and 4-(but-3-enyl) oxyquinolones: Influence of the alkene substitution pattern, photophysical studies, and enantioselective catalysis by a chiral sensitizer." *Chem. Eur. J.* **2013**, *19*, 7461–7472.

[51] Muller, C.; Bauer, A.; Maturi, M.M.; Cuquerella, M.C.; Miranda, M.A.; Bach, T. "Enantioselective intramolecular [2 + 2]-photocycloaddition reactions of 4-substituted quinolones catalyzed by a chiral sensitizer with a hydrogen-bonding motif." *J. Am. Chem. Soc.* **2011**, *133*, 16689–16697.

[52] Maturie, M.M.; Bach, T. "Enantioselective catalysis of the intermolecular [2+2] photocycloaddition between 2-pyridones and acetylenedicarboxylates." *Angew. Chem. Int. Ed.* **2014**, *53*, 7661–7664.

[53] Alonso, R.; Bach, T. "A chiral thioxanthone as an organocatalyst for enantioselective [2+2] photocycloaddition reactions induced by visible light." *Angew. Chem. Int. Ed.* **2014**, *53*, 4368–4371.

[54] Adam, W.; Griesbeck, A.; Staab, E. "A Convenient "One-Pot" Synthesis of Epoxy Alcohols via Photooxygenation of Olefins in the Presence of Titanium(IV) Catalyst." *Tet. Lett.* **1986**, *27*, 2839–2842.

[55] Campestrini, S.; Tonellato, U. "Photoinitiated Olefin Epoxidation with Molecular Oxygen, Sensitized by Free Base Porphyrins and Promoted by Hexacarbonylmolybdenum in Homogeneous Solution." *Eur. J. Org. Chem.* **2002**, 3827–3832.

[56] Krief, A.; Colaux-Castillo, C. "Catalytic asymmetric dihydroxylation of α-methylstyrene by air." *Tet. Lett.* **1999**, *40*, 4189–4192.

[57] Abatjoglou, A. G.; Bryant, D. R. "Organic selenoxides as oxidants in osmium tetroxide catalyzed oxidation of olefins to glycols." *Tetrahedron. Lett.* **1981**, *22*, 2051–2054.

[58] Hevesi, L.; Krief, A. "Photo-Oxygenation of selenides – A New Pathway to Selenoxides." *Angew. Chem. Int. Ed.* **1976**, *15*, 381.

[59] Yoo, W-J.; Tsukamoto, T.; Kobayashi, S. "Visible Light-Mediated Ullmann-Type C-N Coupling Reactions of Carbazole Derivatives and Aryl Iodides." *Org. Lett.* **2015**, *17*, 3640–3642.

[60] (a) Creutz, S.E.; Lotito, K.J.; Fu, G.C.; Peters, J.C. "Photoinduced Ullmann C-N Coupling: Demonstrating the Viability of a Radical Pathway." *Science,* **2012**, *338*, 647–651. (b) Bissember,

A.C.; Lundgren, R.J.; Creutz, S.E.; Peters, J.C.; Fu, G.C. "Transition-Metal-Catalyzed Alkylations of Amines with Alkyl Halides: Photoinduced, Copper-Catalyzed Couplings of Carbazoles." *Angew. Chem. Int. Ed.* **2013**, *52*, 5129–5133. (c) Ratani, T.S.; Bachman, S.; Fu, G.C.; Peters, J.C. "Photoinduced, Copper-Catalyzed Carbon–Carbon Bond Formation with Alkyl Electrophiles: Cyanation of Unactivated Secondary Alkyl Chlorides at Room Temperature *J. Am. Chem. Soc.* **2015**, *137*, 13902–13907.

[61] Sakai, A.; Tani, H.; Aoyama, T.; Shiori, T. "Enantioselective Photosensitized Oxygenation. Its Application to N_b-Methoxycarbonyltryptamine and Determination of Absolute Configuration of the Product." *Synlett*, **1998**, *9*, 257–258.

[62] (a) Córdova, A.; Sundén, H.; Engqvist, M.; Ibrahem, I.; Casasm J. "The direct amino acid-catalyzed asymmetric incorporation of molecular oxygen to organic compounds." *J. Am. Chem. Soc.* **2004**, *126*, 8914–8915. (b) Sundén, H.; Engqvist, M.; Casas, J.; Ibrahem, I.; Córdova, A. "Direct amino acid catalyzed asymmetric α oxidation of ketones with molecular oxygen." *Angew. Chem. Int. Ed.* **2004**, *43*, 6532–6535. (c) Ibrahem, I.; Zhao, G-L.; Sundén, H.; Córdova, A. "A route to 1,2-diols by enantioselective organocatalytic α-oxidation with molecular oxygen." *Tet. Lett.* **2006**, *47*, 4659–4663.

[63] Walaszek, D.J.; Rybicka-Jasinska, K.; Smolen, S.; Karczewski, M.; Gryko, D. "Mechanistic Insights into Enantioselective C–H Photooxygenation of Aldehydes *via* Enamine Catalysis." *Adv. Synth. Catal.* **2015**, *357*, 2061–2070.

[64] Lian, M.; Li, Z.; Cai, Y.; Meng, Q.; Gao, Z. "Enantioselective photooxygenation of α-keto esters by chiral phase-transfer catalysis using molecular oxygen." *Chem. Asian J.* **2012**, *7*, 2019–2023.

[65] Silverman, S.K.; Foote, C.S. "Singlet oxygen and electron-transfer mechanisms in the dicyanoanthracene-sensitized photooxidation of 2,3-diphenyl-1,4-dioxene." *J. Am. Chem. Soc.* **1991**, *113*, 7672–7675.

[66] Manring, L.E.; Kramer, M.K.; Foote, C.S. "Interception of O_2^- by Benzoquinone in Canoaromatic-Sensitized Photooxygenations." *Tet. Lett.* **1984**, *25*, 2523–2526.

[67] Brachet, E.; Ghosh, T.; Ghosh, I.; König, B. "Visible Light C-H Amidation of Heteroarenes with Benzoyl Azides." *Chem. Sci.* **2015**, *6*, 987–992.

[68] Das, A.; Banerjee, T.; Hanson, K. "Protonation of silylenol ether via excited state proton transfer catalysis." *Chem. Comm.* **2015**, 10.1039/c5cc08081A

Chapter 2. Development of a photocatalytic platform for organic oxidation

Portions of this work have been previously published:

Blum, T.R.; Zhu, Y.; Nordeen, S.A.; Yoon, T.P. "Photocatalytic Synthesis of Dihydrobenzofurans by Oxidative [3+2] Cycloaddition of Phenols." *Angew. Chem. Int. Ed.* **2014**, *53*, 11056–11059.

2.1 Introduction

The proper choice of terminal oxidant is an important consideration in the design of oxidative transformations.[1] Many of the most common oxidants used in organic synthesis produce stoichiometric byproducts whose separation and disposal can be both practically and environmentally problematic. Our laboratory has a long-standing interest in the propensity of the photoexcited $Ru^*(bpy)_3^{2+}$ chromophore to undergo efficient redox reactions with a diverse range of quenchers,[2] a feature that has been increasingly exploited in the design of synthetic reactions.[3] We wondered if photoredox catalysis might offer a strategy to employ benign, kinetically inert oxidants in a diverse range of synthetically useful oxidative transformations. The recent surge of research in photoredox catalysis has largely been focused on redox-neutral and net reductive reactions. The limited examples of net oxidative transformations published to date have generally utilized either stoichiometric halocarbon oxidants,[4] which are not ideal from an environmental standpoint, or molecular oxygen,[5] which is a triplet quencher of many photoexcited molecules[6] and therefore can negatively impact the overall efficiency of a photoredox reaction. Thus, there exists a need for a more practical, general approach to the design of oxidative photoredox reactions.

2.2 Oxidative [3+2] Cycloaddition of Phenols

We became interested in studying phenol oxidation as a platform to explore this challenge. Phenols participate in a rich variety of oxidatively induced transformations,[7] and this broad class of reactions can produce a number of complex structures common in bioactive molecules. For example, 2,3-dihydrobenzofurans form the structural cores of many neolignans, resveratrol oligomers, and peptide-derived natural products (Figure 2.1).[8] The biogenic origin of these natural products presumably involves the oxidative [3+2] cycloaddition of phenols with alkenes. Several synthetic approaches to this transformation have been reported,[9] but they often suffer from low yields, limited scope, or a need for specialized equipment.[10,11] The most practical

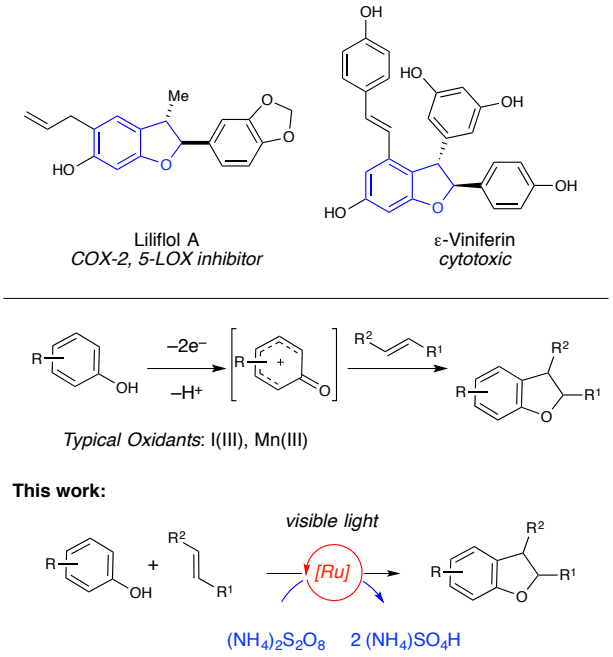

Figure 2.1: Bioactive dihydrobenzofuran-containing natural products and an oxidative [3+2] cycloaddition strategy for their synthesis.

methods for this reaction reported to date exploit hypervalent iodine(III) reagents,[12] which generate iodoarenes as stoichiometric byproducts. This section describes the development and application of an alternate photocatalytic protocol for [3+2] phenol–olefin cycloaddition that enables the use of ammonium persulfate as an inexpensive terminal oxidant with a benign bisulfate salt as the stoichiometric byproduct.[13]

Our initial investigations (Table 2.1) focused upon the photocatalytic reaction of *p*-methoxyphenol (**2.3**) with methylisoeugenol (**2.4**). A screen of oxidants in the presence of $Ru(bpy)_3^{2+}$ (**2.1**) revealed that while inorganic and organic hydroperoxides effected no reaction (entries 1–4), the desired cycloadduct is formed slowly upon irradiation in the presence of Oxone® (entry 5). This observation led us to examine other persulfates, and $K_2S_2O_8$ proved to be a more effective terminal oxidant (entry 6). Peroxydisulfates have long been known as oxidative quenchers of photoexcited ruthenium polypyridyl complexes,[14] but their use as terminal oxidants for synthetic photocatalytic reactions has been limited.[15] A brief screen of photocatalysts revealed

that the more strongly oxidizing $Ru(bpz)_3^{2+}$ (**2.2**) chromophore provided faster rates than $Ru(bpy)_3^{2+}$, affording good yield of the cycloadduct after 24 h. We also examined other commercially available peroxydisulfate salts and found that $(NH_4)_2S_2O_8$ provided optimal yields. Finally, control studies indicated that this reaction requires the presence of both catalyst and light (entries 10–11), validating the photocatalytic nature of this process.

The scope studies summarized in Figure 2.2 revealed that a broad range of coupling partners participate readily in this oxidative [3+2] cycloaddition. The reaction requires electron-rich phenols bearing alkoxy substituents at the 2- or 4-position, consistent with the need to

Table 2.1: Discovery and optimization of the photocatalytic oxidative [3+2] phenol–alkene cycloaddition

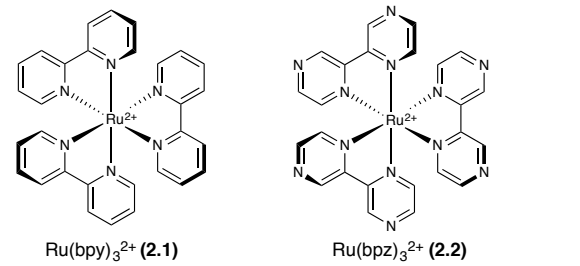

entry	catalyst	oxidant	% yield[a]
1	**2.1**$(PF_6)_2$	H_2O_2 (30% aq.)	0
2	**2.1**$(PF_6)_2$	UHP	0
3	**2.1**$(PF_6)_2$	*t*BuOOH	0
4	**2.1**$(PF_6)_2$	*m*-CPBA	0
5	**2.1**$(PF_6)_2$	oxone	7
6	**2.1**$(PF_6)_2$	$K_2S_2O_8$	20
7	**2.2**$(PF_6)_2$	$K_2S_2O_8$	75
8	**2.2**$(PF_6)_2$	$Na_2S_2O_8$	23
9	**2.2**$(PF_6)_2$	$(NH_4)_2S_2O_8$	78 (79)
10[b]	**2.2**$(PF_6)_2$	$(NH_4)_2S_2O_8$	0
11	-	$(NH_4)_2S_2O_8$	0

All reactions performed using 0.10 mmol phenol, 0.13 mmol styrene, .20 mmol oxidant (2 equiv.), and 0.005 mmol catalyst for 24 hrs. [a]Yield obtained by ^1H NMR spectroscopy using TMSPh as internal standard. Yields in parentheses indicate isolated yields after 30 h. [b]Reaction performed in the dark. UHP = Urea hydrogen preoxide adduct

stabilize the putative phenoxonium intermediate. Within this constraint, however, the scope proved to be quite broad. Benzyl (**2.7**) and allyl (**2.8**) ethers were tolerated easily without any trace of oxidative degradation, as were unprotected alcohols (**2.9**). Other substituents are also tolerated, including aryl substituents (**11**), bulky alkyl groups (**2.12**) and halides (**2.14**). Unsymmetrical 3-substituted phenols undergo clean, highly regioselective [3+2] cycloadditions (**2.15** and **2.16**), suggesting that the reaction is susceptible to steric control. Nevertheless, 3,5-disubstituted phenols do not suffer from significantly lower reactivity (**2.17**). Finally, condensed polycyclic phenols are also excellent substrates for this reaction (**2.18**). We also examined the scope of this reaction with respect to the styrene component. In line with the highly electrophilic nature of the phenoxonium intermediate, electron-rich styrenes bearing *para* or *ortho* alkoxy groups were the most reactive cycloaddition partners (**2.19**–**2.21**). However, styrenes lacking these activating groups still reacted smoothly, albeit with decreased efficiency (**2.22**–**2.24**). As

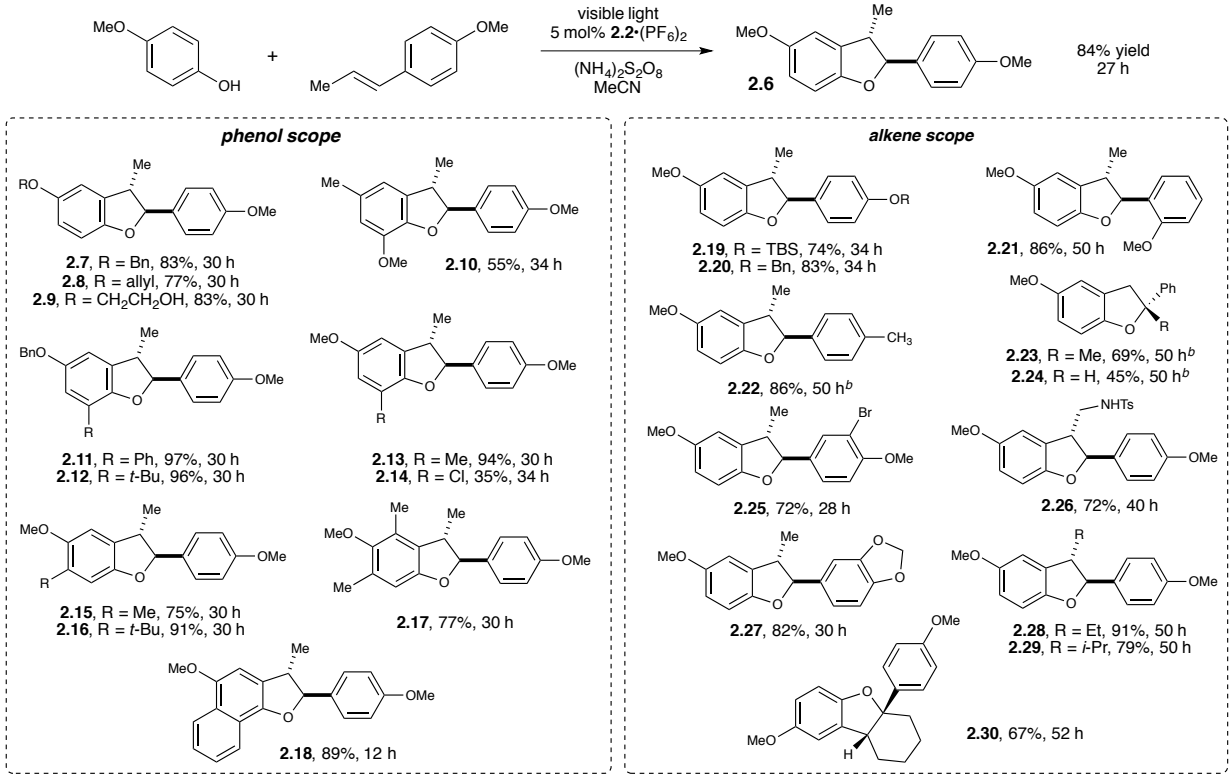

Figure 2.2: Scope and limitations of the photocatalytic oxidative [3+2] phenol–alkene cycloaddition

with the phenol component, a variety of potentially sensitive functional groups could be present on the alkene substrate, including halides (**2.25**), sulfonamides (**2.26**), and acetals (**2.27**). The reaction was also tolerant of steric bulk, both at the α and β positions of the styrene (**2.28**–**2.30**).

One of our principal motivations for this study is the existence of a multitude of bioactive natural products that feature dihydrobenzofuran scaffolds. Indeed, the broad scope of the oxidative [3+2] cycloaddition makes this photocatalytic process readily applicable to the efficient, modular assembly of natural products in this class (Figure 2.3). For instance, the dihydrobenzofuran **2.33**, isolated along with several similar benzofuranoid neolignans from *Piper aequale*,[16] presumably arises from an oxidative [3+2] phenol cycloaddition. This putative biosynthesis can be replicated using photocatalytic [3+2] cycloaddition of **2.31**, available in two high yielding steps from 4-methoxyphenol (**2.3**), with TBS-protected 4-propenylphenol **2.32**. Subsequent TBAF deprotection of the silyl group affords the natural product in 81% yield over these two steps. Similarly, the antiprotozoal neolignan **2.37**, isolated from *K. ixina*,[17] is available in three steps from cycloadduct **2.7**. Selective hydrogenolysis of the primary benzyl ether followed by treatment with triflic anhydride affords aryl triflate **2.36** in 93% yield over two steps. Efficient Suzuki coupling with *trans*-propenyl boronic acid produces **37** in 95% yield. Together, these

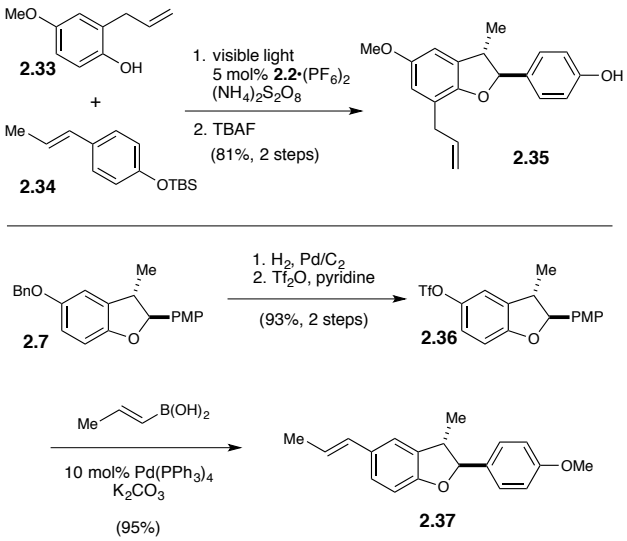

Figure 2.3: Total synthesis of neolignan natural products

syntheses demonstrate the applicability of this photocatalytic method to produce 2,3-dihydrobenzofurans, allowing facile access to this large family of bioactive natural products.

2.3 C–H Functionalization *via* Enolate Oxidation

The broad goal of these investigations is the development of a general strategy for performing net-oxidative transformations using photocatalytic single-electron transfer. Thus we began studies to extend the synthetic reach of the $Ru(bpz)_3^{2+}/S_2O_8^{2-}$ oxidation system that emerged as the optimal strategy for phenol oxidation. We focused particularly upon synthetically attractive known transformations whose state-of-the-art conditions are characterized by inefficient reactivity and suboptimal stoichiometric oxidants.

We elected to focus on enolate oxidation chemistry for our first experimental forays beyond phenol oxidation. A number of C–H functionalization reactions can be readily accessed through malonyl radicals (Figure 2.4).[18] While several routes to these intermediates via single-electron reduction of prefunctionalized β-ketoesters are known,[19,20] methods for direct oxidative

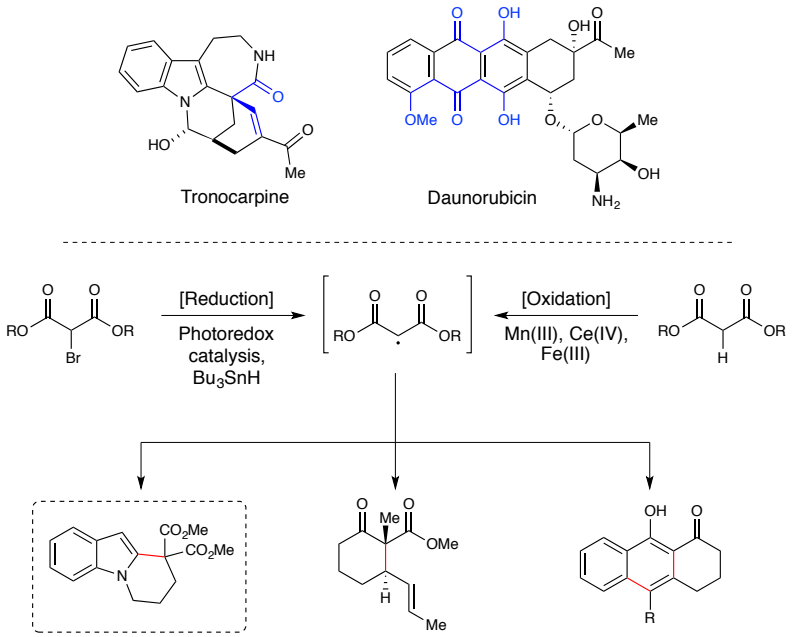

Figure 2.4: Natural product targets, and synthetic strategies to access malonyl radicals.

access to α-ketoradicals are limited. The current state-of-the-art strategies generally use superstoichiometric $Mn(OAc)_3$, or high loadings of $Mn(OAc)_3$ in conjunction with elevated temperatures (120 °C) and extended reaction times to accommodate inefficient catalytic turnover by dioxygen.[18,21] Anticipating that photocatalysis might offer an attractive platform for delivering these intermediates, and aware of the therapeutic and biological relevance of nitrogen heterocycles, we elected to test this hypothesis on the oxidative intramolecular radical cyclization of malonates to generate polycyclic indoles.[21,22]

Reaction optimization:

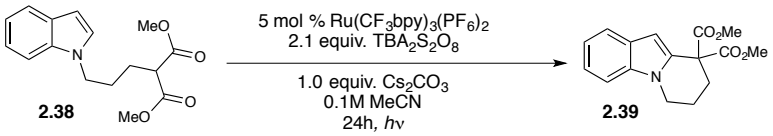

entry	catalyst	oxidant	additive	% yield[a]
1	**2.1**$(PF_6)_2$	$K_2S_2O_8/(NH_4)_2S_2O_8$	none	0%
2	**2.2**$(PF_6)_2$	$K_2S_2O_8/(NH_4)_2S_2O_8$	none	0%
3	**2.2**$(PF_6)_2$	$K_2S_2O_8$	K_2CO_3 (1 equiv.)	3%
4	**2.40**$(PF_6)_2$	$K_2S_2O_8$	K_2CO_3 (1 equiv.)	5%
5*	**2.40**$(PF_6)_2$	$K_2S_2O_8$	Cs_2CO_3 (1 equiv.)	17%
6	**2.40**$(PF_6)_2$	$(NBu_4)_2S_2O_8$	Cs_2CO_3 (1 equiv.)	30%
7	none	$(NBu_4)_2S_2O_8$	Cs_2CO_3 (1 equiv.)	0%

[a]all yields obtained by ^{1}H NMR using TMSPh as an internal standard.

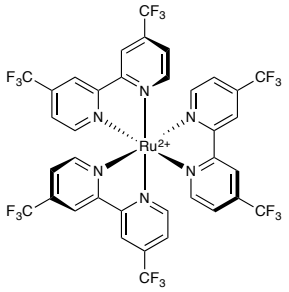

$Ru(CF_3bpy)_3^{2+}$ **(2.40)**

Product Instability:

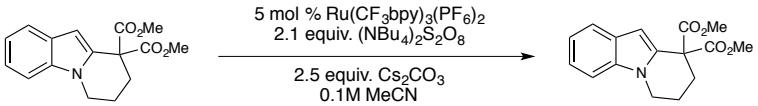

Figure 2.5: Optimization and product stability studies for the oxidative radical cyclization of malonate 2.38

We began our optimization with direct application of the optimized conditions for the oxidative [3+2] cycloaddition to the radical cyclization of malonate **2.38** using both $Ru(bpy)_3^{2+}$ and $Ru(bpz)_3^{2+}$ catalysts (Figure 5), but were disappointed to observe no formation of cyclization products. Hypothesizing that this negligible reactivity might be due to a low concentration of the electron-rich enolate, we investigated the use of carbonate bases in the presence of several catalysts including $Ru(bpz)_3^{2+}$ and $Ru(CF_3bpy)_3^{2+}$, and noted a low but detectable yield of cyclized

product **2.39**. Electing to pursue the strongly oxidizing fluorinated $Ru(CF_3bpy)_3^{2+}$ (**2.40**) catalyst over $Ru(bpz)_3^{2+}$ due to its enhanced stability toward basic additives, a subsequent screen of several bases suggested revealed that more weakly coordinating cations provided better reactivity. To enhance this effect, we moved to the more soluble and less coordinating tetrabutylammonium persulfate as the oxidant, and observed the highest yields to date. However, with these conditions in hand, we were unable to improve yields further, with product instability providing a substantial hurdle to development (Figure 2.5). Several classes of additives, including redox-active and inactive transition metals, redox mediators, and exotic bases were screened, but gave no improvement in yield (data not shown).

Preliminary Optimization

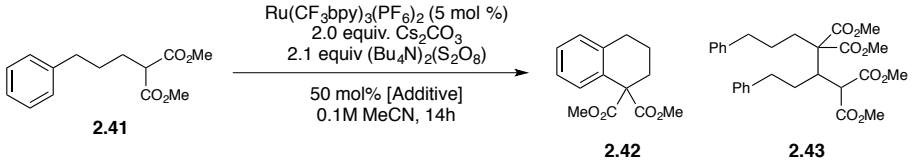

entry	Additive	Remaining **2.41**	Yield **2.42**	Yield **2.43**
1	none	55%	7%	0%
2	**$Fe(SO_4)$**	**59%**	**19%**	**< 2%**
3*	$Fe(SO_4)$	54%	0%	24%
4	**$Mn(SO_4)$**	**40%**	**18%**	**20%**
5*	$Mn(SO_4)$	50%	0%	20%
6	**$Cu(SO_4)$**	**50%**	**16%**	**5%**
7*	$Cu(SO_4)$	4%	0%	5%

[a]all yields obtained by ^1H NMR using TMSPh as an internal standard.
*Reaction performed without $Ru(CF_3bpy)_3(PF_6)_2$

Competing oxidation pathways

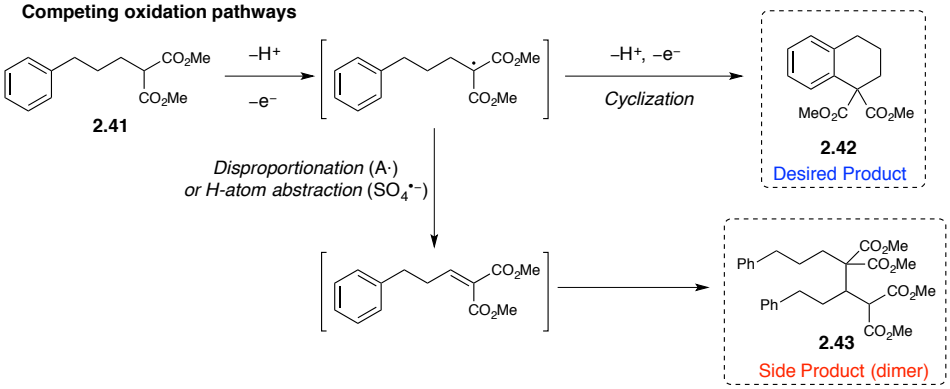

Figure 2.6: Optimization and competing oxidation pathways for the oxidative cyclization of aryl malonate 2.41

Having reached this roadblock, we began to examine several alternative substrate classes that we hypothesized would be both more stable to the strongly oxidizing reaction conditions, and were known to undergo radical cyclization chemistry.[23] As with the cyclization of indoyl malonate **2.38**, attempts to develop an analogous radical cyclization with alternative substrates also proved difficult (Figure 2.6). The cyclization of **2.41** in particular demonstrated the challenges intrinsic to these systems, as low reactivity is present under the optimized conditions for indole cyclization. Promising reactivity was observed in the presence of redox-active transition metal additives, however competing oxidation to the α,β-unsaturated ester affords undesired dimeric side products in many cases (Figure 2.6). Some selectivity has been observed with a number of additives, though the mechanism by which this is achieved has not been studied in detail. Additional work is needed to obtain synthetically useful results in this system.

2.4 Conclusion

In conclusion, we have developed a robust photocatalytic method for the oxidative [3+2] cycloaddition of phenols and electron-rich styrenes. Transition metal photoredox catalysis enables the use of ammonium persulfate as a terminal oxidant, which results in the formation of an innocuous and easily separated inorganic byproduct. Despite the challenges in generalizing the photocatalytic platform for performing synthetic oxidation chemistry, there remain several promising results that suggest potential avenues for further synthetic exploration. Mechanistic studies aimed at identifying the salient features of this catalytic system will be discussed in the following chapter.

2.5 Experimental

General Information: MeCN, THF and CH_2Cl_2 were purified by elution through alumina as described by Grubbs.[24] A 23 W (1200 lumens) SLI Lighting Mini-Lynx compact fluorescent

light bulb (CFL) was used for all photochemical reactions. Flash-column chromatography was performed with Silicycle 40–63Å silica (230–40 mesh). Styrene, α-methylstyrene, *trans*-methylisoeugenol (**4**), *trans*-anethole, 4-methoxyphenol (**3**), 4-(benzyloxy)phenol, 2-methoxy-4-methylphenol, 2-chloro-4-methoxyphenol, and 4-methoxynaphthalen-1-ol were purchased from Sigma Aldrich, then purified by either distillation or recrystallization prior to use. (*E*)-*N*-(3-(4-Methoxyphenyl)allyl)-4-methylbenzenesulfonamide, (*E*)-*tert*-butyldimethyl(4-(prop-1-en-1-yl)phenoxy)silane (**32**), and 4'-methoxy-2,3,4,5-tetrahydro-1,1'-biphenyl were synthesized according to previously reported methods.[25] All other styrene substrates were synthesized according to methods adapted from Lin *et al.*[26] 4-Methoxy-3-methylphenol,[27] 4-(allyloxy)phenol,[28] and 4-(2-hydroxyethoxy)phenol[29] were synthesized according to previously reported methods. The synthesis of *cis*-anethole was carried out according to procedures for hydroboration-protodeboration adapted from Nakamura *et al.*[30] (*E*)-Prop-1-en-1-ylboronic acid was synthesized according to methods adapted from Althaus *et al.*[31] 2,2'-Bipyrazine and $Ru(bpz)_3(PF_6)_2$ were synthesized according to previously reported methods.[26] $Ru(CF_3bpy)_3(PF_6)_2$ was synthesized according to methods derived from Farney *et al.*[32] Malonate **2.38** was synthesized according to reported methods.[22] Unless otherwise noted, all other compounds were purchased from Sigma Aldrich or Strem and used without further purification.

Diastereomer ratios for all compounds were determined by ^1H NMR analysis of unpurified reaction mixtures and assigned based on analogy to literature precedent. Relative stereochemistry for compound **30** was assigned by 1D NOESY (see below). ^1H and ^{13}C NMR data for all previously uncharacterized compounds were obtained using a Bruker AVANCE-400 spectrometer and are referenced to TMS (0.0 ppm) and $CDCl_3$ (77.0 ppm), respectively. IR spectral data were obtained using a Bruker Vector 22 spectrometer (thin film on NaCl). Melting points were obtained using a Mel-Temp II (Laboratory Devices, Inc., USA) melting point apparatus. Mass spectrometry was

performed with a Waters (Micromass) AutoSpec®. These facilities are funded by the NSF (CHE-9974839, CHE-9304546) and the University of Wisconsin.

Substrate Synthesis:

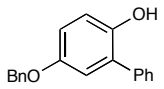

5-(Benzyloxy)-[1,1'-biphenyl]-2-ol: A suspension of [1,1'-biphenyl]-2,5-diol[33] (1.98 g, 10.6 mmol) and K_2CO_3 (1.59 g, 11.5 mmol) in MeCN (27 mL) was placed in a flame-dried 100 mL flask containing a magnetic stirbar. The flask was capped with a septum and flushed with N_2. Benzyl bromide (1.3 mL, 10.9 mmol) was then added to the stirring mixture *via* syringe. The flask was equipped with a reflux condenser and heated to reflux for 21 h. After cooling to room temperature, the flask contents were transferred to a separatory funnel with EtOAc and 1 M HCl. After separating, the aqueous layer was extracted once with EtOAc. The combined organic extracts were then washed with brine, dried over $MgSO_4$, filtered and concentrated *in vacuo*. The crude residue was purified by flash-column chromatography (15–50% EtOAc/Hexanes) to afford the desired product as a white solid (559 mg, 19% yield). All spectral data were in agreement with previously reported values.[34]

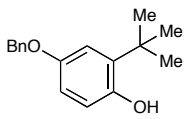

4-(Benzyloxy)-2-(*tert*-butyl)phenol: Into a flame-dried 100 mL round-bottom flask were weighed K_2CO_3 (838 mg, 6.07 mmol) and *tert*-butylhydroquinone (2.00 g, 12.05 mmol). A magnetic stirbar was then added, and the flask was capped with a septum and flushed with N_2. MeCN (30 mL) was then added *via* syringe. Upon stirring, a yellow suspension formed, to which benzyl bromide (1.45 mL, 12.19 mmol) was added *via* syringe. The flask was equipped with a reflux condenser (under N_2) and heated to reflux for 18 h. After cooling, the resulting reddish suspension was transferred into a separatory funnel with H_2O, and Et_2O. The layers were separated, and the aqueous layer was extracted twice more with

Et_2O. The combined organic extracts were then washed with brine, dried over $MgSO_4$, filtered, and concentrated *in vacuo*. The crude residue was purified by flash-column chromatography (7-10% EtOAc/Hexanes) to afford the desired product as a white solid. Mass: 1.44 g, (46% yield). IR (thin film) 3422 (br), 2957, 1506, 1422, 1239, 1079 cm^{-1}; ^1H NMR (400 MHz, $CDCl_3$) δ 7.50 – 7.28 (m, 5H), 6.94 (d, *J* = 2.9 Hz, 1H), 6.67 (dd, *J* = 8.5, 2.9 Hz, 1H), 6.58 (d, *J* = 8.5 Hz, 1H), 4.99 (s, 2H), 4.44 (s, 1H), 1.39 (s, 9H). ^{13}C NMR (101 MHz, $CDCl_3$) δ 152.72, 148.47, 137.64, 137.42, 128.60, 127.95, 127.69, 116.84, 115.28, 111.78, 70.83, 34.76, 29.55. HRMS (ESI) calculated for $[C_{17}H_{20}O_2]^+$ requires *m/z* 256.1457, found *m/z* 256.1466. Melting point: 90–92 °C.

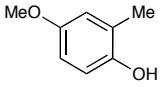

4-Methoxy-2-methylphenol: 4-Methoxyl-2-methylbenzaldehyde (900 μL, 6.63 mmol) was dissolved in dry dichloromethane (10 mL) in a 100 mL round-bottomed flask. After capping with a septum, the flask was flushed with N_2 and cooled to 0 °C in an ice bath. Solid *m*-CPBA (70-77% from Sigma Aldrich, 2.48 g, 10.06 mmol) was added in a single portion. The resulting suspension was stirred for 5 min at 0 °C and then allowed to warm to room temperature, where it was stirred for 3.5 h. The resulting suspension was transferred to a separatory funnel using dichloromethane, and the organic layers were washed twice with 10% aqueous Na_2SO_3. The organic layer was then washed with brine, dried over $MgSO_4$, filtered, and concentrated *in vacuo*. The crude residue was dissolved in 10:1 MeOH:6M HCl (11 mL), and stirred for 12 h under N_2 atmosphere. The orange solution was then concentrated *in vacuo*, and the crude oil was taken up in EtOAc and transferred to a separatory funnel. The organic layer was washed with sat. aq. $NaHCO_3$ (8x) to remove benzoic acid, then washed with brine, dried over $MgSO_4$, filtered, and concentrated *in vacuo*. The crude material was purified by flash-column chromatography (20% EtOAc/Hexanes) to afford the desired product as an off-white solid (725 mg, 79% yield). All spectral data were in agreement with previously reported values.[35]

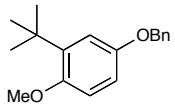

4-(Benzyloxy)-2-(tert-butyl)-1-methoxybenzene (S1): Into a flame-dried round-bottom flask equipped with a magnetic stirbar were weighed 4-(benzyloxy)-2-(*tert*-butyl)phenol (753 mg, 2.94 mmol) and K_2CO_3 (492 mg, 3.56 mmol). A magnetic stirbar and acetone (8.5 mL) were added to the flask, which was then capped with septum and flushed with N_2. To the stirring suspension was added methyl iodide (500 μL, 8.03 mmol) *via* syringe, and the mixture was heated to reflux. The reaction progress was monitored by TLC. Upon reacting full conversion (approx 144 h), the flask was cooled to room temperature, and the reaction was quenched with methanol, then H_2O. The flask contents were concentrated *in vacuo* in a fume hood, and the residue was washed into a separatory funnel with H_2O, and Et_2O. After separating, the organic layer was washed with 1 M NaOH (aq.) and brine, dried over $MgSO_4$, filtered, and concentrated *in vacuo*. The crude residue was purified by flash-column chromatography (10% EtOAc/Hexanes) to afford the desired product as a white solid (757 mg, 95% yield). IR (thin film) 2912, 1587, 1500, 1458, 1283, 1209 cm^{-1}; ^1H NMR (400 MHz, $CDCl_3$) δ 7.55 – 7.25 (m, 5H), 6.94 (d, *J* = 3.0 Hz, 1H), 6.65 (dd, *J* = 8.5, 3.0 Hz, 1H), 6.54 (d, *J* = 8.5 Hz, 1H), 4.98 (s, 2H), 4.54 (s, 1H), 1.38 (s, 9H). ^{13}C NMR (101 MHz, CDCl3) δ 153.11, 152.56, 139.90, 137.52, 128.59, 127.91, 127.65, 115.27, 112.26, 111.04, 70.65, 55.64, 34.99, 29.72. HRMS (EI) calculated for $[C_{18}H_{22}O_2]^+$ requires *m/z* 270.1615, found *m/z* 270.1614. Melting point: 39–40 °C

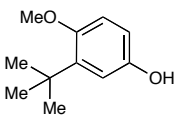

3-(*tert*-Butyl)-4-methoxyphenol: 4-(Benzyloxy)-2-(tert-butyl)-1-methoxybenzene (**S1**, 757 mg, 2.80 mmol) was weighed into a 25 mL round-bottomed flask containing a magnetic stirbar. Dichloromethane (15 mL) was added, and the mixture was stirred until all solids were dissolved. The flask was then capped with a septum and purged with N_2 for 5 min. Solid Pd/C (10 wt%, 239 mg, 0.225 mmol) was then added, and H_2 (introduced with balloon and syringe) was bubbled through the black suspension. After 15 min, the needle was removed from the suspension, and the hydrogen atmosphere was maintained with

rapid stirring for 18 h. The black suspension was filtered over Celite, and the filter cake was washed thoroughly with DCM. The eluent was concentrated in vacuo to afford clean product as a white solid (499 mg, 99% yield). IR (thin film) 3319 (br), 2870, 1500, 1286, 1086 cm^{-1}; ^1H NMR (400 MHz, $CDCl_3$) δ 6.88 – 6.68 (m, 2H), 6.63 (dd, *J* = 8.6, 3.1 Hz, 1H), 4.31 (s, 1H), 3.79 (s, 3H), 1.35 (s, 9H). ^{13}C NMR (101 MHz, $CDCl_3$) δ 152.87, 148.87, 139.96, 114.40, 112.79, 112.47, 55.73, 34.83, 29.64. HRMS (EI) calculated for $[C_{11}H_{16}O_2]^+$ requires *m/z* 180.1145, found *m/z* 180.1149. Melting point: 63–65 °C

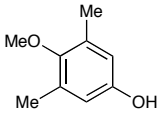

4-Methoxy-3,5-dimethylphenol: 4-Hydroxy-3,5-dimethylbenzaldehyde (996 mg, 6.63 mmol), and K_2CO_3 (1.10 g, 7.97 mg) were weighed into a flame-dried round-bottomed flask. A magnetic stirbar and acetone (8.5 mL) were added to the flask, which was then capped with septum and flushed with N_2. To this stirring suspension was added methyl iodide (600 μL, 9.64 mmol) dropwise *via* needle and syringe. The flask was then equipped with a reflux condenser under N_2, and heated to reflux for 96 h. After cooling to room temperature, methanol and H_2O were added to quench remaining methyl iodide, and the contents of the flask were concentrated *in vacuo* in a fume hood. The resulting residue was transferred to a separatory funnel using H_2O and Et_2O. After separating, the organic layer was washed with 1 M NaOH (aq.) and brine, dried over $MgSO_4$, filtered, and concentrated *in vacuo*. The crude residue was purified by flash-column chromatography (15% EtOAc/Hexanes) to afford 4-methoxy-3,5-dimethylbenzaldehyde as a white solid (507 mg, 47% yield) with spectral properties identical to those previously reported.[36] The isolated benzaldehyde (507 mg, 3.09 mmol) was subsequently dissolved in dichloromethane (4.6 mL) in a 25 mL round-bottomed flask, which was then capped with a septum, and flushed with N_2. After cooling to 0 °C in an ice bath, solid *m*-CPBA (70-77%, 1.06 g, 4.3 mmol) was added in a single portion. The resulting suspension was stirred for 5 min at 0 °C and then allowed to warm to room temperature, where

it was stirred for 2 h. The resulting suspension was transferred to a separatory funnel using dichloromethane and washed twice with 10% aqueous Na_2SO_3. The organic layer was then dried over $MgSO_4$, filtered and concentrated *in vacuo*. The crude residue was dissolved in 10:1 MeOH:6M HCl (11 mL), and stirred for 24 h under N_2. The orange solution that resulted was concentrated *in vacuo*, and the resulting residue was transferred to a separatory funnel with EtOAc. The organic layer was washed with sat. aq. $NaHCO_3$ (8x) to remove benzoic acid, then washed with brine, dried over $MgSO_4$, filtered, and concentrated *in vacuo*. The crude material was purified by flash-column chromatography (20% EtOAc/Hexanes) to afford the desired product as an off-white solid (378 mg, 82% yield). IR (thin film) 3390 (br), 2947, 1603, 1470, 1322, 1215 cm^{-1}; ^1H NMR (400 MHz, $CDCl_3$) δ 6.47 (s, 2H), 5.08 – 4.53 (s br, 1H), 3.67 (s, 3H), 2.23 (s, 6H). ^{13}C NMR (101 MHz, $CDCl_3$) δ 151.25, 150.69, 131.95, 115.03, 60.00, 16.16. HRMS (ESI) calculated for $[C_9H_{12}O_2]^+$ requires *m/z* 152.0832, found *m/z* 152.0833. Melting point: 87–89 °C

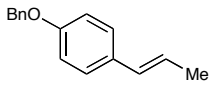

(*E*)-1-(Benzyloxy)-4-(prop-1-en-1-yl)benzene: Ethyltriphenylphosphonium iodide (9.67 g, 23.1 mmol) was weighed into a flame-dried flask containing a magnetic stirbar. The flask was capped with a rubber septum and placed under nitrogen. THF (100 mL) was added, and the flask was cooled to 0 °C. *n*-BuLi (15 mL of a 1.6M solution in hexanes, 24.0 mmol) was then added dropwise over 5 min by syringe, resulting in a red solution. After stirring for 30 minutes at 0 °C, 4-(benzyloxy)benzaldehyde (2.45 g, 11.5 mmol) in THF (10 mL) was added dropwise over 3 min. The flask was allowed to warm slowly to room temperature and stirred until TLC showed complete consumption of starting material. After quenching with dropwise addition of sat. aq. NH_4Cl, the resulting mixture was rinsed into a separatory funnel with water and Et_2O. The aqueous layer was extracted with Et_2O (2 x 30 mL). The combined organic layers were then washed with brine, dried over $MgSO_4$,

filtered, and concentrated *in vacuo*. The crude solid was purified by silica gel chromatography (5% EtOAc/Hexanes) to afford the title compound as a white solid. 2.55 g (98% yield, E:Z = 8:1). To improve the isomer ratio, the purified E/Z mixture was dissolved in benzene (110 mL) in a 250 mL round-bottomed flask, which was then purged with N_2. AIBN (135 mg, 0.82 mmol) and PhSH (200 μL, 1.95 mmol) were then added, and the reaction was heated under N_2 at reflux for 15 h. After cooling to room temperature, the solution was diluted with Et_2O (30 mL) and washed with sat. aq. $NaHCO_3$ (3 x 40 mL). The organic layer was then dried over $MgSO_4$ and concentrated *in vacuo*. The residue was purified by flash-column chromatography (hexanes) to afford the desired product as a single isomer (2.22 g, 87% yield). All spectral data were in agreement with previously reported values.[26]

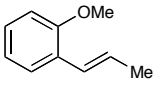

(*E*)-1-Methoxy-2-(prop-1-en-1-yl)benzene: Ethyltriphenylphosphonium bromide (12.46 g, 22.6 mmol) was weighed into a flame-dried flask containing a magnetic stirbar. The flask was capped with a rubber septum and placed under N_2. THF (40 mL) was then added, and the flask contents were stirred vigorously. Potassium *tert*-butoxide (3.55 g, 31.6 mmol) was added in three portions over 5 min, forming a red suspension. After stirring 30 minutes at room temperature, the flask was cooled to –78 °C (dry ice/acetone bath), and 2-methoxybenzaldehyde (2.04 g) in THF (10 mL) was added dropwise over 10 min. The flask was allowed to warm to room temperature, and the reaction was monitored by TLC. After stirring 40 h, the orange mixture was quenched *via* dropwise addition of sat. aq. NH_4Cl. The resulting suspension was diluted with water (10 mL) and transferred to a separatory funnel. The aqueous layer was extracted with EtOAc (3 x 50 mL). The combined organic extracts were dried over Na_2SO_4, filtered, and concentrated *in vacuo*. The crude oil was purified by silica gel chromatography (15% EtOAc/Hexanes) to afford the title compound as a colorless oil. 2.08 g (94% yield, E:Z = 1:2.5). To improve the isomer ratio, 2.08 g of the *E*/*Z* mixture was dissolved in

benzene (110 mL) in a 250 mL round-bottomed flask, which was purged with N_2. AIBN (236.4 mg, 1.44 mmol) and PhSH (145 μL, 1.32 mmol) were added to the solution, and the flask was equipped with a reflux condenser. The flask was then heated to reflux for 16 h under N_2. After cooling to room temperature, Et_2O (100 mL) was added, and the flask contents were transferred to a separatory funnel containing sat. aq. $NaHCO_3$. After separating, the organic layer was washed twice more with sat. aq. $NaHCO_3$ (2 x 20 mL). The organic layer was then dried over Na_2SO_4, and concentrated *in vacuo*. The crude residue was purified by flash-column chromatography (hexanes) to afford the desired product as a single isomer (1.80 g, 86% yield). All spectral data were in agreement with previously reported values.[37]

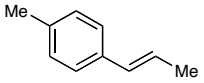

(*E*)-1-Methyl-4-(prop-1-en-1-yl)benzene: Ethyltriphenylphosphonium iodide (8.21 g, 20.0 mmol) was weighed into a flame-dried flask containing a magnetic stirbar. The flask was capped with a rubber septum and placed under nitrogen. THF (100 mL) was added, and the flask was cooled to 0 °C. *n*-BuLi (12.5 mL of a 1.6M solution in hexanes, 20.0 mmol) was then added dropwise over 5 min by syringe, resulting in a red solution. After stirring for 30 minutes at 0 °C, *p*-tolualdehyde (2.45 g, 10.2 mmol) in THF (10 mL) was added dropwise over 3 min. The flask was allowed to warm slowly to room temperature and stirred until TLC showed complete consumption of starting material (45 min). After quenching with dropwise addition of sat. aq. NH_4Cl, the resulting mixture was rinsed into a separatory funnel with water and Et_2O. The aqueous layer was extracted with EtOAc (3 x 50 mL). The combined organic layers were then washed with brine, dried over $MgSO_4$, filtered, and concentrated *in vacuo*. The crude solid was purified by silica gel chromatography (100% Hexanes) to afford the title compound as a colorless oil. 870 mg (65% yield, E:Z = 3:1). To improve the isomer ratio, the purified E/Z mixture was dissolved in benzene (50 mL) in a 100 mL round-bottomed flask, which was then purged with N_2. AIBN (107 mg, 0.65 mmol) and PhSH (70 μL, .64 mmol) were then added, and the reaction was

heated under N_2 at reflux for 15 h. After cooling to room temperature, the solution was diluted with Et_2O (30 mL) and washed with sat. aq. $NaHCO_3$ (3 x 40 mL). The organic layer was then dried over $MgSO_4$ and concentrated *in vacuo*. The residue was purified by flash-column chromatography (hexanes) to afford the desired product as a single isomer (520 mg, 60% yield). All spectral data were in agreement with previously reported values.[38]

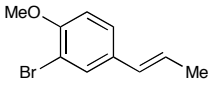

(*E*)-2-Bromo-1-methoxy-4-(prop-1-en-1-yl)benzene: Ethyltriphenylphosphonium bromide (5.94 g, 16.0 mmol) was weighed into a flame-dried flask containing a magnetic stirbar. The flask was capped with a rubber septum and placed under N_2. THF (25 mL) was then added, and the flask contents were stirred vigorously. Potassium *tert*-butoxide (1.79 g, 15 mmol) was added in three portions over 5 min, forming a red suspension. After stirring 30 minutes at room temperature, the flask was cooled to –78 °C (dry ice/acetone bath), and 3-bromo-4-methoxybenzaldehyde (2.15 g) in THF (5 mL) was added dropwise over 10 min. The flask was allowed to warm to room temperature, and the reaction was monitored by TLC. After stirring 14 h, the orange mixture was quenched *via* dropwise addition of sat. aq. NH_4Cl. The resulting suspension was diluted with water (10 mL) and transferred to a separatory funnel. The aqueous layer was extracted with EtOAc (3 x 30 mL). The combined organic extracts were dried over Na_2SO_4, filtered, and concentrated *in vacuo*. The crude oil was purified by silica gel chromatography (5% EtOAc/Hexanes) to afford the title compound as a colorless oil. 1.78 g (78% yield, E:Z = 1:1.5). To improve the isomer ratio, 1.40 g of the *E*/*Z* mixture was dissolved in benzene (20 mL) in a 100 mL round-bottomed flask, which was purged with N_2. AIBN (102 mg, 0.62 mmol) and PhSH (70 μL, 0.62 mmol) were added to the solution, and the flask was equipped with a reflux condenser. The flask was then heated to reflux for 16 h under N_2. After cooling to room temperature, Et_2O (20 mL) was added, and the flask contents were transferred to a separatory funnel containing sat. aq. $NaHCO_3$. After separating, the organic layer

was washed twice more with sat. aq. $NaHCO_3$ (2 x 20 mL). The organic layer was then dried over Na_2SO_4, and concentrated *in vacuo*. The crude residue was purified by flash-column chromatography (hexanes) to afford the desired product as a single isomer (0.919 g, 65% yield). IR (thin film) 2850, 2362, 1277, 1021 cm^{-1}; ^1H NMR (400 MHz, $CDCl_3$) δ 7.53 (d, *J* = 2.1 Hz, 1H), 7.20 (dd, *J* = 8.5, 2.2 Hz, 1H), 6.82 (d, *J* = 8.5 Hz, 1H), 6.27 (dd, *J* = 15.7, 1.7 Hz, 1H), 6.10 (dd, *J* = 15.7, 6.6 Hz, 1H), 3.88 (s, 3H), 1.86 (dd, *J* = 6.6, 1.6 Hz, 3H). ^{13}C NMR (101 MHz, $CDCl_3$) δ 154.69, 132.31, 130.47, 129.12, 125.95, 125.08, 111.87, 111.84, 56.31, 18.39. HRMS (ESI) calculated for $[C_{10}H_{11}BrO]^+$ requires *m/z* 225.9987, found *m/z* 225.9983.

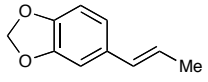

(*E*)-5-(Prop-1-en-1-yl)benzo[*d*][1,3]dioxole: Ethyltriphenylphosphonium iodide (4.10 g, 10.0 mmol) was weighed into a flame-dried flask containing a magnetic stirbar. The flask was capped with a rubber septum and placed under nitrogen. THF (50 mL) was added, and the flask was cooled to 0 °C. *n*-BuLi (7.0 mL of a 1.6M solution in hexanes, 9.8 mmol) was then added dropwise over 5 min by syringe, resulting in a red solution. After stirring for 30 minutes at 0 °C, piperonal (765 mg, 5.03 mmol) in THF (5 mL) was added dropwise over 3 min. The flask was allowed to warm slowly to room temperature and stirred until TLC showed complete consumption of starting material (30 min). After quenching with dropwise addition of sat. aq. NH_4Cl, the resulting mixture was rinsed into a separatory funnel with water and EtOAc. The aqueous layer was extracted with EtOAc (2 x 30 mL). The combined organic layers were then washed with brine, dried over $MgSO_4$, filtered, and concentrated *in vacuo*. The crude solid was purified by silica gel chromatography (20% EtOAc/Hexanes) to afford the title compound as a white solid. 740 mg (90% yield, E:Z = 4:1). To improve the isomer ratio, the purified E/Z mixture was dissolved in benzene (50 mL) in a 100 mL round-bottomed flask, which was then purged with N_2. AIBN (83 mg, 0.51 mmol) and PhSH (55 μL, 0.50 mmol) were then added, and the reaction was heated under N_2 at reflux for 18 h. After

cooling to room temperature, the solution was diluted with Et_2O (30 mL) and washed with sat. aq. $NaHCO_3$ (3 x 40 mL). The organic layer was then dried over $MgSO_4$ and concentrated *in vacuo*. The residue was purified by flash-column chromatography (5% EtOAc/Hexanes) to afford the desired product as a single isomer (516 mg, 75% yield). All spectral data were in agreement with previously reported values.[39]

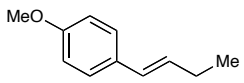

(*E*)-1-(But-1-en-1-yl)-4-methoxybenzene: (4-Methoxybenzyl)triphenylphosphonium bromide[40] (4.63 g, 10.0 mmol) was weighed into a flame-dried flask containing a magnetic stirbar. The flask was capped with a rubber septum and purged with N_2. THF (50 mL) was added, and the flask was cooled to 0 °C in an ice bath. *n*-BuLi (7.2 mL of a 1.6M solution in hexanes, 10.1 mmol) was added dropwise over 4 minutes, forming a red solution. After stirring for 30 minutes at 0 °C, propanal (350 μL, 4.85 mmol) was added dropwise over 3 minutes. The flask was allowed to warm slowly to room temperature, and the reaction was monitored by TLC. Upon complete consumption of starting material (1.5 h), the mixture was the quenched by dropwise addition of sat. aq. NH_4Cl. The resulting suspension was rinsed into a separatory funnel with water and EtOAc. The aqueous layer was extracted with EtOAc (3 x 30 mL). The combined organic layers were then washed with brine, dried over $MgSO_4$, filtered, and concentrated *in vacuo*. The crude solid was purified by silica gel chromatography (15–20% EtOAc/Hexanes) to afford the title compound as a white solid. Mass: 0.740 g (90% yield, E:Z = 1.8:1). To improve the isomer ratio, the purified *E*/*Z* mixture was dissolved in benzene (40 mL) in a 100 mL round-bottomed flask containing a magnetic stirbar. The flask was capped with a septum and purged with nitrogen. AIBN (72 mg, 0.44 mmol) and PhSH (45 μL, 0.44 mmol) were then added, and the flask was equipped with a reflux condenser under N_2. The flask was then heated at reflux for 12 h. After cooling to room temperature, the solution was diluted with Et_2O (20 mL), and then transferred into a separatory funnel. A solution

of sat. aq. $NaHCO_3$ was added, and the layers were separated. The aqueous layer was extracted with Et_2O (3 x 20 mL), and then the combined organics were washed with brine, dried over $MgSO_4$, and concentrated *in vacuo*. The crude residue was purified by flash-column chromatography (1–10% EtOAc/Hexanes) to afford the desired product as a single isomer. Mass: 0.449 g, (63% yield). IR (thin film) 1834, 1603, 1490, 1244, 1202, 1031 cm^{-1}; ^1H NMR (400 MHz, $CDCl_3$) δ 7.32 – 7.22 (m, 2H), 6.91 – 6.73 (m, 2H), 6.32 (dt, *J* = 16.0, 1.5 Hz, 1H), 6.21 – 5.97 (m, 1H), 3.78 (d, *J* = 0.8 Hz, 3H), 2.20 (dtd, *J* = 9.0, 7.5, 6.1 Hz, 2H), 1.07 (td, *J* = 7.5, 1.6 Hz, 3H). ^{13}C NMR (101 MHz, $CDCl_3$) δ 158.62, 130.81, 130.54, 128.14, 126.99, 113.92, 55.30, 26.07, 13.84. HRMS (ESI) calculated for $[C_{11}H_{14}O]^+$ requires *m/z* 162.1040, found *m/z* 162.1033.

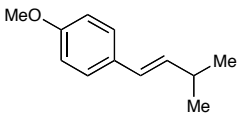

(*E*)-1-Methoxy-4-(3-methylbut-1-en-1-yl)benzene: (4-Methoxybenzyl)triphenylphosphonium bromide[40] (2.07 g, 4.5 mmol) was weighed into a flame-dried flask containing a magnetic stirbar. The flask was capped with a rubber septum and purged with N_2. THF (50 mL) was added, and the flask was cooled to 0 °C in an ice bath. *n*-BuLi (3.70 mL of a 1.6M solution in hexanes, 5.2 mmol) was added dropwise over 4 minutes, forming a red solution. After stirring for 30 minutes at 0 °C, isobutyraldehyde (350 μL, 3.83 mmol) was added dropwise over 3 minutes. The flask was allowed to warm slowly to room temperature, and the reaction was monitored by TLC. Upon complete consumption of starting material (12 h), the mixture was the quenched by dropwise addition of sat. aq. NH_4Cl. The resulting suspension was rinsed into a separatory funnel with water and EtOAc. The aqueous layer was extracted with EtOAc (3 x 30 mL). The combined organic layers were then washed with brine, dried over $MgSO_4$, filtered, and concentrated *in vacuo*. The crude solid was purified by silica gel chromatography (15% EtOAc/Hexanes) to afford the title compound as a colorless oil. Mass: 643 mg (95% yield, E:Z = 2:1). To improve the isomer ratio, the purified *E*/*Z* mixture was dissolved in benzene (30 mL) in a 100 mL round-bottomed flask containing a magnetic stirbar.

The flask was capped with a septum and purged with nitrogen. AIBN (66 mg, 0.40 mmol) and PhSH (40 μL, 0.39 mmol) were then added, and the flask was equipped with a reflux condenser under N_2. The flask was then heated at reflux for 14 h. After cooling to room temperature, the solution was diluted with Et_2O (20 mL), and then transferred into a separatory funnel. A solution of sat. aq. $NaHCO_3$ was added, and the layers were separated. The aqueous layer was extracted with Et_2O (3 x 20 mL), and then the combined organics were washed with brine, dried over $MgSO_4$, and concentrated *in vacuo*. The crude residue was purified by flash-column chromatography (3% EtOAc/Hexanes) to afford the desired product as a single isomer (568 mg, 88% yield. IR (thin film) 2964, 2362, 1606, 1509, 1247, 1176 cm^{-1}; ^1H NMR (400 MHz, $CDCl_3$) δ 7.44 – 7.16 (m, 2H), 6.98 – 6.70 (m, 2H), 6.42 – 6.16 (m, 1H), 6.05 (dd, *J* = 15.9, 6.8 Hz, 1H), 3.80 (s, 3H), 2.60 – 2.28 (m, 1H), 1.08 (d, *J* = 6.7 Hz, 6H). ^{13}C NMR (101 MHz, $CDCl_3$) δ 158.61, 135.97, 130.79, 127.02, 126.14, 113.91, 55.31, 31.50, 22.59. HRMS (EI) calculated for $[C_{12}H_{16}O]^+$ requires *m/z* 176.1196, found *m/z* 176.1191.

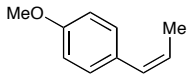

(*Z*)-1-Methoxy-4-(prop-1-en-1-yl)benzene: A solution of cyclohexene (1.42 mL, 14.0 mmol) in THF (6.5 mL) was placed in a flame-dried 100 mL three-necked flask under N_2 atmosphere. The flask was cooled to 0 °C, and a 2.0 M solution of $BH_3{\cdot}SMe_2$ in toluene (3.50 mL, 7.00 mmol) was added dropwise over 5 min *via* syringe. The resulting solution was stirred vigorously, and a white precipitate was observed after ~10 min. The suspension was stirred for 1 h at 0 °C. A solution of 1-methoxy-4-(prop-1-yn-1-yl)benzene[41] (930 mg, 6.37 mmol) in THF (8.5 mL) was added dropwise over 5 min at 0 °C. The resulting white suspension was stirred for 1 h at 0 °C, then for 2 h at room temperature. The flask was then cooled to 0 °C, and glacial acetic acid (1.3 mL) was added *via* syringe. The solution was stirred for 1 h at 0 °C, then an additional 2 h at room temperature. The resulting pale yellow solution was transferred to a separatory funnel with H_2O, sat. aq. $NaHCO_3$, and Et_2O. The layers were

separated, and aqueous phase was extracted with Et_2O. The combined organics were then washed with brine, dried over $MgSO_4$, filtered, and concentrated *in vacuo*. The crude residue was purified by flash-column chromatography (3% EtOAc/Hexanes) to afford the desired product as a single isomer. Mass: 800.8 mg, (85% yield). All spectral data were in agreement with previously reported values.[42]

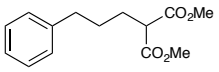

2.41

Compound 2.41: NaH (60% dispersion in mineral oil, 1.161g, 4.42 equiv) was weighed into a flame-dried 250 mL roundbottom flask and suspended in DMF (100 mL). Dimethyl malonate (3.4 mL, 4.53 equiv.) was added dropwise over 5 min. with evolution of hydrogen gas observed. The resulting mixture was stirred at room temperature for 30 min. under a nitrogen atmosphere. In a separate vessel, 1-bromo-3-phenylpropane (1.00 mL, 6.75 mmol, 1 equiv) was dissolved in DMF (20 mL), then added to the stirring suspension of dimethyl malonate and NaH by cannula. The resulting solution was stirred for 18 h at room temperature, then quenched with H_2O. The mixture was transferred to a separatory funnel with Et_2O and H_2O, and the layers separated. The aqueous layer was extracted twice more with Et_2O, then the combined organic layers were washed with H_2O (x2), then brine, dried over $MgSO_4$, filtered, and concentrated *in vacuo*. The crude oil was purified by flash-column chromatography (60% DCM/Hexanes to 90% DCM/Hexanes) to afford the desired product as a clear oil (890.9 mg, 54% yield). Spectral properties mathc those previously reported.[43]

Photocyclization Reactions:

General Procedure: In an oven-dried Schlenk flask were placed the appropriate phenol (1.0 equiv.) and styrene (1.3–2 equiv.) coupling partners, along with $Ru(bpz)_3(PF_6)_2$ (**2**, 5 mol %), and

ammonium peroxydisulfate (2.1 equiv.). A magnetic stirbar was added, and MeCN (1–4 mL) was introduced *via* syringe. The flask was sealed with a glass stopper and degassed by three freeze-pump-thaw cycles in a dry-ice/acetone bath. After the final thaw, the flask was backfilled with nitrogen, and stirred evenly under irradiation with a 23 W (1200 lumens) SLI Mini-Lynx compact fluorescent light bulb (placed 3–4 inches from the reaction flask) for the duration of the reaction. During irradiation, the reaction was sonicated periodically (once in the first 2–6 hours, and once every 6–12 hours afterwards), to maintain an even suspension. After completion, the reaction was diluted with EtOAc (5–10 mL), and eluted through a plug of silica using EtOAc. After concentrating *in vacuo*, the crude product was purified by flash-column chromatography.

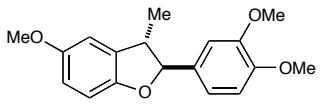

Compound 2.5. *Experiment 1*: Prepared according to the general procedure using 49 mg (0.39 mmol) of 4-methoxyphenol, 92 mg (0.51 mmol) of *trans*-methylisoeugenol (**4**), 186 mg (0.82 mmol) of ammonium persulfate and 17.1 mg (0.02 mmol) of $Ru(bpz)_3(PF_6)_2$. The reaction was irradiated for 27 h. The crude residue was purified by flash-column chromatography using 10% EtOAc/Hexanes to afford 92 mg (0.31 mmol, 78% yield) of the desired cycloadduct as a colorless oil. *Experiment 2*: Prepared according to the general procedure using 49 mg (0.40 mmol) of 4-methoxyphenol, 92 mg (0.52 mmol) of *trans*-methylisoeugenol (**4**), 184 mg (0.92 mmol) of ammonium persulfate and 16.6 mg (0.02 mmol) of $Ru(bpz)_3(PF_6)_2$. The reaction was irradiated for 27 h. The crude residue was purified by flash-column chromatography using 10% EtOAc/Hexanes to afford 92 mg (0.31 mmol, 77% yield) of the desired cycloadduct as a colorless oil. All spectral data were in agreement with previously reported values.[10b]

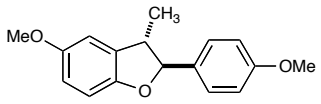

Compound 2.6. *Experiment 1*: Prepared according to the general procedure using 49 mg (0.39 mmol) of 4-methoxyphenol, 75 mg (0.51

mmol) of *trans*-anethole, 209 mg (0.92 mmol) of ammonium persulfate and 15.4 mg (0.02 mmol) of $Ru(bpz)_3(PF_6)_2$. The reaction was irradiated for 27 h. The crude residue was purified by flash-column chromatography using 7% EtOAc/Hexanes to afford 87 mg (0.32 mmol, 82% yield) of the desired cycloadduct as a colorless oil. *Experiment 2*: Prepared according to the general procedure using 50 mg (0.40 mmol) of 4-methoxyphenol, 77 mg (0.52 mmol) of *trans*-anethole, 209 mg (0.92 mmol) of ammonium persulfate and 17.1 mg (0.02 mmol) of $Ru(bpz)_3(PF_6)_2$. The reaction was irradiated for 27 h. The crude residue was purified by flash-column chromatography using 7% EtOAc/Hexanes to afford 95 mg (0.35 mmol, 88% yield) of the desired cycloadduct as a colorless oil. *Experiment 3*: Prepared according to the general procedure using 51 mg (0.41 mmol) of 4-methoxyphenol, 88 mg (0.51 mmol) of *cis*-anethole, 191 mg (0.84 mmol) of ammonium persulfate and 17.6 mg (0.02 mmol) of $Ru(bpz)_3(PF_6)_2$. The reaction was irradiated for 30 h. The crude residue was purified by flash-column chromatography using 7% EtOAc/Hexanes to afford 76 mg (0.28 mmol, 69% yield) of the desired cycloadduct as a colorless oil. *Experiment 4*: Prepared according to the general procedure using 50 mg (0.41 mmol) of 4-methoxyphenol, 86 mg (0.58 mmol) of *cis*-anethole, 189 mg (0.83 mmol) of ammonium persulfate and 17.9 mg (0.02 mmol) of $Ru(bpz)_3(PF_6)_2$. The reaction was irradiated for 30 h. The crude residue was purified by flash-column chromatography using 7% EtOAc/Hexanes to afford 71 mg (0.26 mmol, 64% yield) of the desired cycloadduct as a colorless oil. IR (thin film) 2965, 2837, 1519, 1266 cm^{-1}; ^1H NMR (400 MHz, $CDCl_3$) δ 7.42 – 7.25 (m, 2H), 6.95 – 6.84 (m, 2H), 6.80 – 6.55 (m, 3H), 5.06 (d, J = 9.1 Hz, 1H), 3.78 (s, 3H), 3.76 (s, 3H), 3.47 – 3.24 (m, 1H), 1.36 (d, J = 6.8 Hz, 3H). ^{13}C NMR (101 MHz, $CDCl_3$) δ 159.68, 154.46, 153.32, 133.18, 132.74, 127.71, 114.04, 112.90, 110.13, 109.39, 92.64, 56.06, 55.34, 45.74, 17.62. HRMS (EI) calculated for $[C_{17}H_{18}O_3+NH_4]^+$ requires m/z 288.1595, found m/z 288.1597.

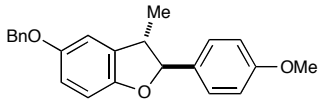

Compound 2.7. *Experiment 1*: Prepared according to the general procedure using 82 mg (0.41 mmol) of 4-benzyloxyphenol, 79 mg (0.53 mmol) of *trans*-anethole, 196 mg (0.86 mmol) of ammonium persulfate and 17.5 mg (0.02 mmol) of $Ru(bpz)_3(PF_6)_2$. The reaction was irradiated for 30 h. The crude residue was purified by flash-column chromatography using 7% EtOAc/Hexanes to afford 108 mg (0.31 mmol, 76% yield) of the desired cycloadduct as a colorless oil. *Experiment 2*: Prepared according to the general procedure using 82 mg (0.41 mmol) of 4-benzyloxyphenol, 80 mg (0.54 mmol) of *trans*-anethole, 197 mg (0.85 mmol) of ammonium persulfate and 17.3 mg (0.02 mmol) of $Ru(bpz)_3(PF_6)_2$. The reaction was irradiated for 30 h. The crude residue was purified by flash-column chromatography using 7% EtOAc/Hexanes to afford 109 mg (0.32 mmol, 77% yield) of the desired cycloadduct as a colorless oil. IR (thin film) 2964, 1613, 1516, 1273, 1199, 1034 cm^{-1}; ^1H NMR (400 MHz, $CDCl_3$) δ 7.52 – 7.25 (m, 7H), 6.96 – 6.83 (m, 2H), 6.83 – 6.66 (m, 3H), 5.06 (d, *J* = 9.1 Hz, 1H), 5.00 (s, 2H), 3.78 (s, 3H), 3.40 (p, 6.8 Hz, 1H), 1.35 (d, *J* = 6.8 Hz, 3H). ^{13}C NMR (101 MHz, $CDCl_3$) δ 159.70, 153.68, 153.57, 137.45, 133.23, 132.71, 128.61, 127.95, 127.73, 127.60, 114.09, 114.06, 111.37, 109.41, 92.69, 71.12, 55.37, 45.73, 17.63. HRMS (ESI) calculated for $[C_{23}H_{22}O_3H]^+$ requires *m/z* 347.1642, found *m/z* 347.1627. Melting point: 87–88 °C

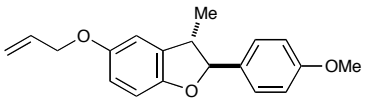

Compound 2.8: *Experiment 1*: Prepared according to the general procedure using 61 mg (0.41 mmol) of 4-allyloxyphenol, 80 mg (0.54 mmol) of *trans*-anethole, 190 mg (0.83 mmol) of ammonium persulfate and 17.8 mg (0.02 mmol) of $Ru(bpz)_3(PF_6)_2$. The reaction was irradiated for 30 h. The crude residue was purified by flash-column chromatography using 7% EtOAc/Hexanes to afford 94 mg (0.32 mmol, 77% yield) of the desired cycloadduct as a colorless oil. *Experiment 2*: Prepared according to the general procedure using 60 mg (0.40 mmol) of 4-allyloxyphenol, 82 mg (0.55 mmol) of

trans-anethole, 186 mg (0.82 mmol) of ammonium persulfate and 17.5 mg (0.02 mmol) of $Ru(bpz)_3(PF_6)_2$. The reaction was irradiated for 30 h. The crude residue was purified by flash-column chromatography using 7% EtOAc/Hexanes to afford 91 mg (0.31 mmol, 76% yield) of the desired cycloadduct as a colorless oil. IR (thin film) 2960, 1613, 1247, 1199, 1034 cm^{-1}; ^1H NMR (400 MHz, $CDCl_3$) δ 7.41 – 7.30 (m, 2H), 7.00 – 6.86 (m, 2H), 6.81 – 6.67 (m, 3H), 6.06 (ddt, *J* = 17.3, 10.6, 5.3 Hz,1H), 5.41 (dt, *J* = 17.3, 1.7 Hz, 1H), 5.27 (dq, *J* = 10.5, 1.4 Hz, 1H), 5.07 (d, *J* = 9.0 Hz, 1H), 4.49 (dt, *J* = 5.3, 1.6 Hz, 2H), 3.81 (s, 4H), 3.48 – 3.31 (m, 1H), 1.37 (d, *J* = 6.8, 3H). ^{13}C NMR (101 MHz, $CDCl_3$) δ 159.65, 153.44, 153.40, 133.73, 133.12, 132.68, 127.67, 117.46, 114.01, 113.99, 111.19, 109.32, 92.63, 69.93, 55.34, 45.67, 17.57. HRMS (EI) calculated for $[C_{19}H_{20}O_3]^+$ requires *m/z* 296.1407, found *m/z* 196.1402.

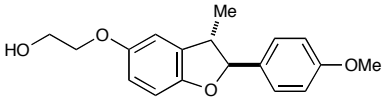

Compound 2.9. *Experiment 1*: Prepared according to the general procedure using 62 mg (0.40 mmol) of 4-(2-hydroxyethoxy)phenol, 80 mg (0.54 mmol) of *trans*-anethole, 191 mg (0.84 mmol) of ammonium persulfate and 17.7 mg (0.02 mmol) of $Ru(bpz)_3(PF_6)_2$. The reaction was irradiated for 30 h. The crude residue was purified by flash-column chromatography using 50% EtOAc/Hexanes to afford 84 mg (0.28 mmol, 70% yield) of the desired cycloadduct as a colorless oil. *Experiment 2*: Prepared according to the general procedure using 62 mg (0.40 mmol) of 4-methoxy-2-methylphenol, 80 mg (0.54 mmol) of *trans*-anethole, 190 mg (0.83 mmol) of ammonium persulfate and 17.2 mg (0.02 mmol) of $Ru(bpz)_3(PF_6)_2$. The reaction was irradiated for 30 h. The crude residue was purified by flash-column chromatography using 50% EtOAc/Hexanes to afford 83 mg (0.28 mmol, 69% yield) of the desired cycloadduct as a colorless oil. IR (thin film) 3419 (br), 2068, 1512, 1459, 1180 cm^{-1}; ^1H NMR (400 MHz, $CDCl_3$) δ 7.46 – 7.29 (m, 2H), 6.97 – 6.81 (m, 2H), 6.81 – 6.63 (m, 3H), 5.07 (d, *J* = 9.1 Hz, 1H), 4.09 – 3.97 (m, 2H), 3.92 (t, *J* = 4.9 Hz, 2H), 3.79 (s, 3H), 3.49 – 3.30 (m, 1H), 2.39 (s, 1H), 1.36 (d, *J* = 6.8 Hz, 3H).

^{13}C NMR (101 MHz, $CDCl_3$) δ 159.67, 153.64, 153.41, 133.25, 132.63, 127.68, 114.05, 113.99, 111.11, 109.44, 92.66, 70.37, 61.60, 55.35, 45.66, 17.61. HRMS (EI) calculated for $[C_{18}H_{20}O_4]^+$ requires *m/z* 300.1357, found *m/z* 300.1353.

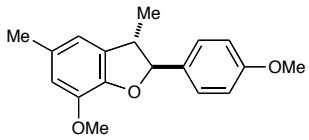

Compound 2.10. *Experiment 1*: Prepared according to the general procedure using 55 mg (0.40 mmol) of 2-methoxy-4-methylphenol, 78 mg (0.53 mmol) of *trans*-anethole, 194 mg (0.85 mmol) of ammonium persulfate and 17.2 mg (0.02 mmol) of $Ru(bpz)_3(PF_6)_2$. The reaction was irradiated for 34 h. The crude residue was purified by flash-column chromatography using 7–10% EtOAc/Hexanes to afford 59 mg (0.21 mmol, 52% yield) of the desired cycloadduct as a colorless oil. *Experiment 2:* Prepared according to the general procedure using 56 mg (0.41 mmol) of 2-methoxy-4-methylphenol, 80 mg (0.54 mmol) of *trans*-anethole, 196 mg (0.86 mmol) of ammonium persulfate and 17.3 mg (0.02 mmol) of $Ru(bpz)_3(PF_6)_2$. The reaction was irradiated for 34 h. The crude residue was purified by flash-column chromatography using 7% EtOAc/Hexanes to afford 66 mg (0.23 mmol, 58% yield) of the desired cycloadduct as a colorless oil. IR (thin film) 2362, 1496, 1458, 1328, 1251, 1034 cm^{-1}; ^{1}H NMR (400 MHz, $CDCl_3$) δ 7.43 – 7.28 (m, 2H), 6.98 – 6.68 (m, 2H), 6.61 (s, 1H), 6.58 (s, 1H), 5.11 (d, *J* = 9.2 Hz, 1H), 3.86 (s, 3H), 3.79 (s, 3H), 3.50 – 3.34 (m, 1H), 2.32 (s, 3H), 1.36 (d, *J* = 6.8 Hz, 3H). ^{13}C NMR (101 MHz, $CDCl_3$) δ 159.61, 145.24, 143.87, 133.06, 132.62, 131.03, 127.91, 116.13, 113.87, 112.32, 93.16, 55.98, 55.31, 45.83, 21.35, 17.79. HRMS (ESI) calculated for $[C_{18}H_{20}O_3H]^+$ requires *m/z* 285.1486, found *m/z* 285.1482.

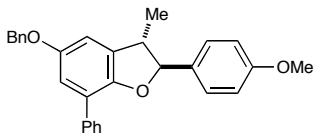

Compound 2.11 *Experiment 1*: Prepared according to the general procedure using 110 mg (0.40 mmol) of 5-(benzyloxy)-[1,1'-biphenyl]-2-ol, 78 mg (0.52 mmol) of *trans*-anethole, 188 mg (0.82 mmol) of ammonium persulfate and 17.1 mg (0.02 mmol) of $Ru(bpz)_3(PF_6)_2$. The reaction was irradiated

for 30 h. The crude residue was purified by flash-column chromatography using 7% EtOAc/Hexanes to afford 159.8 mg (0.378 mmol, 95% yield) of the desired cycloadduct as a white crystalline solid. *Experiment 2*: Prepared according to the general procedure using 111 mg (0.40 mmol) of 5-(benzyloxy)-[1,1'-biphenyl]-2-ol, 83 mg (0.56 mmol) of *trans*-anethole, 194 mg (0.85 mmol) of ammonium persulfate and 17.6 mg (0.02 mmol) of $Ru(bpz)_3(PF_6)_2$. The reaction was irradiated for 30 h. The crude residue was purified by flash-column chromatography using 7% EtOAc/Hexanes to afford 164.0 mg (0.388 mmol, 97% yield) of the desired cycloadduct as a white crystalline solid. IR (thin film) 2362, 1516, 1254, 1176 cm^{-1}; ^1H NMR (400 MHz, $CDCl_3$) δ 7.77 – 7.64 (m, 2H), 7.48 – 7.40 (m, 2H), 7.40 – 7.17 (m, 8H), 7.00 (dd, *J* = 2.7, 0.9 Hz, 1H), 6.95 – 6.83 (m, 2H), 6.77 (dd, *J* = 2.6, 1.2 Hz, 1H), 5.10 (d, *J* = 9.1 Hz, 1H), 5.04 (s, 2H), 3.76 (s, 3H), 3.47 – 3.32 (m, 1H), 1.37 (d, *J* = 6.8 Hz, 3H). ^{13}C NMR (101 MHz, $CDCl_3$) δ 159.66, 154.02, 150.90, 137.44, 137.17, 134.14, 133.08, 128.68, 128.50, 128.47, 128.04, 127.70, 127.27, 123.36, 114.05, 113.90, 110.48, 92.50, 71.20, 55.38, 45.92, 17.79 (One peak missing due to accidental equivalence). HRMS (EI) calculated for $[C_{29}H_{26}O_3]^+$ requires *m/z* 422.1877, found *m/z* 422.1886. Melting point: 113–114 °C

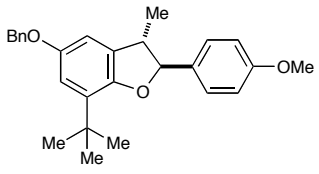

Compound 2.12 *Experiment 1*: Prepared according to the general procedure using 104 mg (0.41 mmol) of 4-(benzyloxy)-2-(tert-butyl)-1-methoxybenzene, 82 mg (0.55 mmol) of *trans*-anethole, 186 mg (0.81 mmol) of ammonium persulfate and 17.6 mg (0.02 mmol) of $Ru(bpz)_3(PF_6)_2$. The reaction was irradiated for 30 h. The crude residue was purified by flash-column chromatography using 5% EtOAc/Hexanes to afford 155 mg (0.38 mmol, 94% yield) of the desired cycloadduct as an off-white solid. *Experiment 2*: Prepared according to the general procedure using 103 mg (0.39 mmol) of 4-(benzyloxy)-2-(tert-butyl)-1-methoxybenzene, 83 mg (0.59 mmol) of *trans*-anethole, 194 mg (0.85 mmol) of ammonium persulfate and 17.4 mg (0.02 mmol) of $Ru(bpz)_3(PF_6)_2$. The

reaction was irradiated for 30 h. The crude residue was purified by flash-column chromatography using 7% EtOAc/Hexanes to afford 152 mg (0.38 mmol, 97% yield) of the desired cycloadduct as an off-white solid. IR (thin film) 2973, 1613, 1254, 1189, 1173 cm^{-1}; ^1H NMR (400 MHz, $CDCl_3$) δ 7.44 (d, *J* = 7.1 Hz, 2H), 7.42 – 7.25 (m, 5H), 6.90 (d, *J* = 8.3 Hz, 2H), 6.80 (d, *J* = 2.5 Hz, 1H), 6.72 – 6.58 (m, 1H), 5.07 (d, *J* = 9.3 Hz, 1H), 5.04 – 4.96 (m, 2H), 3.79 (s, 3H), 3.37 – 3.21 (m, 1H), 1.42 – 1.32 (m, 12H). ^{13}C NMR (101 MHz, $CDCl_3$) δ 159.47, 153.41, 151.47, 137.60, 133.78, 133.73, 132.92, 128.62, 127.95, 127.74, 127.34, 114.00, 112.64, 107.37, 91.84, 71.08, 55.37, 45.95, 34.41, 29.36, 17.72. HRMS (ESI) calculated for $[C_{27}H_{30}O_3H]^+$ requires *m/z* 403.2268, found *m/z* 403.2251. Melting point: 90–92 °C.

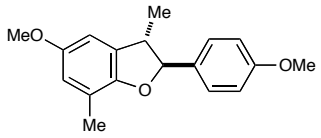

Compound 2.13 *Experiment 1*: Prepared according to the general procedure using 56 mg (0.41 mmol) of 4-methoxy-2-methylphenol, 82 mg (0.56 mmol) of *trans*-anethole, 187 mg (0.82 mmol) of ammonium persulfate and 17.8 mg (0.02 mmol) of $Ru(bpz)_3(PF_6)_2$. The reaction was irradiated for 30 h. The crude residue was purified by flash-column chromatography using 7% EtOAc/Hexanes to afford 109 mg (0.38 mmol, 94% yield) of the desired cycloadduct as a colorless oil. *Experiment 2*: Prepared according to the general procedure using 56 mg (0.40 mmol) of 4-methoxy-2-methylphenol, 80 mg (0.54 mmol) of *trans*-anethole, 190 mg (0.83 mmol) of ammonium persulfate and 17.2 mg (0.02 mmol) of $Ru(bpz)_3(PF_6)_2$. The reaction was irradiated for 30 h. The crude residue was purified by flash-column chromatography using 7% EtOAc/Hexanes to afford 108 mg (0.38 mmol, 94% yield) of the desired cycloadduct as a colorless oil. IR (thin film) 2931, 1616, 1302, 1251, 1144 cm^{-1}; ^1H NMR (400 MHz, $CDCl_3$) δ 7.35 (d, *J* = 8.5 Hz, 2H), 6.89 (d, *J* = 8.5 Hz, 2H), 6.55 (apparent s, 2H), 5.03 (d, *J* = 9.2 Hz, 1H), 3.77 (s, 3H), 3.74 (s, 3H), 3.47 – 3.30 (m, 1H), 2.22 (s, 3H), 1.34 (d, *J* = 6.8 Hz, 3H). ^{13}C NMR (101 MHz, $CDCl_3$) δ 159.67, 154.36, 151.80,

133.07, 132.20, 127.76, 119.91, 114.65, 114.05, 107.10, 92.25, 56.03, 55.34, 46.16, 17.72, 15.61. HRMS (ESI) calculated for $[C_{18}H_{20}O_3H]^+$ requires *m/z* 285.1486, found *m/z* 285.1483.

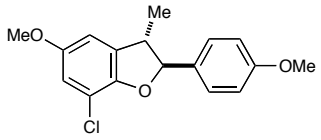

Compound 2.14. *Experiment 1:* Prepared according to the general procedure using 63 mg (0.40 mmol) of 2-chloro-4-methoxyphenol, 78 mg (0.53 mmol) of *trans*-anethole, 193 mg (0.84 mmol) of ammonium persulfate and 17.3 mg (0.02 mmol) of $Ru(bpz)_3(PF_6)_2$. The reaction was irradiated for 34 h. The crude residue was purified by flash-column chromatography using 10–15% EtOAc/Hexanes to afford 48 mg (0.14 mmol, 36% yield) of the desired cycloadduct as a colorless oil. *Experiment 2:* Prepared according to the general procedure using 64 mg (0.40 mmol) of 2-chloro-4-methoxyphenol, 83 mg (0.56 mmol) of *trans*-anethole, 199 mg (0.87 mmol) of ammonium persulfate and 17.6 mg (0.02 mmol) of $Ru(bpz)_3(PF_6)_2$. The reaction was irradiated for 34 h. The crude residue was purified by flash-column chromatography 10–15% EtOAc/Hexanes to afford 46 mg (0.14 mmol, 34% yield) of the desired cycloadduct as a colorless oil. IR (thin film) 2838, 1596, 1480, 1441, 1209 cm^{-1}; ^1H NMR (400 MHz, $CDCl_3$) δ 7.41 – 7.29 (m, 2H), 6.95 – 6.86 (m, 2H), 6.72 (dd, *J* = 2.5, 0.9 Hz, 1H), 6.62 (dd, *J* = 2.5, 1.2 Hz, 1H), 5.15 (d, *J* = 9.0 Hz, 1H), 3.81 (s, 3H), 3.76 (s, 3H), 3.46 (d, *J* = 6.8 Hz, 1H), 1.37 (d, *J* = 6.8 Hz, 3H). ^{13}C NMR (101 MHz, $CDCl_3$) δ 159.80, 154.68, 149.33, 134.41, 131.93, 127.80, 114.44, 114.04, 113.06, 109.12, 93.07, 56.19, 55.35, 46.42, 17.64. HRMS (EI) calculated for $[C_{17}H_{17}ClO_3]^+$ requires *m/z* 304.0861, found *m/z* 304.8074. Melting point: 88–89 °C.

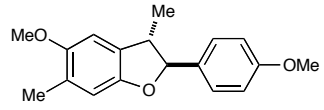

Compound 2.15. *Experiment 1*: Prepared according to the general procedure using 56 mg (0.40 mmol) of 4-methoxy-2-methylphenol, 84 mg (0.55 mmol) of *trans*-anethole, 186 mg (0.81 mmol) of ammonium persulfate and 17.1 mg (0.02 mmol) of $Ru(bpz)_3(PF_6)_2$. The reaction was irradiated for 30 h. The crude residue was

purified by flash-column chromatography using 7–10% EtOAc/Hexanes to afford 85 mg (0.30 mmol, 74% yield) of the desired cycloadduct as a colorless oil. *Experiment 2*: Prepared according to the general procedure using 56 mg (0.40 mmol) of 4-methoxy-2-methylphenol, 82 mg (0.56 mmol) of *trans*-anethole, 170 mg (0.74 mmol) of ammonium persulfate and 17.4 mg (0.02 mmol) of $Ru(bpz)_3(PF_6)_2$. The reaction was irradiated for 30 h. The crude residue was purified by flash-column chromatography using 7–10% EtOAc/Hexanes to afford 87 mg (0.31 mmol, 75% yield) of the desired cycloadduct as a colorless oil. IR (thin film) 2928, 1516, 1467, 1415, 1364 cm^{-1}; ^1H NMR (400 MHz, $CDCl_3$) δ 7.35 (d, *J* = 8.4 Hz, 2H), 6.90 (d, *J* = 8.4 Hz, 2H), 6.63–6.67 (m, 2H), 5.05 (d, *J* = 8.8 Hz, 1H), 3.81 (s, 3H), 3.80 (s, 3H), 3.49 – 3.27 (m, 1H), 2.20 (s, 3H), 1.38 (d, *J* = 6.8 Hz, 3H). ^{13}C NMR (101 MHz, $CDCl_3$) δ 159.59, 152.78, 152.42, 132.99, 129.38, 127.63, 126.55, 113.99, 111.54, 106.65, 92.51, 56.35, 55.34, 45.90, 18.00, 16.58. HRMS (EI) calculated for $[C_{18}H_{20}O_3H]^+$ requires *m/z* 285.1486, found *m/z* 285.1485. Melting point: 82–83 °C.

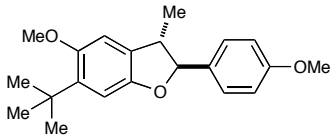

Compound 2.16. *Experiment 1*: Prepared according to the general procedure using 72 mg (0.40 mmol) of 3-(tert-butyl)-4-methoxyphenol, 82 mg (0.55 mmol) of *trans*-anethole, 184 mg (0.80 mmol) of ammonium persulfate and 17.3 mg (0.02 mmol) of $Ru(bpz)_3(PF_6)_2$. The reaction was irradiated for 30 h. The crude residue was purified by flash-column chromatography using 5% EtOAc/Hexanes to afford 118 mg (0.36 mmol, 91% yield) of the desired cycloadduct as a colorless oil. *Experiment 2*: Prepared according to the general procedure using 73 mg (0.41 mmol) of 3-(tert-butyl)-4-methoxyphenol, 78 mg (0.52 mmol) of *trans*-anethole, 183 mg (0.80 mmol) of ammonium persulfate and 17.2 mg (0.02 mmol) of $Ru(bpz)_3(PF_6)_2$. The reaction was irradiated for 30 h. The crude residue was purified by flash-column chromatography using 5% EtOAc/Hexanes to afford 122 mg (0.37 mmol, 92% yield) of the desired cycloadduct as a colorless oil. IR (thin film) 2960, 1516, 1493, 1412, 1196, 1176 cm^{-1}; ^1H NMR (400 MHz, $CDCl_3$) δ 7.45 – 7.29 (m, 2H), 7.00 – 6.88

(m, 2H), 6.70 (s, 1H), 5.05 (d, *J* = 9.3 Hz, 1H), 3.81 (s, 3H), 3.80 (s, 3H), 3.53 – 3.22 (m, 1H), 1.4 – 1.3 (m, 12H). ^{13}C NMR (101 MHz, $CDCl_3$) δ 159.61, 153.42, 152.90, 138.58, 132.95, 129.23, 127.70, 114.00, 107.96, 107.94, 92.62, 56.04, 55.33, 45.91, 35.05, 29.90, 17.63. HRMS (ESI) calculated for $[C_{21}H_{26}O_3]^+$ requires *m/z* 327.1955, found *m/z* 327.1960.

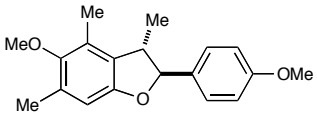

Compound 2.17. *Experiment 1*: Prepared according to the general procedure using 55 mg (0.36 mmol) of 4-methoxy-3,5-dimethylphenol, 124 mg (0.84 mmol) of *trans*-anethole, 182 mg (0.80 mmol) of ammonium persulfate and 17.4 mg (0.02 mmol) of $Ru(bpz)_3(PF_6)_2$. The reaction was irradiated for 30 h. The crude residue was purified by flash-column chromatography using 5-10% EtOAc/Hexanes to afford 84 mg (0.28 mmol, 77% yield) of the desired cycloadduct as a colorless oil. *Experiment 2*: Prepared according to the general procedure using 62 mg (0.41 mmol) of 4-methoxy-3,5-dimethylphenol, 121 mg (0.82 mmol) of *trans*-anethole, 196 mg (0.86 mmol) of ammonium persulfate and 17.6 mg (0.02 mmol) of $Ru(bpz)_3(PF_6)_2$. The reaction was irradiated for 30 h. The crude residue was purified by flash-column chromatography using 5% EtOAc/Hexanes to afford 93 mg (0.31 mmol, 76% yield) of the desired cycloadduct as a colorless oil. IR (thin film) 2934, 2362, 1512, 1251, 1176, 1050 cm^{-1}; ^{1}H NMR (400 MHz, $CDCl_3$) δ 7.30 – 7.18 (m, 2H), 6.90 – 6.79 (m, 2H), 6.52 (s, 1H), 5.14 (d, *J* = 5.4 Hz, 1H), 3.79 (s, 3H), 3.67 (s, 3H), 3.47 – 3.25 (m, 1H), 2.26 (s, 3H), 2.20 (s, 3H), 1.42 (d, *J* = 6.8 Hz, 3H). ^{13}C NMR (101 MHz, $CDCl_3$) δ 159.40, 154.84, 150.96, 134.16, 130.49, 128.45, 127.50, 126.95, 113.96, 108.63, 91.58, 60.14, 55.31, 45.54, 19.67, 16.54, 12.48. HRMS (ESI) calculated for $[C_{19}H_{22}O_3H]^+$ requires *m/z* 299.1642, found *m/z* 299.1638.

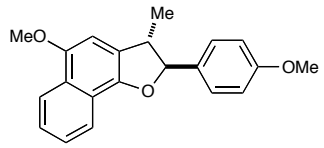

Compound 2.18. *Experiment 1*: Prepared according to the general procedure using 70 mg (0.40 mmol) of 4-methoxynaphthalen-1-ol, 79 mg (0.53 mmol) of *trans*-anethole, 181 mg (0.79 mmol) of ammonium persulfate and 17.1 mg

(0.02 mmol) of $Ru(bpz)_3(PF_6)_2$. The reaction was irradiated for 12 h. The crude residue was purified by flash-column chromatography using 10-15% EtOAc/Hexanes to afford 109 mg (0.34 mmol, 85% yield) of the desired cycloadduct as an off-white solid. *Experiment 2*: Prepared according to the general procedure using 70 mg (0.40 mmol) of 4-methoxynaphthalen-1-ol, 80 mg (0.54 mmol) of *trans*-anethole, 180 mg (0.79 mmol) of ammonium persulfate and 17.9 mg (0.02 mmol) of $Ru(bpz)_3(PF_6)_2$. The reaction was irradiated for 12 h. The crude residue was purified by flash-column chromatography using 10–15% EtOAc/Hexanes to afford 119 mg (0.37 mmol, 92% yield) of the desired cycloadduct as an off-white solid. IR (thin film) 3067, 2838, 1596, 1377, 1247, 1118, 1047 cm^{-1}; ^1H NMR (400 MHz, CDCl3) δ 8.29 – 8.15 (m, 1H), 8.03 – 7.88 (m, 1H), 7.53 – 7.32 (m, 4H), 7.00 – 6.81 (m, 2H), 6.66 (s, 1H), 5.26 (d, J = 8.4 Hz, 1H), 3.96 (s, 3H), 3.78 (s, 3H), 3.58 (p, J = 6.4 Hz, 1H), 1.46 (d, J = 6.8 Hz, 3H). ^{13}C NMR (101 MHz, $CDCl_3$) δ 159.62, 150.41, 147.94, 133.52, 127.63, 126.10, 125.55, 125.08, 123.56, 122.56, 121.43, 121.00, 114.07, 100.44, 92.57, 56.12, 55.37, 47.13, 18.84. HRMS (ESI) calculated for $[C_{21}H_{20}O_3H]^+$ requires m/z 321.1486, found m/z 321.1479. Melting point: 83–84 °C

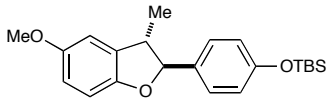

Compound 2.19. *Experiment 1*: Prepared according to the general procedure using 50 mg (0.40 mmol) of 4-methoxyphenol, 132 mg (0.55 mmol) of (*E*)-*tert*-butyldimethyl(4-(prop-1-en-1-yl)phenoxy)silane, 193 mg (0.85 mmol) of ammonium persulfate and 17.5 mg (0.02 mmol) of $Ru(bpz)_3(PF_6)_2$. The reaction was irradiated for 34 h. The crude residue was purified by flash-column chromatography using 3% EtOAc/Hexanes to afford 113 mg (0.31 mmol, 76% yield) of the desired cycloadduct as a colorless oil. *Experiment 2*: Prepared according to the general procedure using 50 mg (0.40 mmol) of 4-methoxyphenol, 137 mg (0.55 mmol) of (*E*)-*tert*-butyldimethyl(4-(prop-1-en-1-yl)phenoxy)silane, 193 mg (0.84 mmol) of ammonium persulfate and 17.2 mg (0.02 mmol) of $Ru(bpz)_3(PF_6)_2$. The reaction was irradiated for 34 h. The crude residue was purified by flash-

column chromatography using 3% EtOAc/Hexanes to afford 108 mg (0.29 mmol, 72% yield) of the desired cycloadduct as a colorless oil. IR (thin film) 2931, 2362, 1609, 1512, 1202 cm^{-1}; ^1H NMR (400 MHz, $CDCl_3$) δ 7.49 – 7.24 (m, 2H), 6.97 – 6.85 (m, 2H), 6.85 – 6.68 (m, 3H), 5.12 (d, *J* = 9.1 Hz, 1H), 3.83 (s, 3H), 3.46 (p, *J* = 6.6 Hz, 1H), 1.43 (d, *J* = 6.8 Hz, 3H), 1.04 (s, 9H), 0.25 (s, 6H). ^{13}C NMR (101 MHz, $CDCl_3$) δ 155.77, 154.43, 153.29, 133.30, 133.18, 127.61, 120.20, 112.85, 110.11, 109.36, 92.70, 56.06, 45.68, 25.73, 18.25, 17.64, -4.36, -4.37. HRMS (ESI) calculated for $[C_{22}H_{30}O_3SiH]^+$ requires *m/z* 371.2037, found *m/z* 371.2044.

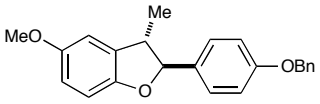

Compound 2.20. *Experiment 1*: Prepared according to the general procedure using 49 mg (0.40 mmol) of 4-methoxyphenol, 117 mg (0.52 mmol) of (*E*)-1-(benzyloxy)-4-(prop-1-en-1-yl)benzene, 197 mg (0.86 mmol) of ammonium persulfate and 17.2 mg (0.02 mmol) of $Ru(bpz)_3(PF_6)_2$. The reaction was irradiated for 34 h. The crude residue was purified by flash-column chromatography using 10% EtOAc/Hexanes to afford 119 mg (0.342 mmol, 86% yield) of the desired cycloadduct as a colorless glass. *Experiment 2*: Prepared according to the general procedure using 49 mg (0.40 mmol) of 4-methoxyphenol, 120 mg (0.54 mmol) of (*E*)-1-(benzyloxy)-4-(prop-1-en-1-yl)benzene, 193 mg (0.84 mmol) of ammonium persulfate and 17.1 mg (0.02 mmol) of $Ru(bpz)_3(PF_6)_2$. The reaction was irradiated for 34 h. The crude residue was purified by flash-column chromatography using 10% EtOAc/Hexanes to afford 111 mg (0.32 mmol, 80% yield) of the desired cycloadduct as a colorless glass. IR (thin film) 2362, 1613, 1512, 1244, 1202 cm^{-1}; ^1H NMR (400 MHz, $CDCl_3$) δ 7.45 – 7.27 (m, 7H), 6.96 (m, 2H), 6.78 – 6.65 (m, 3H), 5.06 (m, 3H), 3.75 (s, 3H), 3.39 (p, *J* = 6.9 Hz, 1H), 1.36 (d, *J* = 6.9, 3H). ^{13}C NMR (101 MHz, $CDCl_3$) δ 158.88, 154.47, 153.32, 136.98, 133.17, 133.05, 128.66, 128.05, 127.73, 127.53, 115.01, 112.92, 110.15, 109.41, 92.61, 70.09, 56.09, 45.74, 17.69. HRMS (ESI) calculated for $[C_{23}H_{22}O_3H]^+$ requires *m/z* 347.1642, found *m/z* 347.1649.

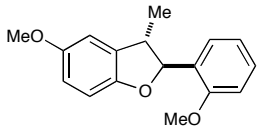

Compound 2.21. *Experiment 1*: Prepared according to the general procedure using 48 mg (0.38 mmol) of 4-methoxyphenol, 78 mg (0.53 mmol) of (*E*)-1-methoxy-2-(prop-1-en-1-yl)benzene, 190 mg (0.83 mmol) of ammonium persulfate and 16.8 mg (0.02 mmol) of $Ru(bpz)_3(PF_6)_2$. The reaction was irradiated for 50 h. The crude residue was purified by flash-column chromatography using 10% EtOAc/Hexanes to afford 89 mg (0.33 mmol, 86% yield) of the desired cycloadduct as a colorless oil. *Experiment 2*: Prepared according to the general procedure using 49 mg (0.40 mmol) of 4-methoxyphenol, 83 mg (0.56 mmol) of (*E*)-1-methoxy-2-(prop-1-en-1-yl)benzene, 191 mg (0.84 mmol) of ammonium persulfate and 17.4 mg (0.02 mmol) of $Ru(bpz)_3(PF_6)_2$. The reaction was irradiated for 50 h. The crude residue was purified by flash-column chromatography using 10% EtOAc/Hexanes to afford 95 mg (0.36 mmol, 90% yield) of the desired cycloadduct as a colorless oil. IR (thin film) 2960, 1487, 1264, 1205 cm^{-1}; ^1H NMR (400 MHz, $CDCl_3$) δ 7.46 – 7.32 (m, 1H), 7.32 – 7.19 (m, 1H), 6.99 – 6.85 (m, 2H), 6.85 – 6.74 (m, 1H), 6.74 – 6.62 (m, 2H), 5.59 (d, *J* = 6.5 Hz, 1H), 3.85 (s, 3H), 3.75 (s, 3H), 3.43 – 3.27 (m, 1H), 1.44 (d, *J* = 6.9 Hz, 3H). ^{13}C NMR (101 MHz, $CDCl_3$) δ 156.56, 154.32, 153.44, 133.29, 130.03, 128.67, 126.25, 120.64, 112.82, 110.43, 110.41, 109.21, 87.00, 56.04, 55.38, 45.50, 19.83. HRMS (ESI) calculated for $[C_{17}H_{18}O_3H]^+$ requires *m/z* 271.1329, found *m/z* 271.1327.

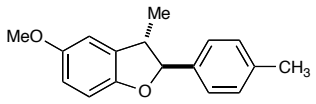

Compound 2.22. *Experiment 1*: Prepared according to the general procedure using 50 mg (0.40 mmol) of 4-methoxyphenol, 110 mg (0.83 mmol) of (*E*)-1-methyl-4-(prop-1-en-1-yl)benzene, 192 mg (0.84 mmol) of ammonium persulfate and 17.1 mg (0.02 mmol) of $Ru(bpz)_3(PF_6)_2$. The reaction was irradiated for 50 h.The crude residue was purified by flash-column chromatography using 7% EtOAc/Hexanes to afford 90 mg (0.36 mmol, 89% yield) of the desired cycloadduct as a colorless oil. *Experiment 2*: Prepared

according to the general procedure using 50 mg (0.40 mmol) of 4-methoxyphenol, 113 mg (0.85 mmol) of (*E*)-1-methyl-4-(prop-1-en-1-yl)benzene, 194 mg (0.85 mmol) of ammonium persulfate and 17.2 mg (0.02 mmol) of $Ru(bpz)_3(PF_6)_2$. The reaction was irradiated for 50 h. The crude residue was purified by flash-column chromatography using 7% EtOAc/Hexanes to afford 83 mg (0.33 mmol, 82% yield) of the desired cycloadduct as a colorless oil. IR (thin film) 2938, 1487, 1180, 1034 cm^{-1}; ^1H NMR (400 MHz, $CDCl_3$) δ 7.31 (d, *J* = 7.7 Hz, 2H), 7.18 (d, *J* = 7.7 Hz, 2H), 6.85 – 6.61 (m, 3H), 5.09 (d, *J* = 9.0 Hz, 1H), 3.76 (s, 3H), 3.39 (p, *J* = 6.8 Hz, 1H), 2.35 (s, 3H), 1.38 (d, *J* = 6.8 Hz, 3H). ^{13}C NMR (101 MHz, $CDCl_3$) δ 154.46, 153.38, 138.01, 137.83, 133.12, 129.33, 126.20, 112.91, 110.14, 109.39, 92.73, 56.08, 45.91, 21.25, 17.79. HRMS (ESI) calculated for $[C_{17}H_{18}O_2H]^+$ requires *m/z* 255.1380, found *m/z* 255.1388.

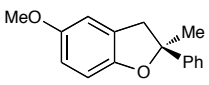

Compound 2.23. *Experiment 1*: Prepared according to the general procedure using 50 mg (0.41 mmol) of 4-methoxyphenol, 111 mg (0.94 mmol) of α-methylstyrene, 194 mg (0.85 mmol) of ammonium persulfate and 17.1 mg (0.02 mmol) of $Ru(bpz)_3(PF_6)_2$. The reaction was irradiated for 50 h. The crude residue was purified by flash-column chromatography using 7% EtOAc/Hexanes to afford 64 mg (0.27 mmol, 65% yield) of the desired cycloadduct as a colorless oil. *Experiment 2*: Prepared according to the general procedure using 49 mg (0.40 mmol) of 4-methoxyphenol, 98 mg (0.83 mmol) of α-methylstyrene, 192 mg (0.84 mmol) of ammonium persulfate and 17.1 mg (0.02 mmol) of $Ru(bpz)_3(PF_6)_2$. The reaction was irradiated for 50 h. The crude residue was purified by flash-column chromatography using 7% EtOAc/Hexanes to afford 69 mg (0.29 mmol, 72% yield) of the desired cycloadduct as a colorless oil. IR (thin film) 2973, 1487, 1448, 1225, 1150, 1034 cm^{-1}; ^1H NMR (400 MHz, $CDCl_3$) δ 7.59 – 7.40 (m, 2H), 7.33 (t, *J* = 7.6 Hz, 2H), 7.24 (t, *J* = 7.4 Hz, 1H), 6.79 (d, *J* = 8.5 Hz, 1H), 6.75 – 6.57 (m, 2H), 3.73 (s, 3H), 3.52 – 3.20 (m, 2H), 1.75 (s, 3H). ^{13}C NMR (101 MHz, $CDCl_3$) δ 154.16,

153.06, 146.90, 128.37, 127.49, 127.04, 124.56, 113.01, 111.38, 109.42, 89.22, 56.03, 45.19, 29.27. HRMS (EI) calculated for $[C_{16}H_{16}O_2]^+$ requires *m/z* 240.1145, found *m/z* 240.1143.

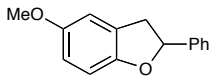

Compound 2.24. *Experiment 1*: Prepared according to the general procedure using 50 mg (0.40 mmol) of 4-methoxyphenol, 100 μL (0.87 mmol) of styrene, 190 mg (0.84 mmol) of ammonium persulfate and 17.3 mg (0.02 mmol) of $Ru(bpz)_3(PF_6)_2$. The reaction was irradiated for 50 h. The crude residue was purified by flash-column chromatography using 5-6% EtOAc/Hexanes to afford 40 mg (0.18 mmol, 44% yield) of the desired cycloadduct as a colorless oil. *Experiment 2*: Prepared according to the general procedure using 50 mg (0.41 mmol) of 4-methoxyphenol, 100 μL (0.87 mmol) of styrene, 195 mg (0.85 mmol) of ammonium persulfate and 17.5 mg (0.02 mmol) of $Ru(bpz)_3(PF_6)_2$. The reaction was irradiated for 50 h. The crude residue was purified by flash-column chromatography using 5–6% EtOAc/Hexanes to afford 42 mg (0.18 mmol, 45% yield) of the desired cycloadduct as a colorless oil. IR (thin film) 2938, 1487, 1205, 1034 cm^{-1}; ^1H NMR (400 MHz, $CDCl_3$) δ 7.51 – 7.21 (m, 5H), 6.88 – 6.52 (m, 3H), 5.72 (t, *J* = 8.7 Hz, 1H), 3.75 (s, 3H), 3.58 (dd, *J* = 15.7, 9.3 Hz, 1H), 3.18 (dd, *J* = 15.7, 8.2 Hz, 1H). ^{13}C NMR (101 MHz, $CDCl_3$) δ 154.35, 153.83, 142.06, 128.65, 128.00, 127.53, 125.79, 113.07, 111.25, 109.23, 84.26, 56.07, 38.91. HRMS (EI) calculated for $[C_{15}H_{14}O_2]^+$ requires *m/z* 226.0989, found *m/z* 226.0988.

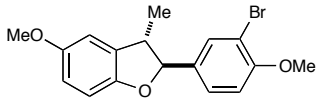

Compound 2.25. *Experiment 1*: Prepared according to the general procedure using 50 mg (0.40 mmol) of 4-methoxyphenol, 119 mg (0.52 mmol) of (*E*)-2-bromo-1-methoxy-4-(prop-1-en-1-yl)benzene, 193 mg (0.85 mmol) of ammonium persulfate and 16.4 mg (0.02 mmol) of $Ru(bpz)_3(PF_6)_2$. The reaction was irradiated for 28 h. The crude residue was purified by flash-column chromatography using 5% EtOAc/Hexanes to afford 95 mg (0.27 mmol, 68% yield) of the desired cycloadduct as a colorless

oil. *Experiment 2*: Prepared according to the general procedure using 49 mg (0.40 mmol) of 4-methoxyphenol, 117 mg (0.52 mmol) of (*E*)-2-bromo-1-methoxy-4-(prop-1-en-1-yl)benzene, 194 mg (0.85 mmol) of ammonium persulfate and 17.0 mg (0.02 mmol) of $Ru(bpz)_3(PF_6)_2$. The reaction was irradiated for 28 h. The crude residue was purified by flash-column chromatography using 5% EtOAc/Hexanes to afford 103 mg (0.30 mmol, 75% yield) of the desired cycloadduct as a colorless oil. IR (thin film) 2960, 1614, 1519, 1372 cm^{-1}; ^1H NMR (400 MHz, $CDCl_3$) δ 7.62 (d, *J* = 2.1 Hz, 1H), 7.31 (dd, *J* = 8.4, 2.1 Hz, 1H), 6.88 (d, *J* = 8.5 Hz, 1H), 6.80 – 6.63 (m, 3H), 5.03 (d, *J* = 8.9 Hz, 1H), 3.88 (s, 3H), 3.76 (s, 3H), 3.50 – 3.22 (m, 1H), 1.38 (d, *J* = 6.8 Hz, 3H). ^{13}C NMR (101 MHz, $CDCl_3$) δ 155.82, 154.58, 153.06, 134.41, 132.76, 131.24, 126.54, 113.03, 111.88, 111.87, 110.12, 109.45, 91.63, 56.35, 56.07, 45.90, 17.76. HRMS (ESI) calculated for $[C_{17}H_{17}O_3BrH]^+$ requires *m/z* 349.0434, found *m/z* 349.0427.

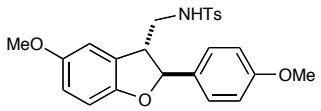

Compound 2.26. *Experiment 1*: Prepared according to the general procedure using 50 mg (0.40 mmol) of 4-methoxyphenol, 166 mg (0.52 mmol) of (*E*)-*N*-(3-(4-methoxyphenyl)allyl)-4-methylbenzenesulfonamide, 197 mg (0.86 mmol) of ammonium persulfate and 17.4 mg (0.02 mmol) of $Ru(bpz)_3(PF_6)_2$. The reaction was irradiated for 40 h. The crude residue was purified by flash-column chromatography using 20–40% EtOAc/Hexanes to afford 121 mg (0.27 mmol, 68% yield) of the desired cycloadduct as a white solid. *Experiment 2*: Prepared according to the general procedure using 50 mg (0.40 mmol) of 4-methoxyphenol, 169 mg (0.53 mmol) of (*E*)-*N*-(3-(4-methoxyphenyl)allyl)-4-methylbenzenesulfonamide, 196 mg (0.86 mmol) of ammonium persulfate and 17.1 mg (0.02 mmol) of $Ru(bpz)_3(PF_6)_2$. The reaction was irradiated for 40 h. The crude residue was purified by flash-column chromatography using 25% EtOAc/Hexanes + 2% Acetone to afford 133 mg (0.31 mmol, 75% yield) of the desired cycloadduct as a white solid. IR (thin film) 3277 (br), 2838, 1490, 1160 cm^{-1}; ^1H NMR (400 MHz, $CDCl_3$) δ 7.69 (d, *J* = 7.9 Hz, 2H), 7.27 (d, *J* = 8.0 Hz, 2H), 7.24 –

7.14 (m, 2H), 6.91 – 6.77 (m, 2H), 6.77 – 6.56 (m, 3H), 5.40 (d, *J* = 6.4 Hz, 1H), 4.89 (t, *J* = 6.5 Hz, 1H), 3.76 (s, 3H), 3.71 (s, 3H), 3.46 (q, *J* = 6.0 Hz, 1H), 3.24 (m, 2H), 2.41 (s, 3H). ^{13}C NMR (101 MHz, $CDCl_3$) δ 159.59, 154.38, 153.93, 143.72, 136.58, 133.01, 129.88, 127.34, 127.11, 127.05, 114.32, 114.09, 110.39, 109.93, 87.12, 56.05, 55.32, 50.89, 45.35, 21.57. HRMS (ESI) calculated for $[C_{24}H_{25}NO_5S+NH_4]^+$ requires *m/z* 457.1792, found *m/z* 457.1798. Melting point: 88–89 °C

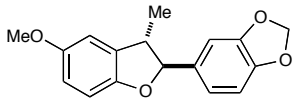

Compound 2.27. *Experiment 1*: Prepared according to the general procedure using 50 mg (0.41 mmol) of 4-methoxyphenol, 90 mg (0.55 mmol) of (*E*)-isosafrole, 196 mg (0.86 mmol) of ammonium persulfate and 17.3 mg (0.02 mmol) of $Ru(bpz)_3(PF_6)_2$. The reaction was irradiated for 30 h. The crude residue was purified by flash-column chromatography using 15% EtOAc/Hexanes to afford 92 mg (0.32 mmol, 79% yield) of the desired cycloadduct as a colorless oil. *Experiment 2*: Prepared according to the general procedure using 50 mg (0.41 mmol) of 4-methoxyphenol, 83 mg (0.54 mmol) of (*E*)-isosafrole, 199 mg (0.87 mmol) of ammonium persulfate and 17.2 mg (0.02 mmol) of $Ru(bpz)_3(PF_6)_2$. The reaction was irradiated for 30 h. The crude residue was purified by flash-column chromatography using 15% EtOAc/Hexanes to afford 98 mg (0.34 mmol, 85% yield) of the desired cycloadduct as a colorless oil. IR (thin film) 2964, 1613, 1487, 1251, 1147, 1034 cm^{-1}; ^{1}H NMR (400 MHz, $CDCl_3$) δ 6.98 – 6.66 (m, 6H), 5.95 (s, 2H), 5.03 (d, *J* = 8.9 Hz, 1H), 3.77 (s, 3H), 3.37 (m, 1H), 1.38 (d, *J* = 6.8 Hz, 3H). ^{13}C NMR (101 MHz, $CDCl_3$) δ 154.48, 153.16, 148.00, 147.61, 134.64, 132.94, 119.96, 112.93, 110.11, 109.38, 108.19, 106.60, 101.15, 92.69, 56.07, 45.85, 17.73. HRMS (ESI) calculated for $[C_{17}H_{16}O_4+NH_4]^+$ requires *m/z* 302.1387, found *m/z* 302.1386.

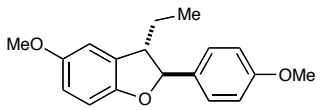

Compound 2.28. *Experiment 1*: Prepared according to the general procedure using 51 mg (0.41 mmol) of 4-methoxyphenol, 89 mg (0.55 mmol) of (*E*)-1-(but-1-en-1-yl)-4-methoxybenzene, 194 mg (0.85 mmol) of ammonium persulfate

and 17.3 mg (0.02 mmol) of $Ru(bpz)_3(PF_6)_2$. The reaction was irradiated for 50 h. The crude residue was purified by flash-column chromatography using 7% EtOAc/Hexanes to afford 104 mg (0.36 mmol, 89% yield) of the desired cycloadduct as a colorless oil. *Experiment 2*: Prepared according to the general procedure using 51 mg (0.41 mmol) of 4-methoxyphenol, 87 mg (0.54 mmol) of (*E*)-1-(but-1-en-1-yl)-4-methoxybenzene, 192 mg (0.84 mmol) of ammonium persulfate and 17.2 mg (0.02 mmol) of $Ru(bpz)_3(PF_6)_2$. The reaction was irradiated for 50 h. The crude residue was purified by flash-column chromatography using 7% EtOAc/Hexanes to afford 109 mg (0.38 mmol, 93% yield) of the desired cycloadduct as a colorless oil. IR (thin film) 2964, 1516, 1487, 1247, 1144, 1037 cm^{-1}; ^1H NMR (400 MHz, $CDCl_3$) δ 7.49 – 7.24 (m, 2H), 7.01 – 6.81 (m, 2H), 6.81 – 6.64 (m, 3H), 5.25 (d, *J* = 6.7 Hz, 1H), 3.79 (s, 3H), 3.77 (s, 3H), 3.32 (q, *J* = 6.6 Hz, 1H), 2.06 – 1.62 (m, 2H), 1.00 (t, *J* = 7.5 Hz, 3H). ^{13}C NMR (101 MHz, $CDCl_3$) δ 159.49, 154.24, 153.60, 134.15, 131.55, 127.48, 114.02, 112.96, 110.86, 109.20, 89.78, 56.05, 55.32, 52.24, 27.27, 11.30. HRMS (ESI) calculated for $[C_{19}H_{20}O_3]^+$ requires *m/z* 284.1407, found *m/z* 284.1411.

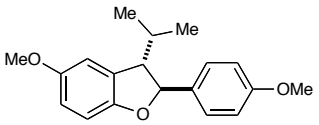

Compound 2.29. *Experiment 1*: Prepared according to the general procedure using 50 mg (0.40 mmol) of 4-methoxyphenol, 92 mg (0.52 mmol) of (*E*)-1-methoxy-4-(3-methylbut-1-en-1-yl)benzene, 197 mg (0.86 mmol) of ammonium persulfate and 17.5 mg (0.02 mmol) of $Ru(bpz)_3(PF_6)_2$. The reaction was irradiated for 50 h. The crude residue was purified by flash-column chromatography using 7% EtOAc/Hexanes to afford 95 mg (0.32 mmol, 79% yield) of the desired cycloadduct as a colorless oil. *Experiment 2*: Prepared according to the general procedure using 50 mg (0.40 mmol) of 4-methoxyphenol, 100 mg (0.57 mmol) of (*E*)-1-methoxy-4-(3-methylbut-1-en-1-yl)benzene, 195 mg (0.86 mmol) of ammonium persulfate and 17.2 mg (0.02 mmol) of $Ru(bpz)_3(PF_6)_2$. The reaction was irradiated for 50 h. The crude residue was purified by flash-column chromatography using 7% EtOAc/Hexanes to afford 96 mg (0.32 mmol, 79% yield) of the desired cycloadduct as a colorless

oil. IR (thin film) 2834, 2367, 1516, 1247, 1176, 1037 cm^{-1}; ^1H NMR (400 MHz, $CDCl_3$) δ 7.33 – 7.12 (m, 2H), 6.98 – 6.81 (m, 2H), 6.81 – 6.62 (m, 3H), 5.38 (d, *J* = 4.7 Hz, 1H), 3.76 (s, 3H), 3.75 (s, 3H), 3.27 (t, *J* = 4.7 Hz, 1H), 2.10 – 2.00 (m, 1H), 0.99 (d, *J* = 6.8 Hz, 3H), 0.97 (d, *J* = 6.8 Hz, 3H). ^{13}C NMR (101 MHz, $CDCl_3$) δ 159.29, 154.14, 154.03, 135.25, 129.77, 126.94, 114.02, 113.07, 111.64, 109.00, 86.41, 57.38, 56.02, 55.30, 32.06, 19.61, 18.94. HRMS (ESI) calculated for $[C_{19}H_{22}O_3+NH_4]^+$ requires *m/z* 316.1908, found *m/z* 316.1917.

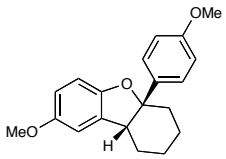

Compound 2.30. *Experiment 1*: Prepared according to the general procedure using 50 mg (0.40 mmol) of 4-methoxyphenol, 154 mg (0.82 mmol) of 4'-methoxy-2,3,4,5-tetrahydro-1,1'-biphenyl, 197 mg (0.86 mmol) of ammonium persulfate and 16.8 mg (0.02 mmol) of $Ru(bpz)_3(PF_6)_2$. The reaction was irradiated for 52 h. The crude residue was purified by flash-column chromatography using 7% EtOAc/Hexanes to afford 82 mg (0.27 mmol, 66% yield) of the desired cycloadduct as a colorless oil. *Experiment 2*: Prepared according to the general procedure using 51 mg (0.41 mmol) of 4-methoxyphenol, 153 mg (0.81 mmol) of 4'-methoxy-2,3,4,5-tetrahydro-1,1'-biphenyl, 194 mg (0.85 mmol) of ammonium persulfate and 17.4 mg (0.02 mmol) of $Ru(bpz)_3(PF_6)_2$. The reaction was irradiated for 52 h. The crude residue was purified by flash-column chromatography using 7% EtOAc/Hexanes to afford 86 mg (0.28 mmol, 68% yield) of the desired cycloadduct as a colorless oil. IR (thin film) 2938, 1613, 1516, 1180, 1034 cm^{-1}; ^1H NMR (400 MHz, $CDCl_3$) δ 7.51 – 7.40 (m, 2H), 6.90 – 6.80 (m, 2H), 6.76 (d, *J* = 8.4 Hz, 1H), 6.70 – 6.58 (m, 2H), 3.78 (s, 3H), 3.74 (s, 3H), 3.54 (t, *J* = 5.9 Hz, 1H), 2.12 – 1.92 (m, 3H), 1.92 – 1.76 (m, 1H), 1.70 – 1.56 (m, 1H), 1.55 – 1.43 (m, 3H). ^{13}C NMR (101 MHz, $CDCl_3$) δ 158.62, 154.19, 152.53, 137.95, 133.59, 126.75, 113.50, 112.27, 110.25, 109.84, 90.72, 55.93, 55.26, 47.31, 35.36, 27.79, 21.28, 20.91. HRMS (EI) calculated for $[C_{20}H_{22}O_3]^+$ requires *m/z* 310.1564, found *m/z* 310.1572.

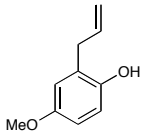

2-Allyl-4-methoxyphenol (2.33): 4-Methoxyphenol (1.80 g, 14.6 mmol) and potassium carbonate (2.13 g, 15.4 mmol) were combined in a 25 mL flame-dried round-bottomed flask containing a magnetic stirbar. Acetone (5 mL) was added, and flask was capped with a septum and flushed with N_2. Allyl bromide (1.90 mL, 22.0 mmol) was then added dropwise *via* syringe to the stirring suspension, and the flask was fitted with a reflux condenser under N_2. The stirring mixture was heated to reflux for 3.5 h. After cooling to room temperature, the mixture was rinsed into a separatory funnel with dichloromethane and 2 M NaOH. The layers were separated, and the organic layer was washed once more with 2 M NaOH. The organic extract was then dried over $MgSO_4$, filtered and concentrated *in vacuo* to afford 1-(allyloxy)-4-methoxybenzene (2.22 g, 93% yield) as a viscous oil. All spectral data were in agreement with previously reported values.[44] This material was carried on without further purification. The unpurified product (2.22 g, 13.5 mmol) was transferred into a round-bottomed flask containing a magnetic stirbar. The flask was equipped with a reflux condenser and heated (neat) to 195 °C for 5 h. The crude reaction mixture was then cooled to room temperature, and purified directly by flash-column chromatography (20% EtOAc/hexanes) to afford the title compound as a pale yellow oil (2.01 g, 91% yield). All spectral data were in agreement with previously reported values.[44]

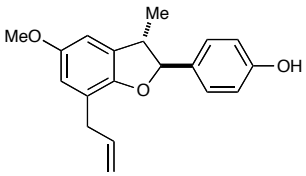

Compound 2.35: Phenol **2.33** (66 mg, 0.40 mmol), (*E*)-*tert*-butyldimethyl(4-(prop-1-en-1-yl)phenoxy)silane (**2.34**, 196 mg, 0.79 mmol), $Ru(bpz)_3(PF_6)_2$ (17.4 mg, 0.02 mmol), and ammonium peroxydisulfate (191 mg, 0.84 mmol) were combined in an oven-dried Schlenk flask. A magnetic stirbar was added, and MeCN (4 mL) was introduced by syringe. The flask was sealed with a glass stopper, and the solution was degassed by three freeze-pump-thaw cycles in dry-ice/acetone. The

flask was then backfilled with N_2, and the reaction was stirred evenly under irradiation with a 23 W (1200 lumens) SLI Mini-Lynx compact fluorescent light bulb (placed 3-4 inches from the reaction flask) for 40 h. During irradiation, the reaction was sonicated as needed to maintain catalyst suspension (see general procedure above). At 40 h, the reaction was diluted with EtOAc (7 mL), and eluted through a plug of silica using EtOAc. After concentrating *in vacuo*, the eluent was transferred to a 10 mL round-bottomed flask containing a magnetic stirbar, and dissolved in 2 mL THF under N_2. The flask was cooled to 0 °C in an ice bath, and solid tetrabutylammonium fluoride trihydrate (TBAF·H_2O, 186 mg, 0.59 mmol) was added in one portion. The resulting solution was stirred for 15 min at room temperature, and TLC analysis showed reaction completion. The solution was transferred to a separatory funnel, and the reaction was quenched by the addition of saturated aqueous ammonium chloride. The resulting aqueous layer was extracted with EtOAc (3x). The combined organic extracts were then washed with sat. aq. $NaHCO_3$, then brine, dried over $MgSO_4$, filtered, and concentrated *in vacuo*. The crude residue was purified by flash-column chromatography to afford pure **2.35** (96 mg, 81% yield) as a yellow oil. IR (thin film) 3422 (br), 2964, 1454, 1199, 1041 cm^{-1}; ^1H NMR (400 MHz, $CDCl_3$) δ 7.36 – 7.25 (m, 2H), 6.88 – 6.65 (m, 2H), 6.58 (apparent s, 2H), 5.99 (ddt, *J* = 16.8, 10.1, 6.6 Hz 1H), 5.28 (br s, 1H), 5.20 – 4.93 (m, 3H), 3.77 (s, 3H), 3.52 – 3.26 (m, 3H), 1.36 (d, *J* = 6.8 Hz, 3H). ^{13}C NMR (101 MHz, $CDCl_3$) δ 155.59, 154.37, 151.31, 136.20, 133.19, 132.52, 127.79, 122.11, 115.94, 115.45, 113.66, 107.76, 92.20, 56.17, 46.13, 34.03, 17.80. HRMS (EI) calculated for $[C_{19}H_{20}O_3]^+$ requires *m/z* 296.1407, found *m/z* 296.1415.

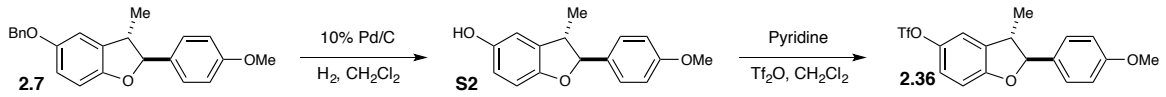

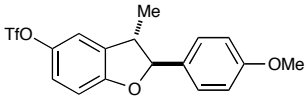

Compound 2.36: Compound **7** (231 mg, 0.67 mmol) was weighed into a 100 mL round-bottom flask containing a magnetic stirbar. THF (40 mL) was added, and the mixture was stirred until all solids were dissolved. The flask was then capped with a septum and purged with N_2 for 5 min. Solid Pd/C (10 wt%, 72 mg, 0.067 mmol) was then added, and hydrogen gas (balloon equipped with a syringe needle) was bubbled through the black suspension for 15 min. After 15 min, the needle was removed from the suspension, and the hydrogen atmosphere was maintained with rapid stirring for 4.5 h. The black mixture was then filtered over Celite, and the filter cake was washed thoroughly with CH_2Cl_2. The eluent was concentrated *in vacuo* to afford phenol (**S2**) cleanly as a colorless glass (177 mg, quantitative yield). The crude product was carried on without further purification. **S2** was weighed into a flame-dried 12 mL vial, then dissolved in toluene and concentrated *in vacuo* to azeotropically remove water. A magnetic stirbar was added, and the vial was capped with a septum and flushed with N_2. Dichloromethane (2.5 mL) was added by syringe, and after the mixture became homogenous, the vial was cooled to 0 °C in an ice bath. Pyridine (250 μL, 3.1 mmol) was added in one portion *via* syringe, and then triflic anhydride (200 μL, 1.2 mmol) was added dropwise over 5 min. After stirring the yellow-green solution for 5 min at 0 °C, the vial was allowed to warm to room temperature. The reaction was stirred for an additional 3 h under N_2 and subsequently quenched by addition of 5 mL of 1 M HCl. The resulting mixture was transferred to a separatory funnel using dichloromethane and H_2O. The layers were separated, and the aqueous layer was extracted once with dichloromethane. The combined organic extracts were washed once with sat. aq. $NaHCO_3$, then washed with brine, the dried over $MgSO_4$, filtered, and concentrated *in vacuo*. The crude residue was purified by flash-column chromatography (10% EtOAC/hex) to afford **2.36**

(241 mg, 93% yield) as a white crystalline solid. IR (thin film) 2359, 1422, 1251, 1144 cm^{-1}; ^1H NMR (400 MHz, $CDCl_3$) δ 7.45 – 7.29 (m, 2H), 7.15 – 6.98 (m, 2H), 6.98 – 6.54 (m, 3H), 5.18 (d, *J* = 9.2 Hz, 1H), 3.82 (s, 3H), 3.56 – 3.36 (m, 1H), 1.40 (d, *J* = 6.8 Hz, 3H). ^{13}C NMR (101 MHz, CDCl3) δ 159.95, 158.67, 143.35, 134.29, 131.61, 127.69, 121.25, 118.8 (q, J_{CF} = 322 Hz) 117.16, 114.17, 110.12, 93.54, 55.36, 45.23, 17.47. HRMS (EI) calculated for $[C_{17}H_{15}F_3O_5S]^+$ requires *m/z* 388.0587, found *m/z* 388.0588. Melting point: 32–33 °C

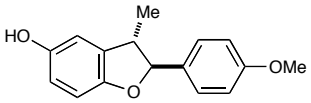

An analytically pure sample of **S2** could be isolated as intermediate in synthesis of **2.37**. It was purified by flash-column chromatography (30% EtOAc/Hexanes) to afford desired product as a white glass. IR (thin film) 3403 (br), 2964, 1616, 1454, 1251 cm^{-1}; ^1H NMR (400 MHz, $CDCl_3$) δ 7.51 – 7.28 (m, 2H), 7.00 – 6.81 (m, 2H), 6.77 – 6.50 (m, 3H), 5.20 – 4.88 (m, 2H), 3.80 (s, 3H), 3.48 – 3.25 (m, 1H), 1.33 (d, *J* = 6.8 Hz, 3H). ^{13}C NMR (101 MHz, $CDCl_3$) δ 159.63, 153.07, 149.97, 133.31, 132.61, 127.75, 114.47, 114.07, 111.19, 109.53, 92.66, 55.38, 45.58, 17.53. HRMS (EI) calculated for $[C_{16}H_{16}O_3]^+$ requires *m/z* 256.1094, found *m/z* 256.1097.

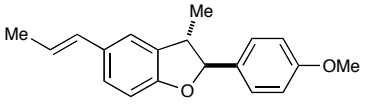

Compound 2.37: Compound **2.36** (148 mg, 0.44 mmol) and *trans*-1-propen-1-ylboronic acid (75 mg, 0.88 mmol) were combined in a 50 mL round bottomed flask containing a magnetic stirbar. Toluene (12 mL), ethanol (3.5 mL) and H_2O (5.2 mL) were added to the flask, which was then capped with a septum and flushed with N_2. The mixture was stirred, and solid $Pd[PPh_3]_4$ (50.6 mg, 0.44 mmol) and potassium carbonate (172 mg, 1.25 mmol) were added to the flask. The flask was then equipped with a reflux condenser attached to a vacuum manifold and carefully evacuated until gentle bubbling of solvent was observed, whereupon the atmosphere was immediately backfilled with N_2. The system was evacuated and refilled in the same way three more times, then heated to reflux (110–120 °C) for 7.5 h with vigorous stirring. The flask was then cooled to room temperature, and

the reaction was quenched by addition of 1 M HCl. The resulting mixture was transferred to a separatory funnel with EtOAc and H_2O. The layers were separated, and the organic phase was washed with saturated aqueous $NaHCO_3$ and brine, dried over $MgSO_4$, filtered, and concentrated *in vacuo*. The crude residue was purified by flash-column chromatography (5–10% EtOAc/Hexanes) to afford **35** (117 mg, 95% yield) as a colorless oil. Spectral data matched those previously reported.[17] IR (thin film) 3022, 2952, 1422, 1212, 1144 cm^{-1}; ^1H NMR (400 MHz, $CDCl_3$) δ 7.43 – 7.26 (m, 2H), 7.11 (d, *J* = 10.3 Hz, 2H), 6.97 – 6.83 (m, 2H), 6.75 (d, *J* = 8.1 Hz, 1H), 6.35 (dq, *J* = 15.7, 1.7 Hz, 1H), 6.07 (dq, *J* = 15.7, 6.6 Hz, 1H), 5.07 (d, *J* = 8.9 Hz, 1H), 3.78 (s, 3H), 3.38 (p, *J* = 6.8 Hz, 1H), 1.85 (dd, *J* = 6.6, 1.7 Hz, 3H), 1.37 (d, *J* = 6.8 Hz, 3H). ^1H NMR (400 MHz, Acetone-d_6) δ 7.48 – 7.31 (m, 2H), 7.24 (s, 1H), 7.18 – 7.07 (m, 1H), 7.05 – 6.89 (m, 2H), 6.71 (d, *J* = 8.2 Hz, 1H), 6.38 (d, *J* = 15.7 Hz, 1H), 6.12 (dq, *J* = 15.7, 6.6 Hz, 1H), 5.12 (d, *J* = 8.7 Hz, 1H), 3.80 (s, 3H), 3.46 – 3.25 (m, 1H), 1.82 (dd, *J* = 6.6, 1.6 Hz, 3H), 1.38 (d, *J* = 6.8 Hz, 3H). ^{13}C NMR (101 MHz, $CDCl_3$) δ 159.71, 158.42, 132.73, 132.47, 131.28, 130.87, 127.71, 126.37, 123.01, 120.80, 114.07, 109.34, 92.72, 55.35, 45.29, 18.51, 17.86. ^{13}C NMR (101 MHz, Acetone-d_6) δ 159.79, 158.54, 132.93, 132.61, 131.17, 131.01, 127.59, 126.28, 122.20, 120.90, 113.86, 108.85, 92.33, 54.69, 45.21, 17.66, 17.26. HRMS (EI) calculated for $[C_{19}H_{20}O_2]^+$ requires *m/z* 280.1458, found *m/z* 280.1457.

Photocatalytic enolate oxidation:

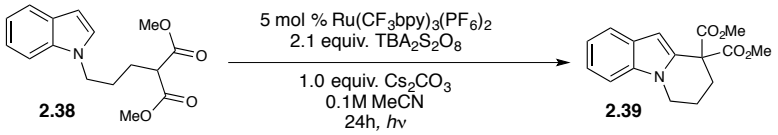

Compound 2.39: Into an oven-dried Schlenk flask containing a magnetic stirbar were weighed indole **2.38** (88.9 mg, 0.307 mmol, 1.0 equiv), cesium carbonate (250.6 mg, 2.56 equiv), tetrabutylammonium persulfate (431.3 mg, 2.08 equiv), and $Ru(CF_3bpy)_3(PF_6)_2$ (**2.40**, 18.7 mg,

0.05 equiv.). Acetonitrile (3 mL) was added, the mixture was stirred to dissolve soluble reagents, and the flask was sealed with a glass stopper. The reaction vessel was then degassed by three freeze-pump-thaw cycles, then backfilled with nitrogen gas. The resulting mixture was then stirred under 23W CFL irradiation for 10 hours, forming a brownish solution with grey-white precipitate. At 10 hours, the reaction mixture was diluted with Et_2O and flushed through a silica plug with excess Et_2O. The eluent was collected, and concentrated *in vacuo*. Trimethyl(phenyl)silane was then added as an external standard, and submitted for ^1H NMR analysis (25% yield versus TMSPh). The desired product could be isolated by flash column chromatography (20% EtOAc/Hexanes) to afford **2.39** (28.6 mg, 32% yield) as a colorless glass. Spectral properties are in agreement with those previously reported.[22]

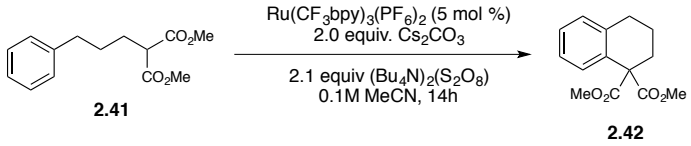

2.41 **2.42**

Compound 2.42: Into an oven-dried Schlenk flask containing a magnetic stirbar were weighed malonate **2.41** (51.2 mg, 0.205 mmol, 1.0 equiv), cesium carbonate (135.6 mg, 2.03 equiv.), tetrabutylammonium persulfate (206.6 mg, 1.49 equiv), and $Ru(CF_3bpy)_3(PF_6)_2$ (**2.40**, 12.8 mg, 0.05 equiv.). Acetonitrile (2 mL) was added, the mixture was stirred to dissolve soluble reagents, and the flask was sealed with a glass stopper. The reaction vessel was then degassed by three freeze-pump-thaw cycles, then backfilled with nitrogen gas. The resulting mixture was then stirred under 23W CFL irradiation for 18 hours, forming a brownish solution with grey-white precipitate. At 18 hours, the reaction mixture was diluted with Et_2O and flushed through a silica plug with excess Et_2O. The eluent was collected, and concentrated *in vacuo*. Trimethyl(phenyl)silane was then added as an external standard, and submitted for ^1H NMR analysis (7% yield relative to TMSPh). The desired product could be isolated by flash column chromatography (30% EtOAc/Hexanes) to afford **2.42** as a colorless glass. ^1H NMR (400 MHz,

Chloroform-d) δ 7.36 – 7.22 (m, 2H), 7.22 – 7.10 (m, 2H), 3.70 (s, 6H), 2.62 (t, J = 7.9 Hz, 2H), 2.16 – 1.99 (m, 2H), 1.80 – 1.61 (m, 2H).

2.6 References

[1] (a) Desai, L.V.; Malik, H. A.; Sanford, M. S. "Oxone as an inexpensive, safe, and environmentally benign oxidant for C-H bond oxygenation." *Org. Lett.* **2006**, *8*, 1141–1144. (b) Campbell, A. N.; Stahl, S. S. "Overcoming the "oxidant problem": Strategies to use O2 as the oxidant in organometallic C-H oxidation reactions catalyzed by Pd (and Cu)." *Acc. Chem. Res.* **2012**, *45*, 851–863.

[2] Kalyanasundaram, K. "Photophysics, photochemistry and solar energy conversion with tris(bipyridyl)ruthenium(II) and its analogues." *Coord. Chem. Rev.* **1982**, *46*, 159–244.

[3] (a) Zeitler, K. "Photoredox catalysis with visible light." *Angew. Chem.* **2009**, *121*, 9969–9974; *Angew. Chem. Int. Ed.* **2009**, *48*, 9785–9789. (b) Yoon, T. P.; Ischay, M. A.; Du, J. "Visible light photocatalysis as a greener approach to photochemical synthesis." *Nat. Chem.* **2010**, *2*, 527–532. (c) Narayanam, J. M. R.; Stephenson, C. R. J. "Visible light photoredox catalysis: applications in organic synthesis." *Chem. Soc. Rev.* **2011**, *40*, 102–113. (d) Xuan, J.; Xiao, W.-J. "Visible-Light Photoredox Catalysis." *Angew. Chem.* **2012**, *124*, 6934–6944; *Angew. Chem. Int. Ed.* **2012**, *51*, 6828–6838. (e) Prier, C. K.; Rankic, D. A.; MacMillan, D. W. C. "Visible Light Photoredox Catalysis with Transition Metal Complexes: Applications in Organic Synthesis." *Chem. Rev.* **2013**, 5322–5363.

[4] (a) Bergonzini, G.; Schindler, C. S.; Wallentin, C-J.; Jacobsen, E. N.; Stephenson, C. R. J. "Photoredox Activation and Anion Binding Catalysis in the Dual Catalytic Enantioselective Synthesis of β-Amino Esters." *Chem. Sci.* **2014**, *5*, 112–116. (b) Konieczynska, M. D.; Dai, C.; Stephenson, C. R. J. "Synthesis of symmetric anhydrides using visible light-mediated photoredox catalysis." *Org. Biomol. Chem.* **2012**, *10*, 4509–4511. (c) Freeman, D. B.; Furst, L.; Condie, A. G.; Stephenson, C. R. J. "Functionally diverse nucleophilic trapping of iminium intermediates generated utilizing visible light." *Org. Lett.* **2012**, *14,* 94–97. (d) Zhao, Y.; Li, Z.; Yang, C.; Lin, R.; Xia, W. "Visible-light photoredox catalysis enabled bromination of phenols and alkenes." *Beilstein J. Org. Chem.* **2014,** *10,* 622–627.

[5] (a) Su, Y.; Zhang, L.; Jiao, N. "Utilization of natural sunlight and air in the aerobic oxidation of benzyl halides." *Org. Lett.* **2011**, *13*, 2168–2171. (b) Zou, Y.-Q.; Chen, J.-R.; Liu, X.-P.; Lu, J.-Q.; Davis, R. L.; Jorgensen, K. A.; Xiao, W.-J. "Highly Efficient Aerobic Oxidative Hydroxylation of Arylboronic Acids: Photoredox Catalysis Using Visible Light." *Angew. Chem.* **2012**, *124*, 808–812; *Angew. Chem. Int. Ed.* **2012**, *51*, 784–788. (d) Cheng, Y.; Yang, J.; Qu, Y.; Li, P. "Aerobic visible-light photoredox radical C-H functionalization: Catalytic synthesis of 2-substituted benzothiazoles." *Org. Lett.* **2012**, *14*, 98–101. (e) Cai, S.; Zhao, X.; Wang, X.; Liu, Q.; Li, Z.; Wang, D. Z. "Visible-light-promoted C-C bond cleavage: Photocatalytic generation of iminium ions and amino radicals." *Angew. Chem.* **2012**, *124*, 8174–8177; *Angew. Chem., Int. Ed.* **2012**, *51*, 8050–8053. (h) Rueping, M.; Vila, C.; Koenigs, R. M.; Poscharny, K.; Fabry, D. C. "Dual catalysis: combining photoredox and Lewis base catalysis for direct Mannich reactions." *Chem. Commun.* **2011**, *47*, 2360–2362. (m) Hari, D. P.; König, B. "Eosin Y catalyzed visible light oxidative C–C

and C–P bond formation." *Org. Lett.* **2011**, *13*, 3852–3855. (t) Zou, Y.-Q.; Lu, L.-Q.; Fu, L.; Chang, N.-J.; Rong, J.; Chen, J.-R.; Xiao, W.-J. "Visible-light-induced oxidation/[3+2] cycloaddition/oxidative aromatization sequence: A photocatalytic strategy to construct pyrrolo[2,1-*a*]isoquinolines." *Angew. Chem.* **2011**, *123*, 7309–7313; *Angew. Chem., Int. Ed.* **2011**, *50*, 7171–7175.

[6] Mulazzani, Q. G.; Sun, H.; Hoffman, M. Z.; Ford, W. E.; Rodgers, M. A. J. "Quenching of the Excited States of Ruthenium(II)-Diimine Complexes by Oxygen." *J. Phys. Chem.* **1994**, *98*, 1145–1150.

[7] (a) Quideau, S.; Pouységu, L.; Deffieux, D. "Chemical and Electrochemical Oxidative Activation of Arenol Derivatives for Carbon-Carbon Bond Formation." *Curr. Org. Chem.* **2004**, *8*, 113-148. (b) Yamamura, S.; Nishiyama, S. "Anodic Oxidation of Phenols Towards the Synthesis of Bioactive Natural Products." *Synlett* **2002**, 533–543.

[8] (a) Coy, E. D.; Cuca, L. E.; Sefkow, M. "COX, LOX and platelet aggregation inhibitory properties of Lauraceae neolignans." *Bioorg. Med. Chem. Lett.* **2009**, *19*, 6922–6925. (b) Barrera, E. D. C.; Suarez, L. E. C. "Three new 7.3',8.5'-connected bicyclo[3.2.1]octanoids and other neolignans from leaves of *Nectandra amazonum* NEES." *Chem. Pharm. Bull.* **2009**, *57,* 639–642. (c) Shen, T.; Wang, X.-N.; Lou, H.-X. "Natural stilbenes: an overview." *Nat. Prod. Rep.* **2009**, *26*, 916–935. (d) Zhang, H.; Qiu, S.; Tamez, P.; Tan, G. T.; Aydogmus, Z.; Hung, N. V.; Cuong, N. M.; Angerhofer, C.; Soejarto, D. D.; Pezzuto, J. M.; Fong, H. H. S. "Antimalarial Agents from Plants II. Decursivine, A New Antimalarial Indole Alkaloid from Rhaphidophora decursiva." *Pharm. Biol.* **2002**, *40*, 221–224. (e) Lachia, M.; Moody, C. J. "The synthetic challenge of diazonamide A, a macrocyclic indole bis-oxazole marine natural product." *Nat. Prod. Rep.* **2008**, *25*, 227–253.

[9] For recent reviews of dihydrobenzofuran synthesis, see: (a) Bertolini, F.; Pineschi, M. "Recent Progress in the Synthesis of 2,3-Dihydrobenzofurans." *Org. Prep. Proc. Int.* **2009**, *41*, 385–418. (b) Sheppard, T. D. "Strategies for the synthesis of 2,3-dihydrobenzofurans." *J. Chem. Res.* **2011**, 377–385. (c) Sefkow, M. "The Stereoselective Synthesis of Neolignans." *Synthesis* **2003**, *17*, 2595–2625.

[10] For examples using preparative electrochemistry, see: (a) Shizuri, Y.; Nakamura, K.; Yamamura, S. "Reactions of alkenes with unstable cations electrogenerated from phenols." *J. Chem. Soc. Chem. Comm.* **1985**, 530–531. (b) Gates, B. D.; Dalidowicz, P.; Tebben, A.; Wang, S.; Swenton, J. S. "Mechanistic Aspects and Synthetic Applications of the Electrochemical and Iodobenzene Bis(trifluoroacetate) Oxidative 1,3-Cycloadditions of Phenols and Electron-Rich Styrene Derivatives." *J. Org. Chem.* **1992**, *57*, 2135–2143. (c) Kerns, M. L.; Conroy, S. M.; Swenton, J. S. *Tet. Lett.* **1994**, *35*, 7529–7532. (d) Chiba, K.; Fukuda, M.; Kim, S.; Kitano, Y.; Tada, M. "Dihydrobenzofuran Synthesis by an Anodic [3+2] Cycloaddition of Phenols and Unactivated Alkenes." *J. Org. Chem.* **1999**, *64*, 7654–7656. (e) El-Seedi, H. R.; Yamamura, S.; Nishiyama, S. "Reactivity of naphthol towards nucleophiles in anodic oxidation." *Tetrahedron* **2002**, *43*, 3301–3304.

[11] Oxidative [3+2] cycloadditions using $Mn(OAc)_3$: Snider, B. B.; Han, L.; Xie, C. "Synthesis of 2,3-dihydrobenzofurans by $Mn(OAc)_3$-based oxidative cycloaddition of 2-cyclohexenones with alkenes. Synthesis of (±)-conocarpan." *J. Org. Chem.* **1997**, *62*, 6978–6984.

[12] Oxidative [3+2] cycloadditions using hypervalent iodide: (a) Wang, S.; Gates, B. D.; Swenton, J. S. "A Convergent Route to Dihydrobenzofuran Neolignans via a Formal 1,3-Cycloaddition

to Oxidized Phenols." *J. Org. Chem.* **1991**, *56*, 1979–1981. (b) Bérard, D.; Jean, A.; Canesi, S. *Tet. Lett.* **2007**, *48*, 8238–8241. (c) Bérard, D.; Giroux, M.; Racicot, L.; Sabot, C.; Canesi, S. "Intriguing formal [2+3] cycloaddition promoted by a hypervalent iodine reagent." *Tetrahedron* **2008**, *64*, 7537–7544. (d) Bérard, D.; Racicot, L.; Sabot, C.; Canesi, S. "Formal [2+3] cycloaddition between substituted phenols and allylsilane." *Synlett* **2008**, 1076–1080. (e) Mohr, A. L.; Lombardo, V. M.; Arisco, T. M.; Morrow, G. W. "Synthesis of Pterocarpan-Type Heterocycles via Oxidative Cycloadditions of Phenols and Electron-Rich Arenes." *Syn. Comm.* **2009**, *39*, 3845–3855.

[13] A very recent report describes the photocatalytic dimerization of resveratrol oligomers: Song, T.; Zhou, B.; Peng, G.-W.; Zhang, Q.-B.; Wu, L-Z.; Liu, Q.; Wang, Y. "Aerobic Oxidative Coupling of Resveratrol and its Analogues by Visible Light Using Mesoporous Graphitic Carbon Nitride (mpg-C_3N_4) as a Bioinspired Catalyst." *Chem. Eur. J.* **2014**, *20*, 678-682.

[14] For leading references, see: (a) Bolletta, F.; Juris, A.; Maestri, M.; Sandrini, D. "Quantum Yield of Formation of the Lowest Excited State of $Ru(bpy)_3^{2+}$ and $Ru(phen)_3^{2+}$." *Inorg. Chim. Acta* **1980**, *44*, L175–L176 (b) White, H. S.; Becker, W. G.; Bard, A. J. "Photochemistry of the tris(2,2'-bipyridine)ruthenium(II)-peroxydisulfate system in aqueous and mixed acetonitrile-water solutions. Evidence for a long-lived photoexcited ion pair." *J. Phys. Chem.* **1984**, *88*, 1840–1846.

[15] (a) Dai, C.; Meschini, F.; Narayanam, J. M. R.; Stephenson, C. R. J. "Friedel-Crafts amidoalkylation via thermolysis and oxidative photocatalysis." *J. Org. Chem.* **2012**, *77*, 4425–4431. (b) Fancy, D. A.; Denison, C.; Kim, K.; Xie, Y.; Holdeman, T.; Amini, F.; Kodadek, T. "Scope, limitations and mechanistic aspects of the photo-induced cross-linking of proteins by water-soluble metal complexes." *Chemistry & Biology* **2000**, *7*, 697–708. (c) Nickel, U.; Chen, Y.-H.; Schneider, S.; Silva, M. I.; Burrows, H. D.; Formosinho, S. J. "Mechanism and kinetics of Photocatalyzed Oxidation of *p*-Phenylenediamines by Peroxydisulfate in the Presence of Tri-2,2'-Bipyridilruthenium(II)." *J. Phys. Chem.* **1994**, *98*, 2883–2888. (d) Minisci, T.; Citterio, A.; Giordano, C. "Electron-transfer processes: peroxydisulfate, a useful and versatile reagent in organic chemistry." *Acc. Chem. Res.* **1983**, *16*, 27–32.

[16] Maxwell, A.; Dabideen, D.; Reynolds, W. F.; McLean, S. "Neolignans from Piper aequale." *Phytochemistry* **1999**, *50*, 499–504.

[17] Achenbach, H.; Utz, W.; Usubillaga, A.; Rodriguez, H. A. "Lignans from *Krameria Ixina*." *Phytochemistry*, **1991**, *30*, 3753–3757.

[18] (a) Snider, B.S. "Manganese(III)-based Oxidative Free-Radical Cyclizations." *Chem. Rev.* **1996**, *96*, 339–363. (b) Melikyan, G.G. "Manganese(III) Mediated Reactions of Unsaturated Systems." *Synthesis* **1993**, 833–850. (c) Iqbal, J.; Bhatia, B.; Nayyar, N.K. "Transition metal-promoted free-radical reactions in organic synthesis: The formation of carbon-carbon bonds." *Chem. Rev.* **1994**, *94*, 519–564.

[19] For a general review traditional methods for the generation of radicals by reduction of activated C–X bonds, see: Curran, D.P. "The Design and Application of Free Radical Chain Reactions in Organic Synthesis. Part 2." *Synthesis*, **1988**, 489–513.

[20] For selected examples using photoredox catalysis, see Ref 3.

[21] For a catalytic variant, see: Oisaki, K.; Abe, J.; Kanai, M. "Manganese-catalyzed aerobic dehydrogenative cyclization toward ring-fused indole skeletons." *Org. Biomol. Chem.* **2013**, *11*, 4569–4572.

[22] Magolan, J.; Kerr, M.A. "Expanding the Scope of $Mn(OAc)_3$ Mediated Cyclizations; Synthesis of the Tetracyclic Core of Tronocarpine." *Org. Lett.* **2006,** *8*, 4561–4564.

[23] (a) Citterio, A.; Sebastiano, R.; Carvayal, M.C. "Synthesis of Substituted Tetrahydronaphthalenes by Mn(III), Ce(IV), and Fe(III) Oxidation of Substituted Diethyl α-Benzylmalonates in the Presence of Olefins." *J. Org. Chem.* **1991**, *56*, 5328–5335. (b) Citterio, A.; Sebastiano, R.; Nicolini, M. "Oxidation of Diethyl ω-Phenylalkenylmalonates by High Valent Metal Salts." *Tetrahedron,* **1993**, *49*, 7743–7760. (c) Citterio, A.; Fancelli, D.; Finzi, C.; Pesce, L. "Manganese(III) Acetate Induced Cyclization of α-Arylalkyl and α-(Aryloxy)alkyl β-Dicarbonyl Derivatives." *J. Org. Chem.* **1989**, *54*, 2713–2718.

[24] Pangborn, A. B.; Giardello, M. A.; Grubbs, R. H.; Rosen, R. K.; Timmers, F. J. "Safe and Convenient Procedure for Solvent Purification." *Organometallics,* **1996**, *15*, 1518–1520.

[25] Ischay, M. A.; Ament, M. S.; Yoon, T. P. "Crossed intermolecular [2+2] cycloaddition of styrenes by visible light photocatalysis." *Chem. Sci.* **2012**, *3*, 2807–2811.

[26] Lin, S.; Ischay, M. A.; Fry, C. G.; Yoon, T. P. "Radical Cation Diels–Alder Cycloadditions by Visible Light Photocatalysis." *J. Am. Chem. Soc.* **2012**, *133*, 19350–19353.

[27] Chuang, K. V.; Navarro, R.; Riesman, S. E. "Benzoquinone-derived sulfinyl imines as versatile intermediates for alkaloid synthesis: Total synthesis of (–)-3-demethoxyerythratidinone." *Chem. Sci.* **2011**, *2*, 1086–1089.

[28] Gautier, A.; Mulatier, J-C.; Crassous, J.; Dutasta, J-P. "Chiral Trialkanolamine-Based Hemicryptophanes: Synthesis and Oxovanadium Complex." *Org. Lett.* **2005**, *7*, 1207–1210.

[29] Crombie, L.; Ryan, A. P.; Whiting, D. A.; Yeboah, S. O. "Synthesis of 4′-*o*-methyl- and 4′,6-di-*o*-methyl-chalaurenol." *J. Chem. Soc. Perkin Trans. I* **1987**, 2783.

[30] Nakamura, H.; Kuroda, H.; Saito, H.; Suzuki, R.; Yamori, T.; Maruyama, K.; Haga, T. "Synthesis and Biological Evaluation of Boronic Acid Containing cis-Stilbenes as Apoptotic Tubulin Polymerization Inhibitors." *ChemMedChem.* **2006**, *1*, 729–740.

[31] Althaus, M.; Mahmood, A.; Suárez, J. R.; Thomas, S. P.; Aggarwal, V. K. "Application of the lithiation-borylation reaction to the preparation of enantioenriched allylic boron reagents and subsequent in situ conversion into 1,2,4-trisubstituted homoallylic alcohols with complete control over all elements of stereochemistry." *J. Am. Chem. Soc.* **2010**, *132*, 4025–4028.

[32] Farney, E.P. "Visible light photocatalysis in the chemistry of radical ions and triplet nitrenes." [dissertation] **2015**, The University of Wisconsin - Madison.

[33] Jeong, M-H.; Lee, K-S.; Hong, Y-T.; Lee, J-S. "Selective and quantitative sulfonation of poly(arylene ether ketone)s containing pendant phenyl rings by chlorosulfonic acid." *J. Membr. Sci.* **2008**, *314*, 212–220.

[34] Wilson, A. A.; Hicks, J. W.; Sadovski, O.; Parkes, J.; Tong, J.; Houle, S.; Fowler, C. J.; Vasdev, N. " Radiosynthesis and Evaluation of [11C-Carbonyl]-Labeled Carbamates as Fatty Acid Amide Hydrolase Radiotracers for Positron Emission Tomography."*J. Med. Chem.* **2013**, *56*, 201–209.

[35] Mori, T.; Inoue, Y.; Grimme, S. "A Combined Experimental and Theoretical Study on the Conformation of Multiarmed Chiral Aryl Ethers." *J. Org. Chem.* **2007**, *72*, 6998–7010.

[36] Johnson, S. M.; Connelly, S.; Wilson, I. A.; Kelly, J. W. "Toward Optimization of the Linker Substructure Common to Transthyretin Amyloidogenesis Inhibitors Using Biochemical and Structural Studies." *J. Med. Chem.* **2008**, *51*, 6348–6358.

[37] Hogan, A-M. L.; Tricotet, T.; Meek, A.; Khokhar, S. S.; O'Shea, D. F. "Applications of Enantioselective Carbolithiation of Ortho-Substituted β-Methylstyrenes." *J. Org. Chem.* **2008**, *73*, 6041–6044.

[38] Rauf, W.; Brown, J. M. "Catalytic Amide-Mediated Methyl Transfer from Silanes to Alkenes in Fujiwara–Moritani Oxidative Coupling." *Angew. Chem. Int. Ed.* **2008**, *47*, 4228–4230.

[39] Gauthier, D.; Lindhardt, A. T.; Olsen, E. P. K.; Overgaard, J.; Skrydstrup, T. "In Situ Generated Bulky Palladium Hydride Complexes as Catalysts for the Efficient Isomerization of Olefins. Selective Transformation of Terminal Alkenes to 2-Alkenes." *J. Am. Chem. Soc.* **2010**, *132*, 7998–8009.

[40] Harrowven, D. C.; Guy, I. L.; Nanson, L. " Efficient Phenanthrene, Helicene, and Azahelicene Syntheses" *Angew. Chem. Int. Ed.* **2006**, *45*, 2242–2245.

[41] Swenson, A. K.; Higgins, K. E.; Brewer, M. G.; Brennessel, W. W.; Coleman, M. G. "Highly selective synthesis of tetra-substituted furans and cyclopropenes: copper(I)-catalyzed formal cycloadditions of internal aryl alkynes and diazoacetates." *Org. & Biomol. Chem.* **2012**, *10*, 7483–7486.

[42] Vassilikogiannakis, G.; Hatsimarinaki, M.; Orfanoloulos, M. "Mechanism of the [2+2] Photocycloaddition of Fullerene C60 with Styrenes." *J. Org. Chem.* **2000**, *65*, 8180–8187.

[43] Guyon, C.; Duclos, M-C.; Sutter, M.; Metay, E.; Lemaire, M. "Reductive alkylation of active methylene compounds with carbonyl derivatives, calcium hydride and a heterogeneous catalyst." *Org. Biomol. Chem.* **2015**, *13*, 7067–7075.

[44] Yoshida, M.; Higuchi, M.; Shishido, K. "Stereoselective Construction of Substituted Chromans by Palladium-Catalyzed Cyclization of Propargylic Carbonates with 2-(2-Hydroxyphenyl)acetates." *Org. Lett.* **2009**, *11*, 4752–4755.

Chapter 3. Mechanistic studies on photocatalytic oxidative [3+2] cycloadditions of phenols

Portions of this work have been previously published:

Blum, T.R.; Zhu, Y.; Nordeen, S.A.; Yoon, T.P. "Photocatalytic Synthesis of Dihydrobenzofurans by Oxidative [3+2] Cycloaddition of Phenols." *Angew. Chem. Int. Ed.* **2014**, *53*, 11056–11059.

3.1 Introduction

With the broad goal of developing strategies for the design of net-oxidative transformations through photocatalysis, we became interested in examining the mechanism of the oxidative [3+2] cycloaddition discussed in Chapter 2. We hoped that a detailed understanding of the mechanism would enable us to both predict viable synthetic applications and to identify problematic steps in the mechanism that could then be improved. This chapter will relate the sum of these mechanistic investigations and highlight results that are of note for further synthetic or mechanistic investigations.

Important mechanistic precedent has been put forward for several oxidative cycloadditions with phenols for both electrochemical and homogenous chemical oxidation. The most complete work has been performed by the lab of Swenton, who outlined several of the potential radical and cationic bond-forming mechanisms in both electrochemical and iodine(III)-mediated oxidative cycloadditions.[1] Phenolic oxidation and deprotonation is proposed to give a resonance-stabilized cationic intermediate (**3.2**). This species can undergo a concerted [5+2] cycloaddition (**3.4**) followed by rearrangement to afford **3.3**, or can afford **3.3** directly by electrophilic attack on **3.2**. Deprotonation and cyclization affords the desired dihydrobenzofuran (**3.5**). Despite the unresolved mechanistic ambiguity between these pathways, distinguishing between them lies outside the scope of this investigation. Seeking to apply our system for photocatalytic oxidation as broadly as possible, our primary goals were instead to validate the ability of the $Ru(bpz)_3^{2+}/S_2O_8^{2-}$ system to perform phenolic oxidation, to identify the species responsible for substrate oxidation in this work, and to interrogate the efficiency of this photocatalytic system. The results of these experimental endeavors are reported herein.

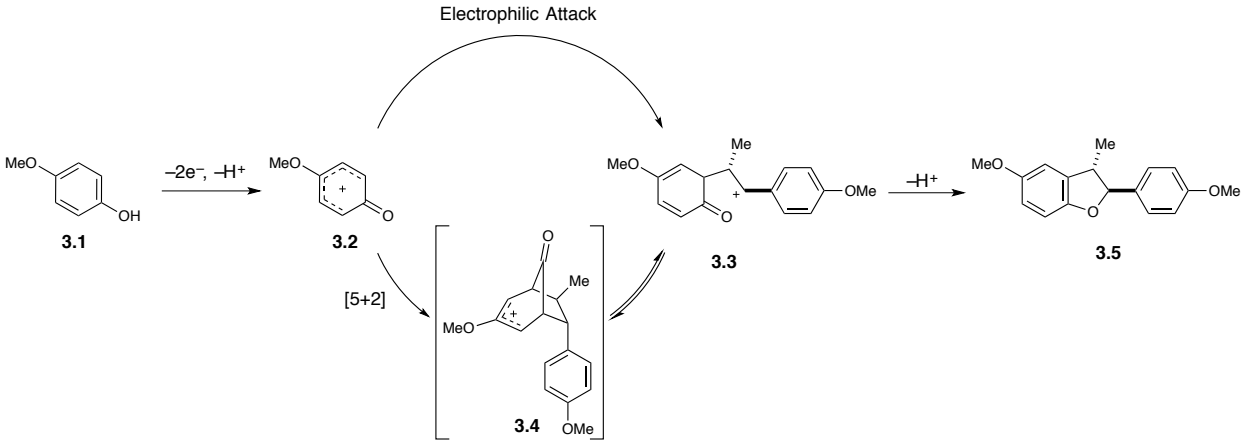

Figure 3.1: Selected proposed bond forming mechanisms in oxidative [3+2] cycloaddition of phenols and alkenes

3.2 Results and Discussion

Our first objective was to confirm the ability of the $Ru(bpz)_3^{2+}/S_2O_8^{2-}$ system to perform phenolic oxidation. While this may initially seem self-evident given the success of the desired cycloaddition, the umpolung nature of this reaction requires that both coupling partners be electron-rich. This provides two substrates that are potentially capable of acting as single electron donors. For example, the initial optimization studies for this reaction were conducted using anethole (**3.9**) and *p*-methoxyphenol (**3.1**), both of which possess quite positive redox potentials and thus react readily with a variety of one-electron oxidants. However, reactions conducted with readily oxidized phenols such as (**3.1**) (E_{ox} = +1.05 V vs. SCE)[1] proceed even in the presence of alkenes that possess oxidation potentials outside of the working range for the photocatalyst ($[Ru]^{3+/2+}$, +1.98 V; styrene, **3.6**, +2.05 V, Figure 3.2).[2] On the other hand, readily oxidized alkenes, such as anethole (**3.9**, +1.10 V)[3] do not generate product in the presence of a less electron

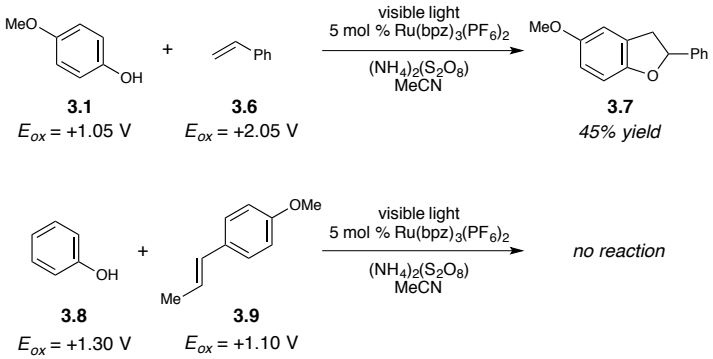

Figure 3.2: Effect of substrate redox potentials on reactivity in the [3+2] cycloaddition

rich phenol (**3.8**, E_{ox} = +1.30 V).[4] This suggests that phenol oxidation, rather than alkene oxidation, is the key step that initiates the cycloaddition.

Second, we wished to identify the species responsible for substrate oxidation. Under the photocatalytic conditions employed, both of the strongly oxidizing species $Ru(bpz)_3^{3+}$ and $SO4^{\cdot-}$ are likely to be present.[5] To investigate this question, we took advantage of the highly tunable nature of Ru(II) polypyridyl catalysts, and examined the effects of photocatalyst oxidizing power on the relative reaction rate (see Table 2.1, entries 6 and 7). The faster rates observed in the presence of the more strongly oxidizing $Ru(bpz)_3^{2+}$ catalyst suggest that direct interaction with the photocatalyst is likely responsible for substrate oxidation. This is supported by fluorescence quenching studies (Figure 3.3D), indicating that, $Ru^*(bpy)_3^{2+}$ reacts with persulfate much more rapidly than the more electron-deficient $Ru^*(bpz)_3^{2+}$ catalyst. Thus the observation that the more reducing catalyst generates increased amounts of sulfate radical ($SO4^{\cdot-}$), but functions as a slower catalyst for the overall transformation suggests that substrate oxidation is performed predominantly by the photocatalyst, and not by sulfate radical anion produced through oxidative quenching of the Ru* excited state.

Finally, several key observations were made regarding the nature and efficiency of the catalytic platform developed in the previous chapter. We observed an induction period coupled with the formation of an orange precipitate over the course of several hours (see Figure 3.2A). The precipitate formed during the induction period is both catalytically competent and necessary for reactivity (see Experimental Section 3.4, Figures 3.5–3.7). These observations suggest that a heterogeneous ruthenium persulfate complex is either a functional catalyst in the oxidative [3+2]

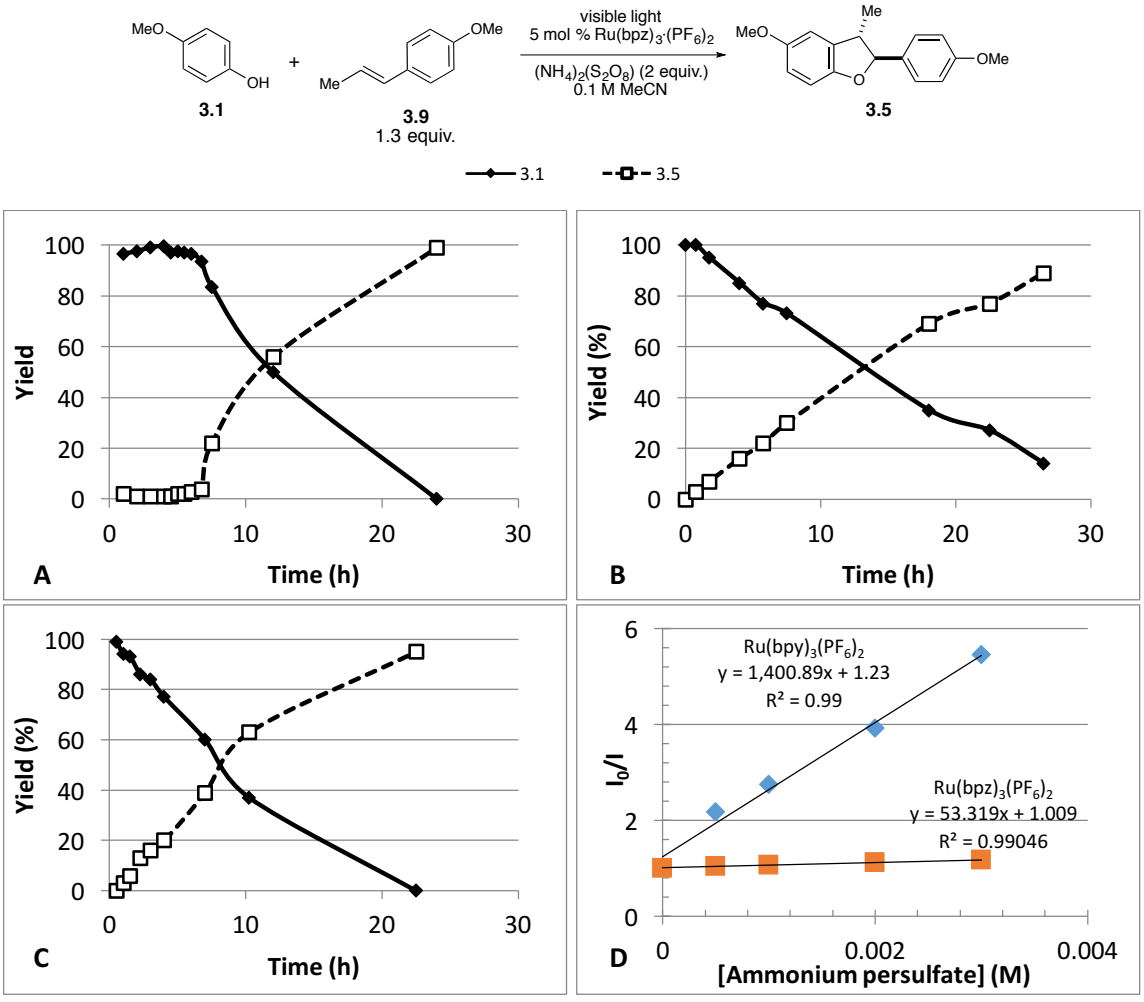

Figure 3.3: Timecourse and kinetic data for the oxidative [3+2] cycloaddition. (A) Reaction timecourse under standard conditions. (B) Reaction timecourse using $Ru(bpz)_3(S_2O_8)$ with 0.5 equiv. ammonium hexafluorophosphate (C) Reaction timecourse under standard conditions with an additional 0.5 equiv. ammonium hexafluorophosphate. (D) Fluorescence quenching studies of Ru photocatalysts with aqueous ammonium persulfate.

cycloaddition, or represents the catalyst resting state. Indeed, when authentic $Ru(bpz)_3(S_2O_8)$ was prepared and directly used in the oxidative [3+2] cycloaddition, this insoluble complex proved to be a competent catalyst, and there was no induction period associated with its use (Figure 3.3B). Intriguingly, the presence of non-sulfate or persulfate counterions in the reaction mixture is essential for the reaction to proceed efficiently. Isolation of the reaction precipitate (presumably a mixture of $Ru(bpz)_3(S_2O_8)$ and $Ru(bpz)_3(SO_4)$) proved catalytically impotent in the absence of ammonium hexaflorophosphate. Additionally, the addition of exogenous ammonium hexafluorophosphate eliminates the induction period observed under the standard reaction conditions, and suggests a key role for this counterion in promoting reactivity. We suggest this anionic hexafluorophosphate may be assisting in turning over the insoluble $Ru(bpz)_3(SO_4)$ salt that is expected to be the product of substrate oxidation.

Based upon these observations, we have proposed the mechanistic model outlined in Figure 3.4. The induction period is consistent with a slow salt metathesis that results in the precipitation of $Ru(bpz)_3(S_2O_8)$. Photoexcitation of this salt followed by oxidative quenching then generates the active oxidant, $Ru(bpz)_3^{3+}$ with concomitant production of sulfate radical anion. Oxidation of phenol (**3.1**) generates the corresponding radical cation (**3.10**), which can be further

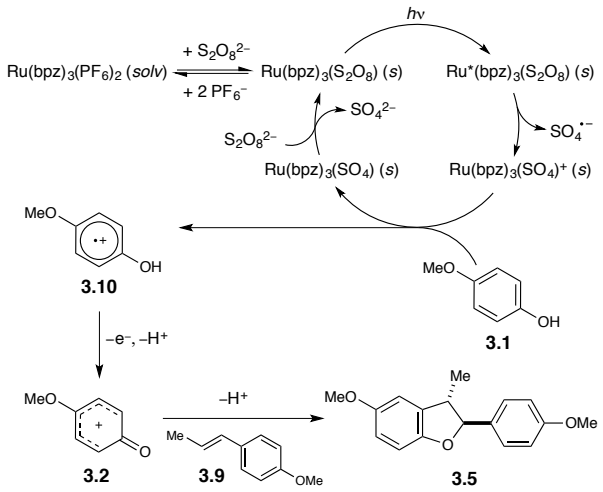

Figure 3.4: Proposed mechanism for the photocatalytic oxidative [3+2] cycloaddition of phenols

oxidized to generate a resonance-stabilized phenoxonium cation (**3.2**) that is trapped by an electron rich olefin to afford dihydrobenzofuran (**3.5**).

3.3 Conclusion

In conclusion, we have investigated several salient features of the mechanism by which the photocatalytic $Ru(bpz)_3^{2+}/S_2O_8^{2-}$ system performs phenol oxidation to drive [3+2] cycloadditions with alkenes. While these experiments validate our initial hypotheses, they also serve to identify several important facets of this chemistry that require further investigation. Due to the densely heterogeneous nature of the reaction medium, and the presence of an induction period, detailed kinetic analyses were not feasible by traditional methods under the optimized reaction conditions. This begs the question whether the reaction is mass-transport or photon limited, and both of these cases could be improved by developing homogenous reaction conditions. Additionally, the fate of the excess oxidizing equivalents present in the reaction is currently not understood, and is intriguing given the high degree of product stability under the strongly oxidizing conditions. Resolution of these questions, and extension of this oxidative platform remains an open investigation in the group.

3.4 Experimental

MeCN was purified by elution through alumina as described by Grubbs.[6] A 23 W (1200 lumens) SLI Lighting Mini-Lynx compact fluorescent light bulb (CFL) was used for all photochemical reactions. Styrene, *trans*-anethole, and 4-methoxyphenol were purchased from Sigma Aldrich, then purified by either distillation or recrystallization prior to use. Synthesis of 2,2'-bipyrazine and Ru(bpz)3(PF6)2 were performed according to previously reported methods.[7]

Unless otherwise noted, all other compounds were purchased from Sigma Aldrich or Strem and used without further purification.

General Procedure: In an oven-dried Schlenk flask were placed the appropriate phenol (1.0 equiv.) and styrene (1.3–2 equiv.) coupling partners, along with $Ru(bpz)_3(PF_6)_2$ (**2**, 5 mol %), and ammonium peroxydisulfate (2.1 equiv.). A magnetic stirbar was added, and MeCN (1–4 mL) was introduced *via* syringe. The flask was sealed with a glass stopper and degassed by three freeze-pump-thaw cycles in a dry-ice/acetone bath. After the final thaw, the flask was backfilled with nitrogen, and stirred evenly under irradiation with a 23 W (1200 lumens) SLI Mini-Lynx compact fluorescent light bulb (placed 3–4 inches from the reaction flask) for the duration of the reaction. During irradiation, the reaction was sonicated periodically (once in the first 2–6 hours, and once every 6–12 hours afterwards), to maintain an even suspension. After completion, the reaction was diluted with EtOAc (5–10 mL), and eluted through a plug of silica using EtOAc. After concentrating *in vacuo*, the crude product was purified by flash-column chromatography.

Representative Reaction Timecourse:

The reaction was set up according to the general procedure with 4-methoxyphenol (**3**, 1 equiv.), *trans*-anethole (1.3 equiv.), ammonium persulfate (2.1 equiv.), $Ru(bpz)_3(PF_6)_2$ (0.05 equiv), and trimethyl(phenyl)silane as an internal standard in MeCN (0.1 M). After degassing by three freeze-pump-thaw cycles, the reaction flask was irradiated with a 23 W CFL light source and reaction progress was monitored by ^1H NMR using reaction aliquots taken under N_2 purge to maintain an oxygen-free environment. The resulting data (Figure 3.3A) revealed an induction period of several hours corresponding to the formation of a red precipitate in the reaction.

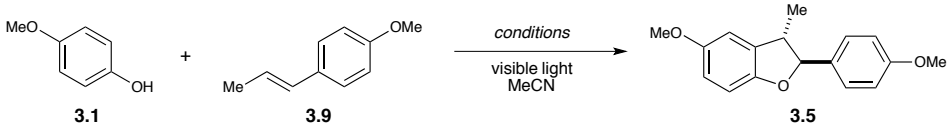

Precipitate removal experiments

Reactions were set up according to the general procedure with 4-methoxyphenol (1 equiv.), *trans*-anethole (1.3 equiv.), ammonium persulfate (2.1 equiv.), $Ru(bpz)_3(PF_6)_2$ (0.05 equiv), and trimethyl(phenyl)silane as an internal standard in MeCN (0.1M). After degassing by three freeze-pump-thaw cycles, the reaction flasks were irradiated with a 23 W CFL light source, and stirred for 4.5 h. The reaction media were then filtered separately through medium frits into clean, dry Schlenk flasks containing magnetic stirbars. The resulting solutions were then either immediately degassed again by three freeze-pump-thaw cycles (Figure S1-A), or degassed by 3x freeze-pump-thaw cycles following the addition of ammonium persulfate (2.1 equiv.) (Figure S1-B). The resulting reactions were then monitored by ^1H NMR using reaction aliquots taken under N_2 purge to maintain an oxygen-free environment. Both experiments resulted in negligible further consumption of **3**, indicating that the majority of the active catalyst was likely removed by filtration.

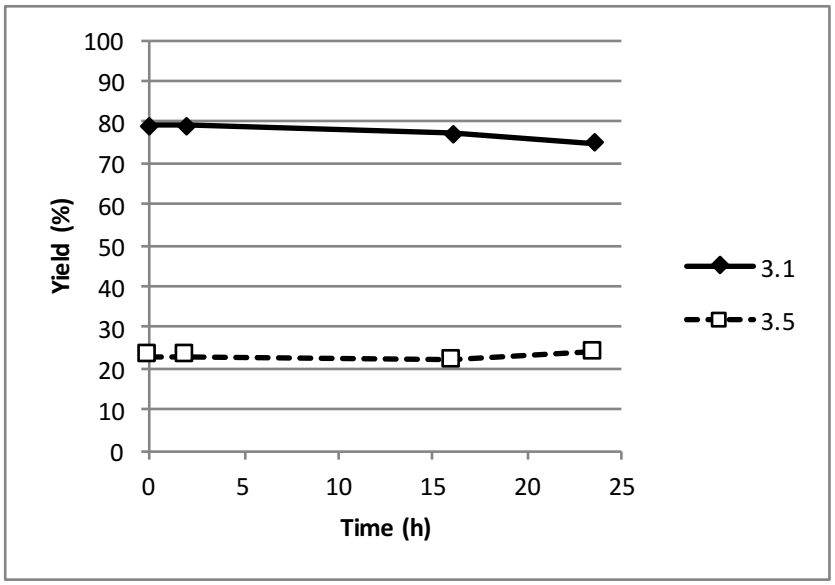

Figure 3.5: Precipitate removal experiment with no added ammonium persulfate

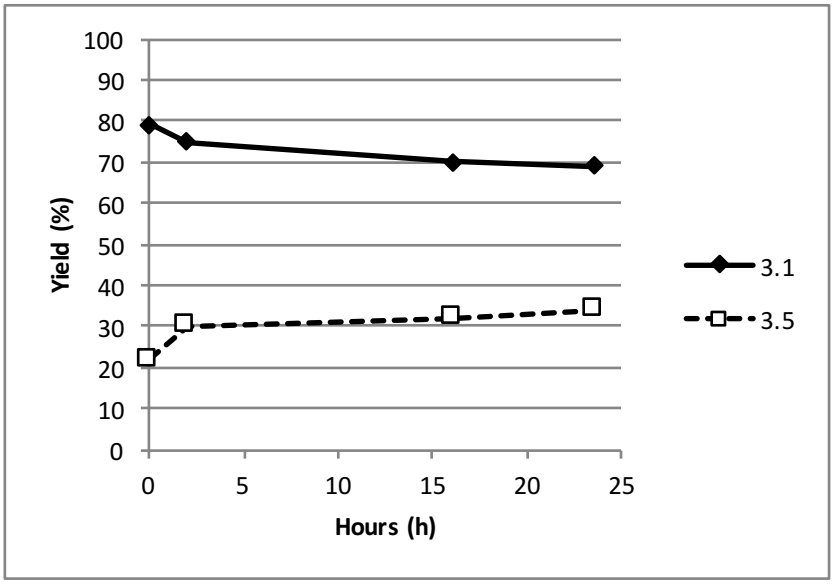

Figure 3.6: Precipitate removal experiment with 2.1 equiv of added ammonium persulfate.

Catalyst filtration experiment

The reaction was set up according to the general procedure with 4-methoxyphenol (**3**, 1 equiv.), *trans*-anethole (1.3 equiv.), ammonium persulfate (2.1 equiv.), $Ru(bpz)_3(PF_6)_2$ (0.05 equiv) in MeCN (0.1 M). After degassing by three freeze-pump-thaw cycles, the reaction flask was irradiated with a 23 W CFL light source and stirred for 7 h. The reaction medium was then filtered through a medium frit, and the collected orange-brown solid was washed thoroughly with MeCN. The solid was then dried thoroughly on the frit, and care was taken to exclude light wherever possible. The dry solid was then added to a new Schlenk flask containing 4-methoxyphenol (**5**, 1 equiv.), *trans*-anethole (1.3 equiv.), ammonium persulfate (2.1 equiv.), and trimethyl(phenyl)silane in MeCN (0.1 M). The resulting mixture was then degassed by three freeze-pump-thaw cycles. The reaction was then monitored by ^{1}H NMR using reaction aliquots taken under N_2 purge to maintain an oxygen-free environment. The resulting data (Figure S2) suggest that the solid precipitate contains the active catalyst.

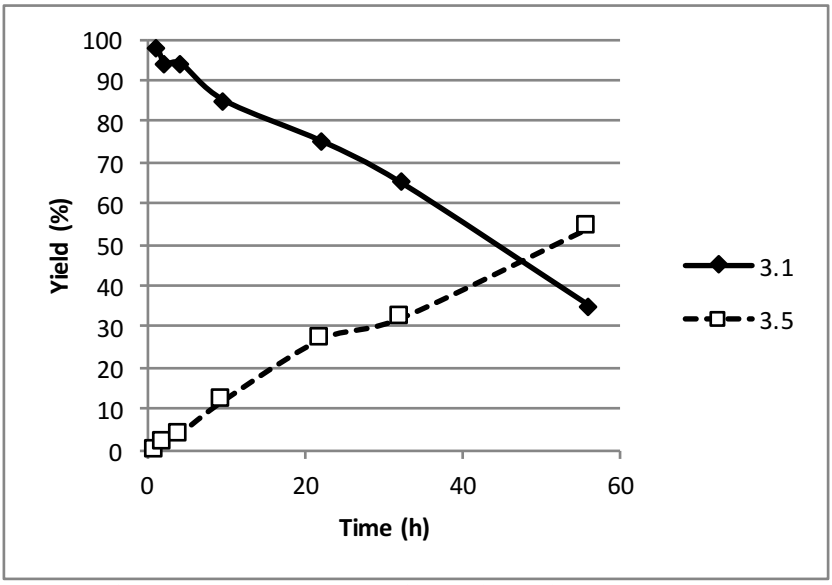

Figure 3.7: Catalyst filtration timecourse

Synthesis and Reactivity of $Ru(bpz)_3(S_2O_8)$

*Note: All manipulations were undertaken in a manner that would minimize light exposure due to the potential photosensitivity of the $Ru(bpz)_3(S_2O_8)$ salt. The synthesis of this salt was thus performed in a darkened lab, inside a fume hood made opaque with aluminum foil to exclude light scattered from external sources.

$Ru(bpz)_3(PF_6)_2$ (1 equiv.) and $(NBu_4)_2(S_2O_8)$[8] (1 equiv.) were combined in a 15 mL flame-dried vial containing a magnetic stirbar. MeCN (0.1 M) was added to the vial, which was then sealed, and the contents were stirred for 20 h in the dark forming a dark precipitate as observed by red light. The resulting suspension was filtered through a medium frit, and the solid was washed generously with MeCN, then with Et_2O, and finally dried under vacuum. The isolated solid was then used as a catalyst without further purification. The photochemical reaction was set up according to the general procedure in a dark lab with 4-methoxyphenol (**3**, 1 equiv.), *trans*-anethole (1.3 equiv.),

ammonium persulfate (2.1 equiv.), $Ru(bpz)_3(S_2O_8)$ (0.05 equiv), ammonium hexafluorophosphate (0.5 equiv) and trimethyl(phenyl)silane as an internal standard in MeCN (0.1 M). After degassing by three freeze-pump-thaw cycles, the reaction flask were irradiated with a 23 W CFL light source, and reaction progress was monitored by ^1H NMR using reaction aliquots taken under N_2 purge to maintain an oxygen-free environment. The resulting data can be seen in Figure 3.3B.

3.5 References

[1] Gates, B.D.; Dalidowicz, P.; Tebben, A.; Wang, S.; Swenton, J.S. "Mechanistic Aspects and Synthetic Applications of the Electrochemical and Iodobenzene Bis(trifluoroacetate) Oxidative 1,3-Cycloadditions of Phenols and Electron-Rich Styrene Derivatives." *J. Org. Chem.* **1992**, *57*, 2135–2143.

[2] (a) Rillema, D.P.; Allen, G.; Meyer, T.J.; Conrad, D. "Redox properties of ruthenium (II) tris chelate complexes containing the ligands 2,2'-bipyrazine, 2,2'-bipyridine, and 2,2'-bipyrimidine." *Inorg. Chem.* **1983**, *22*, 1617-1622. (b) Schepp, N. P.; Johnston, L.J. "Reactivity of Radical Cations. Effect of Radical Cation and Alkene Structure on the Absolute Rate Constants of Radical Cation Mediated Cycloaddition Reactions." *J. Am. Chem. Soc.* **1996**, *118*, 2872–2881.

[3] Yueh, W.; Bauld, N.L. "Mechanistic Aspects of Aminium Salt-Catalyzed Diels–Alder Reactions: The Substrate Ionization Step." *J. Phys. Org. Chem.* **1996**, *9*, 529–538.

[4] Pratt, D.A.; Pesavento, R. P.; Van der Donk, W. A. "Model studies of the histidine-tyrosine cross-link in cytochrome C oxidase reveal the flexible substituent effect of the imidazole moiety." *Org. Lett.* **2005**, *7*, 2735–2738.

[5] (a) White, H.S.; Becker, W.G.; Bard, A.J. "Photochemistry of the tris(2,2'-bipyridine) ruthenium(II)-peroxydisulfate system in aqueous and mixed acetonitrile-water solutions. Evidence for a long-lived photoexcited ion pair." *J. Phys. Chem.* **1984**, *88*, 1840–1846. (b) White, H.S.; Bar, A.J. "Electrogenerated chemiluminescence. 41. Electrogenerated chemiluminescence and chemiluminescence of the $Ru(2,2'\text{-bpy})_3^{2+}$-$S_2O_8^{2-}$ system in acetonitrile-water solutions." *J. Am. Chem. Soc.* **1982**, *104*, 6891–6895. (c) Nickel, U.; Chen. Y-H.; Schneider, S.; Silva, M.I.; Burrows, H.D.; Formosinho, S.J. "Mechanism and kinetics of Photocatalyzed Oxidation of P-Phenylenediamines by Peroxydisulfate in the Presence of Tri-2,2'-Bipyridilruthenium(II)." *J. Phys. Chem.* **1994**, *98*, 2883–2888.

[6] Pangborn, A. B.; Giardello, M. A.; Grubbs, R. H.; Rosen, R. K.; Timmers, F. J. "Safe and Convenient Procedure for Solvent Purification." *Organometallics,* **1996**, *15*, 1518–1520.

[7] Lin, S.; Ischay, M.A.; Fry, C.G.; Yoon, T.P. "Radical Cation Diels–Alder Cycloadditions by Visible Light Photocatalysis." *J. Am. Chem. Soc.* **2012**, *133*, 19350–19353.

[8] J-H. Lee, D. Bhattarai, G. Keum, **2013**. Tetrabutylammonium peroxydisulfate. *E-EROS Encyclopedia of Reagents for Organic Synthesis*.

Chapter 4. Lewis acid-coupled asymmetric energy transfer cycloadditions of 2'-hydroxychalcones

4.1 Introduction

The control of absolute stereochemistry in organic synthesis has emerged as a powerful capability in the construction of useful molecular scaffolds for a wide range of applications. In considering the totality of asymmetric synthesis, it is notable that the vast majority of strategies in enantioselective catalysis function through controlling the reactivity of ground-state species with chiral catalysts or auxiliaries.[1,2] Despite the power of photochemical methods to facilitate access to unique molecular topologies, progress in asymmetric photochemistry has traditionally lagged behind other classes of synthetic transformations. Even among the few highly enantioselective catalytic photoreactions, the majority involve stereocontrol of reactive species in their electronic ground state. These are often photogenerated open-shell radicals, which participate in downstream enantioselective bond forming steps.[3] The ability to directly control the generation and reactivity of *electronically excited* molecules has proven a significant challenge in organic synthesis.

Catalytic strategies for using electronically excited intermediates in organic synthesis are often hampered by the limited lifetime of these species, which result from the fast unimolecular deactivation pathways available to excited singlet and triplet states. Because of this limited lifetime, electronically excited species are present in exceedingly low concentrations in solution, and this constrains their ability to interact with other species in solution. To compound this difficulty, electronically exited intermediates are also highly destabilized, and therefore participate in thermodynamically favorable reactions at generally fast rates. As a result of these two general characteristics, the ability of exogenous catalysts to intercept and influence the reactivity of electronically excited intermediates is often difficult. Successful methods for controlling the enantioselectivity in reactions of electronically excited species thus require the selective generation of the excited intermediates within a well-defined chiral environment. Several elegant catalytic methods for achieving this have been reported in the context of [2+2]

cycloadditions, including the use of chiral sensitizers,[4] chiral exciplexes,[5] and chiral Lewis acid catalysis.[6] Because Lewis acid catalysis in particular offers a mature catalytic platform with a diverse array of well-studied catalysts and ligand scaffolds, a general method for leveraging this knowledge in the catalysis of excited state photoreactions would offer a powerful tool for photochemical synthesis.

Seminal work from Bach has established two modes of Lewis acid catalysis as viable strategies for performing enantioselective photocycloadditions with electronically excited species.[6] The first catalytic strategy operates through Lewis acid promoted stabilization of the photoexcited singlet state, resulting in accelerated intersystem crossing and faster reactivity in Lewis acid complexed coumarins. In the second, Lewis acid coordination affords a bathochromic shift in the absorption spectrum of an enone, allowing for the selective excitation of only a chiral Lewis acid complex using a monochromatic light source that avoids excitation of the free achiral substrate. These impressive studies, however, require direct irradiation of the substrate, and thus high enantioselectivities require a complex matching of substrate and Lewis acid properties to effectively tune the absorption, lifetime, and intersystem crossing (ISC) properties of the chiral Lewis acid-substrate complex. Because of this, the range of substrates that have been shown to provide high ee's using Bach's chiral Lewis acid strategy have, to date, occupied a relatively narrow range. Only intramolecular [2+2] cycloadditions of a small set of cyclic enones have thus far been reported.

A potentially more general approach to this challenge would be to decouple the sensitive photophysical properties of a Lewis acid-bound substrate from its excited state reactivity via triplet sensitization. In this chapter, we describe the realization of this strategy and describe a dual catalyst system comprising a transition metal photocatalyst and a chiral Lewis acid co-catalyst that enables highly enantioselective [2+2] cycloaddition reactions via Lewis acid catalyzed energy transfer sensitization.

4.2 Results and Discussion

Our interest in this system arose serendipitously during an investigation into the known cycloaddition reactions of 2'-hydroxychalcone (**4.1**) from the work of Porco and coworkers.[7] In this work, single electron transfer is believed to promote [4+2] cycloaddition reactivity in the presence of electron rich dienes.[8] In an attempt to study this process under photocatalytic conditions, we observed the unexpected and efficient formation of [2+2] cycloaddition product **4.2** in the presence of a number of Lewis acid additives under visible light irradiation with Ru(II) polypyridyl photocatalysts. Several oxophilic d^0 Lewis acids including $Sc(OTf)_3$ were found to catalyze the photochemical cycloaddition of 2'-hydroxychalcone with isoprene in good yields (Figure 4.1). Because control reactions demonstrated that the reaction proceeded only in the presence of both Lewis acid and photocatalyst, we wondered if the use of a chiral Lewis acid might

Table 4.1: Discovery and optimization of Lewis acid-catalyzed [2+2] cycloaddition of 2'-hydroxychalcones

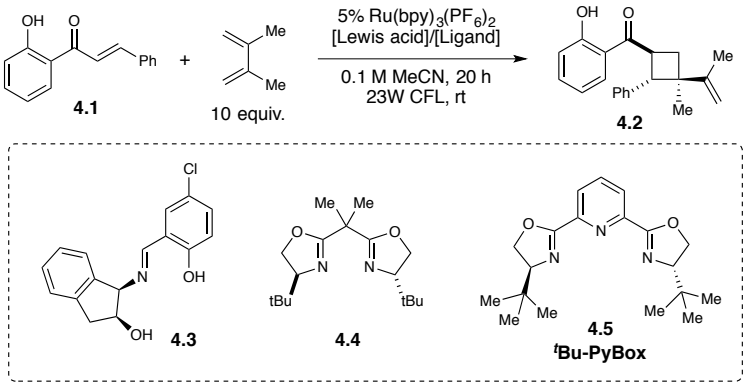

Entry	[Lewis acid]	Ligand	Note	Yield	%ee
1	-none-	none	–	< 5%	–
2	$Sc(OTf)_3$ (1 equiv.)	none	–	70%	–
3	$Sc(OTf)_3$ (1 equiv.)	none	No light	< 5%	–
4	$Sc(OTf)_3$ (1 equiv.)	none	No $Ru(bpy)_3(PF_6)_2$	< 5%	–
5	$Sc(OTf)_3$ (20 mol%)	**4.3** (30 mol%)	–	25%	4%
6	$Sc(OTf)_3$ (20 mol%)	**4.4** (30 mol%)	–	34%	0%
7	$Sc(OTf)_3$ (20 mol%)	**4.5** (30 mol%)	–	79%	75%
8	$Sc(OTf)_3$ (20 mol%)	**4.5** (30 mol%)	0.03 M 3:1 ^{i}PrOAc: MeCN	65%	96%
9	$Sc(OTf)_3$ (10 mol%)	**4.5** (15 mol%)	2.5 mol% $Ru(bpy)_3(PF_6)_2$, 0.03 M 3:1 ^{i}PrOAc: MeCN	89%	93%

All yields obtained by ^{1}H NMR using phenanthrene as an internal standard.

enable the development of an enantioselective version of this photoreaction. After examining several classes of chiral ligands, including *cis*-iminoindanols (**4.3**) and bisoxazolines (**4.4**), we were pleased to find that Sc(III) PyBox complexes generally worked well in the chemistry, and ^{t}Bu-PyBox (**4.5**) in particular provided particularly promising results (Table 4.1, entries 5–7). Subsequent optimization of solvent, concentration, and catalyst loading afforded our optimized conditions (Table 4.1, entries 8–9), which produced cyclobutane **4.2** in high yields and excellent enantioselectivity.

This highly enantioselective cycloaddition presents an intriguing improvement upon the state of the art [2+2] cycloaddition methods previously reported in the literature. First, the reaction requires substantially lower loadings of chiral Lewis acid catalyst than the methods described by Bach (10 mol% vs. ca. 50 mol%). This is also one of the the first highly

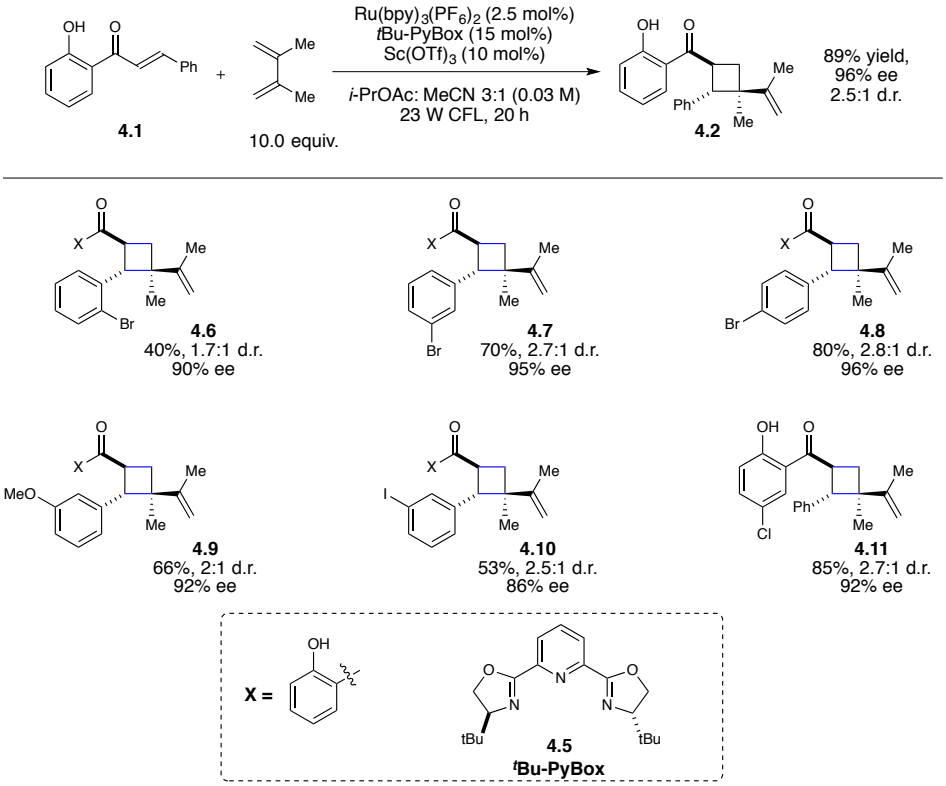

Figure 4.1: Preliminary scope of the enantioselective Lewis acid catalyzed photocycloaddition of 2'-hydroxychalcones

enantioselective catalytic versions of an intermolecular photocycloaddition, and one of the few examples involving an acyclic enone.[9] We have consequently begun an exploration of the synthetic scope and limitations of this transformation. Preliminary results are briefly outlined in Figure 4.2. Steric and electronic perturbation of the hydroxychalcone β-phenyl substituent is well-tolerated, with all positional isomers of the bromine-substituted chalcone affording high

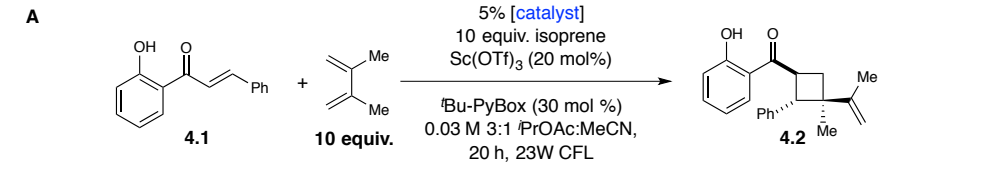

Entry	[catalyst]	Excited state potentials (vs. SCE) 2**/3+	2**/1+	Yield [2+2]
1	$Ru(bpy)_3(PF_6)_2$	–0.81 V	+0.77 V	89%
2	$Ru(CF_3bpy)_3(PF_6)_2$ (**4.12**)	–	+1.11	15%
3	$Ru(deeb)_3(PF_6)_2$ (**4.13**)	–0.42 V	+1.07 V	68%
4	$Ru(dmb)_3(PF_6)_2$ (**4.14**)	–1.16 V	+0.20 V	78%
5	$Ru(dtbbpy)_3(PF_6)_2$ (**4.15**)	–1.05 V	+0.72	41%

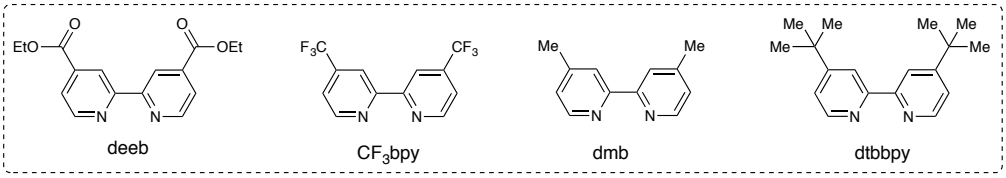

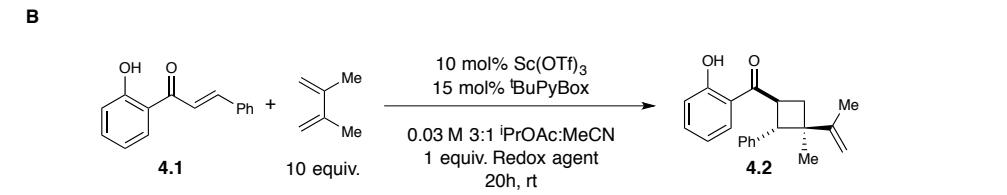

Oxidant	Result
CAN	0% yield, 69% RSM
$Fe(acac)_3$	0% yield, 85% RSM
$K_3[Fe(CN)_6]$	0% yield, 105% RSM
$Mn(OAc)_3$	0% yield, 104% RSM
$(Ar_3N)\cdot SbCl_6$	0% yield, 96% RSM

Reductant	Result
TDAE	0% yield, 88% RSM
SmI_2	0% yield, 34% Chalcone reduction 2% RSM**
Li[Naphthalenide]	0% yield, 70% RSM**
Cobaltocene	0% yield, 54% chromanone 26% RSM

**iPrOAc replaced with THF due to known reactivity of esters

Figure 4.2: Investigations into a photoinduced electron transfer pathway in the asymmetric [2+2] cycloaddition of 2'-hydroxychalcones

yields and enantioselectivities (**4.6**–**4.8**), and electron-donating methoxy substituents affording good yields and excellent enantioselectivities (**4.9**). The hydroxyphenyl ring has also proven amenable to modification, with halogen substitution also providing efficient access to highly enantioenriched cyclobutanes (**4.11**). Additional scope studies examining elaboration of the hydroxychalcone scaffold, as well as additional olefin cycloaddition partners are currently underway.

While several groups, including our own, have published on the feasibility of [2+2] cycloadditions facilitated by electron transfer, several features of this reaction argue against this mechanism of activation being relevant to this new enantioselective cycloaddition.[10] First, we observe no correlation between the redox potential of the Ru(II) photocatalyst on the rate or yield of the [2+2] cycloaddition (Figure 4.2A). For a reaction initiated by electron transfer, sensitivity to the electrochemical properties of the photocatalyst would be expected, but was not observed. Additionally, when exposed to a number of chemical single electron oxidants and reductants, the chalcone and diene partners proved unreactive toward each other under conditions both with and without $Sc(OTf)_3$/*t*Bu-PyBox (Figure 4.3). These results suggested to us that an electron transfer mechanism for the photocycloaddition is unlikely.

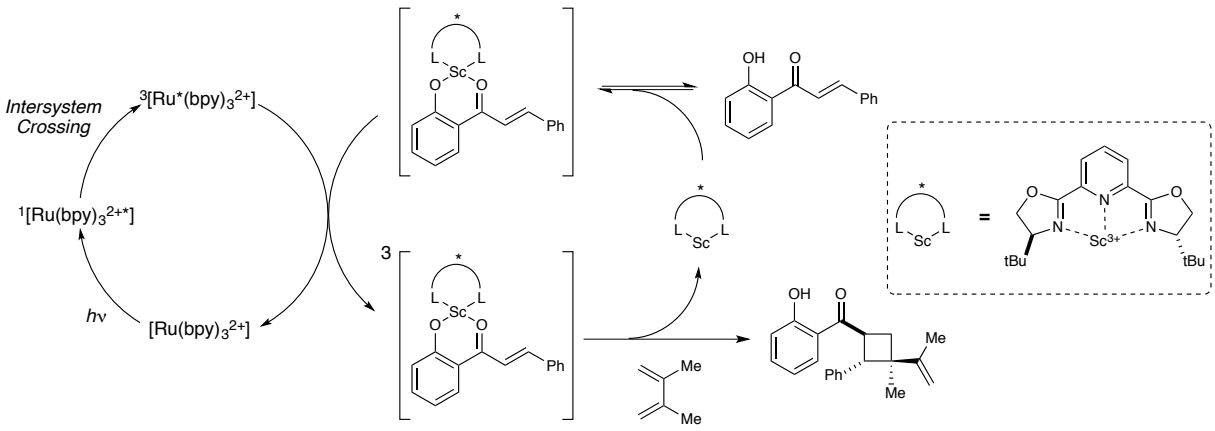

Figure 4.3: Proposed mechanism for the enantioselective Lewis acid-coupled energy transfer [2+2] cycloaddition of 2'-hydroxychalcones

Thus we became interested in studying whether the mechanism of photoactivation in this dual catalyst system involved *energy transfer*. The binding of a Lewis acid to an enone is known to alter the energetics of its excited states.[11] We thus hypothesized that this enantioselective photoreaction might involve Lewis acid-catalyzed energy transfer from the photoexcited $Ru(bpy)_3(PF_6)_2$ catalyst to the Lewis acid bound hydroxychalcone.

Based upon this hypothesis, we have proposed the mechanism outlined in Figure 4.3. Irradiation of $Ru(bpy)_3^{2+}$ results in rapid excitation and intersystem crossing to the photoexcited triplet state. This then selectively performs energy transfer to an equivalent of Sc-bound hydroxychalcone. The resulting electronically excited chalcone complex undergoes a [2+2] cycloaddition on the triplet hypersurface to afford the products shown. Because the energy transfer event occurs only in the presence of the chiral Lewis acid and not to the free achiral substrate, the [2+2] cycloadduct is produced in excellent ee while avoiding competitive racemic background photoreactions.

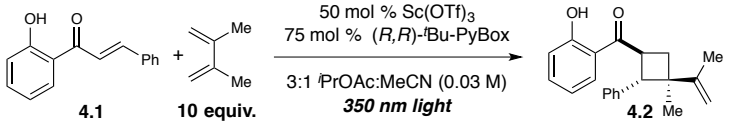

4.1 **10 equiv.** **4.2**

Entry	Photocatalyst (loading)	Result
1	$Ru(bpy)_3(PF_6)_2$ (5 mol %)	86% yield, 94% ee
2	Benzil (50 mol %)	38% yield, 89% ee
3	1-naphthylphenyl ketone (50 mol %)	73% yield, 90% ee

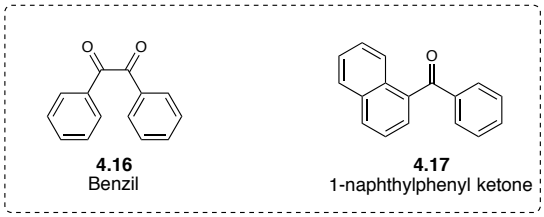

4.16 Benzil

4.17 1-naphthylphenyl ketone

Figure 4.4: Reconstitution of [2+2] cycloaddition with alternative energy transfer photosensitizers

A number of preliminary mechanistic considerations support this mechanistic model. The S_0-T_1 gap (E_T) for 2'-hydroxychalcones has been reported to be 54 kcal/mol.[12] This is in agreement with our experimental results showing that $Ru(bpy)_3^{2+}$ (E_T = 46 kcal/mol) is incapable of facilitating the [2+2] cycloaddition in the absence of Lewis acid. Importantly, if an energy transfer process is relevant to the Lewis acid catalyzed cycloaddition, it should be feasible to promote the reaction using other similarly energetic triplet sensitizers. Indeed, when the cycloaddition of 2'-hydroxychalcone and 2,3-dimethyl-1,3-butadiene was performed under 350 nm irradiation in the presence of benzil (**4.16**) or 1-naphthylphenyl ketone (**4.17**), we observed moderate yields of the desired [2+2] cycloaddition product in comparable enantioselectivity to the $Ru(bpy)_3(PF_6)_2$ catalyzed reaction (Figure 4.4). Because of the high sensitivity of asymmetric catalysis to changes in mechanism, we interpret this as strong evidence for Lewis acid catalyzed triplet sensitization as the operative pathway. We believe that the binding of Sc^{3+} lowers the S_0-T_1 energy gap of 2'-hydroxychalones, which affords an energetically favorable energy transfer process from the $^3[Ru^*(bpy)_3^{2+}]$ photocatalyst. Experimental observation and characterization of these electronically excited species is the subject of ongoing research.

Given the elegant work of Bach in the area of Lewis acid catalyzed asymmetric photochemistry,[6] it is instructive to consider the possibility of direct photoexcitation of the Lewis acid-chalcone complex without sensitizer intermediacy. In analogy to other enones,[6d,e] the

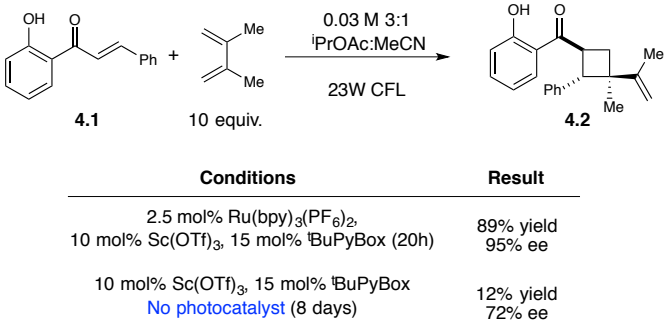

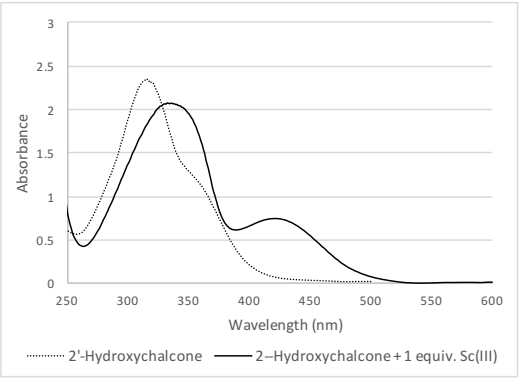

Figure 4.5: Background Lewis acid catalyzed photochemical [2+2] cycloaddition.

putative π,π* transtition of the 2'-hydroxychalcone undergoes a large bathochromic shift upon exposure to $Sc(OTf)_3$, affording strong absorption in the visible spectrum (λ_{max} = 421 nm, ε = 7490 $M^{-1}cm^{-1}$). Despite this, the Lewis acid-chalcone complex undergoes exceedingly inefficient [2+2] cycloaddition in the absence of photocatalyst, requiring several days to reach only 12% yield with 72% ee (figure 4.5). We believe that this is due to inefficient intersystem crossing from S_1 to T_1, resulting in fast relaxation from the singlet photoexcited state in the Lewis acid bound chalcone. We therefore posit that triplet sensitization is essential for efficient access to the long-lived, reactive triplet excited state of the Lewis acid chalcone complex, and that triplet sensitization offers a strategy around inefficient singlet state behavior in a co-catalytic paradigm.

4.3 Conclusion

Because the current state-of-the-art methods for performing enantioselective photochemistry using Lewis acid catalysis rely on direct irradiation of a chiral Lewis acid-substrate complex, they are highly sensitive to structural perturbations in either the substrate or Lewis acid species, since these changes can directly impact the photochemical properties of the complex. Lewis acid-coupled triplet sensitization offers a means around several of the inherent challenges in this strategy by circumventing the short lived singlet state of the Lewis acid-substrate complex, and enabling both efficient *and* selective access to a chiral reactive species in an electronically excited state. We are optimistic that this paradigm will expand both the *substrate classes* and *Lewis acid catalysts* that can be applied to asymmetric energy transfer photochemistry. Exploring the generality of this strategy, as well as exploring new modes of energy transfer co-catalysis, such as amine-enamine organocatalysis, remains a primary goal of this research moving forward.

4.4 Contributions

Dr. Zachary Miller performed the scope studies described above, and is responsible for confirming the structure of **4.2** by X-ray crystallographic analysis with Dr. Ilia Guzei.

4.5 Experimental

General Information: MeCN solvent was purified by elution through alumina as described by Grubbs.[13] A 23 W (1200 lumens) SLI Lighting Mini-Lynx compact fluorescent light bulb (CFL) was used for all photochemical reactions uless otherwise noted. Flash-column chromatography was performed with Silicycle 40–63Å silica (230–40 mesh). 2,3-Dimethyl-1,3-butadiene was purchased from Sigma Aldrich and distilled prior to use. Bisoxazoline ligand **4.3** and Pyridine Bisoxazoline ligand **4.5** were prepared according to literature methods.[14] $Ru(bpy)_3(PF_6)_2$ was prepared according to known procedures.[15] Unless otherwise noted, all other compounds were purchased from Sigma Aldrich or Strem and used without further purification.

Enantiomeric excesses were determined by chiral SFC of isolated material using a Waters Investigator system with Daicel CHIRALPAK® columns and Chromasolv®-grade MeOH. Diastereomer ratios for all compounds were determined by ^{1}H NMR analysis of unpurified reaction mixtures and assigned based on analogy to compound **4.2**, which was assigned by 1D NOESY (Blum, T.R.) and X-ray crystallographic analysis (Dr. Zachary Miller). ^{1}H and ^{13}C NMR data for all previously uncharacterized compounds were obtained using a Bruker AVANCE-400 spectrometer and are referenced to TMS (0.0 ppm) and $CDCl_3$ (77.0 ppm), respectively. These facilities are funded by the NSF (CHE-9974839, CHE-9304546) and the University of Wisconsin.

Substrate Synthesis

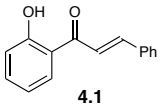

4.1

2'-hydroxychalcone (**4.1**)*:* 2'-Hydroxyacetophenone (2.5 mL, 20.4 mmol) and benzaldehyde (2.1 mL, 20.7 mmol) were dissolved in MeOH (100 mL) in a 250 mL roundbottom flask, a magnetic stirbar was added, and the solution cooled to 4 °C in an ice bath. To the vigorously stirring solution was added 40 mL of 50% aq. KOH over 5 min. The starting solution changed gradually from yellow to dark red ovar the course of the addition, and at 5 min a fine precipitate was observed. After the addition was complete, the reaction mixture was allowed to warm to room temperature, and was stirred for 20 hours. Periodic mixing (every 4–8 hrs) with a metal spatula was required to break up clumps of precipitated yellow solid, which prevented efficient mixing. At 20 hours, the reaction medium was poured into 150 mL of ice water in an Erlenmeyer flask, and rinsed in with additional H_2O and MeOH. The resulting mixture was acidified to pH = 1 with 6M HCl, and allowed to stir vigorously for 20 min, forming a brilliant yellow precipitate. The yellow solid was filtered, and washed extensively with dH_2O, then allowed to dry on the frit, and subsequently under vacuum. The resulting solid was purified further by recrystallization from EtOH if necessary to afford the title compound as a fine yellow powder (3.30 g, 72% yield). Spectroscopic data are in agreement with reported literature values.[16]

General procedure for probe-scale racemic photochemical cycloadditions:

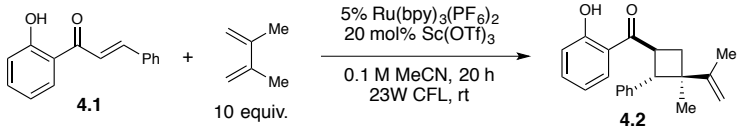

4.1 10 equiv. **4.2**

In an oven-dried 2 dram vial were combined 2'-hydroxychalcone (22.4 mg, 0.100 mmol), $Sc(OTf)_3$ (9.8 mg, 0.20 equiv.), $Ru(bpy)_3Cl_2 \cdot 6H_2O$ (3.6 mg, 0.05 equiv), and phenanthrene (10-15 mg as internal standard). A magnetic stirbar was added, and the contents were dissolved in MeCN (1 mL). To the resulting solution was added 2,3-dimethyl-1,3-butadiene (110 μL, 9.72 equiv.) by syringe, then the vial was sealed with a Teflon-lined cap and stirred under 23W CFL irradiation

for 20 h at room temperature. The reaction progress can be monitored by TLC (10% EtOAc/Hexanes). At 20 h, the reaction mixture was diluted with H_2O and Et_2O (approx. 1.5 mL each), and mixed vigorously. After allowing the layers to separate, the organic layer was removed by pipette, dried by passing through a plug of $MgSO_4$, and concentrated *in vacuo*. The yield of **4.2** was obtained by ^1H NMR spectroscopic analysis of the crude reaction mixture (relative to phenanthrene internal standard), then the crude material was purified by flash-column chromatorgraphy (2.5% EtOAc/Hexanes) to afford analytically pure material for analysis.

General procedure for probe-scale enantioselective photochemical cycloadditions:

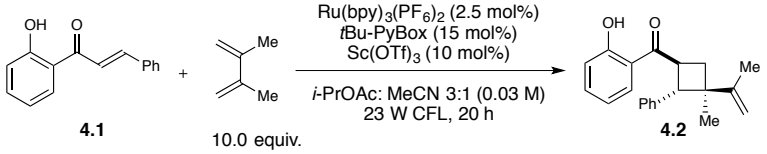

4.1 10.0 equiv. **4.2**

In an oven-dried 2 dram vial were combined 2'-hydroxychalcone (22.4 mg, 0.100 mmol), $Sc(OTf)_3$ (4.9 mg, 0.10 equiv.), *t*BuPyBox (5.0 mg, 0.15 equiv.), and $Ru(bpy)_3(PF_6)_2$ (1.3 mg, 0.025 equiv), and phenanthrene (10-15 mg as internal standard). A magnetic stirbar was added, and the contents were dissolved in 3:1 ^{i}PrOAc:MeCN (3 mL). To the resulting solution was added 2,3-dimethyl-1,3-butadiene (110 μL, 9.72 equiv.) by syringe, then the vial was sealed with a Teflon-lined cap and stirred under 23W CFL irradiation for 20 h at room temperature. The reaction progress can be monitored by TLC (10% EtOAc/Hexanes). At 20 h, the reaction mixture was diluted with H_2O and Et_2O (approx. 2.0 mL each), and mixed vigorously. After allowing the layers to separate, the organic layer was removed by pipette, dried by passing through a plug of $MgSO_4$, and concentrated *in vacuo*. The yield of **4.2** was obtained by ^1H NMR spectroscopic analysis of the crude reaction mixture (relative to phenanthrene internal standard), then the crude material was purified by flash-column chromatorgraphy (2.5% EtOAc/Hexanes) to afford analytically pure material for analysis.

General procedure for photoreactions under 350 nm Irradiation:

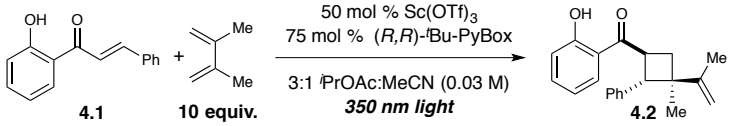

4.1 10 equiv. 4.2

In a 25 mL schlenck flask were combined 2'-hydroxychalcone (22.5 mg, 0.100 mmol), Sc(OTf)3 (24.1 mg, 0.49 equiv.), ^{t}BuPyBox (24.5 mg, 0.74 equiv.), and sensitizer (see below for amounts). Solvent (3:1 iPrOAc:MeCN, 3 mL) was then added to the flask, and the mixture stirred to dissolve. After addition of 2,3-dimethyl-1,2-butadiene (110 μL, 9.72 equiv.) by syringe, the flask was sealed, and degassed by three freeze-pump-thaw cycles. After the final thaw, the flask was backfilled with nitrogen gas, and sealed. The resulting solution was then stirred in a Rayonet photoreactor (bulb emission λ_{max} = 350 nm) for 18 hours. At 18 hours, irradiation was ceased, phenanthrene was added as an internal standard and allowed to dissolve. The reaction mixture was diluted with H_2O and Et_2O (approx. 2.0 mL each), and mixed vigorously. After allowing the layers to separate, the organic layer was removed by pipette, dried by passing through a plug of $MgSO_4$, and concentrated *in vacuo*. The yield of **4.2** was obtained by ^{1}H NMR spectroscopic analysis of the crude reaction mixture (relative to phenanthrene internal standard), and the crude material was purified by flash-column chromatorgraphy (2.5% EtOAc/Hexanes) to afford analytically pure material for SFC analysis.

Experiment A: *Sensitizer*: $Ru(bpy)_3(PF_6)_2$ (2.1 mg, 0.025 equiv.)

Experiment B: *Sensitizer*: Benzil (10.5 mg, 0.50 equiv.)

Experiment C: *Sensitizer*: 1-phenylnaphthyl ketone (11.4 mg, 0.50 equiv.)

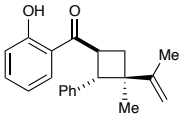

Compound 4.2*:* The title compound was synthesized according to the general procedures specified above, and isolated as a colorless glass after flash column chromatography. ^{1}H NMR (500 MHz, Chloroform-*d*) δ 12.35 (s, 1H), 7.72 (dd, *J* = 8.0, 1.6 Hz, 1H), 7.45 (ddd, *J* = 8.7, 7.2, 1.7 Hz, 1H), 7.31 (d, *J* = 8.3, 6.9 Hz, 2H), 7.23 (d, *J* = 7.7 Hz, 3H), 6.98 (dd, *J* =

8.4, 1.1 Hz, 1H), 6.86 (ddd, *J* = 8.2, 7.2, 1.2 Hz, 1H), 4.91 (s, 1H), 4.84 (s, 1H), 4.25 (q, *J* = 9.3 Hz, 1H), 4.19 (d, *J* = 9.8 Hz, 1H), 2.40 (t, *J* = 10.0 Hz, 1H), 2.23 (dd, *J* = 10.7, 8.9 Hz, 1H), 1.75 (s, 3H), 1.17 (s, 3H).

Figure 4.6: SFC chromatogram for racemic cyclobutane **4.2**

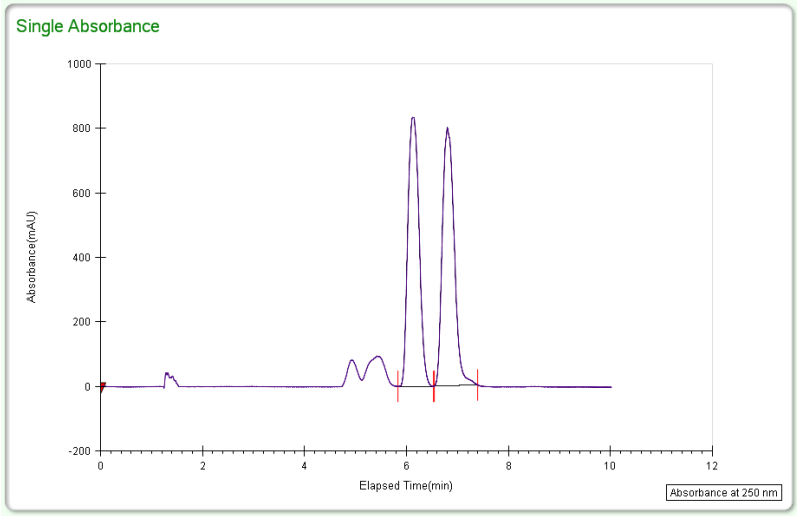

Peak Info

Peak	**Area %**	**Area**	**Retention Time**
1	49.6955	12733.513	6.12 min
2	50.3045	12889.5794	6.8 min
Total:	100	25623.0924	

Figure 4.7: SFC chromatogram for enantioenriched cyclobutane **4.2** (Table 4.1, entry 9)

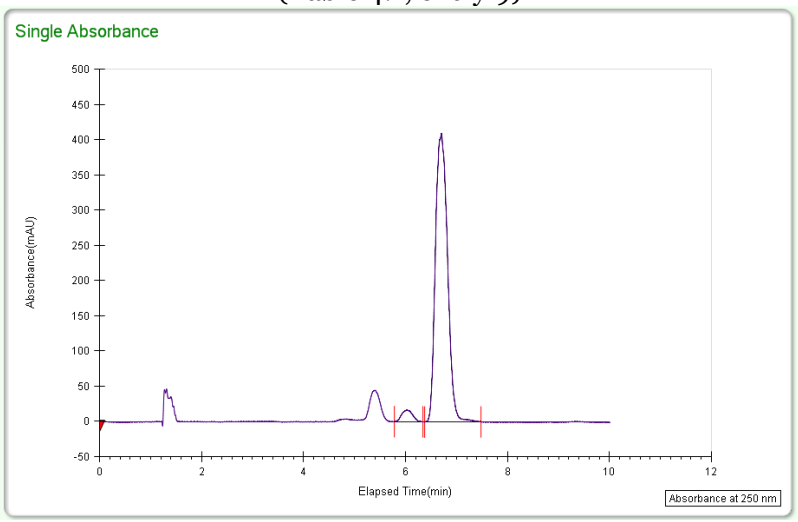

Peak Info

Peak	Area %	Area	Retention Time
1	3.5295	246.711	6.02 min
2	96.4705	6743.3156	6.7 min
Total:	100	6990.0266	

4.6 References

[1] Jacobsen, E. N.; Pfaltz, A.; Yamamoto, H. *Comprehensive Asymmetric Catalysis* **1999** (Springer, Berlin, New York).

[2] Ojima, I. *Catalytic Asymmetric Synthesis* **2010**, (Wiley, Hoboken, NJ, ed. 3).

[3] Brimioulle, R.; Lenhart, D.; Maturi, M.M.; Bach, T. "Enantioselective Catalysis of Photochemical Reactions." *Angew. Chem. Int. Ed.* **2015**, *54*, 3872–3890.

[4] (a) Cauble, D.F.; Lynch, V.; Krische, M.J. "Studies on the enantioselective catalysis of photochemically promoted transformations: "Sensitizing receptors" as chiral catalysts." *J. Org. Chem.* **2003**, *68*, 15–21. (b) Muller, C.; Bauer, A.; Bach, T. "Light-driven enantioselective organocatalysis." *Angew. Chem. Int. Ed.* **2009**, *48*, 6640–6642. (c) Muller, C.; Bauer, A.; Maturi, M.M.; Cuquerella, M.C.; Miranda, M.A.; Bach, T. "Enantioselective intramolecular [2 + 2]-photocycloaddition reactions of 4-substituted quinolones catalyzed by a chiral sensitizer with a hydrogen-bonding motif." *J. Am. Chem. Soc.* **2011**, *133*, 16689–16697. (d) Maturi, M.M.; Menninger, M.; Alonso, R.; Bauer, A.; Pothig, A.; Riedle, E.; Bach, T. "Intramolecular [2+2] photocycloaddition of 3- and 4-(but-3-enyl) oxyquinolones: Influence of the alkene substitution pattern, photophysical studies, and enantioselective catalysis by a chiral sensitizer." *Chem. Eur. J.* **2013**, *19*, 7461–7472. (e) Alonso, R.; Bach, T. "A chiral thioxanthone as an organocatalyst for enantioselective [2+2] photocycloaddition reactions induced by visible light." *Angew. Chem. Int. Ed.* **2014**, *53*, 4368–4371. (f) Maturi, M.; Bach, T. "Enantioselective catalysis of the

intermolecular [2+2] photocycloaddition between 2-pyridones and acetylenedicarboxylates." *Angew. Chem. Int. Ed.* **2014**, *53*, 7661–7664.

[5] (a) Vallavoju, N.; Selvakumar, S.; Jockusch, S.; Sibi, M.P.; Sivaguru, J. "Enantioselective organo-photocatalysis mediated by atropisomeric thiourea derivatives." *Angew. Chem. Int. Ed.* **2014**, *53*, 5604–5714. (b) Vallavoju, N.; Selvakumar, S.; Jockusch, S.; Prabhakaran, M.T.; Sibi, M.P.; Sivaguru, J. "Evaluating Thiourea Architecture for Intramolecular [2 + 2] Photocycloaddition of 4-Alkenylcoumarins." *Adv. Synth. Catal.* **2014**, *356*, 2763–2768.

[6] (a) Guo, H.; Herdtweck, E.; Bach, T. "Enantioselective Lewis acid catalysis in intramolecular [2+2] photocycloaddition reactions of coumarins." *Angew, Chem. Int. Ed.* **2010**, *53*, 7948–7951. (b) Brimioulle, R.; Bach, T. "[2+2] Photocycloaddition of 3-Alkenyloxy-2-cycloalkenones: Enantioselective Lewis Acid Catalysis and Ring Expansion." *Angew. Chem. Int. Ed.* **2014**, *53*, 5604–5608. (c) Brimioulle, R.; Guo, H.; Bach, T. "Enantioselective intramolecular [2+2] photocycloaddition reactions of 4-substituted coumarins catalyzed by a chiral Lewis acid." *Chem. Eur. J.* **2012**, *18*, 7552–7560. (d) Brimioulle, R.; Bach, T. "Enantioselective Lewis Acid Catalysis of Intramolecular Enone Photocycloaddition Reactions." *Science* **2013**, *342*, 840–843. (e) Brimioulle, R.; Bauer, A.; Bach, T. "Enantioselective Lewis Acid Catalysis in Intramolecular [2+2] Photocycloaddition Reactions: A Mechanistic Comparison between Representative Coumarin and Enone Substrates." *J. Am. Chem. Soc.* **2015**, *137*, 5170–5176.

[7] (a) Cong, H.; Becker, C.; Elliott, S.; Grinstaff, M.W.; Porco, J.A. "Silver Nanoparticle-Catalyzed Diels–Alder Cycloadditions of 2'-Hydroxychalcones." *J. Am. Chem. Soc.* **2010**, 132, 7514–7518. (b) Cong, H.; Ledbetter, D.; Rowe, G.T.; Caradonna, J.P.; Porco, J.A. "Electron Transfer-Initiated Diels–Alder Cycloadditions of 2′-Hydroxychalcones." *J. Am. Chem. Soc.* **2008**, *130*, 9214–9215.

[8]Recent publications suggest that simple Lewis acid catalysis may also explain the results of these studies: (a) Li, X.; Han, J.; Jones, A.X.; Lei, X. "Chiral Boron Complex-Promoted Asymmetric Diels–Alder Cycloaddition and its Application in Natural Product Synthesis." *J. Org. Chem.* **2015**, DOI: 10.1021/acs.joc.5b02248. (b) Qi, C.; Xiong, Y.; Eschenbrenner-Lux, V.; Cong, H.; Porco, J.A. "Asymmetric Synthesis of the Flavonoid Diels–Alder Natural Products Sanggenons C and O." *J. Am. Chem. Soc.* **2016**, DOI: 10.1021/jacs.5b12778.

[9] Du, J.; Skubi, K.L.; Schultz, D.M.; Yoon, T.P. "A dual-catalysis approach to enantioselective [2 + 2] photocycloadditions using visible light." *Science* **2014**, *344*, 392–396.

[10] (a) Baik, T.-G.; Luiz, A. L.; Wang, L.-C.; Krische, M. J. "A diastereoselective metal-catalyzed [2+2] cycloaddition of bis-enones." *J. Am. Chem. Soc.* **2001**, *123*, 6716–6717. (b) Wang, L.-C.; Jang, H.-Y.; Roh, Y.; Lynch, V.; Schultz, A. J.; Wang, X.; Krische, M. J. "Diastereoselective cycloreductions and cycloadditions catalyzed by Co(dpm)2-silane (dpm = 2,2,6,6-tetramethylheptane-3,5-dionate): Mechanism and partitioning of hydrometallative versus anion radical pathways." *J. Am. Chem. Soc.* **2002**, *124*, 9448–9453. (c) Yang, J.; Cauble, D. F.; Berro, A. J.; Bauld, N. L.; Krische, M. J. "Anion radical [2 + 2] cycloaddition as a mechanistic probe: Stoichiometry- and concentration-dependent partitioning of electron-transfer and alkylation pathways in the reaction of the Gilman reagent $Me_2CuLi{\bullet}LiI$ with bis(enones)." *J. Org. Chem.* **2004**, *69*, 7979–7984. (d) Roh, Y.; Jang, H.-Y.; Lynch, V.; Bauld, N. L.; Krische, M. J. "Anion radical chain cycloaddition of tethered enones: Intramolecular cyclobutanation and Diels–Alder cycloaddition." *Org. Lett.* **2002**, *4*, 611–613. (e) Yang, J.; Felton, G. A. N.; Bauld, N. L.; Krische, M. J. "Chemically induced anion radical cycloadditions: intramolecular cyclobutanation of

bis(enones) via homogeneous electron transfer." *J. Am. Chem. Soc.* **2004**, *126*, 1634–1635. (f) Ischay, M.A.; Anzovino, M.E.; Du, J.; Yoon, T.P. "Efficient visible light photocatalysis of [2+2] enone cycloadditions." *J. Am. Chem. Soc.* **2008**, *130*, 12886–12887. (g) Ischay, M.A.; Lu, Z.; Yoon, T.P. "Cycloadditions by oxidative visible light photocatalysis." *J. Am. Chem. Soc.* **2010**, *132*, 8572–8574. (h) Ischay, M.A.; Ament, M.S.; Yoon, T.P. "Crossed intermolecular [2 + 2] cycloaddition of styrenes by visible light photocatalysis." *Chem. Sci.* **2012**, *3*, 2807–2811. (i) Riener, M.; Nicewicz, D.A. "Synthesis of cyclobutane lignans via an organic single electron oxidant-electron relay system." *Chem. Sci.* **2013**, *4*, 2625–2629. (j) Pabon, R.A.; Bellville, D.J.; Bauld, N.L. "Selective cyclobutane adduct formation in competition with Diels-Alder addition in cation radical cycloadditions." *J. Am. Chem. Soc.* **1984**, *106*, 2730–2731.

[11] Lewis acid coordination has been shown to lower π,π* transitions in enones. See Ref 6(d,e) and Guner, O.F.; Ottenbrite, R.M.; Shillady, D.D.; Alston, P.V. "An ab initio molecular orbital evaluation of Lewis acid catalysis on Diels-Alder reactions of acrolein." *J. Org. Chem.* **1987**, *52*, 391–394. for selected examples.

[12] Norikane, Y.; Itoh, H; Arai, T. "Photochemistry of 2'-hydroxychalcone. One-way cis-trans photoisomerization induced by adiabatic intramolecular hydrogen atom transfer." *J. Phys. Chem. A.* **2002**, *106*, 2766–2776.

[13] Pangborn, A. B.; Giardello, M. A.; Grubbs, R. H.; Rosen, R. K.; Timmers, F. J. "Safe and Convenient Procedure for Solvent Purification." *Organometallics,* **1996**, *15*, 1518–1520.

[14] Cornejo, A.; Fraile, J. M.; García, J. I.; Gil, M. J.; Martínez-Merino, V.; Mayoral, J. A.; Pires, E.; Villalba, I "An efficient and general one-pot method for the synthesis of chiral bis(oxazoline) and pyridine bis(oxazoline) ligands." *Synlett* **2005**, 2321–2324.

[15] Ischay, M. A.; Lu, Z.; Yoon, T. P. "[2+2] Cycloadditions by Oxidative Visible Light Photocatalysis." *J. Am. Chem. Soc.* **2010**, *132*, 8572–8574.

[16] Shi, Z.; Schroder, N.; Glorius F. "Rhodium(III)-Catalyzed Dehydrogenative Heck Reaction of Salicylaldehydes." *Angew. Chem. Int. Ed.* **2012**, *51*, 8092–8096.

Appendix A. ^{1}H NMR and ^{13}C NMR spectra for new compounds

A.1 List of compounds for Chapter 2

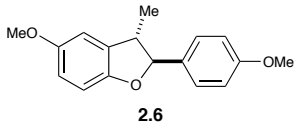

2.6

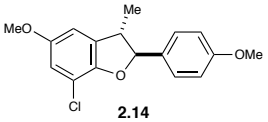

2.14

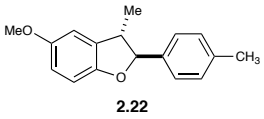

2.22

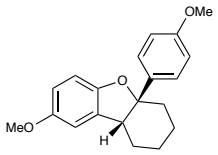

2.30

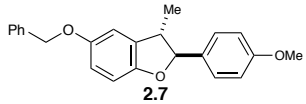

2.7

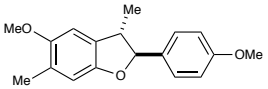

2.15

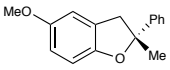

2.23

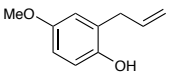

2.33

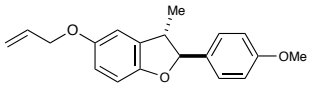

2.8

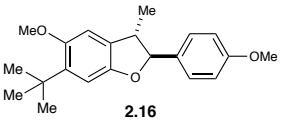

2.16

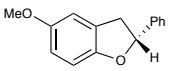

2.24

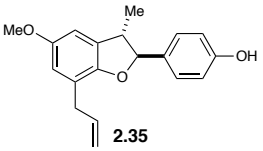

2.35

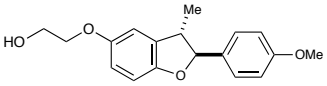

2.9

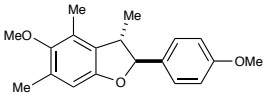

2.17

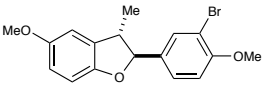

2.25

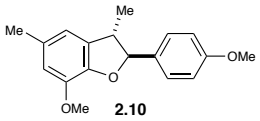

2.10

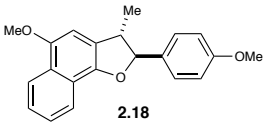

2.18

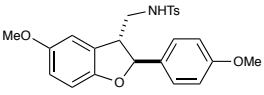

2.26

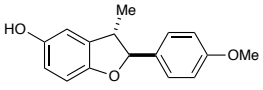

S2

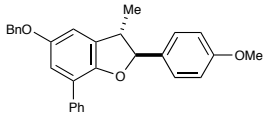

2.11

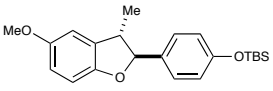

2.19

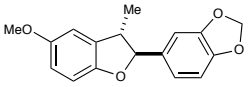

2.27

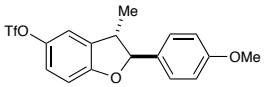

2.36

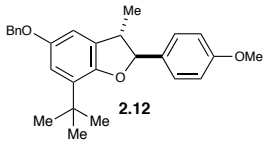

2.12

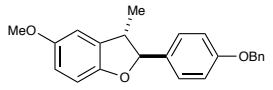

2.20

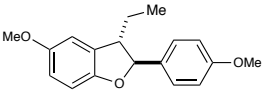

2.28

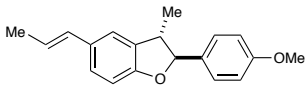

2.37

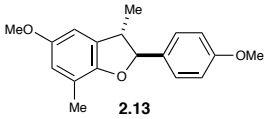

2.13

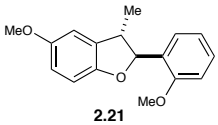

2.21

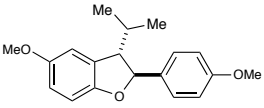

2.29

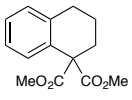

2.42

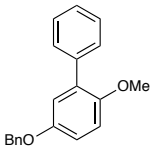

A.1

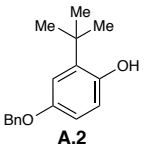

A.2

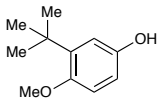

A.3

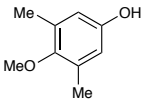

A.4

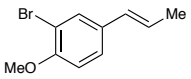

A.5

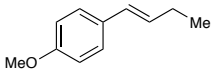

A.6

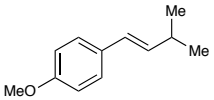

A.7

^{1}H NMR (400 MHz, $CDCl_3$)

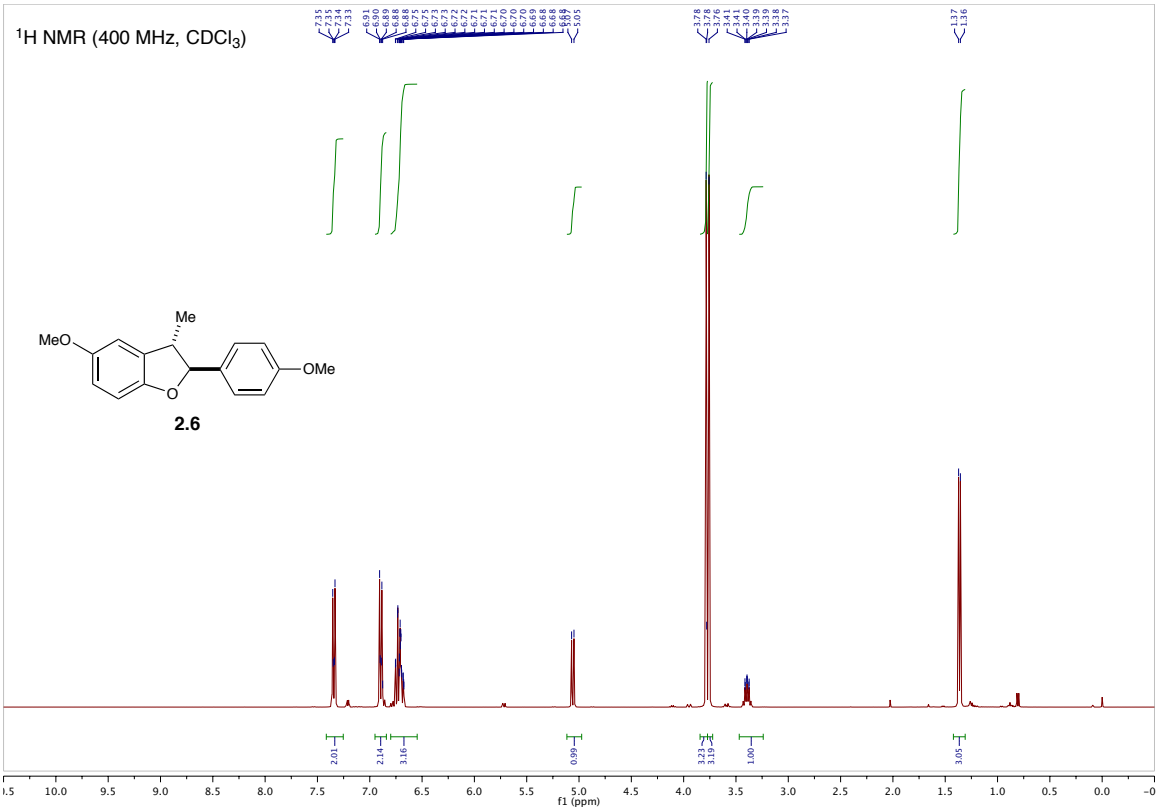

^{13}C NMR (100 MHz, $CDCl_3$)

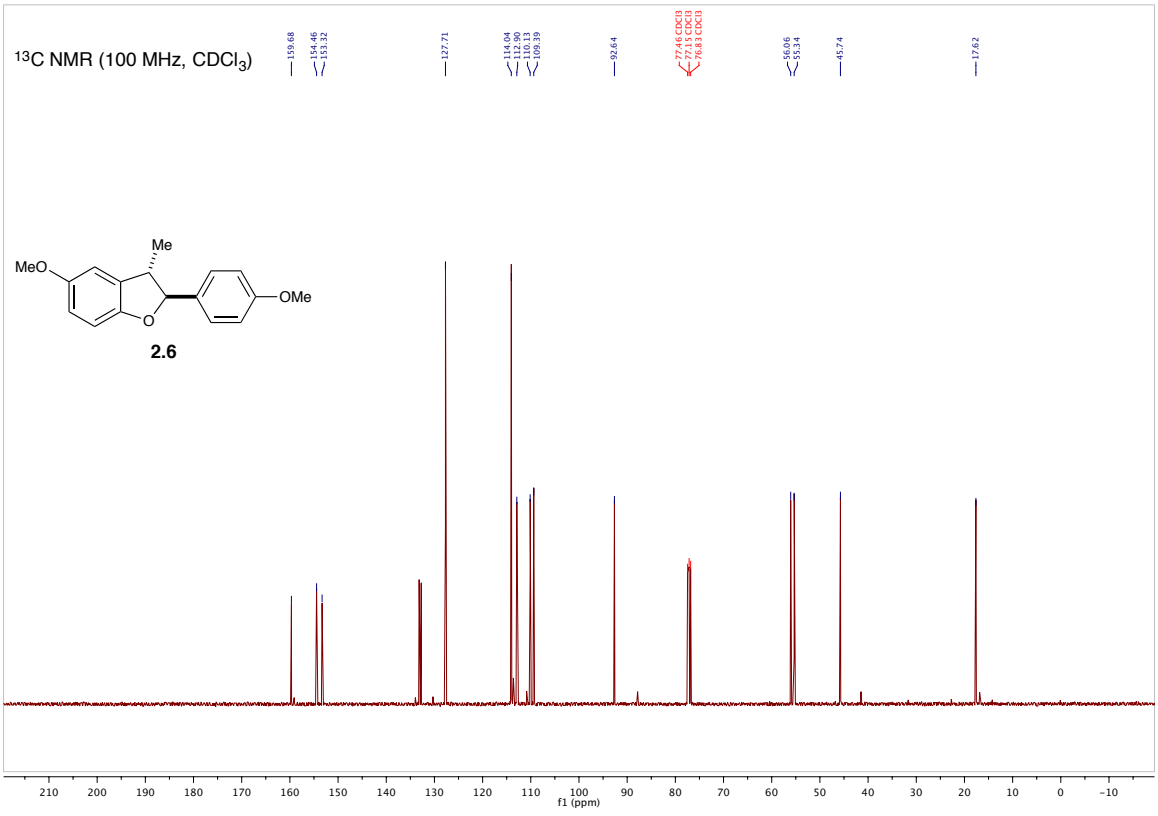

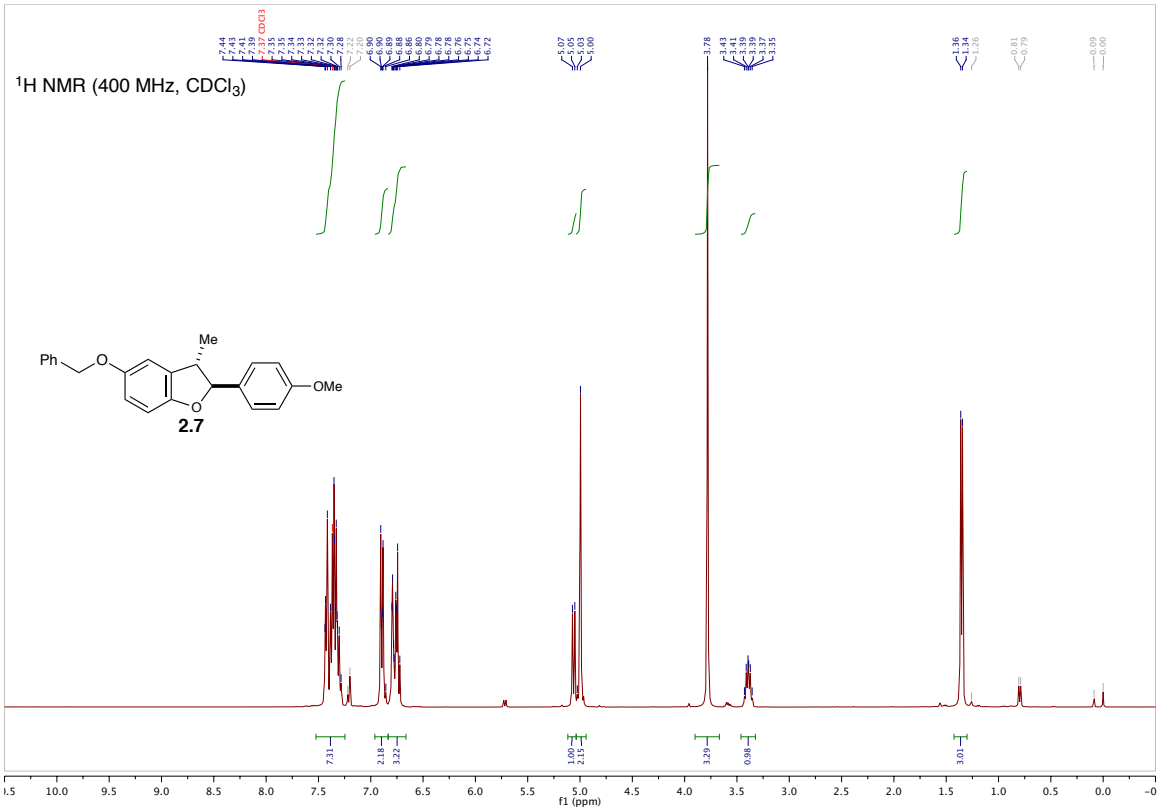
^{1}H NMR (400 MHz, $CDCl_3$)
Ph
O
Me
O
OMe
2.7
f1 (ppm)

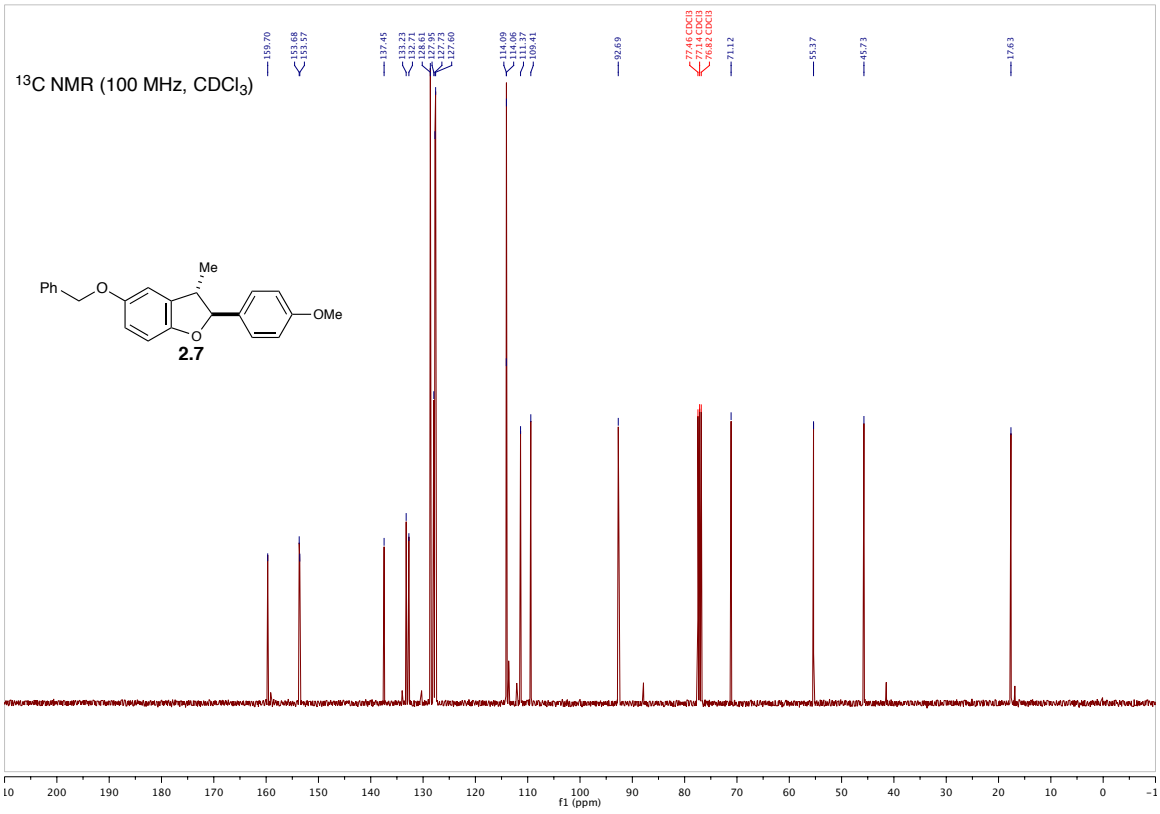
^{13}C NMR (100 MHz, $CDCl_3$)
Ph
O
Me
O
OMe
2.7
f1 (ppm)

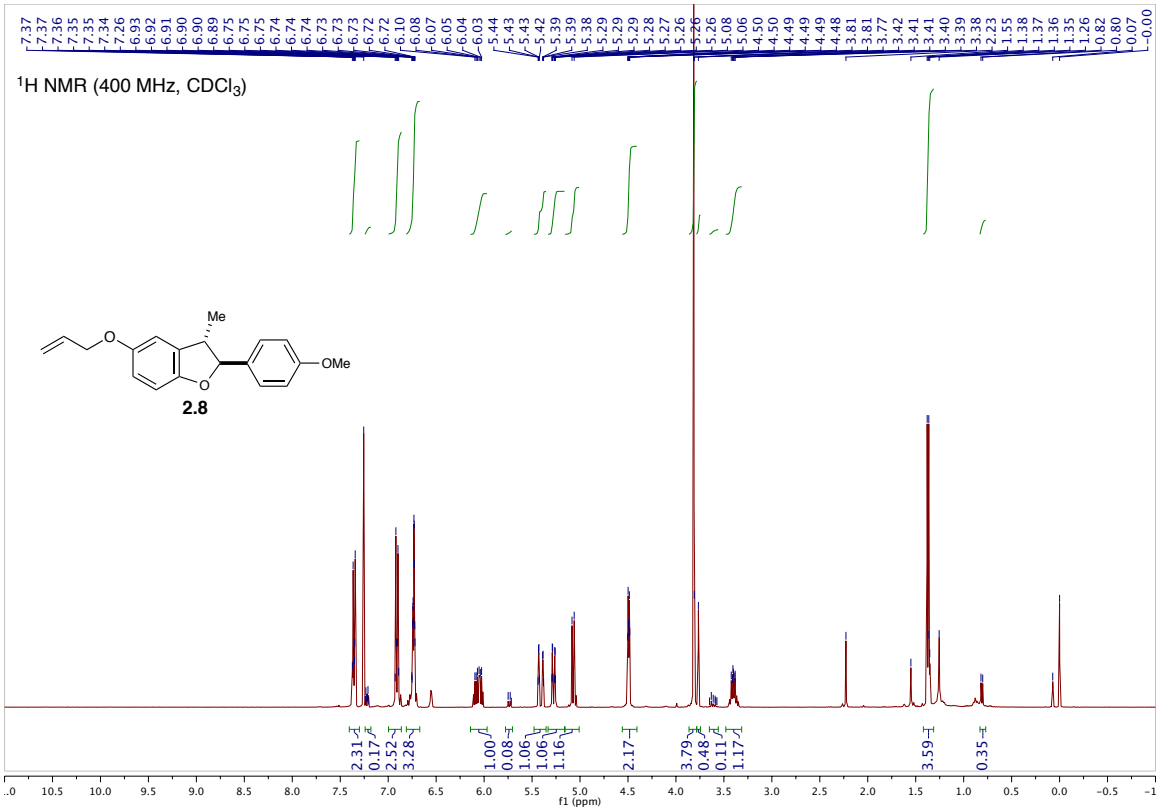
^{1}H NMR (400 MHz, $CDCl_3$)
Me
O
OMe
2.8
f1 (ppm)

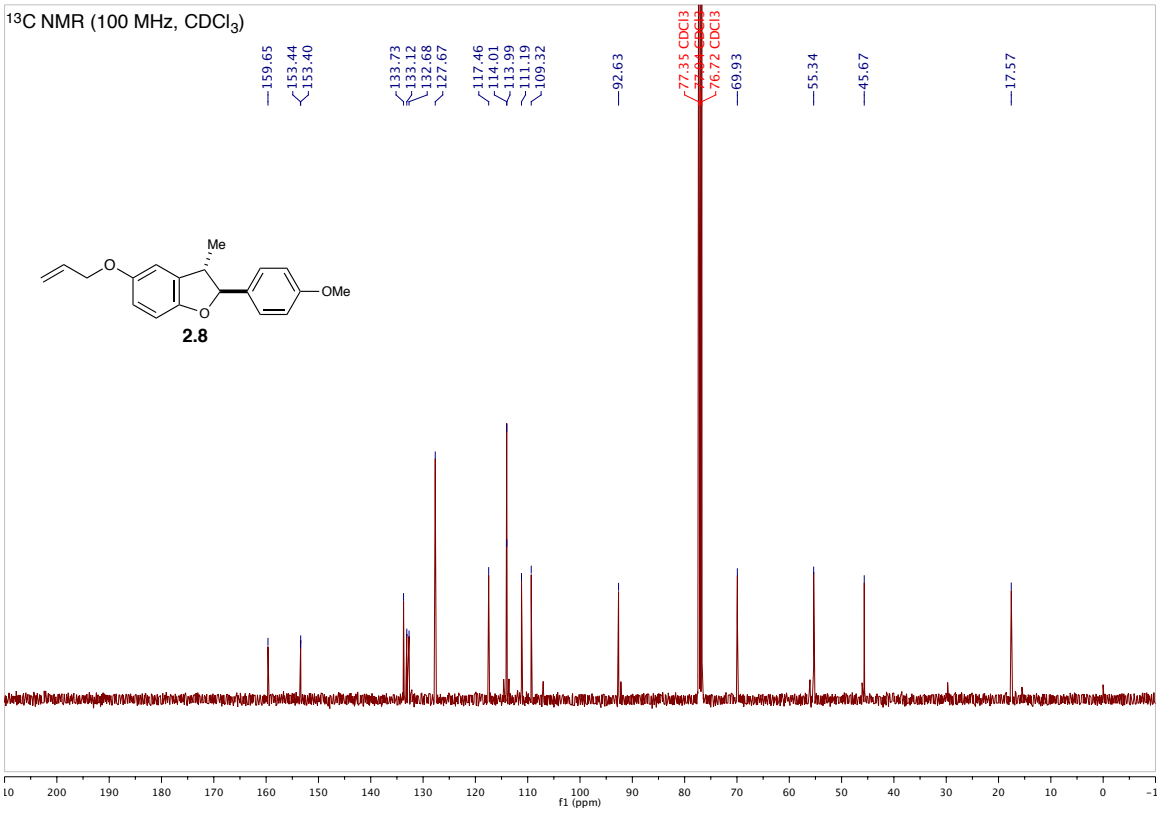
^{13}C NMR (100 MHz, $CDCl_3$)
159.65
153.44
153.40
133.73
133.12
132.68
127.67
117.46
114.01
113.99
111.19
109.32
92.63
77.35 CDCl3
77.04 CDCl3
76.72 CDCl3
69.93
55.34
45.67
17.57
Me
O
OMe
2.8
f1 (ppm)

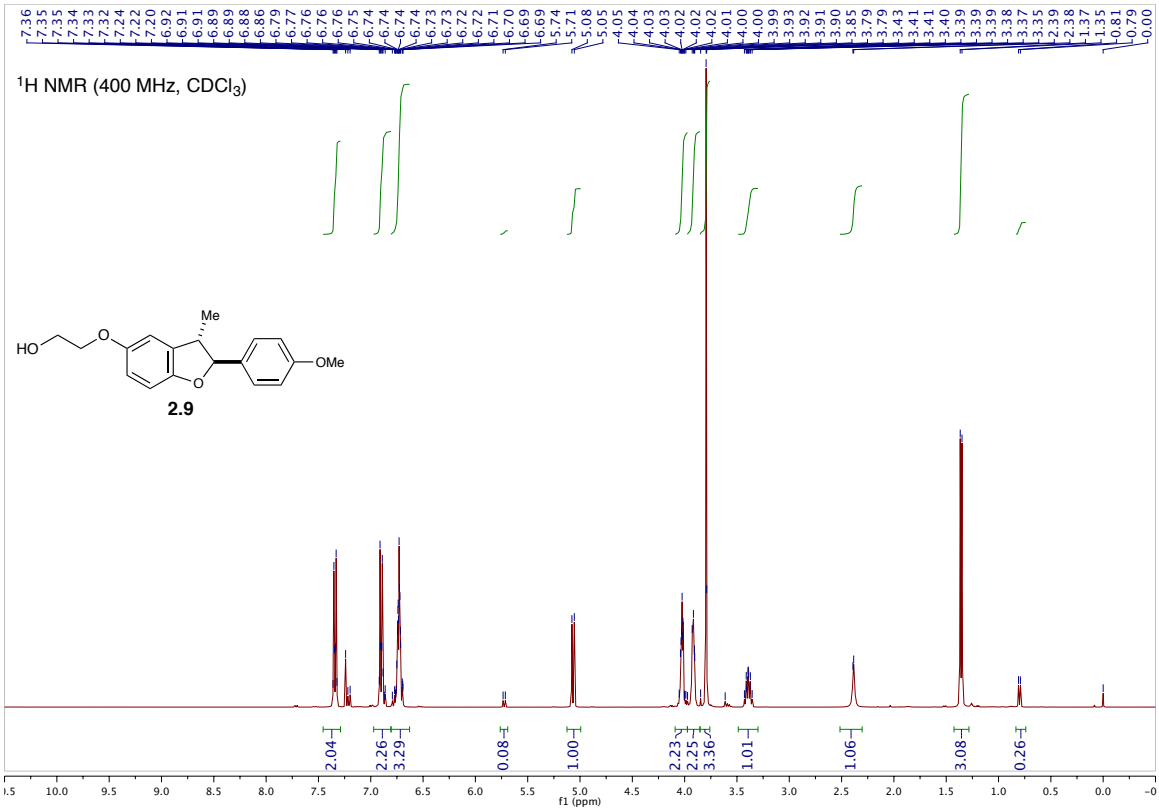
^{1}H NMR (400 MHz, $CDCl_3$)
HO
O
Me
O
OMe
2.9
f1 (ppm)

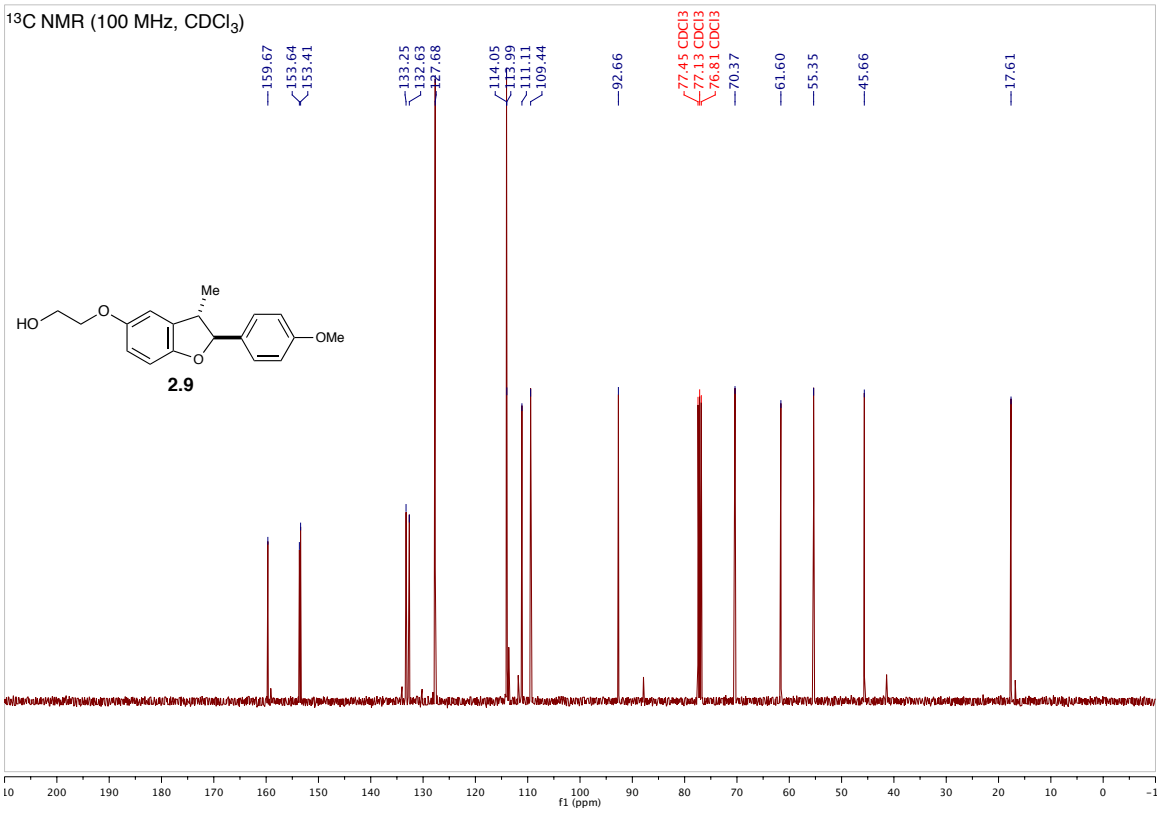
^{13}C NMR (100 MHz, $CDCl_3$)
HO
O
Me
O
OMe
2.9
f1 (ppm)

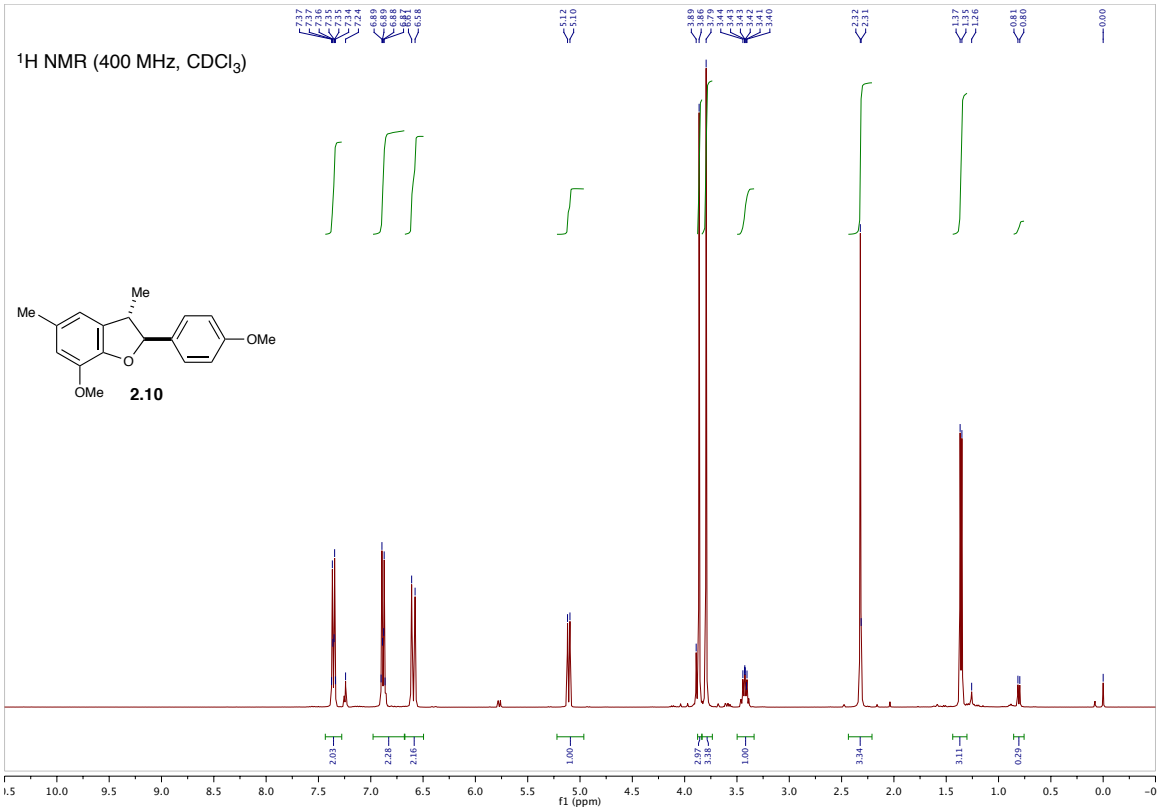
^{1}H NMR (400 MHz, $CDCl_3$)
Me
Me
OMe
OMe
2.10
f1 (ppm)

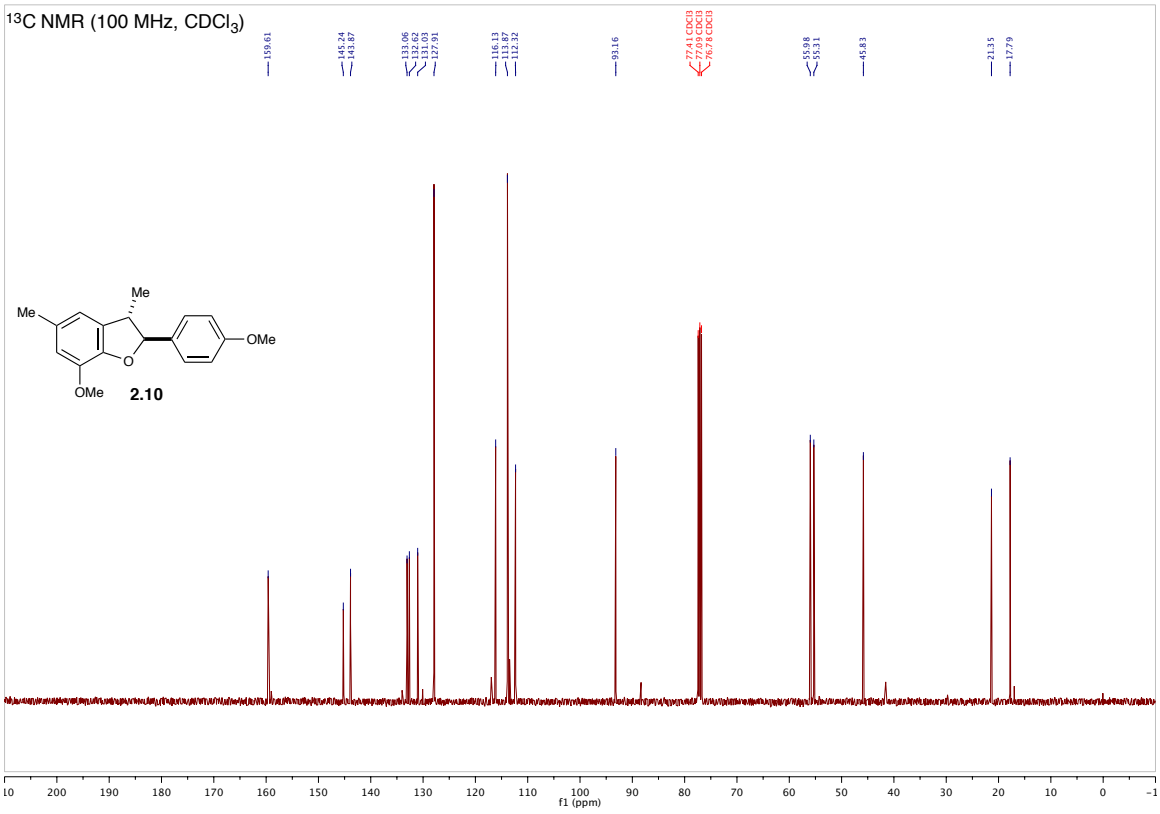
^{13}C NMR (100 MHz, $CDCl_3$)
Me
Me
OMe
OMe
2.10
f1 (ppm)

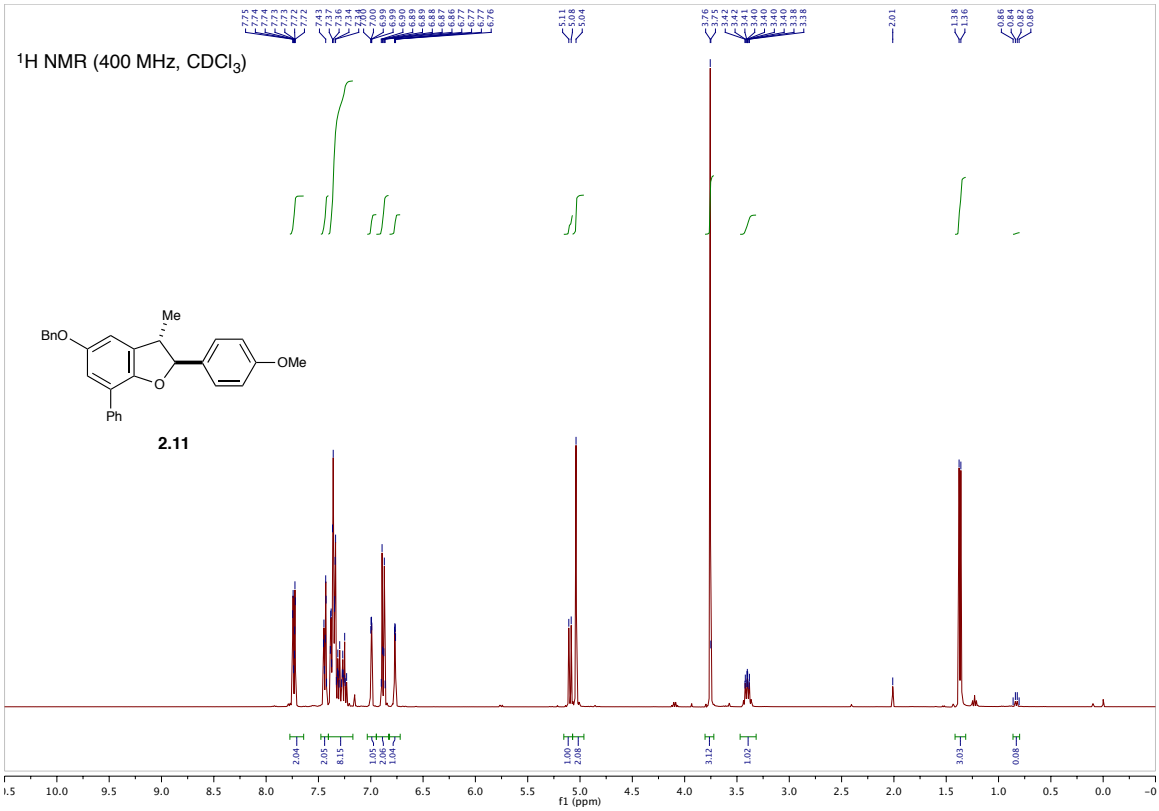
^{1}H NMR (400 MHz, $CDCl_3$)
BnO
Me
OMe
O
Ph
2.11
f1 (ppm)

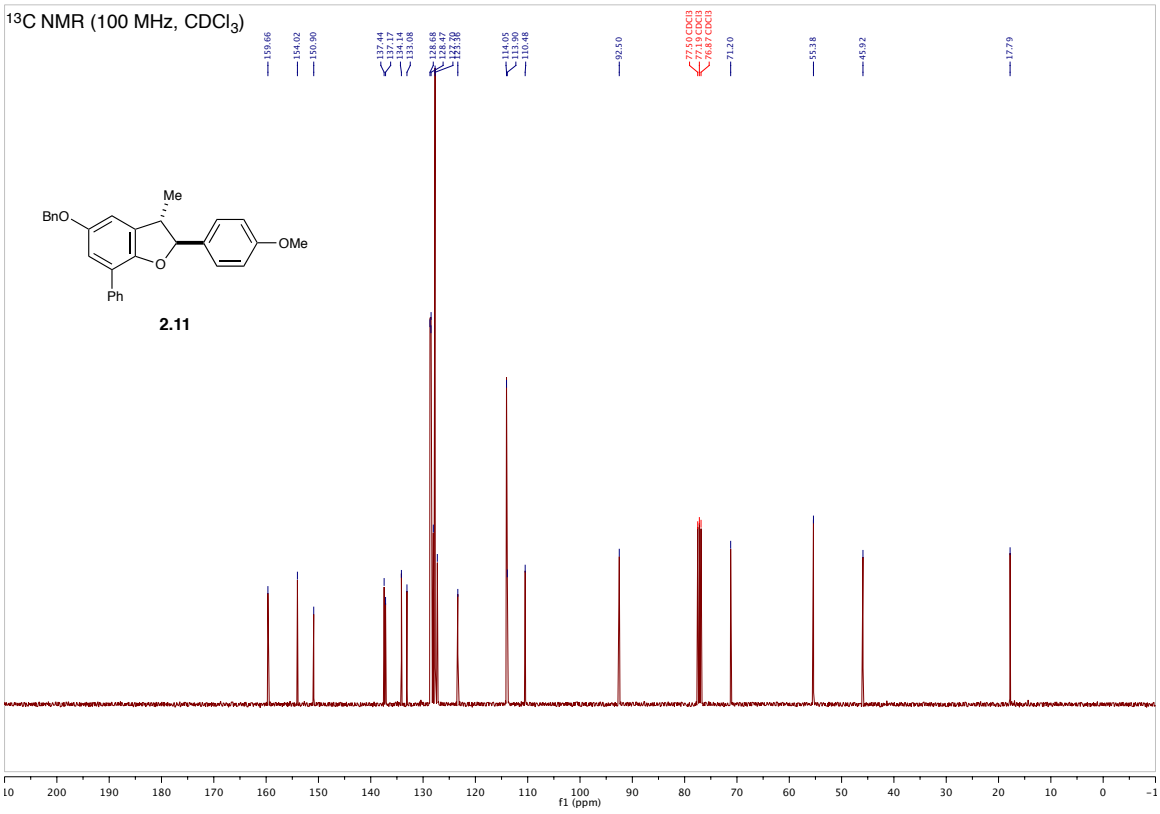
^{13}C NMR (100 MHz, $CDCl_3$)
BnO
Me
OMe
O
Ph
2.11
f1 (ppm)

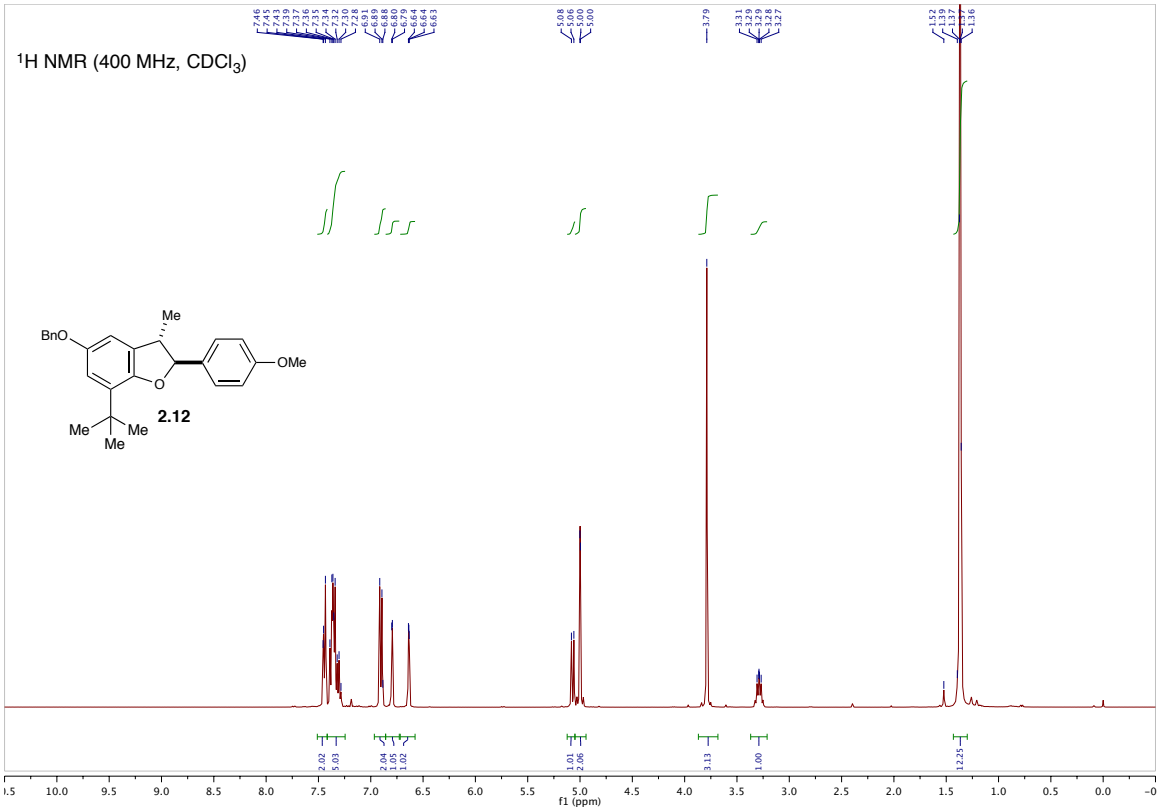
^{1}H NMR (400 MHz, $CDCl_3$)
BnO
Me
OMe
O
Me
Me
Me
2.12
f1 (ppm)

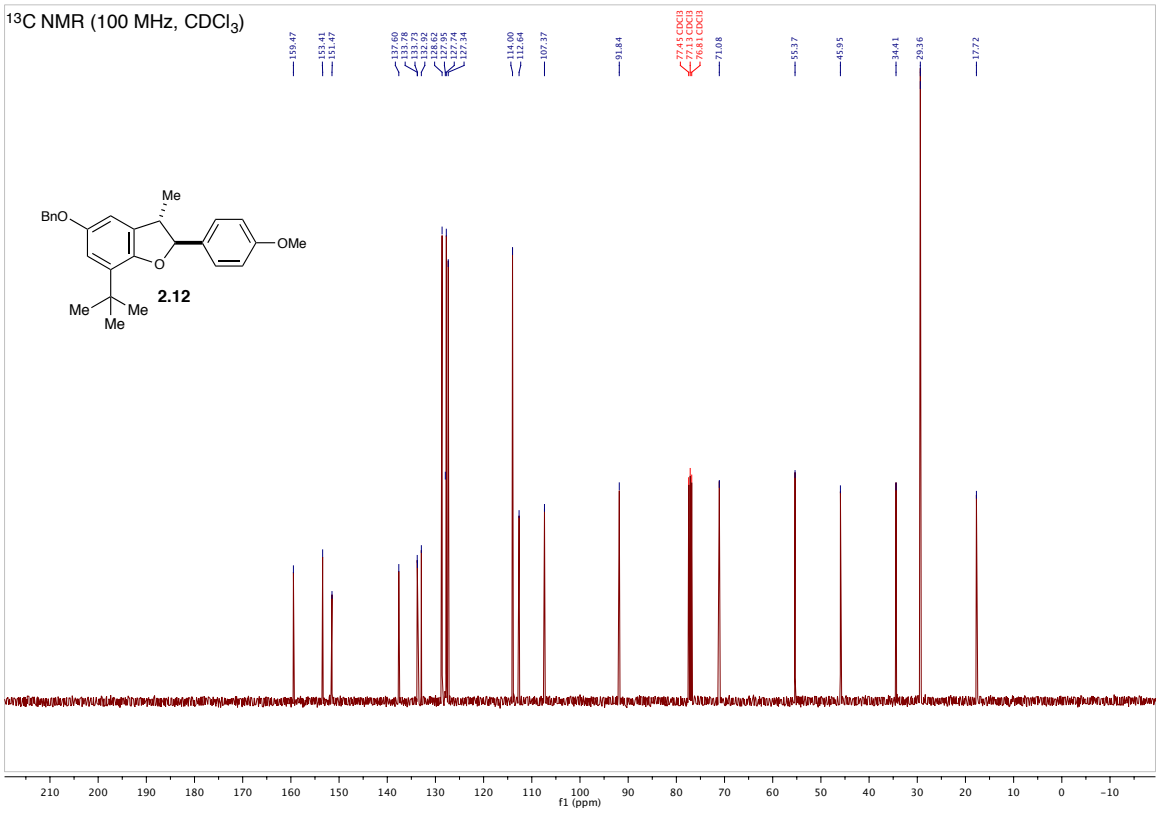
^{13}C NMR (100 MHz, $CDCl_3$)
BnO
Me
OMe
O
Me
Me
Me
2.12
f1 (ppm)

^{1}H NMR (400 MHz, $CDCl_3$)

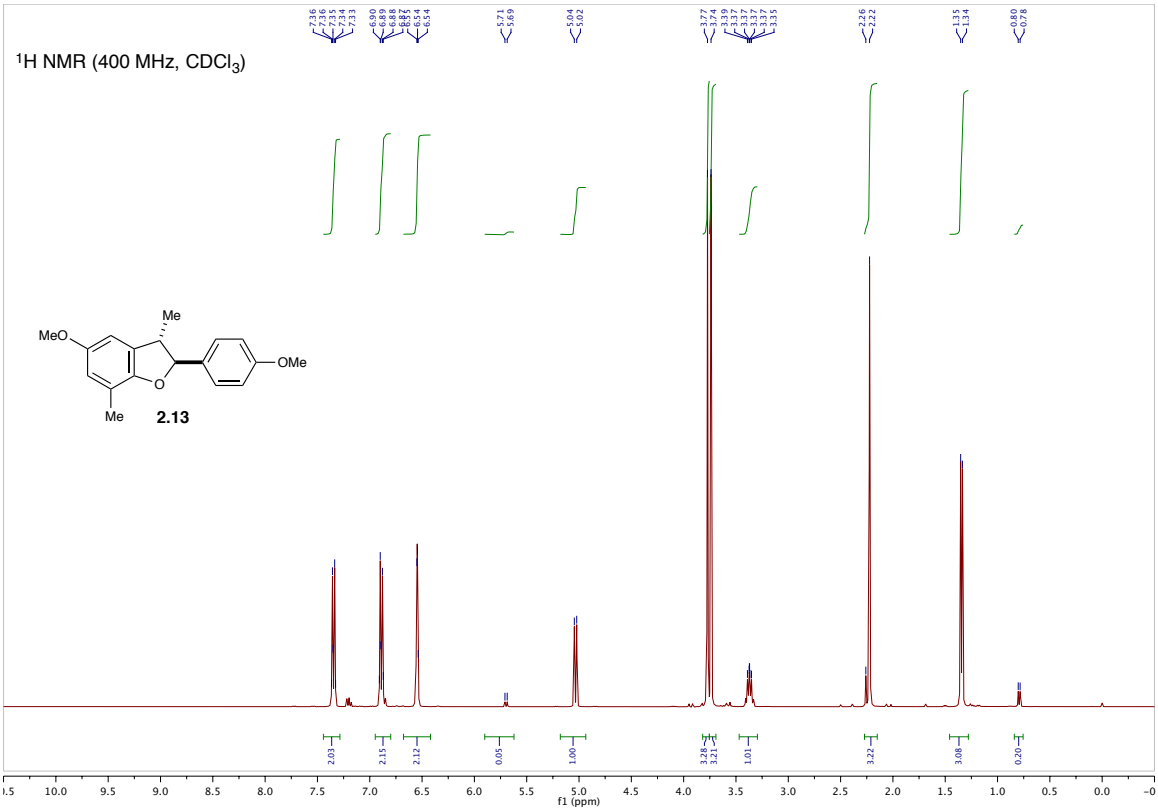

2.13

^{13}C NMR (100 MHz, $CDCl_3$)

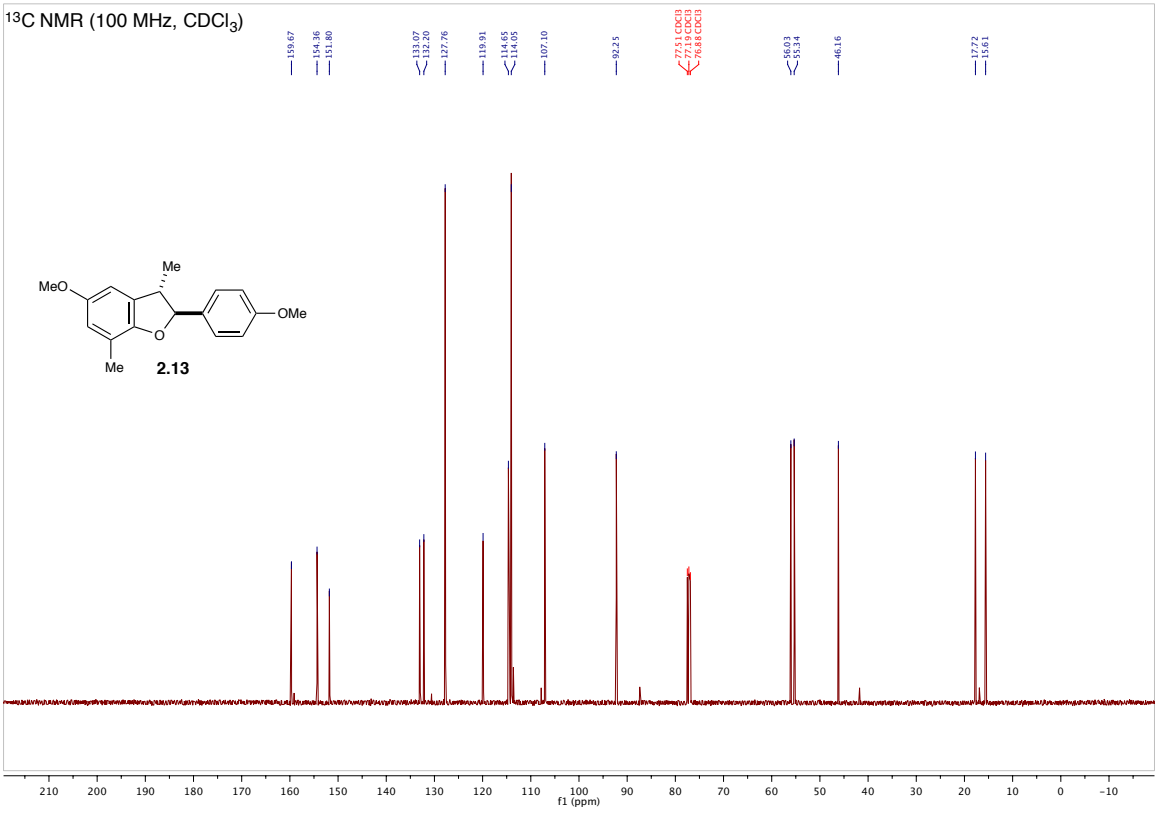

2.13

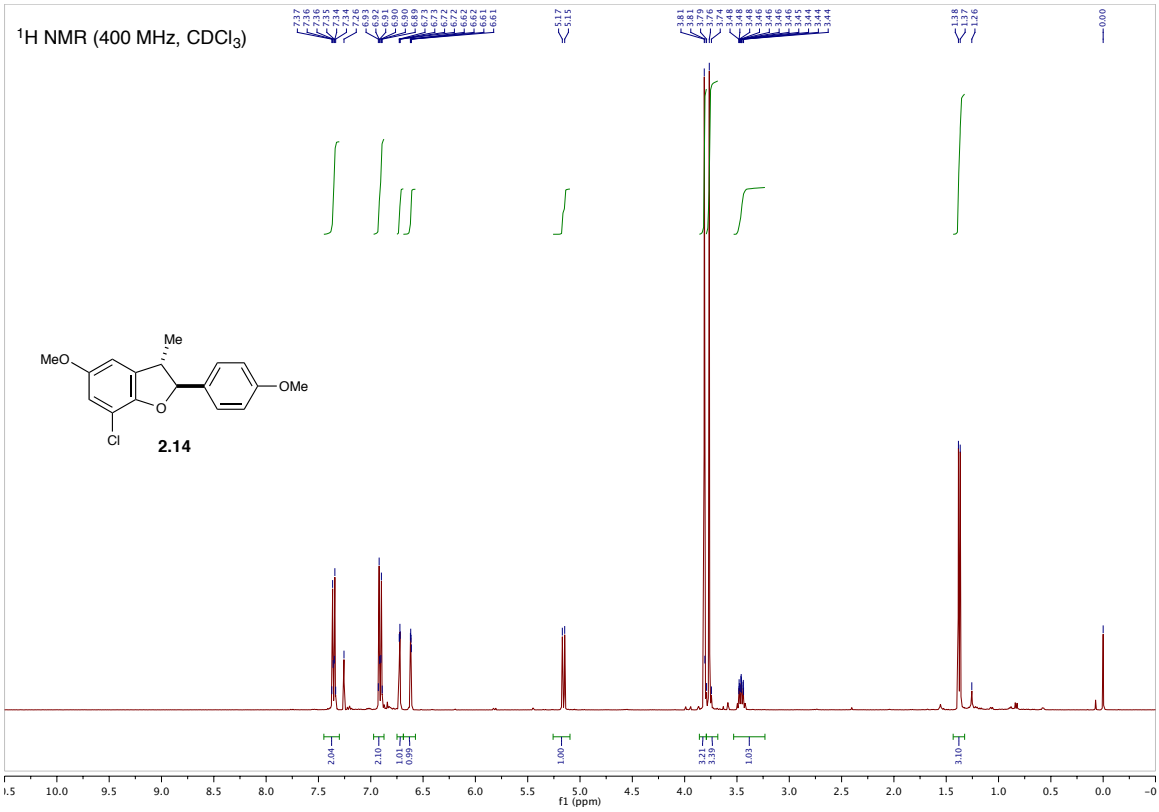
^{1}H NMR (400 MHz, $CDCl_3$)
Me
MeO
OMe
O
Cl
2.14
f1 (ppm)

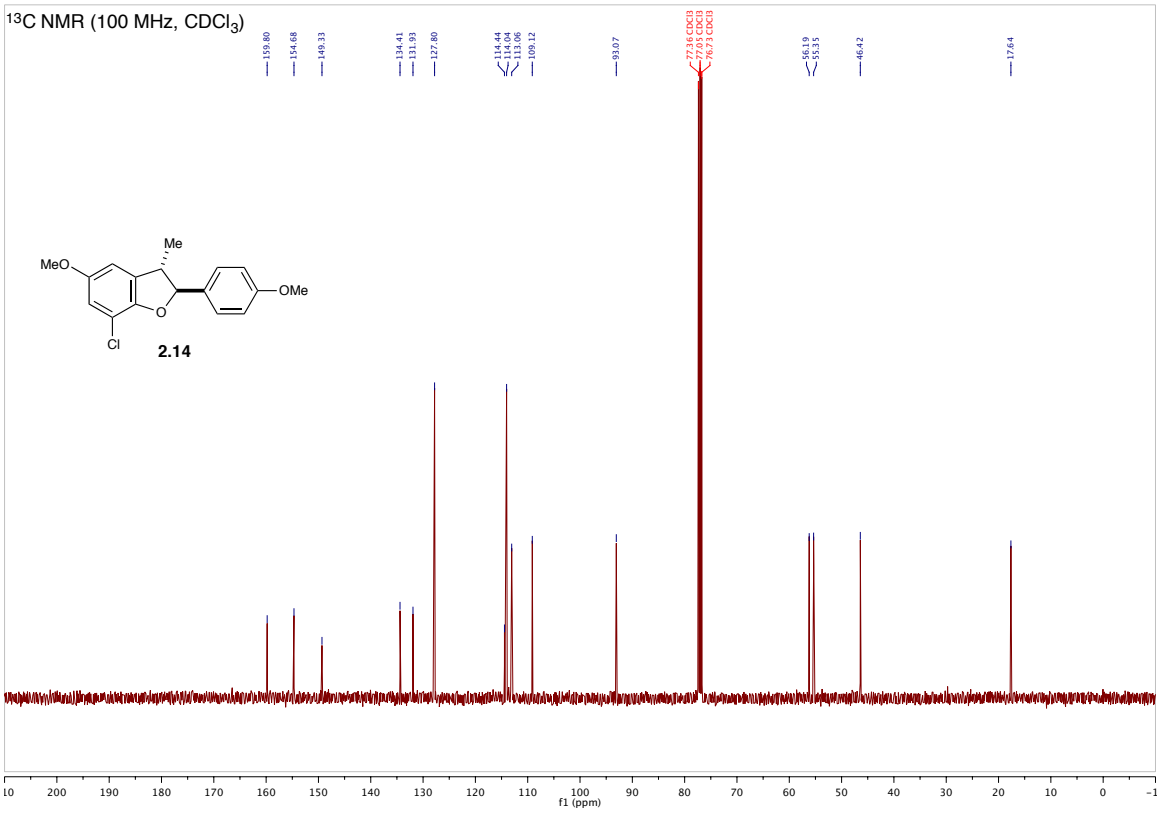
^{13}C NMR (100 MHz, $CDCl_3$)
Me
MeO
OMe
O
Cl
2.14
f1 (ppm)

^{1}H NMR (400 MHz, $CDCl_3$)

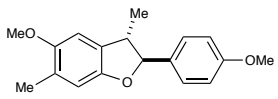

2.15

^{13}C NMR (100 MHz, $CDCl_3$)

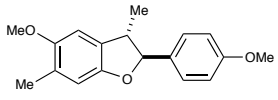

2.15

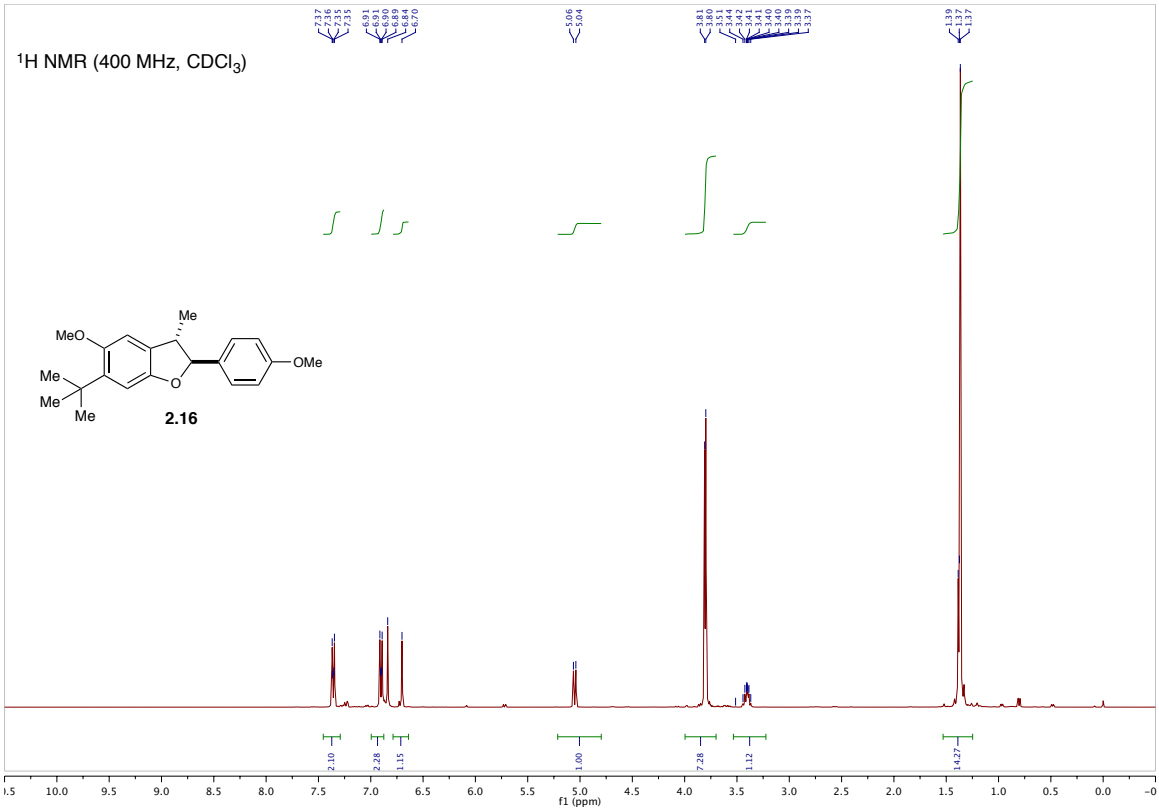
^{1}H NMR (400 MHz, $CDCl_3$)
MeO
Me
Me
Me
Me
OMe
O
2.16
f1 (ppm)

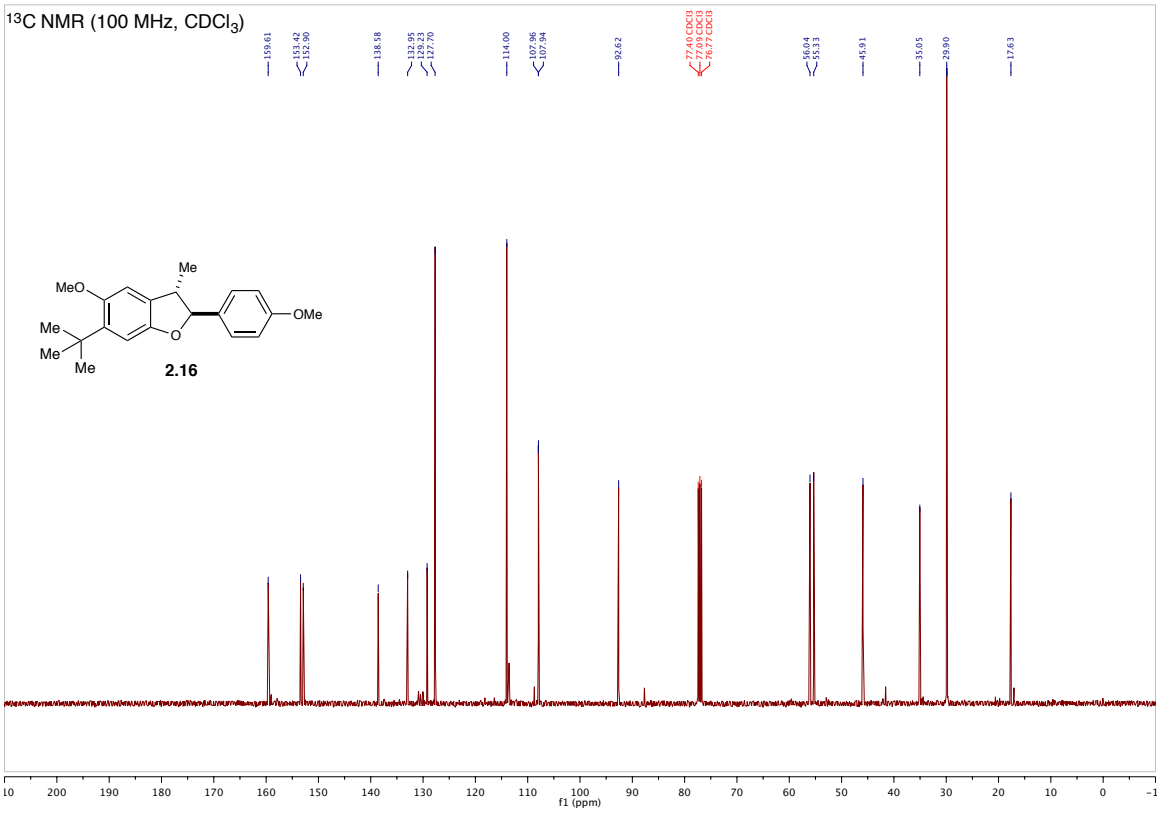
^{13}C NMR (100 MHz, $CDCl_3$)
MeO
Me
Me
Me
Me
OMe
O
2.16
f1 (ppm)

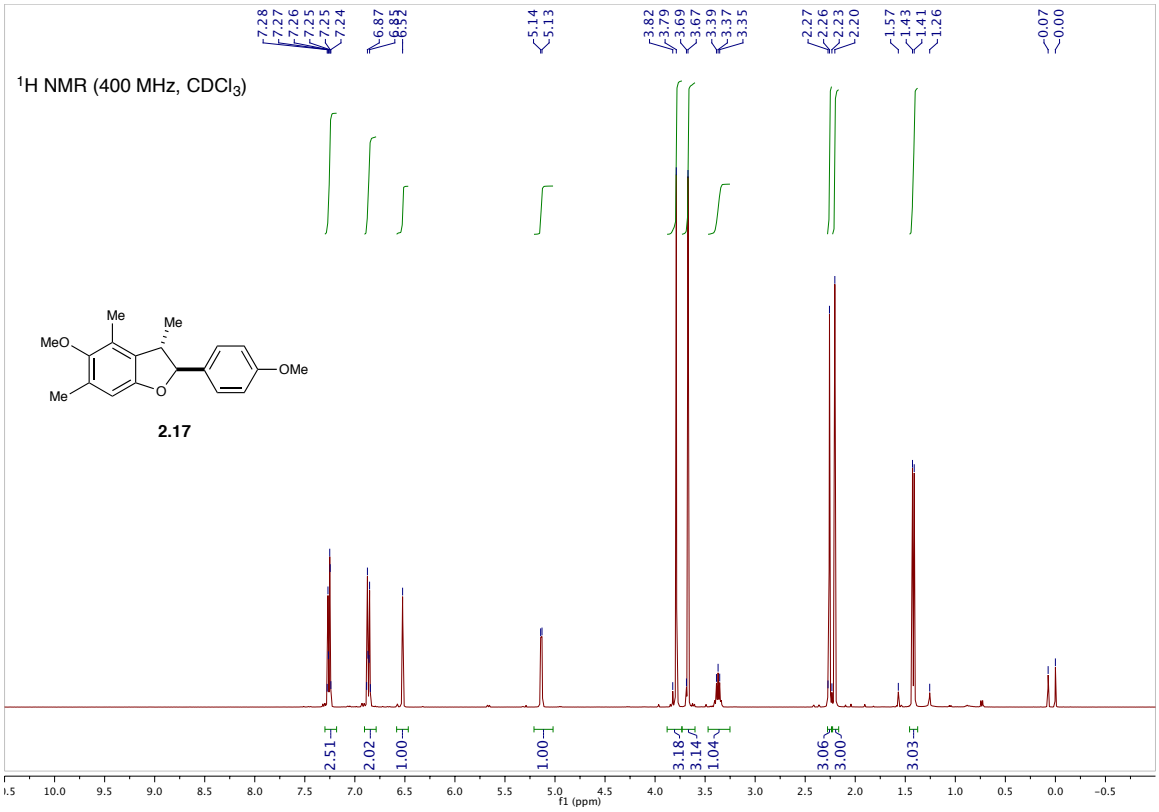
^{1}H NMR (400 MHz, $CDCl_3$)
7.28
7.27
7.26
7.25
7.25
7.24
6.87
6.85
6.85
5.14
5.13
3.82
3.79
3.69
3.67
3.39
3.37
3.35
2.27
2.26
2.23
2.20
1.57
1.43
1.41
1.26
0.07
0.00
2.51
2.02
1.00
1.00
3.18
3.14
1.04
3.06
3.00
3.03
f1 (ppm)
Me
Me
MeO
Me
O
OMe
2.17

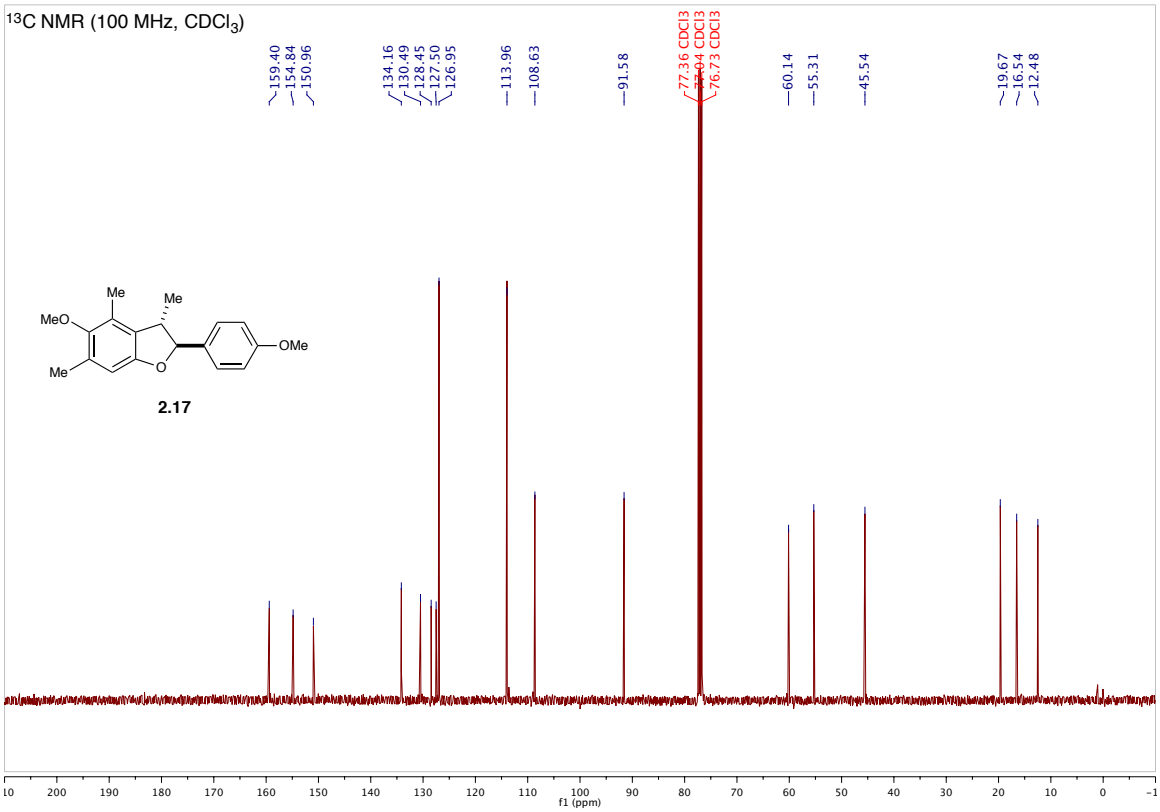
^{13}C NMR (100 MHz, $CDCl_3$)
159.40
154.84
150.96
134.16
130.49
128.45
127.50
126.95
113.96
108.63
91.58
77.36 CDCl3
77.04 CDCl3
76.73 CDCl3
60.14
55.31
45.54
19.67
16.54
12.48
f1 (ppm)
Me
Me
MeO
Me
O
OMe
2.17

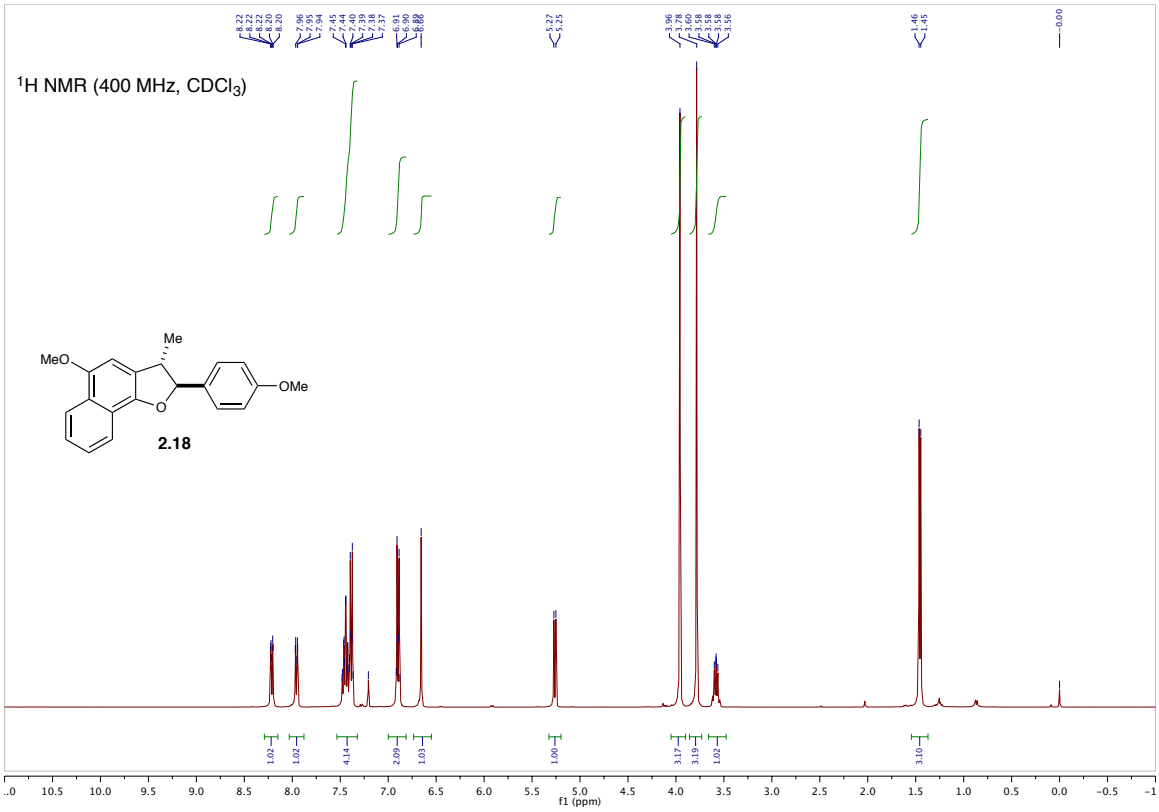
^{1}H NMR (400 MHz, $CDCl_3$)
Me
MeO
OMe
O
2.18
f1 (ppm)

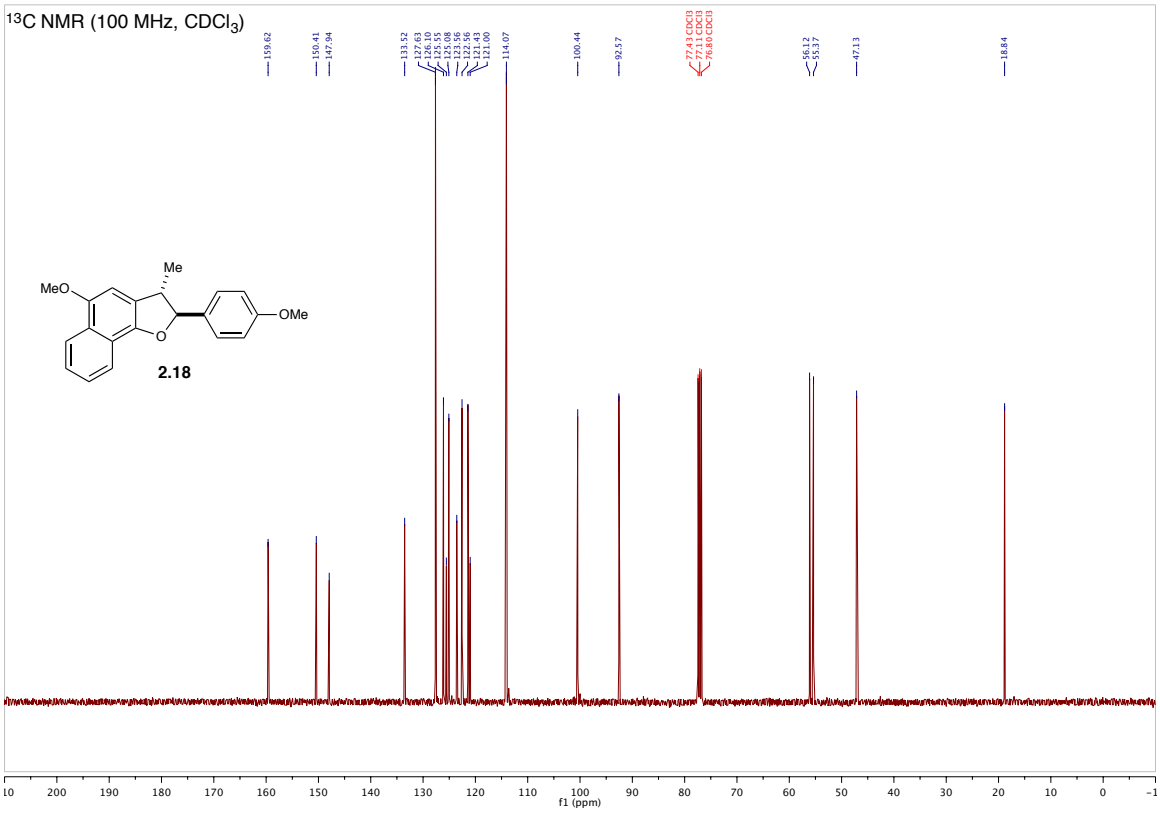
^{13}C NMR (100 MHz, $CDCl_3$)
Me
MeO
OMe
O
2.18
f1 (ppm)

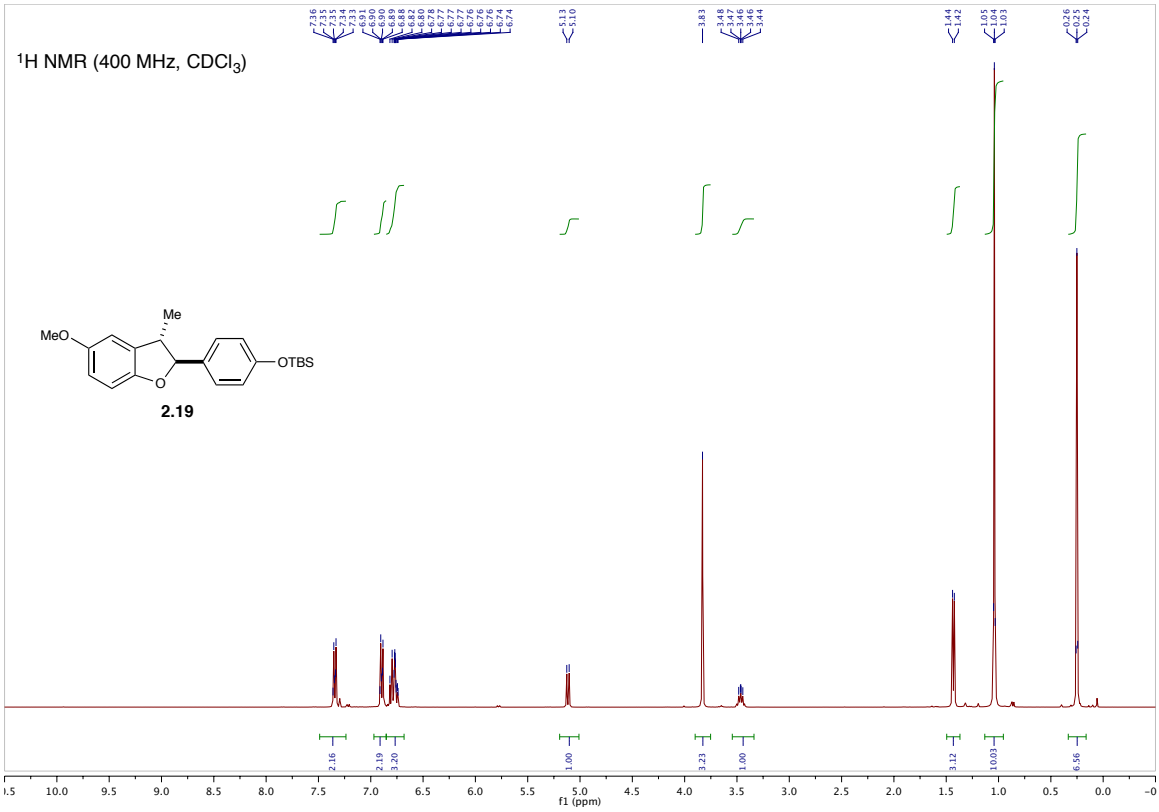
^{1}H NMR (400 MHz, $CDCl_3$)
Me
MeO
OTBS
O
2.19
f1 (ppm)

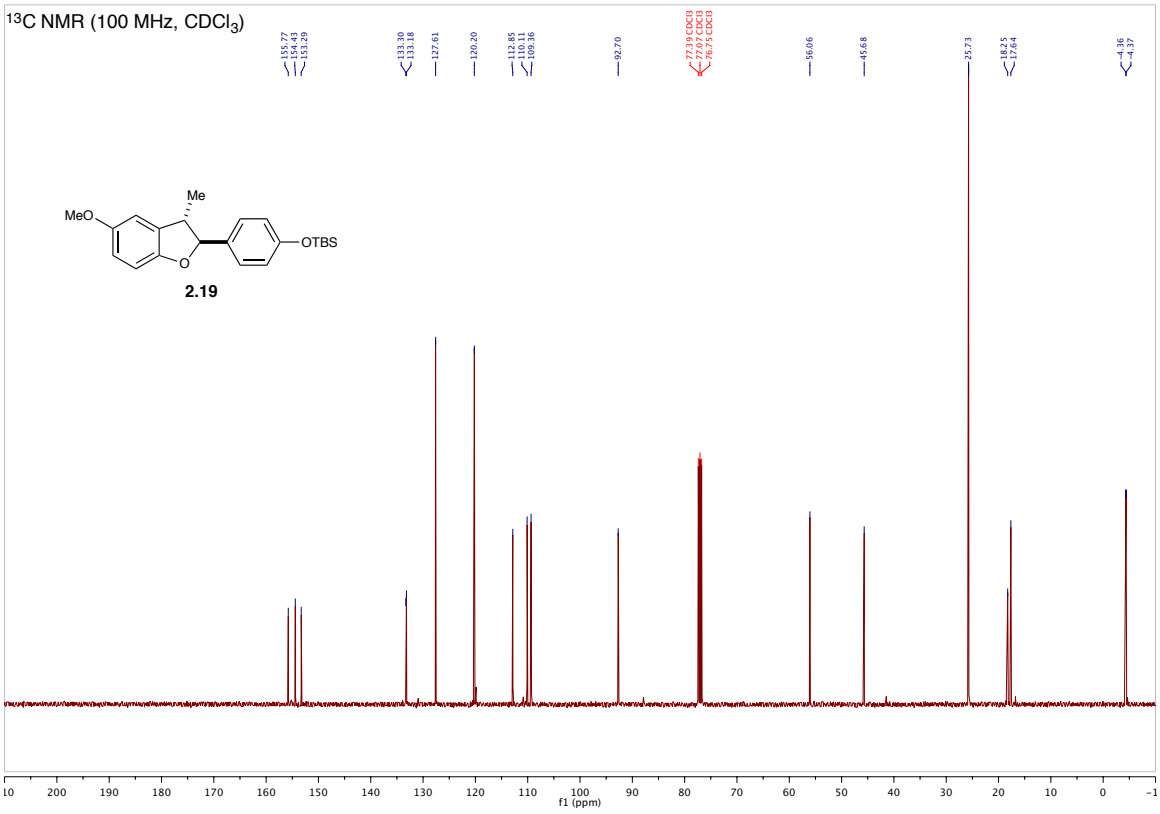
^{13}C NMR (100 MHz, $CDCl_3$)
Me
MeO
OTBS
O
2.19
f1 (ppm)

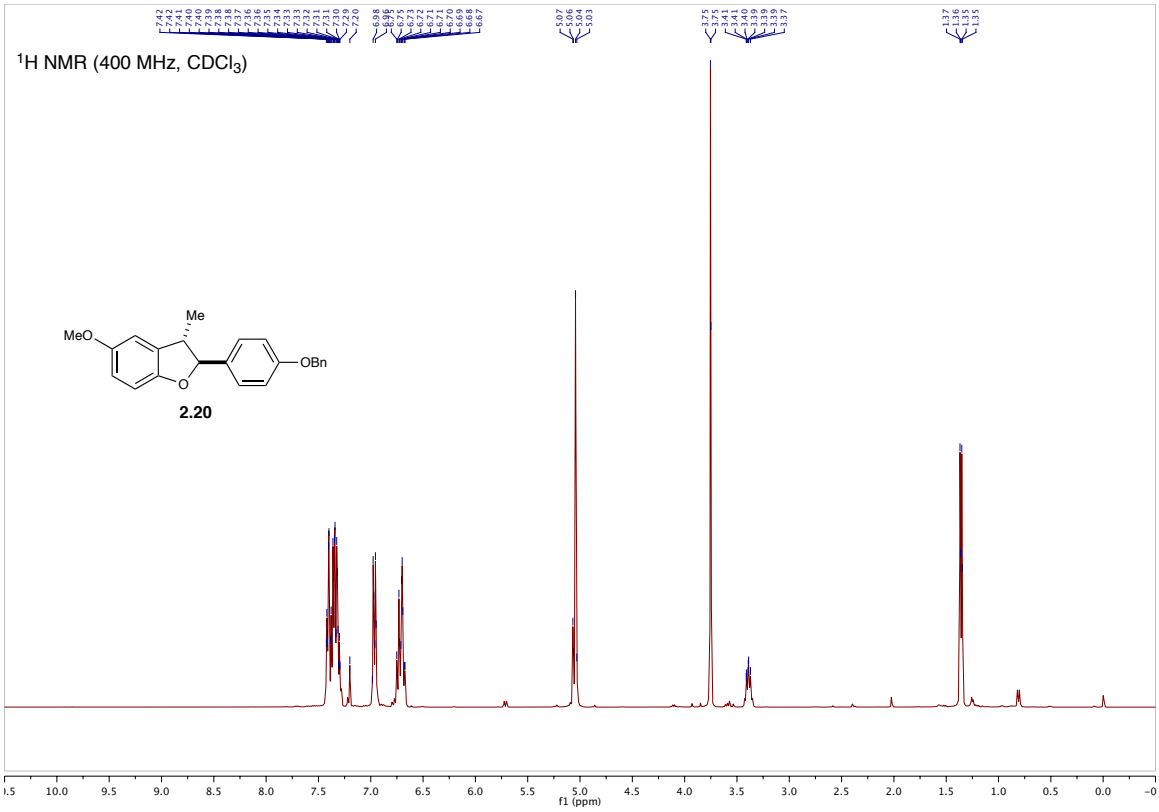
^{1}H NMR (400 MHz, $CDCl_3$)
Me
MeO
OBn
O
2.20
f1 (ppm)

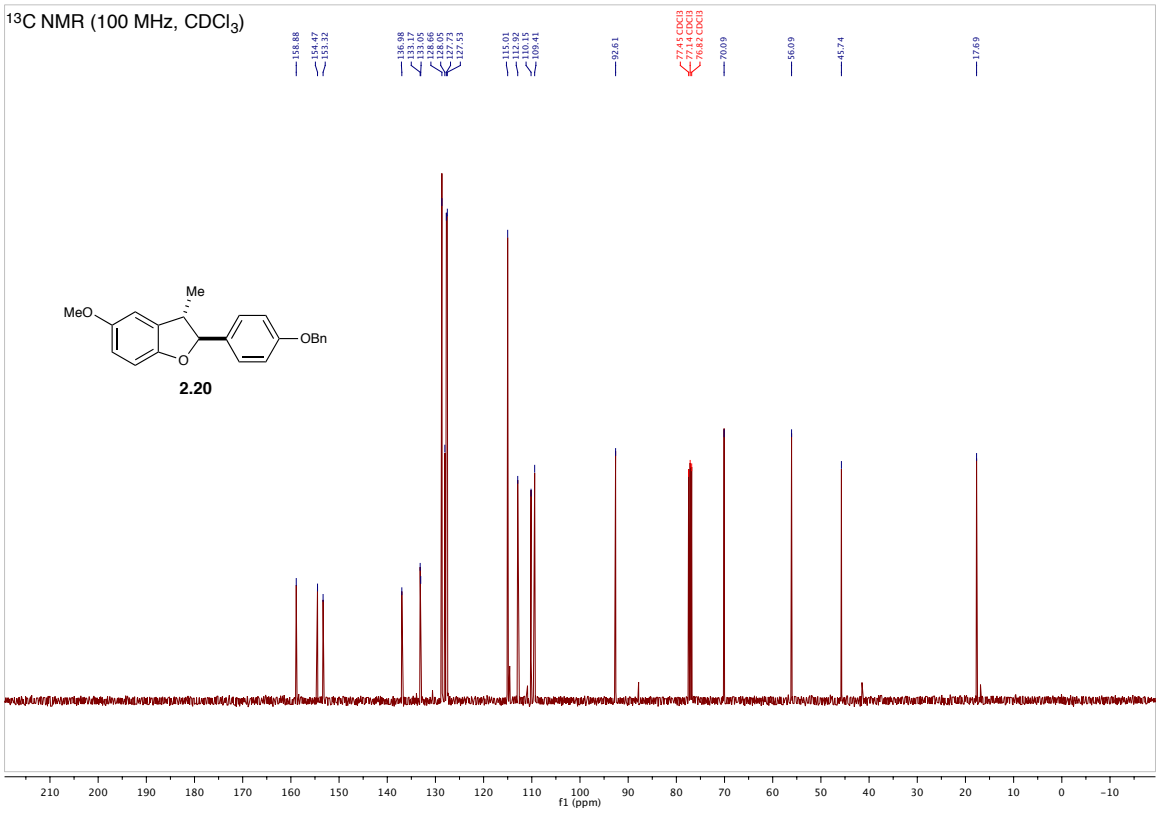
^{13}C NMR (100 MHz, $CDCl_3$)
Me
MeO
OBn
O
2.20
f1 (ppm)

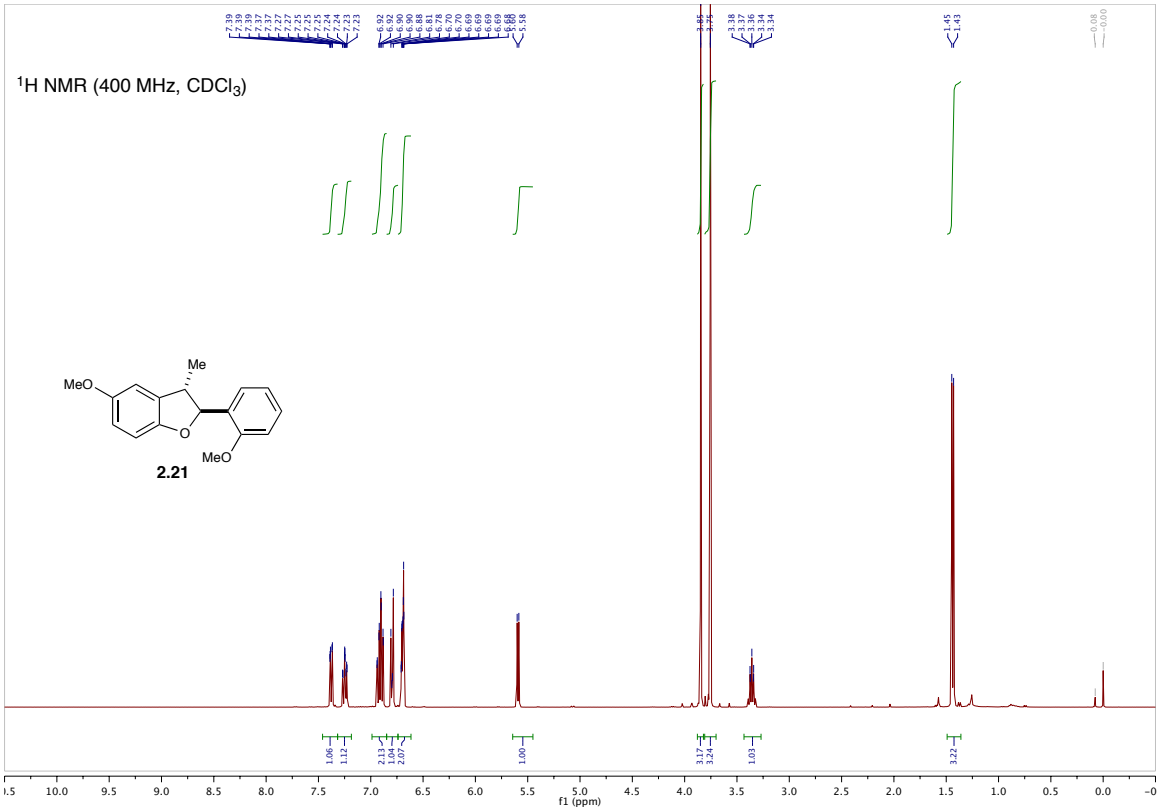
^{1}H NMR (400 MHz, $CDCl_3$)
Me
MeO
O
MeO
2.21
f1 (ppm)

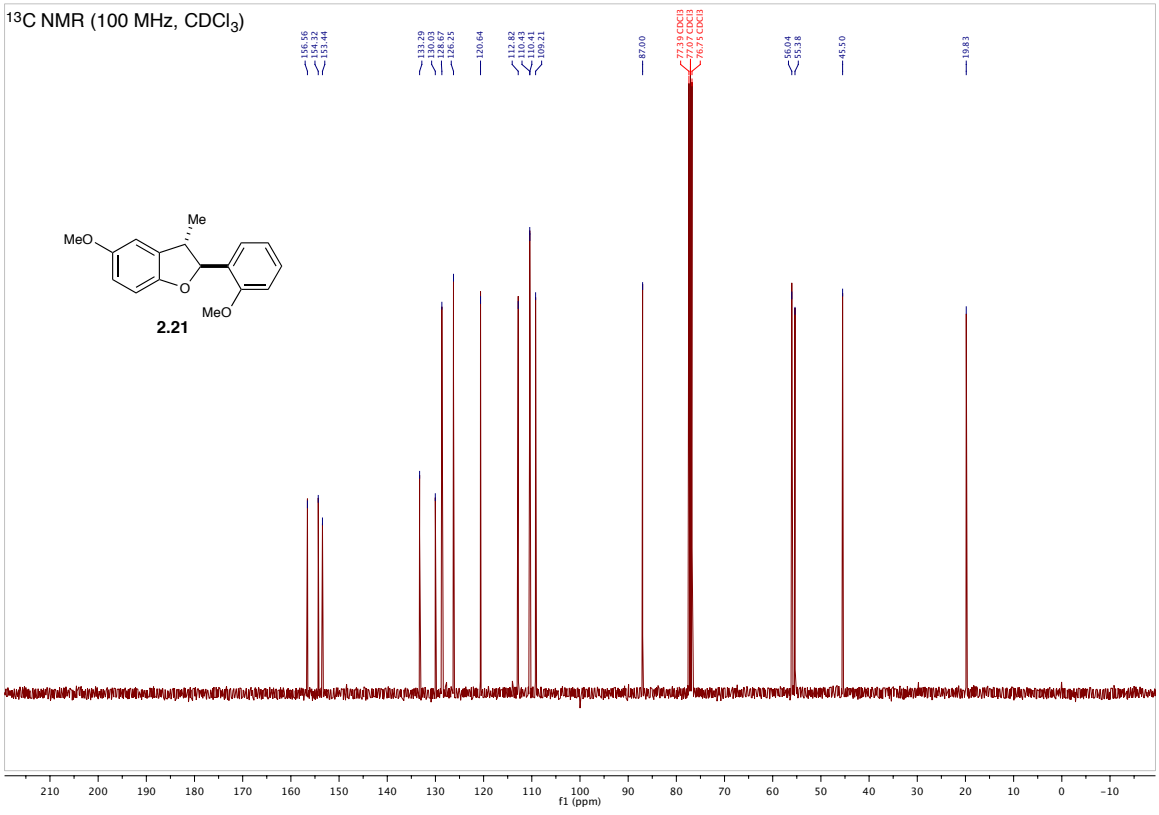
^{13}C NMR (100 MHz, $CDCl_3$)
Me
MeO
O
MeO
2.21
f1 (ppm)

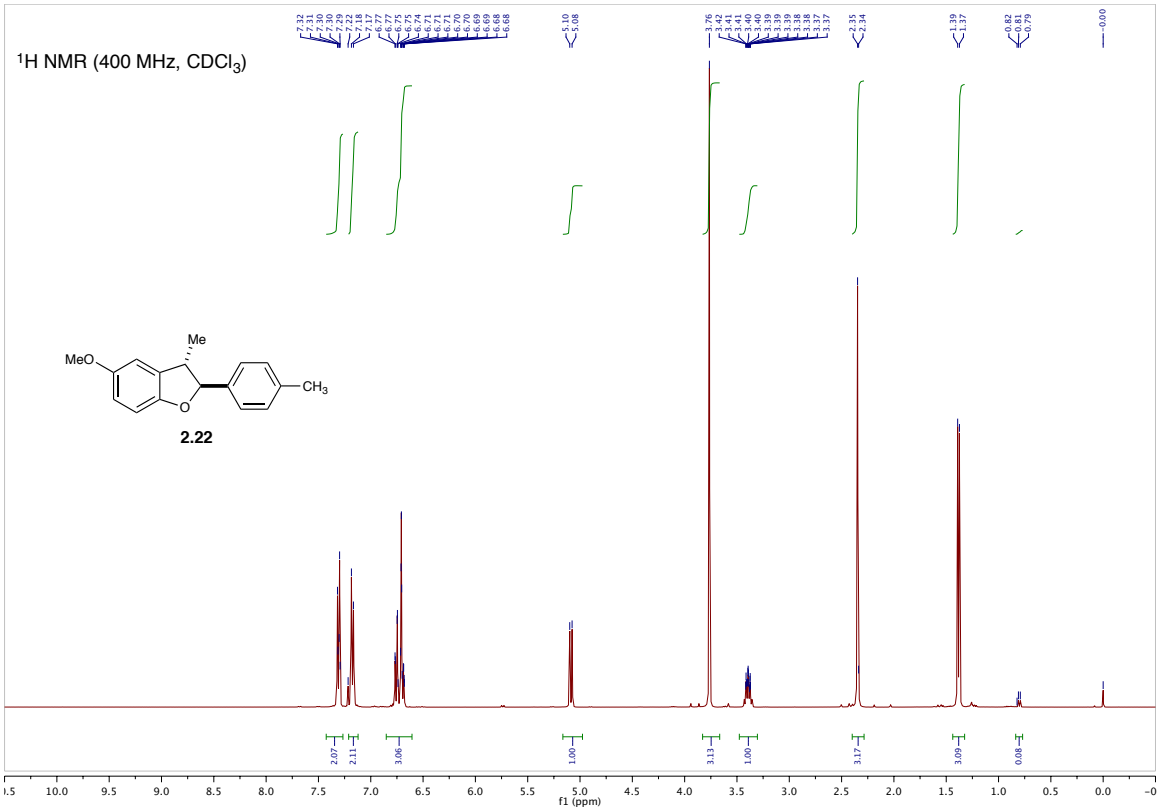
^{1}H NMR (400 MHz, $CDCl_3$)
MeO
Me
CH_3
O
2.22
f1 (ppm)

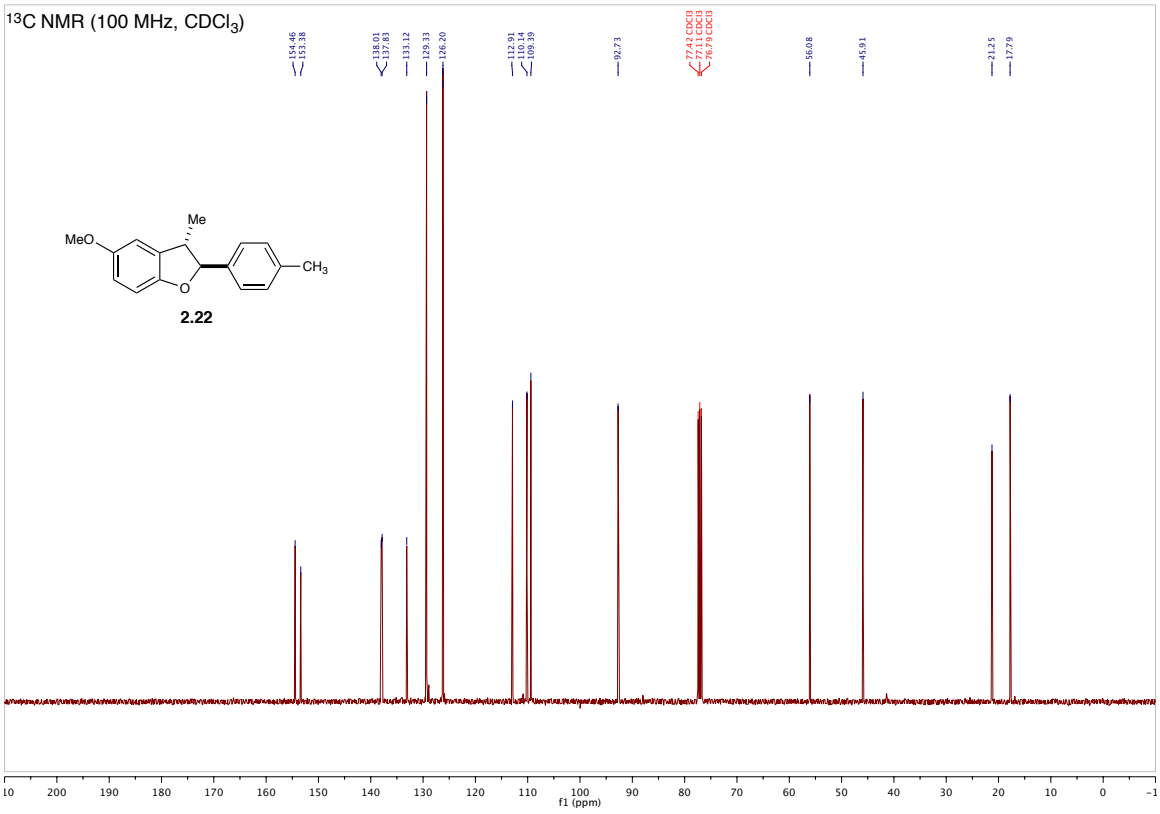
^{13}C NMR (100 MHz, $CDCl_3$)
MeO
Me
CH_3
O
2.22
f1 (ppm)

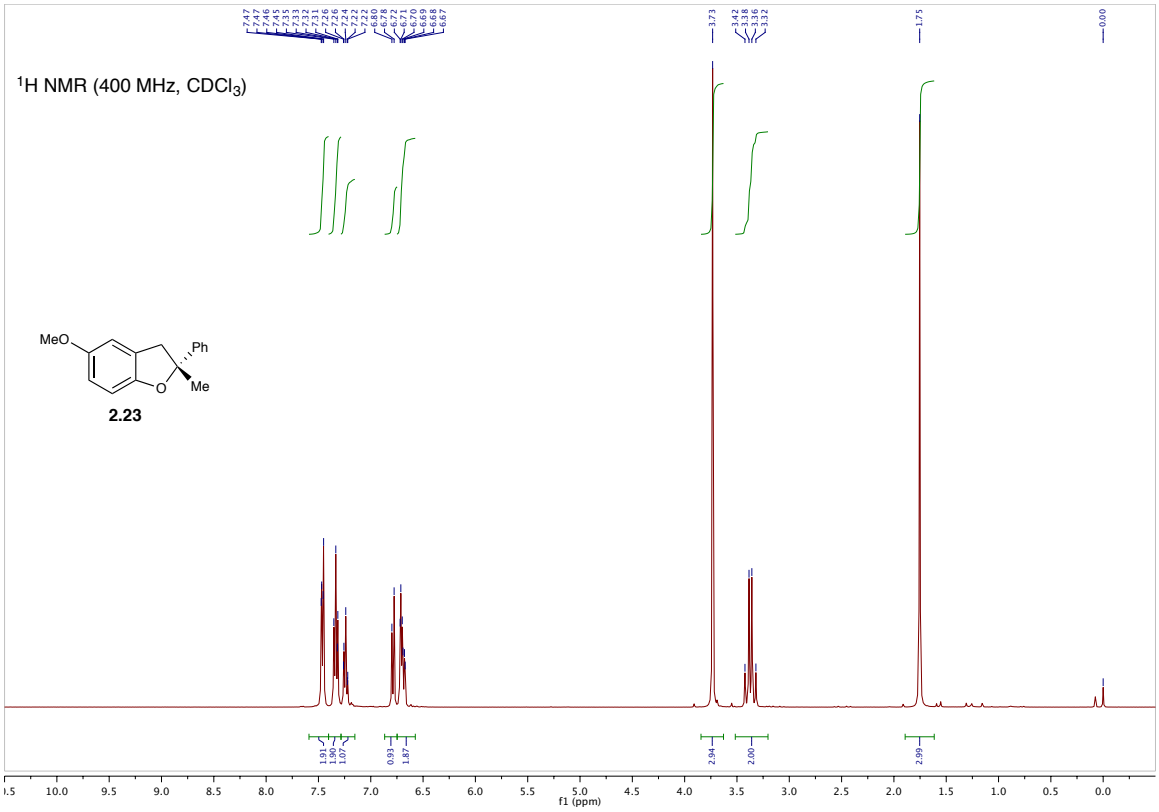
^{1}H NMR (400 MHz, $CDCl_3$)
MeO
Ph
Me
O
2.23
f1 (ppm)

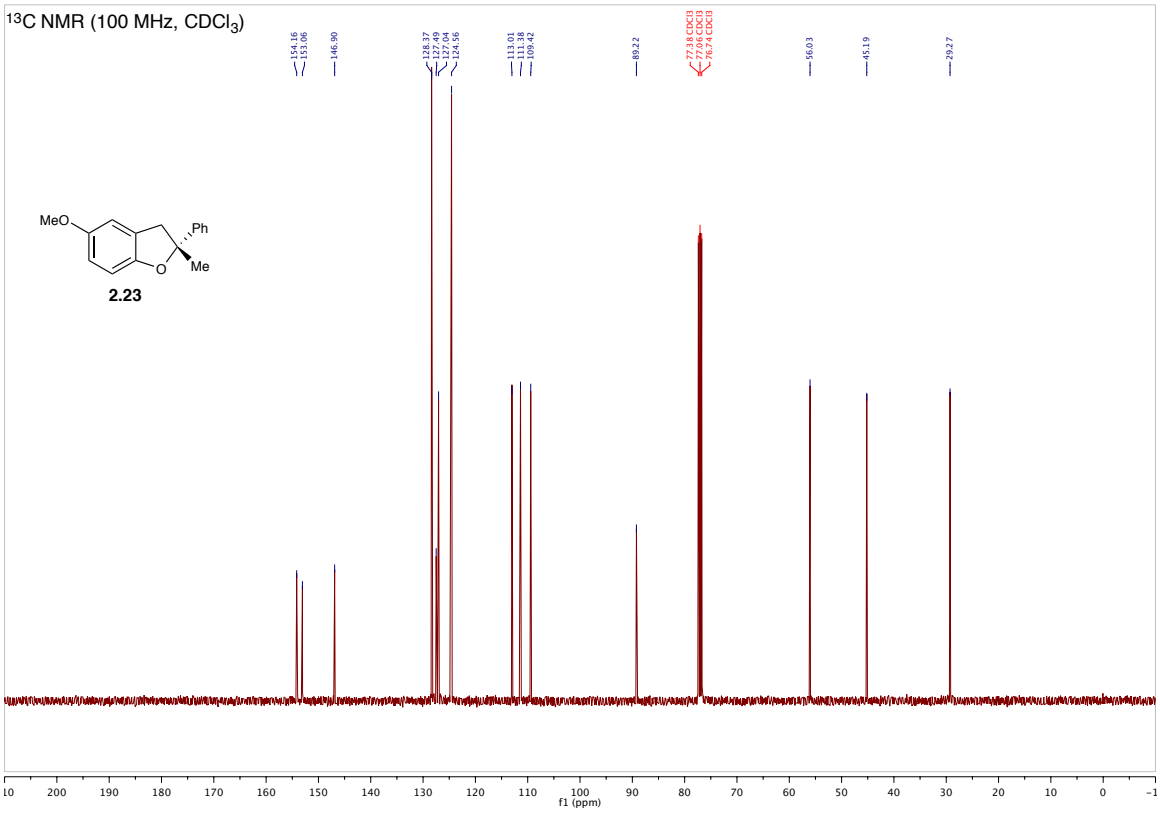
^{13}C NMR (100 MHz, $CDCl_3$)
MeO
Ph
Me
O
2.23
f1 (ppm)

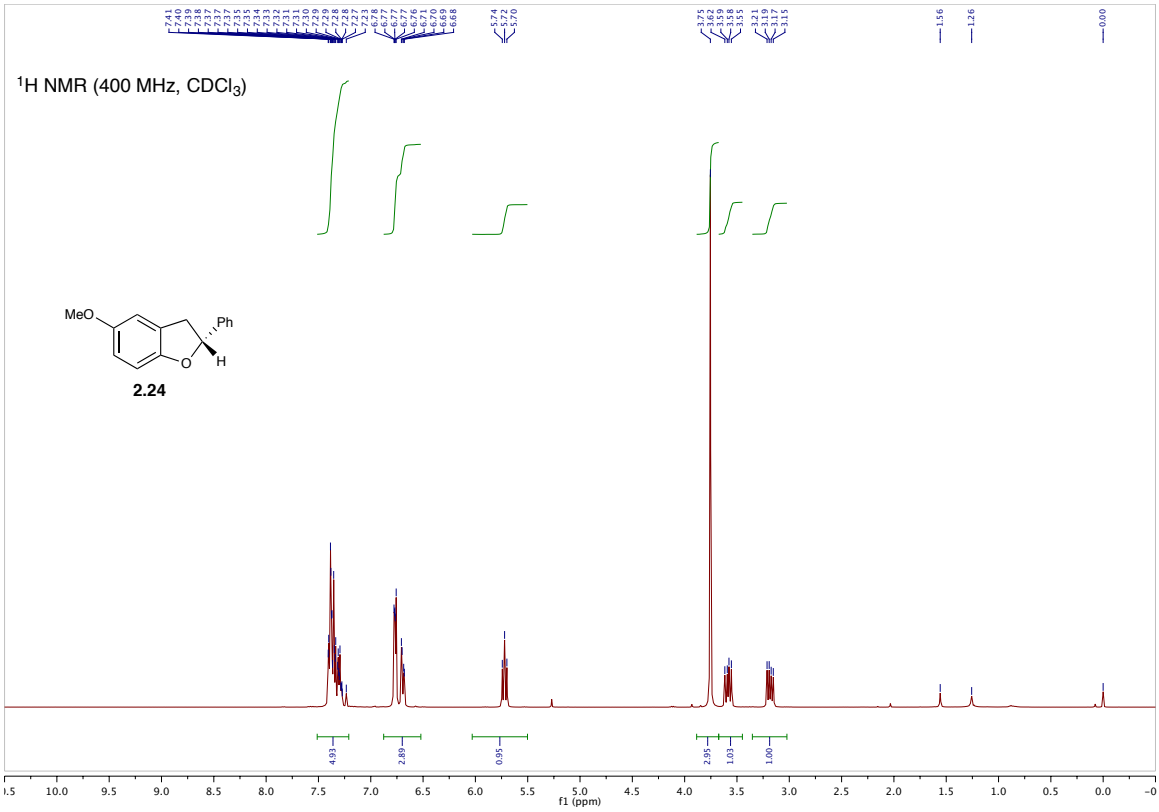
^{1}H NMR (400 MHz, $CDCl_3$)
MeO
Ph
O
H
2.24
f1 (ppm)

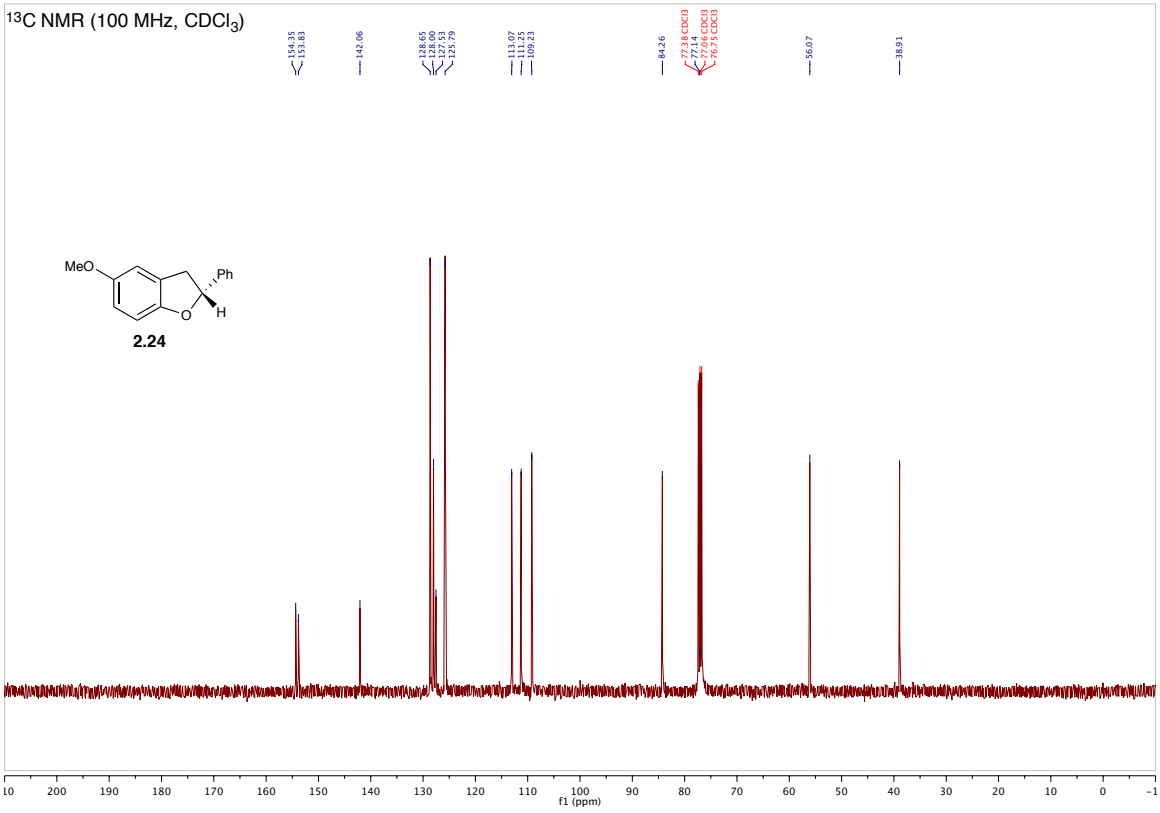
^{13}C NMR (100 MHz, $CDCl_3$)
MeO
Ph
O
H
2.24
f1 (ppm)

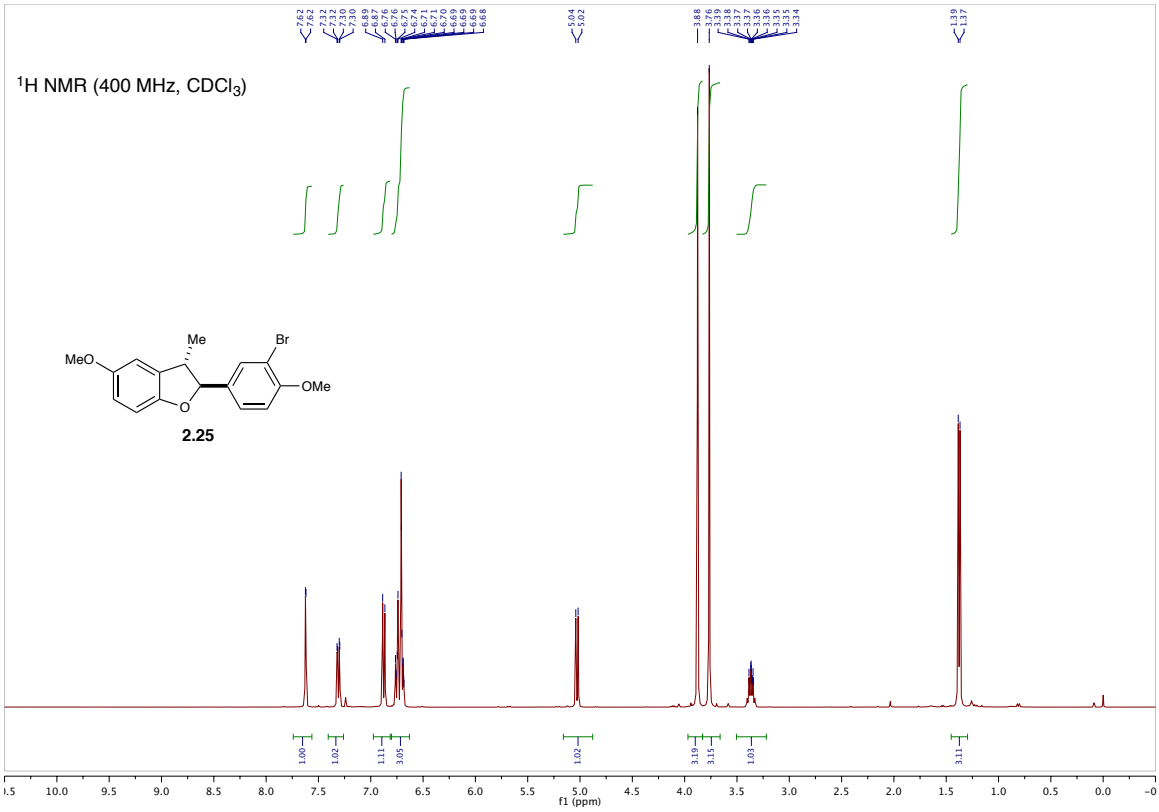
^{1}H NMR (400 MHz, $CDCl_3$)
Me
Br
MeO
OMe
O
2.25
f1 (ppm)

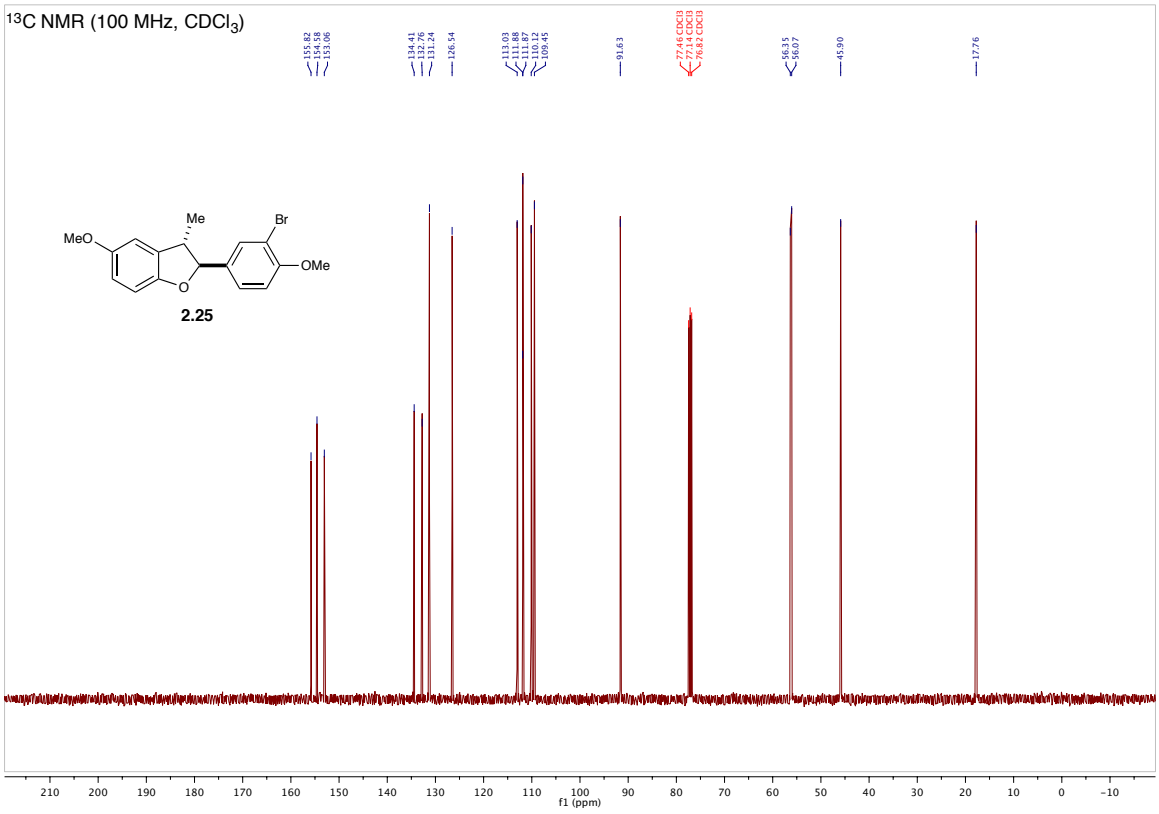
^{13}C NMR (100 MHz, $CDCl_3$)
Me
Br
MeO
OMe
O
2.25
f1 (ppm)

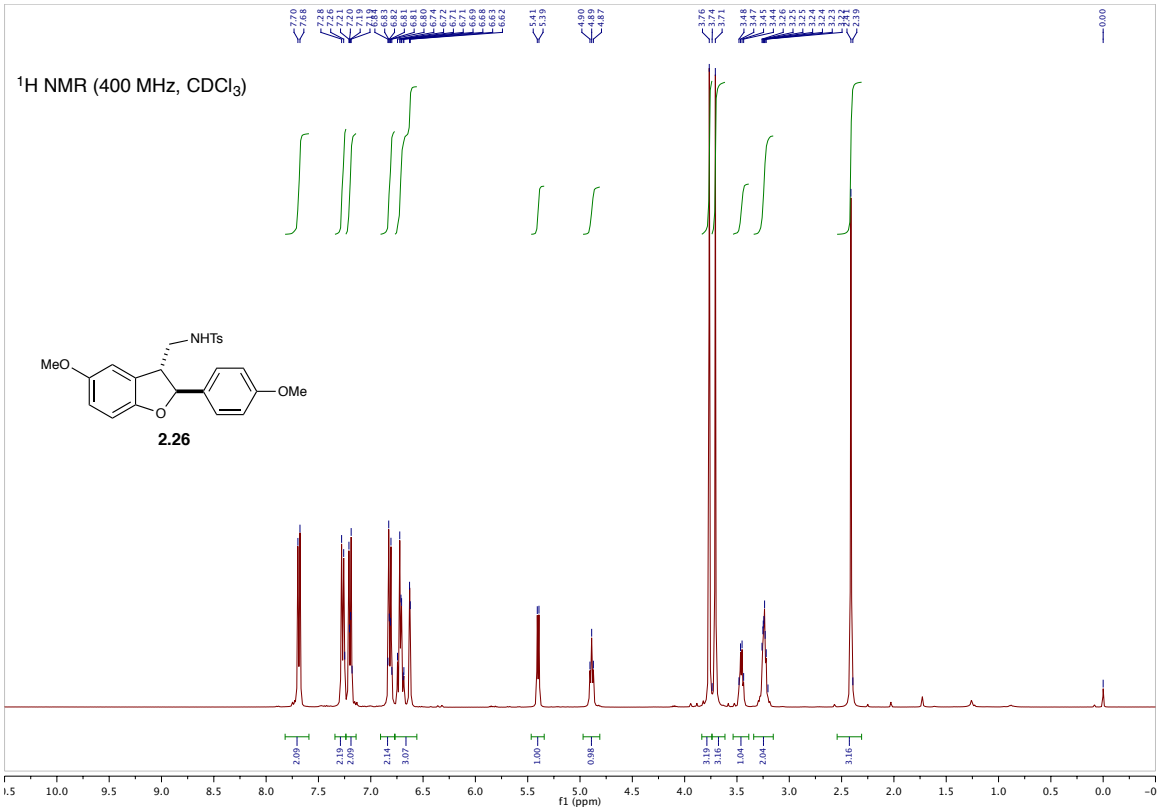
^{1}H NMR (400 MHz, $CDCl_3$)
NHTs
MeO
OMe
O
2.26
f1 (ppm)

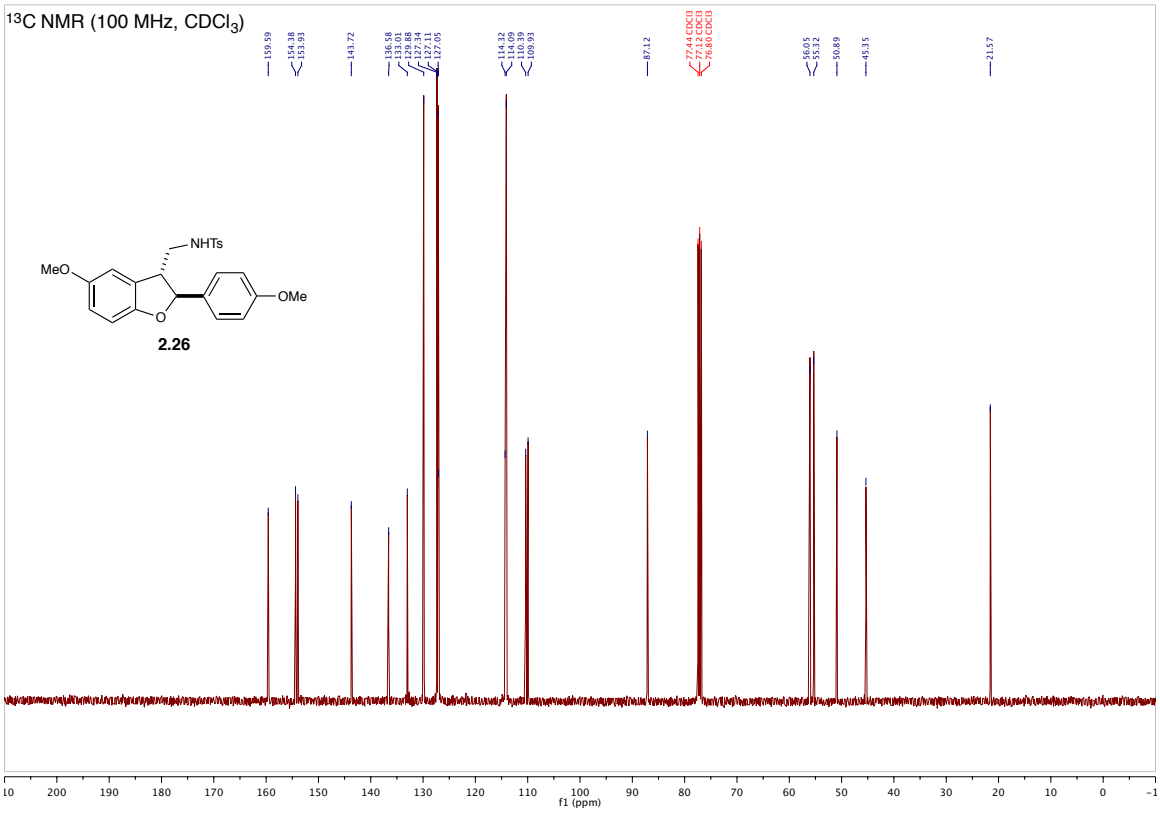
^{13}C NMR (100 MHz, $CDCl_3$)
NHTs
MeO
OMe
O
2.26
f1 (ppm)

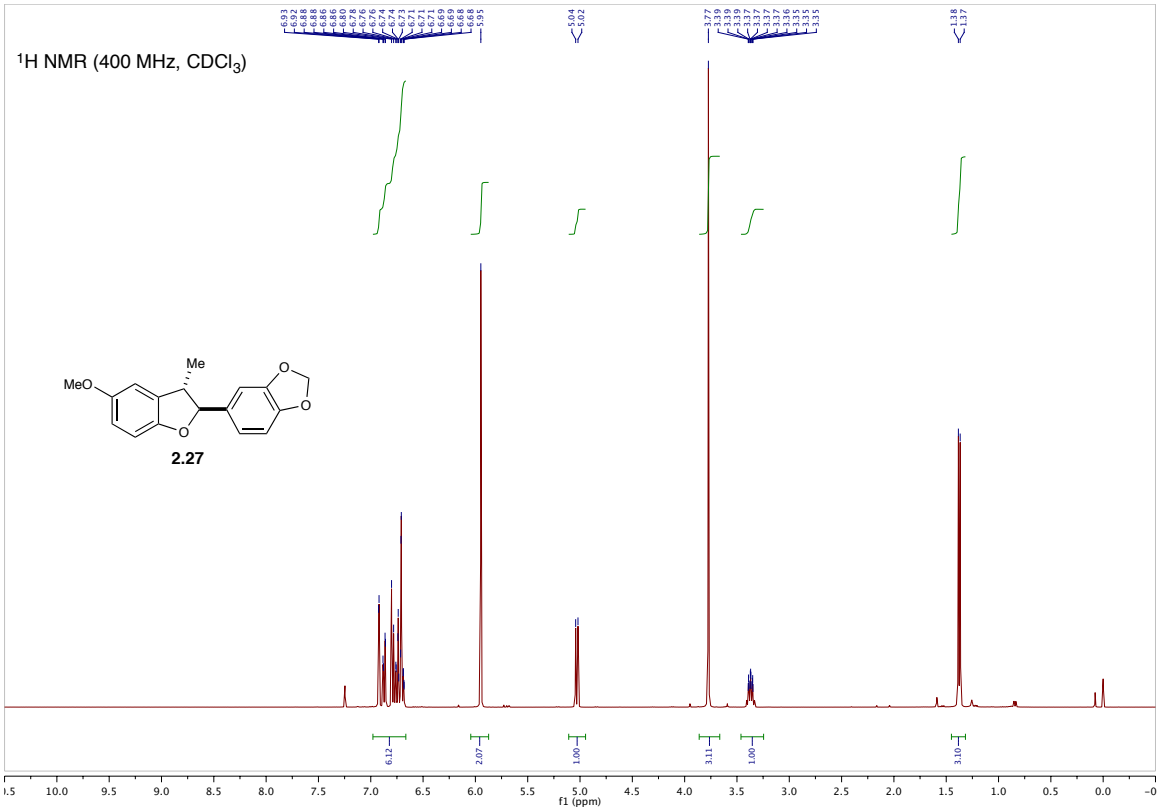
^{1}H NMR (400 MHz, $CDCl_3$)
MeO
Me
O
O
O
2.27
f1 (ppm)

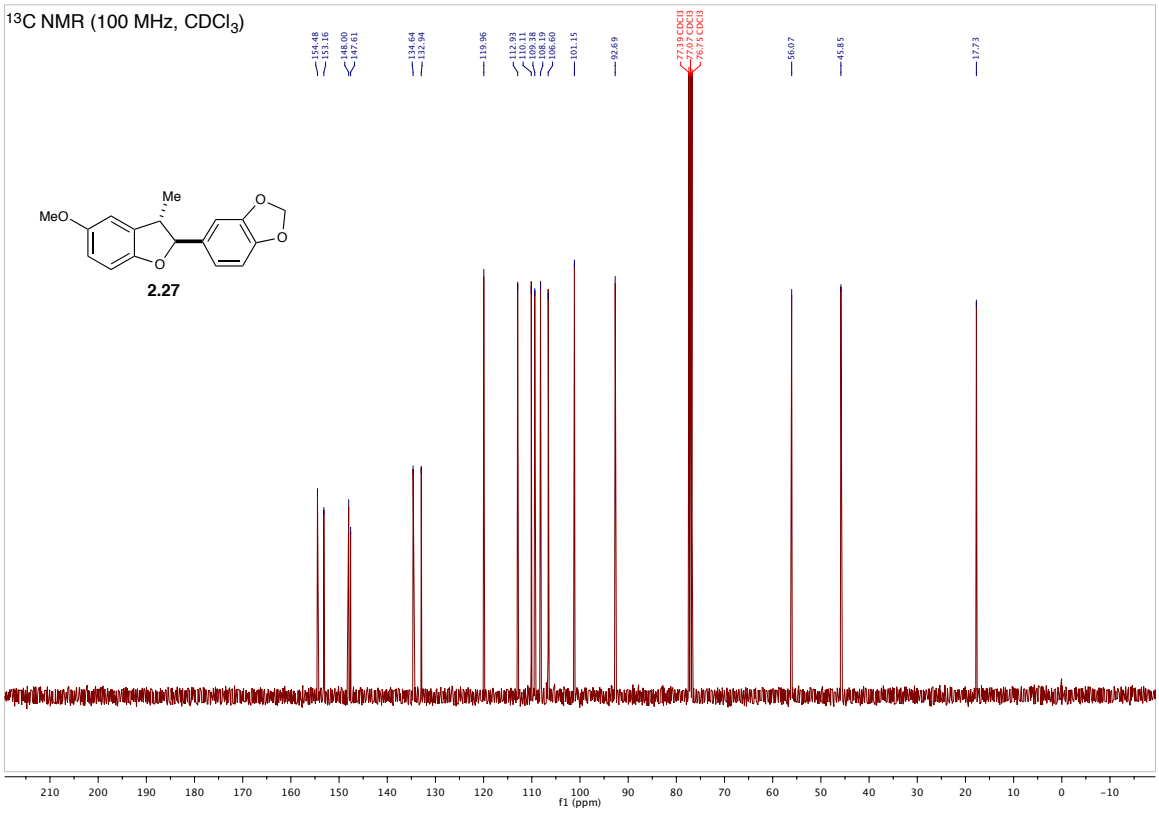
^{13}C NMR (100 MHz, $CDCl_3$)
MeO
Me
O
O
O
2.27
f1 (ppm)

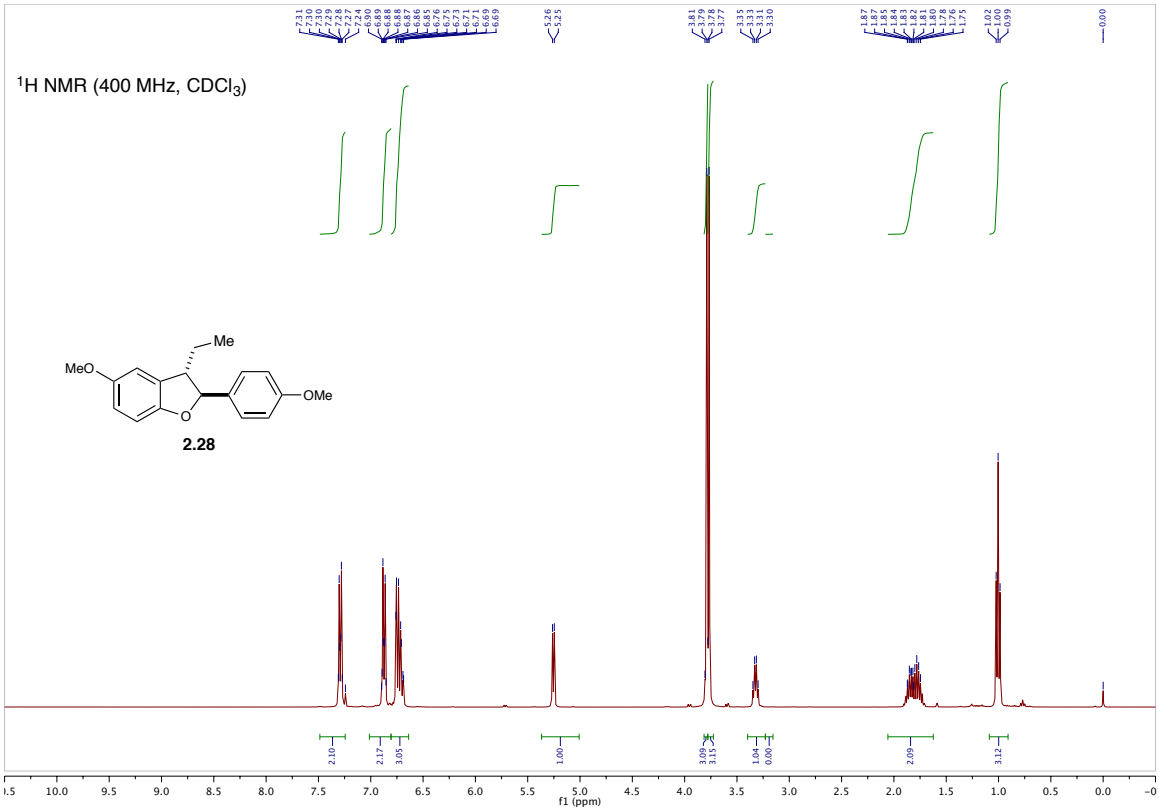
^{1}H NMR (400 MHz, $CDCl_3$)
Me
MeO
OMe
O
2.28
f1 (ppm)

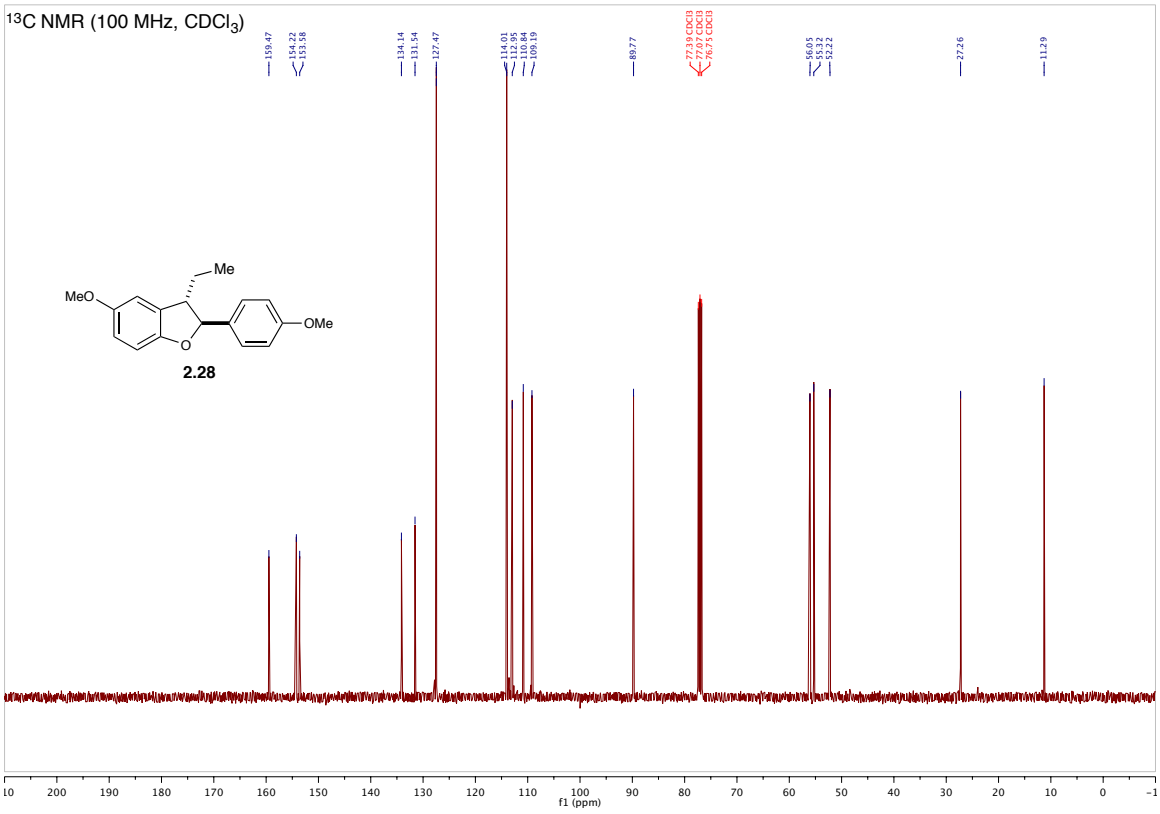
^{13}C NMR (100 MHz, $CDCl_3$)
Me
MeO
OMe
O
2.28
f1 (ppm)

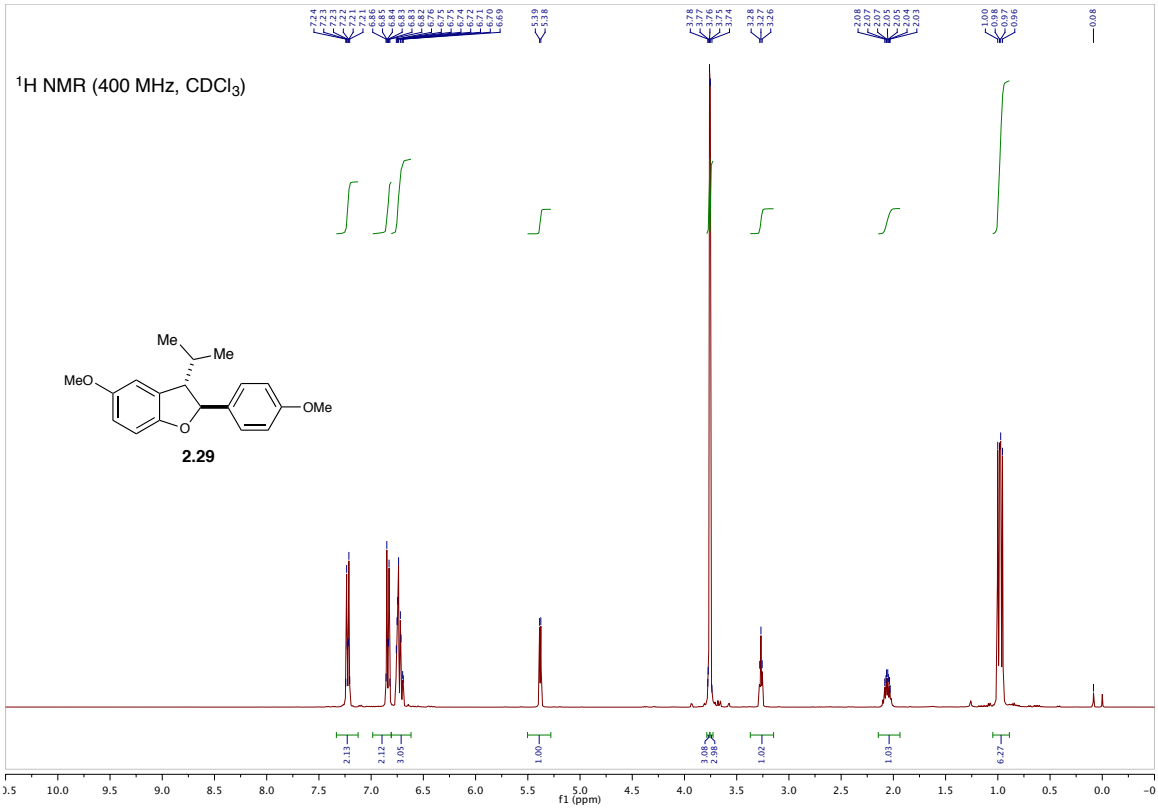
^{1}H NMR (400 MHz, $CDCl_3$)
Me
Me
MeO
OMe
O
2.29
f1 (ppm)

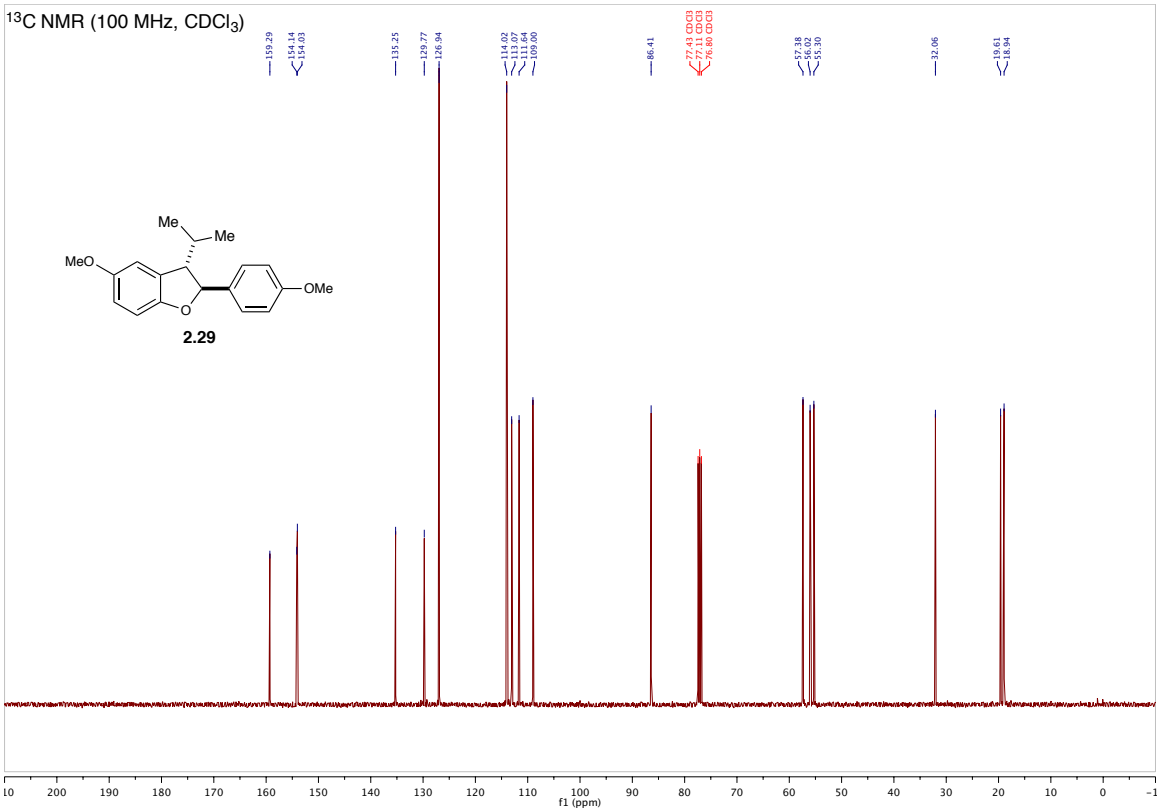
^{13}C NMR (100 MHz, $CDCl_3$)
Me
Me
MeO
OMe
O
2.29
f1 (ppm)

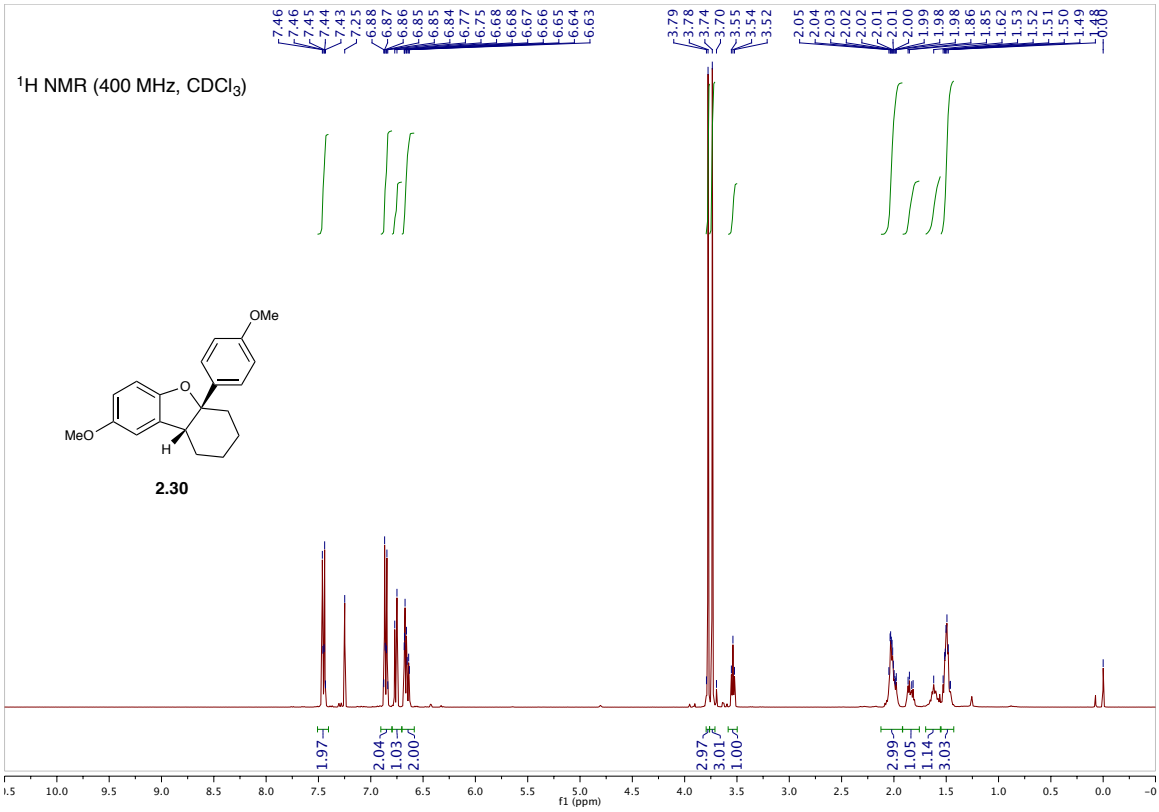
^{1}H NMR (400 MHz, $CDCl_3$)
OMe
MeO
O
H
2.30
f1 (ppm)

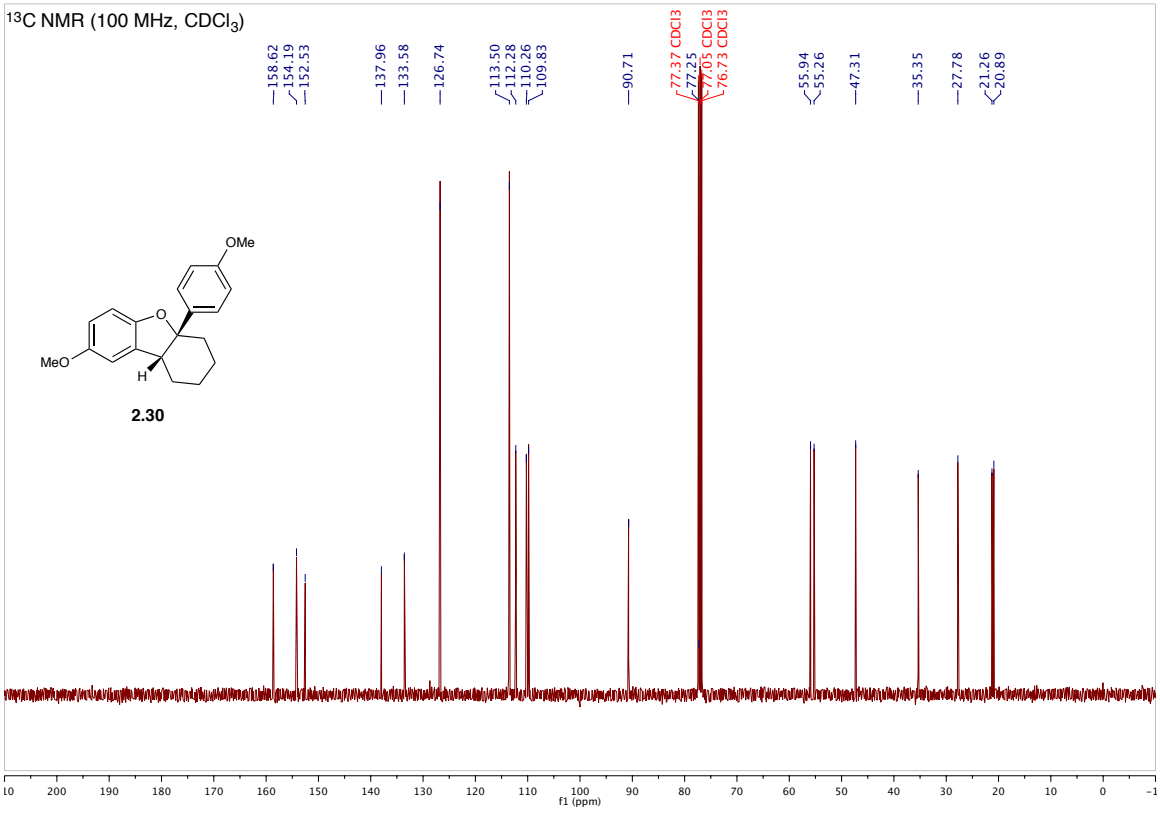
^{13}C NMR (100 MHz, $CDCl_3$)
OMe
MeO
O
H
2.30
f1 (ppm)

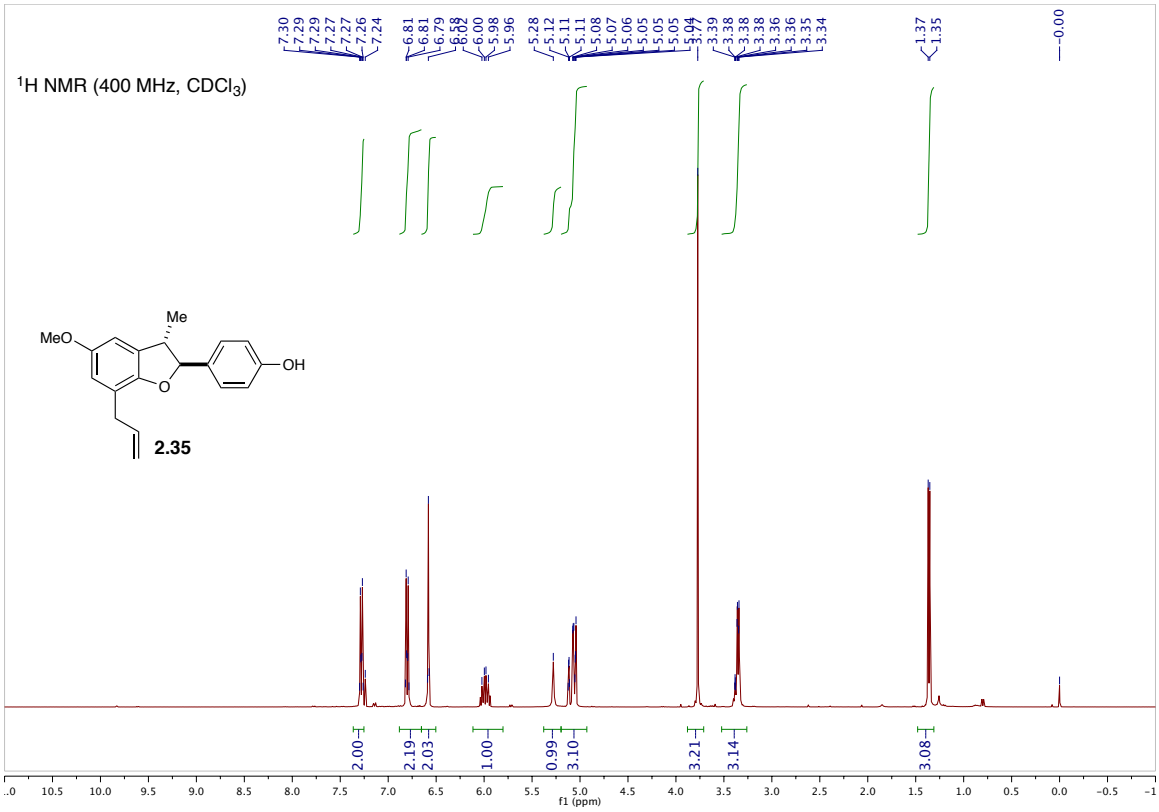
^{1}H NMR (400 MHz, $CDCl_3$)
Me
MeO
OH
O
2.35
f1 (ppm)

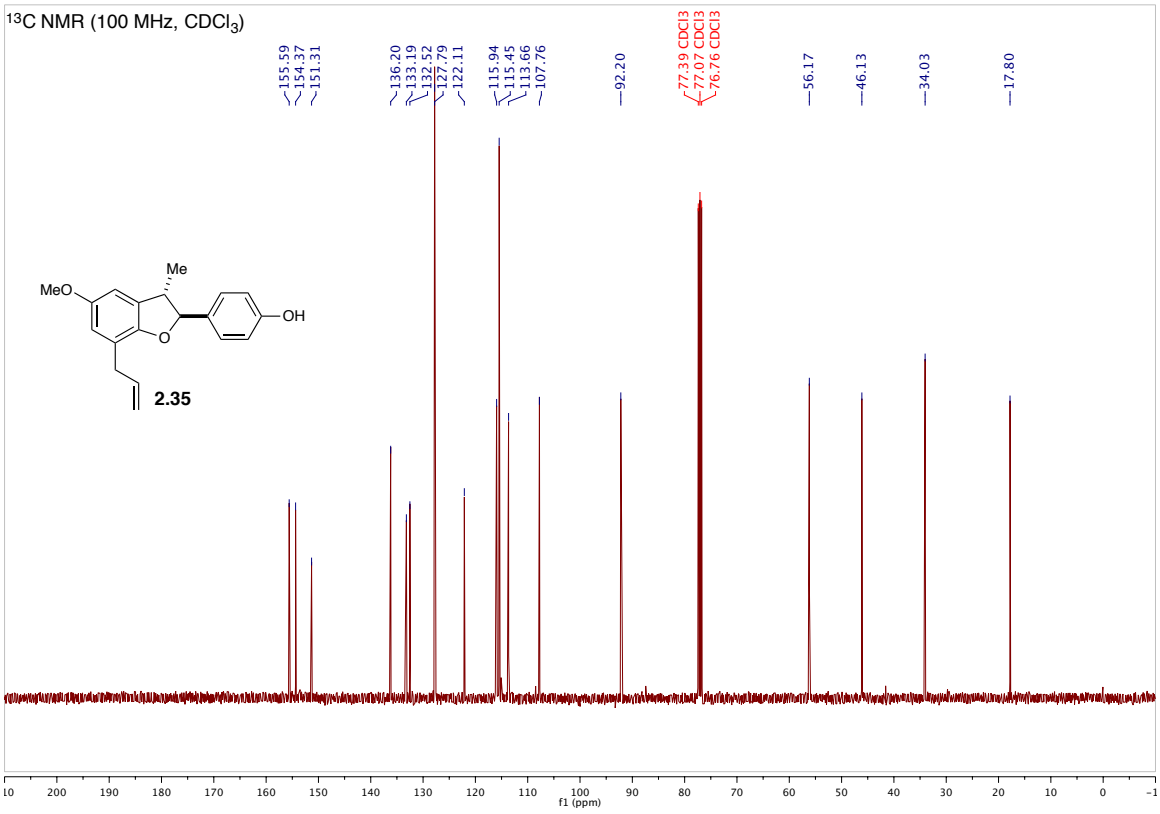
^{13}C NMR (100 MHz, $CDCl_3$)
Me
MeO
OH
O
2.35
f1 (ppm)

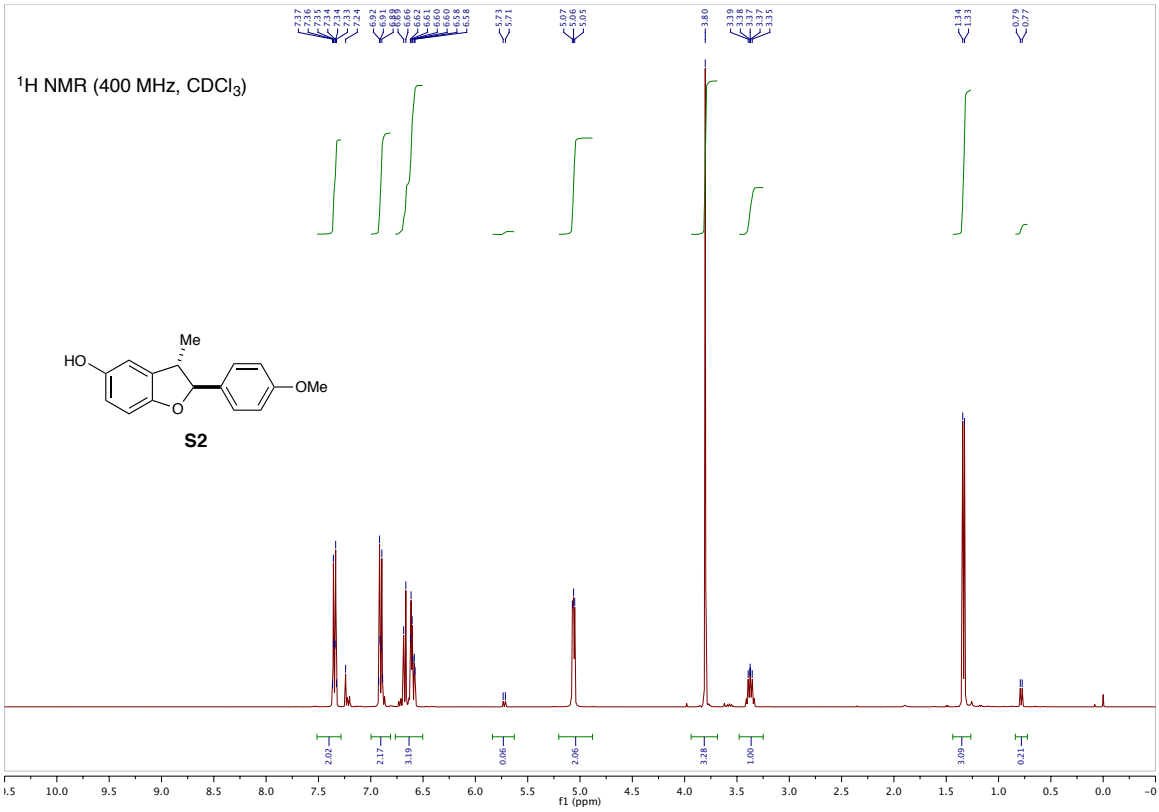
^{1}H NMR (400 MHz, $CDCl_3$)
HO
Me
OMe
O
S2
f1 (ppm)

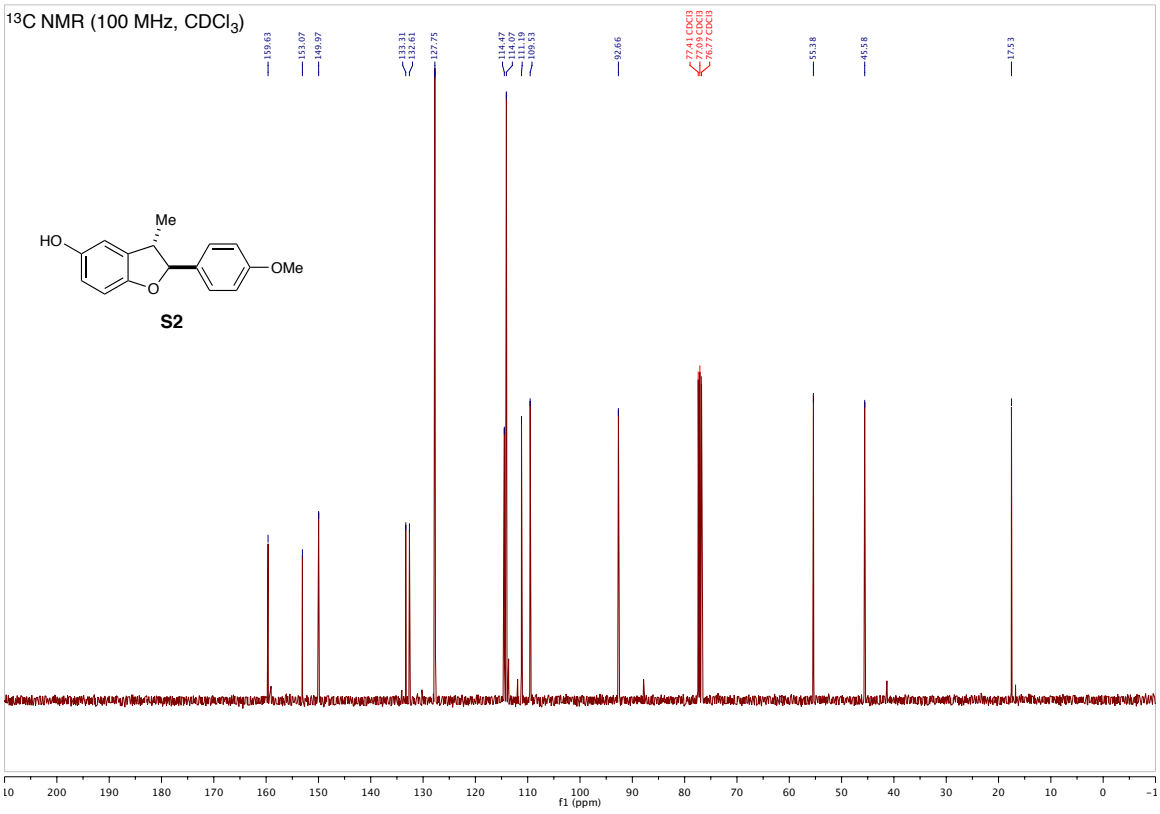
^{13}C NMR (100 MHz, $CDCl_3$)
HO
Me
OMe
O
S2
f1 (ppm)

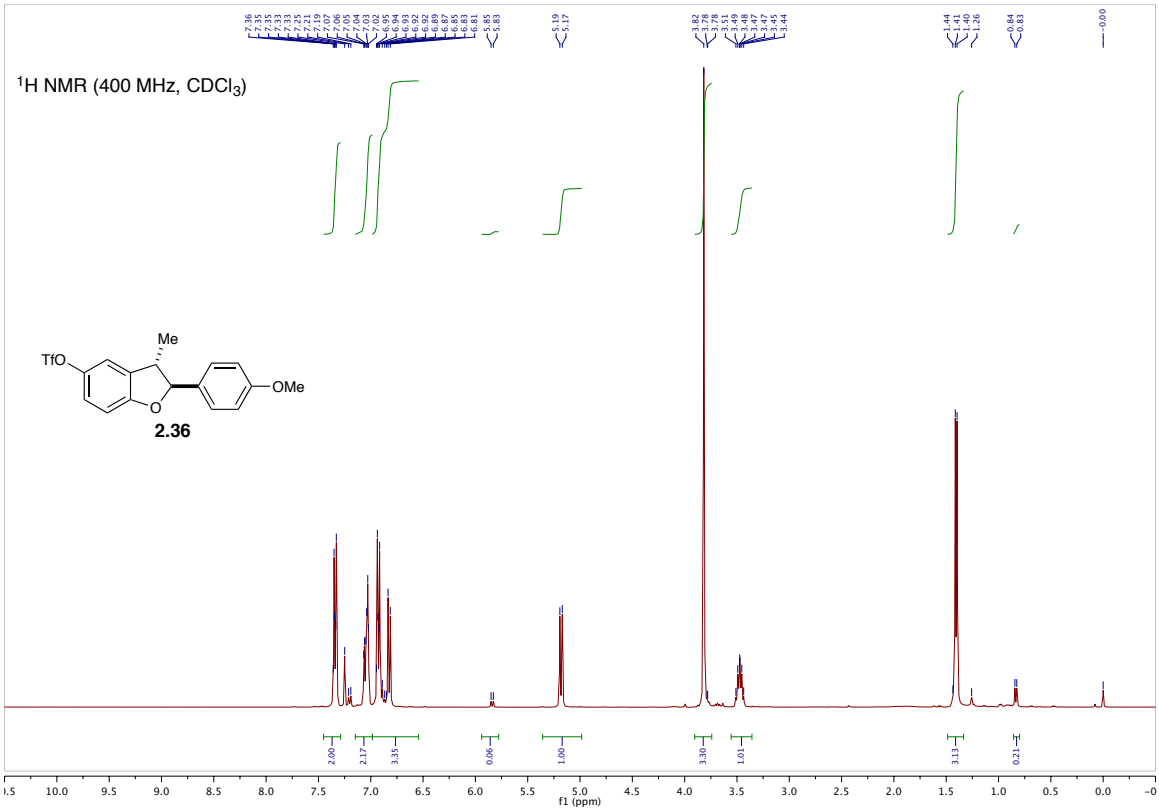
^{1}H NMR (400 MHz, $CDCl_3$)
Me
TfO
OMe
O
2.36
f1 (ppm)

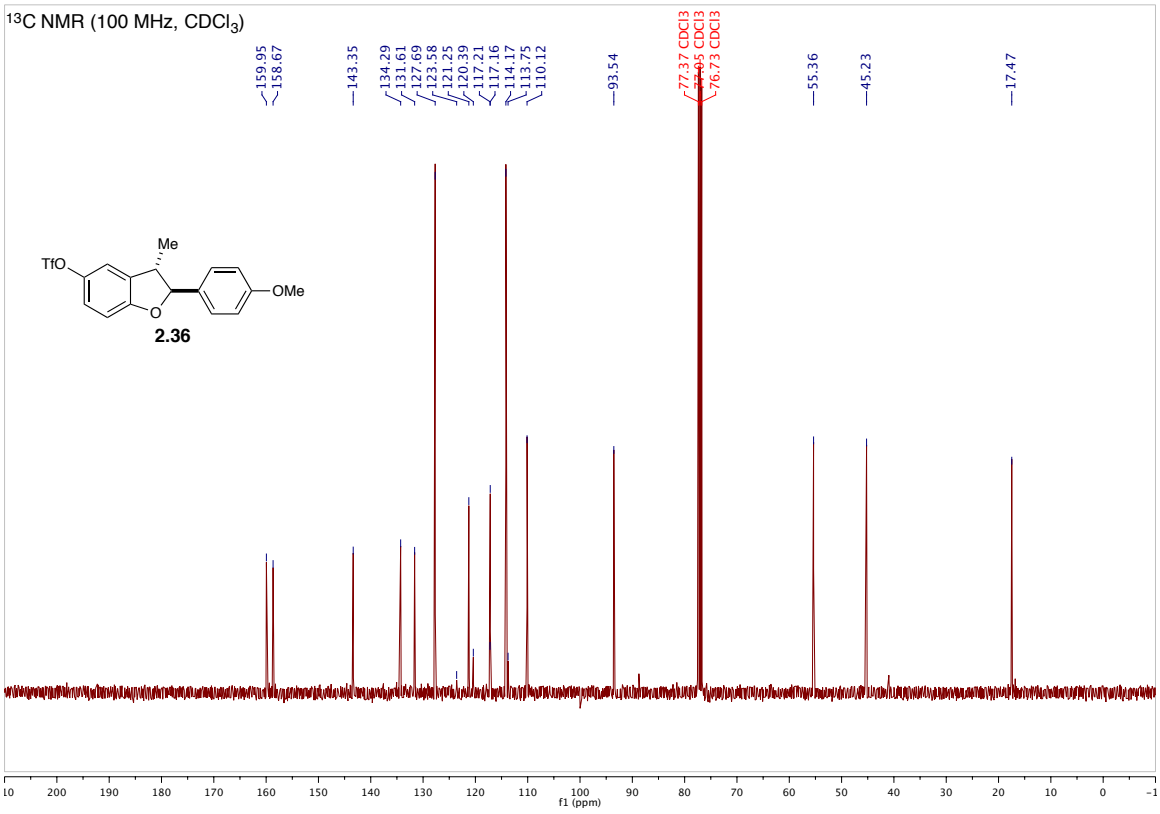
^{13}C NMR (100 MHz, $CDCl_3$)
159.95
158.67
143.35
134.29
131.61
127.69
123.58
121.25
120.39
117.21
117.16
114.17
113.75
110.12
93.54
77.37 CDCl3
77.05 CDCl3
76.73 CDCl3
55.36
45.23
17.47
Me
TfO
OMe
O
2.36
f1 (ppm)

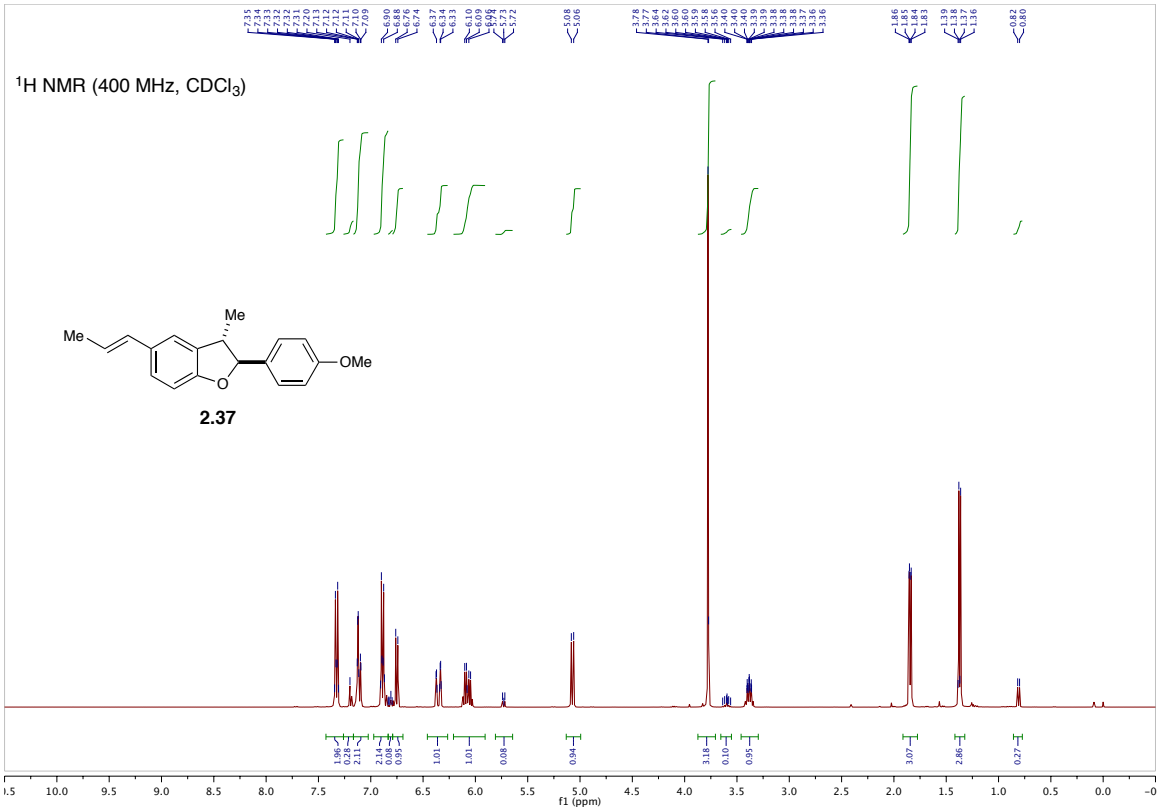
^{1}H NMR (400 MHz, $CDCl_3$)
Me
Me
OMe
O
2.37
f1 (ppm)

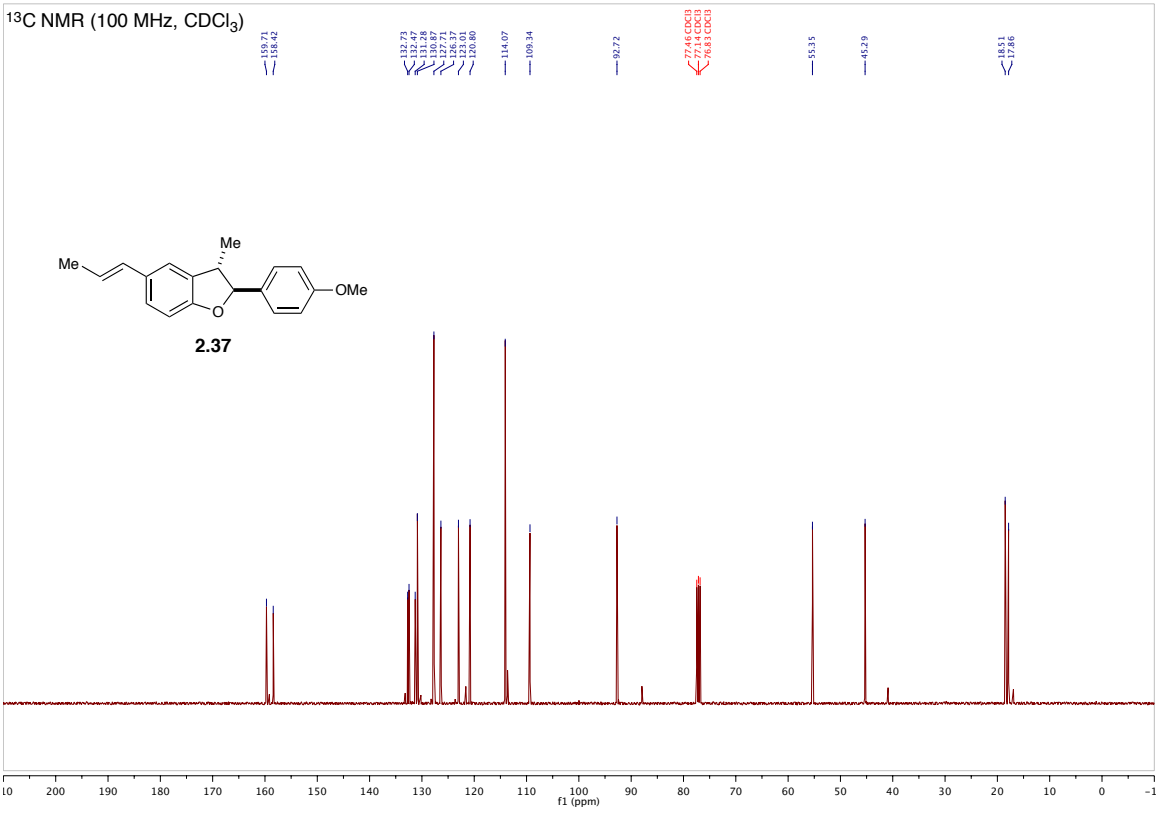
^{13}C NMR (100 MHz, $CDCl_3$)
Me
Me
OMe
O
2.37
f1 (ppm)

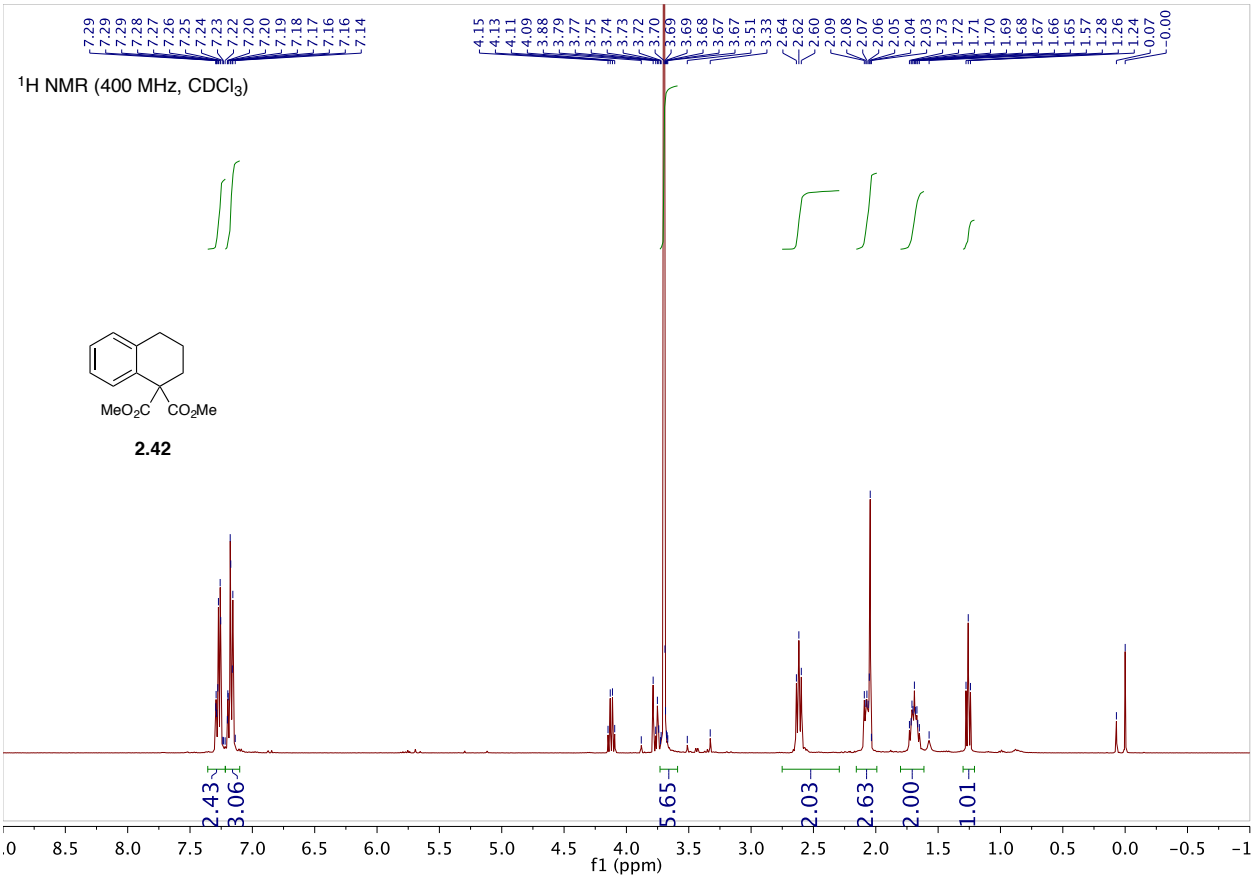
^{1}H NMR (400 MHz, $CDCl_3$)
MeO$_2$C CO$_2$Me
2.42
2.43
3.06
5.65
2.03
2.63
2.00
1.01
f1 (ppm)

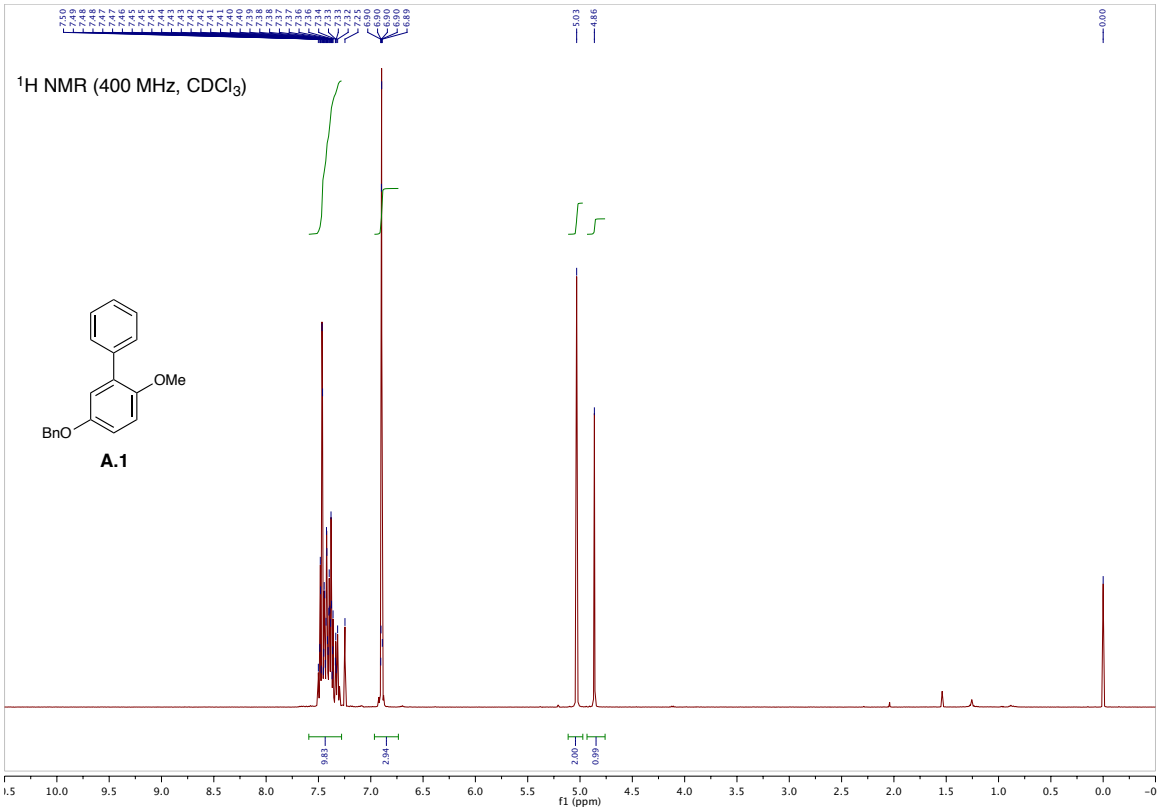
^{1}H NMR (400 MHz, $CDCl_3$)
OMe
BnO
A.1
f1 (ppm)

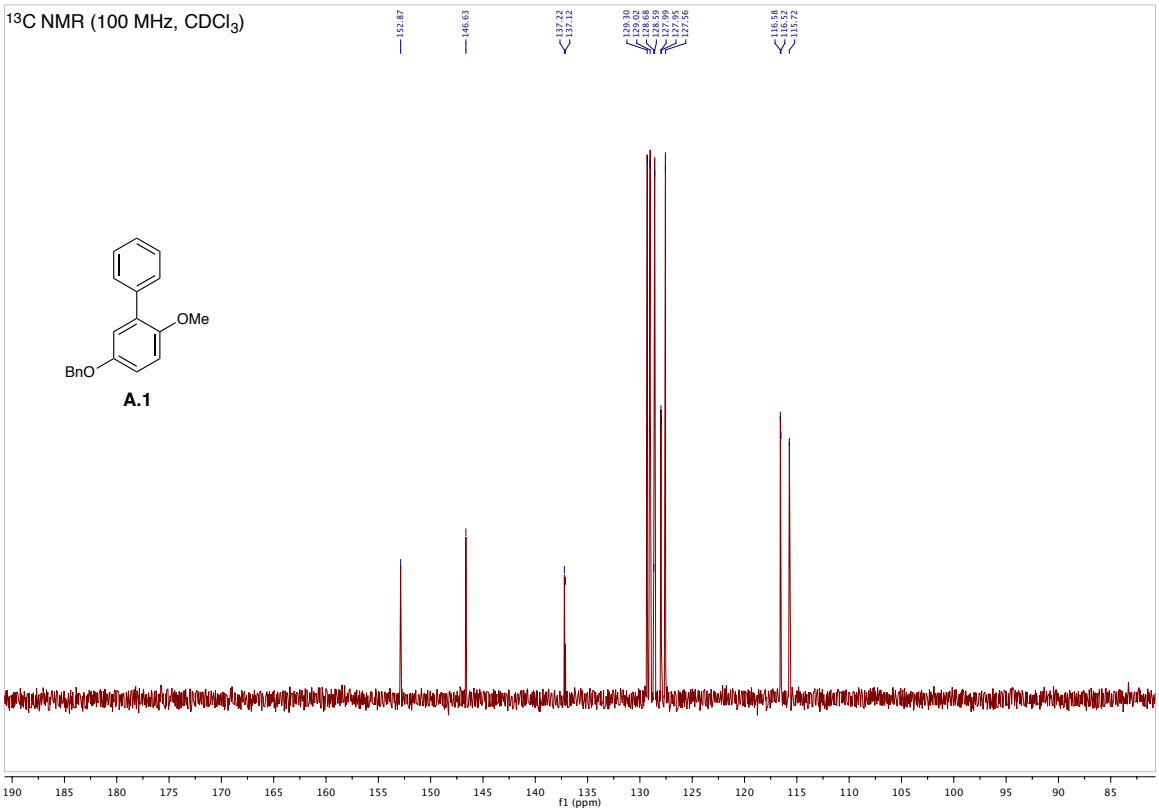
^{13}C NMR (100 MHz, $CDCl_3$)
OMe
BnO
A.1
f1 (ppm)

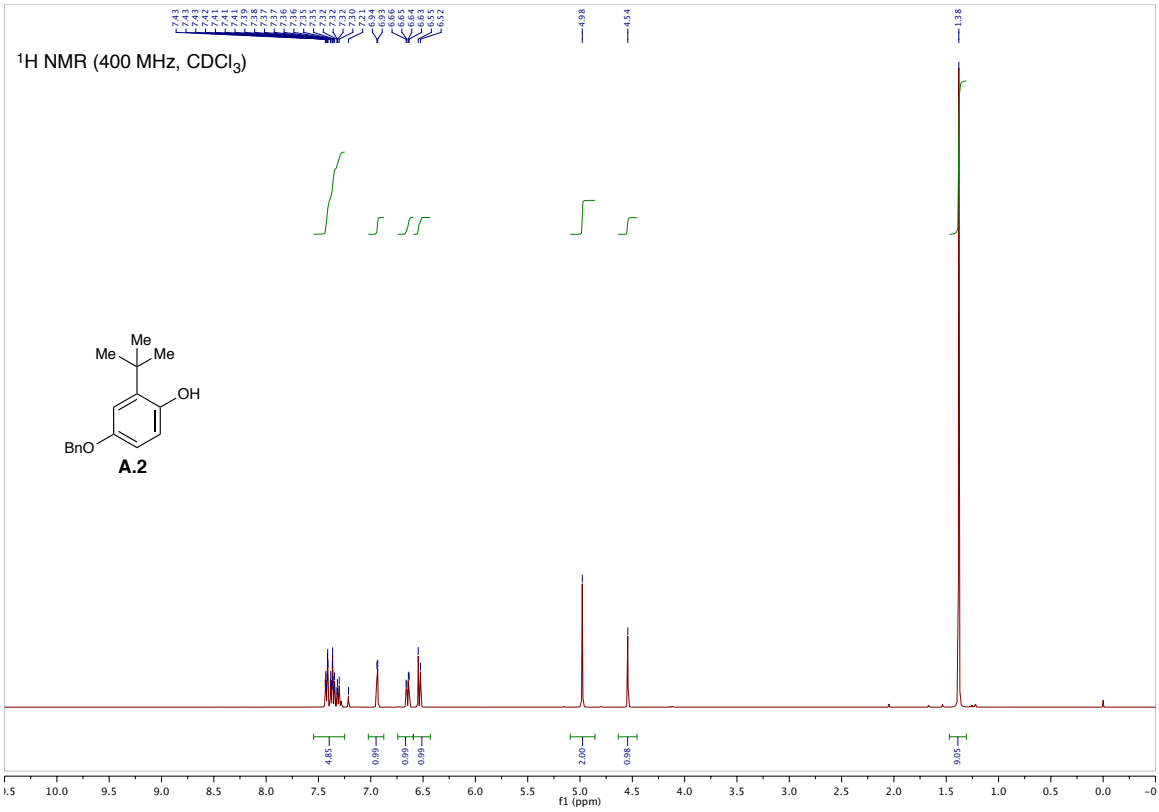
^{1}H NMR (400 MHz, $CDCl_3$)
Me
Me
Me
OH
BnO
A.2
f1 (ppm)

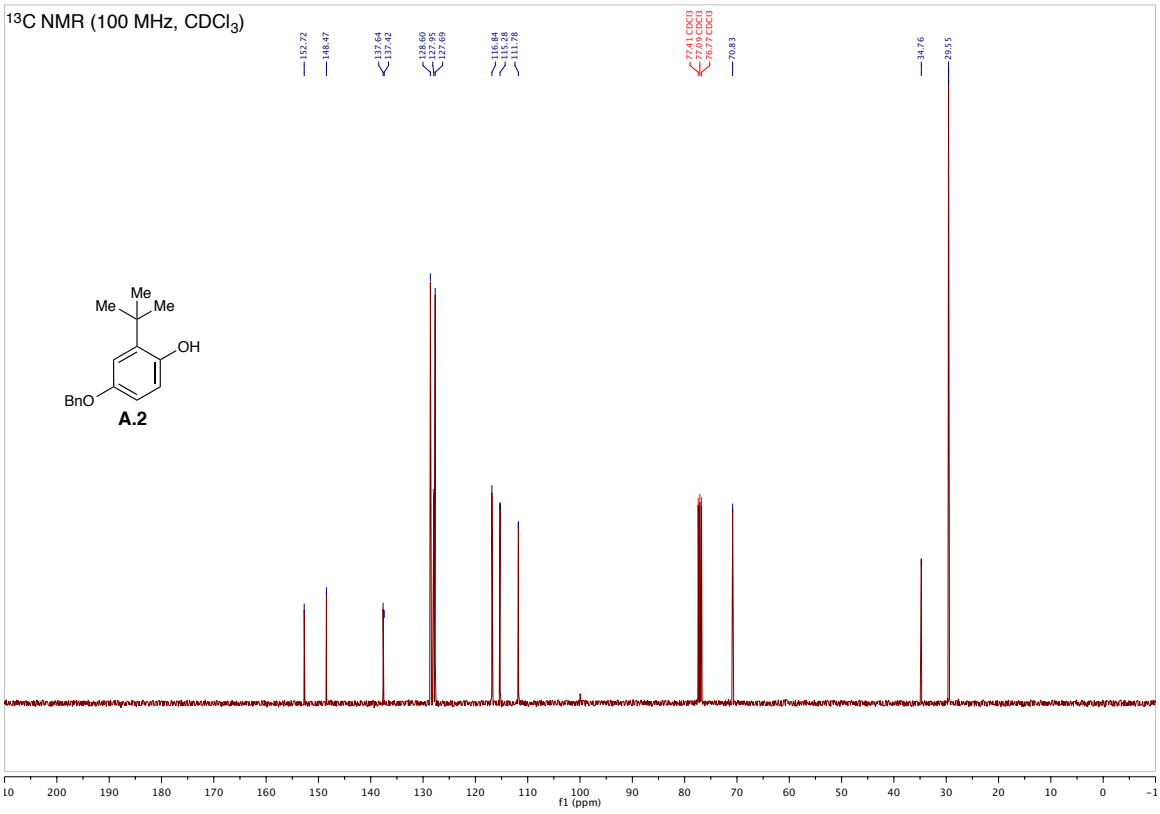
^{13}C NMR (100 MHz, $CDCl_3$)
Me
Me
Me
OH
BnO
A.2
f1 (ppm)

^{1}H NMR (400 MHz, $CDCl_3$)

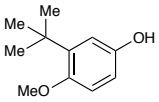

A.3

^{13}C NMR (100 MHz, $CDCl_3$)

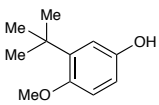

A.3

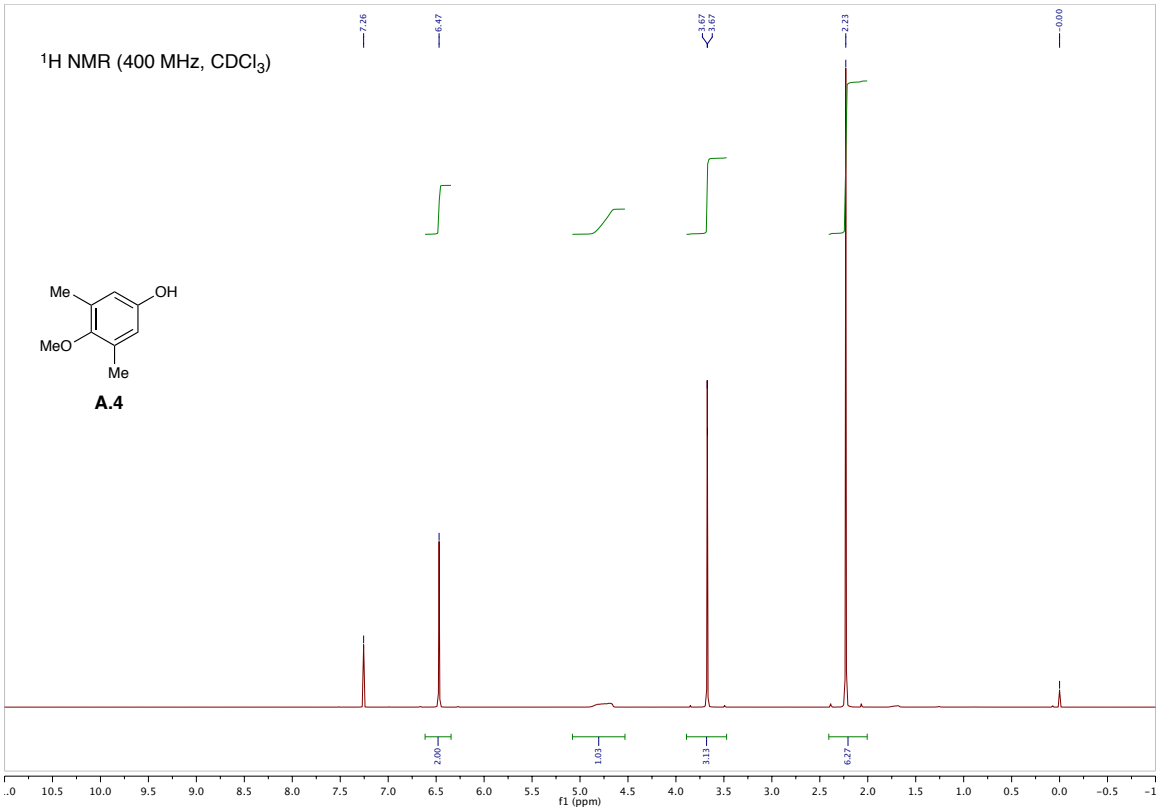
^{1}H NMR (400 MHz, $CDCl_3$)
7.26
6.47
3.67
3.67
2.23
0.00
Me
OH
MeO
Me
A.4
2.00
1.03
3.13
6.27
f1 (ppm)

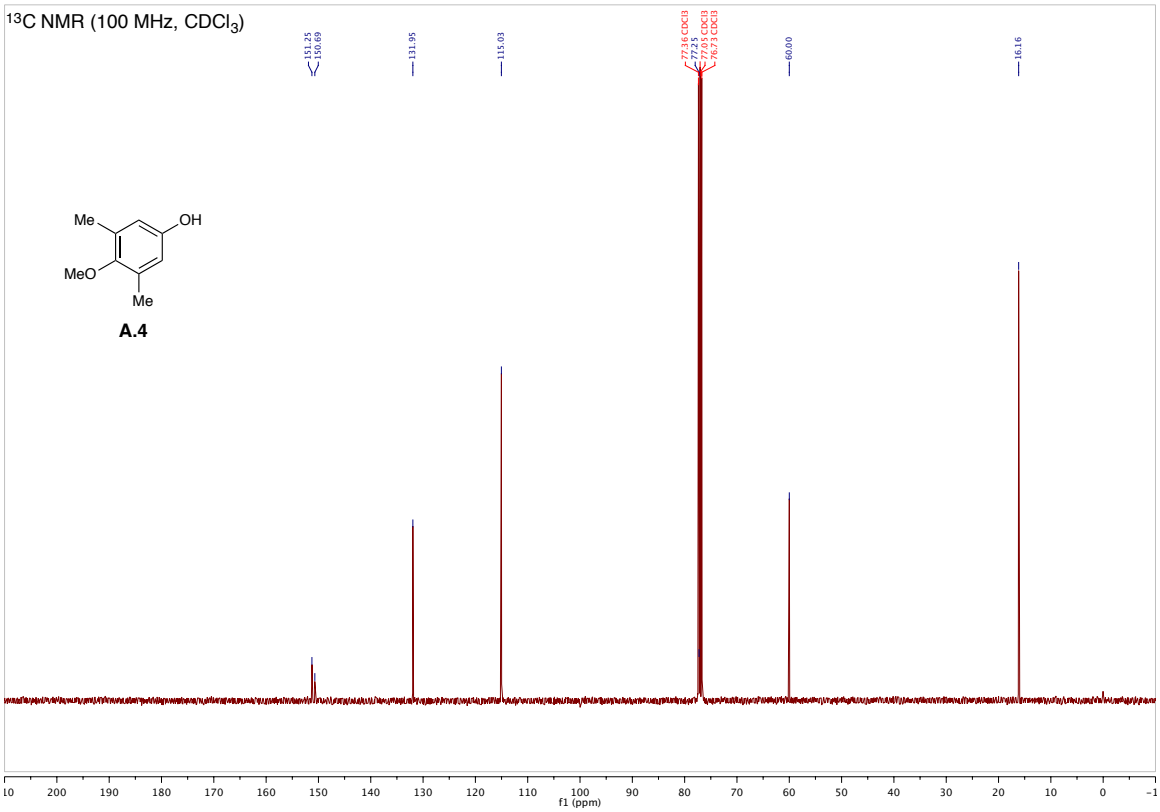
^{13}C NMR (100 MHz, $CDCl_3$)
151.25
150.69
131.95
115.03
77.36 CDCl3
77.25
77.05 CDCl3
76.73 CDCl3
60.00
16.16
Me
OH
MeO
Me
A.4
f1 (ppm)

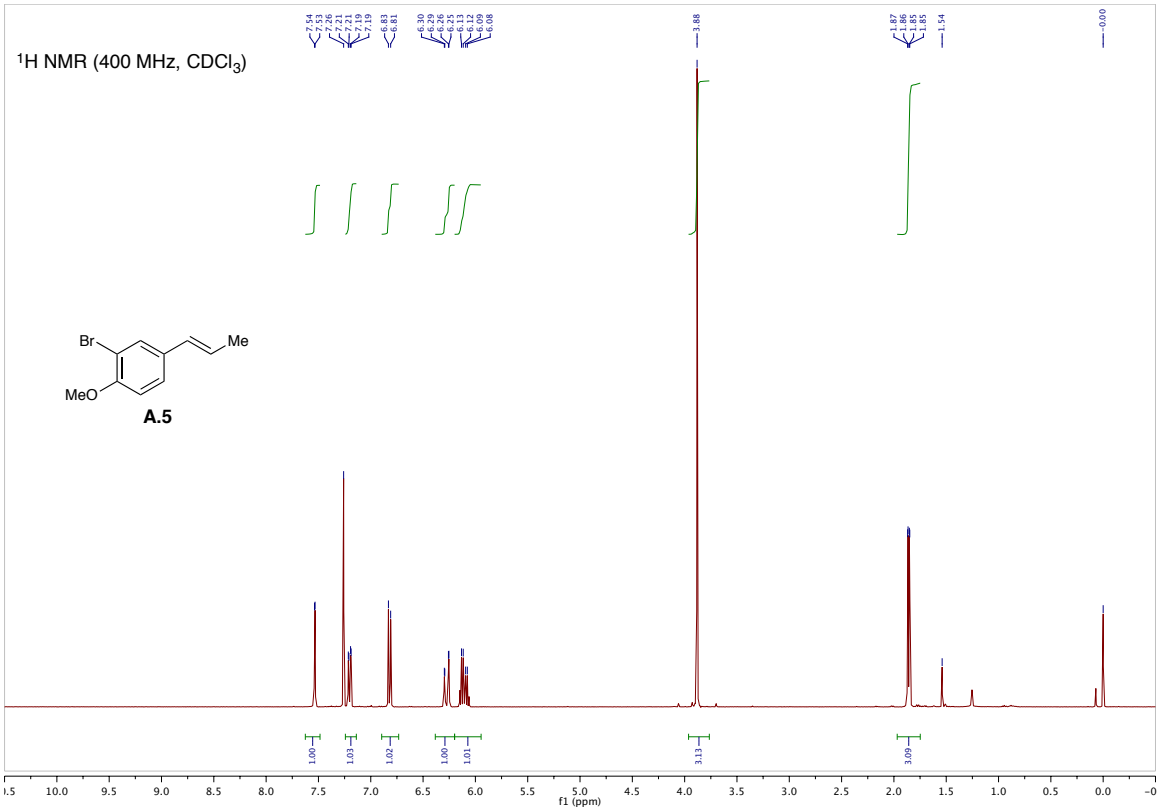
^{1}H NMR (400 MHz, $CDCl_3$)
Br
Me
MeO
A.5
f1 (ppm)

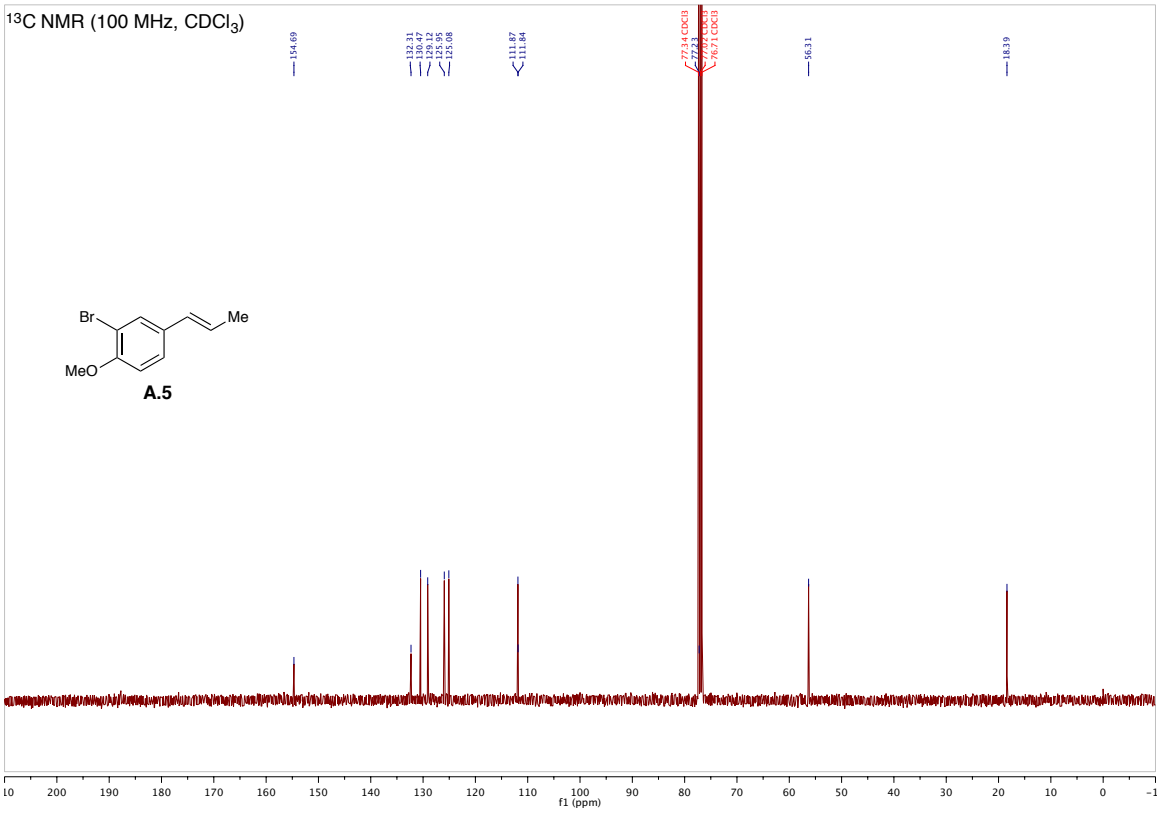
^{13}C NMR (100 MHz, $CDCl_3$)
Br
Me
MeO
A.5
f1 (ppm)

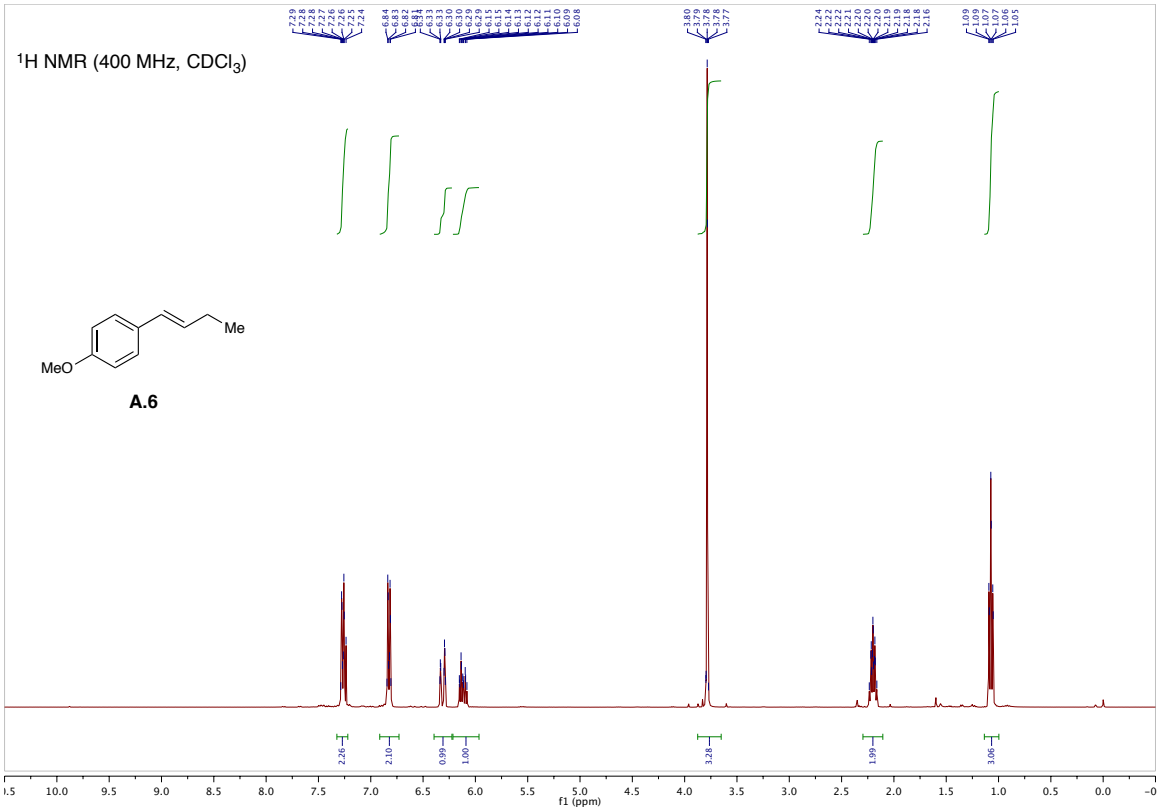
^{1}H NMR (400 MHz, $CDCl_3$)
Me
MeO
A.6
f1 (ppm)

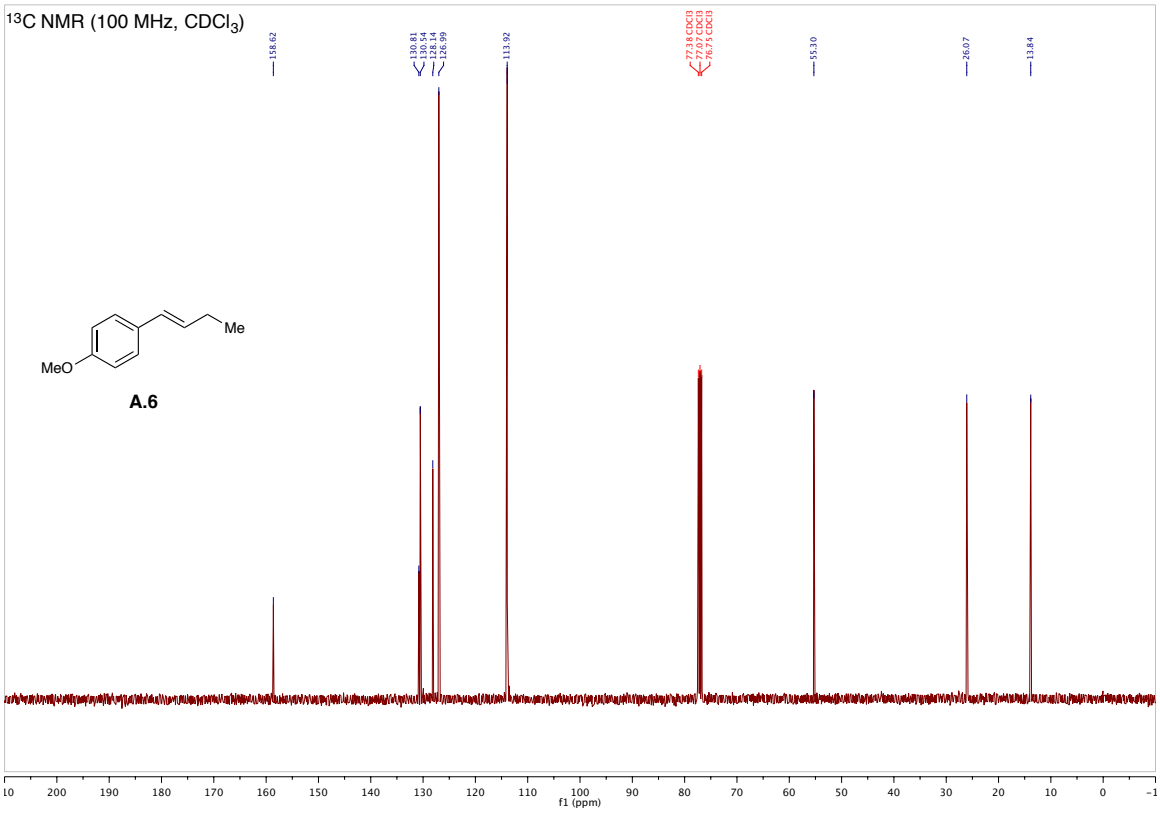
^{13}C NMR (100 MHz, $CDCl_3$)
158.62
130.81
130.54
128.45
126.99
113.92
77.38 CDCl3
77.00 CDCl3
76.71 CDCl3
55.30
26.07
13.84
Me
MeO
A.6
f1 (ppm)

^{1}H NMR (400 MHz, $CDCl_3$)

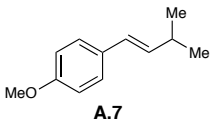

A.7

^{13}C NMR (100 MHz, $CDCl_3$)

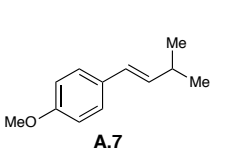

A.7

A.2: List of new compounds for Chapter 4

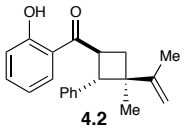

4.2

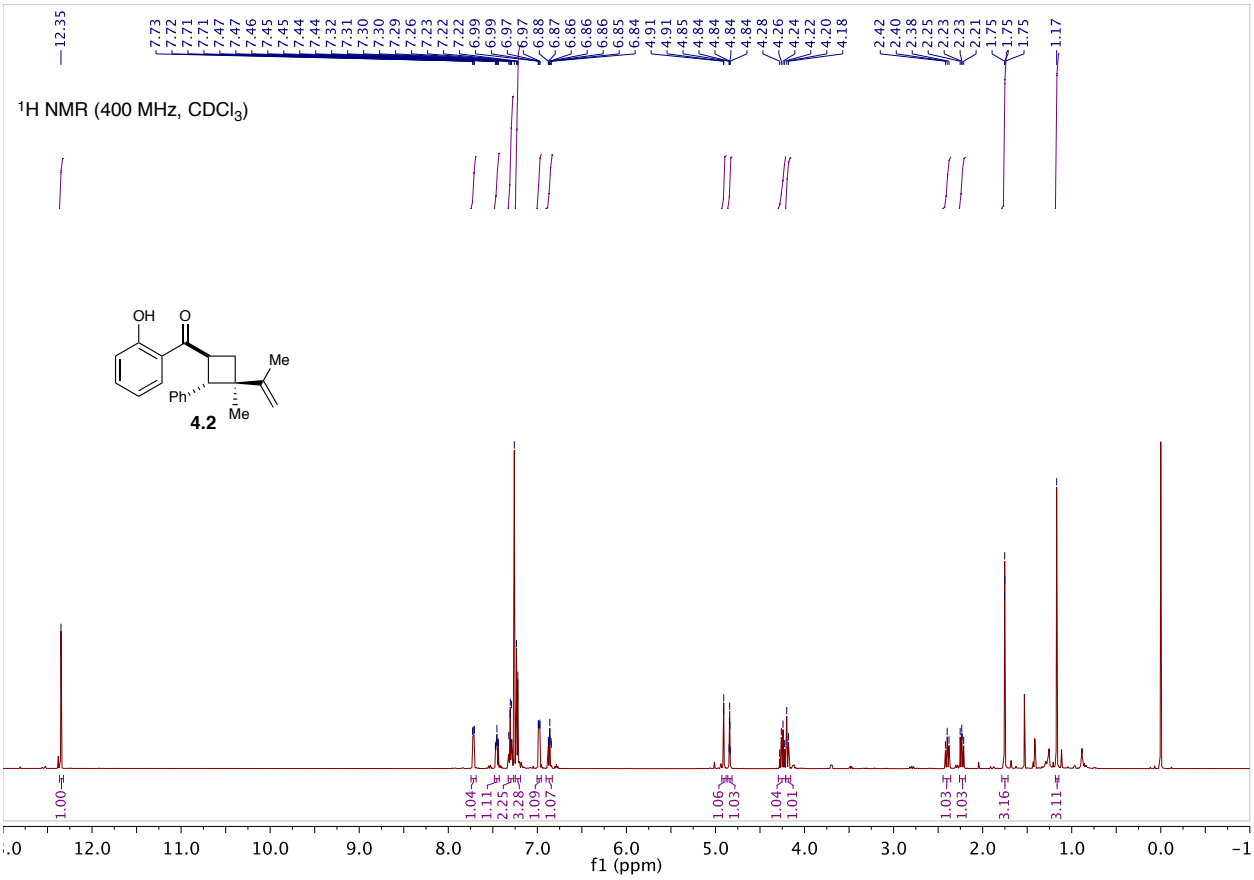
12.35
7.73
7.72
7.71
7.71
7.47
7.47
7.46
7.45
7.45
7.44
7.44
7.32
7.31
7.30
7.30
7.29
7.26
7.23
7.22
7.22
6.99
6.99
6.97
6.97
6.88
6.87
6.86
6.86
6.86
6.85
6.84
4.91
4.91
4.85
4.84
4.84
4.84
4.84
4.28
4.26
4.24
4.22
4.20
4.18
2.42
2.40
2.38
2.25
2.23
2.23
2.21
1.75
1.75
1.75
1.17
1H NMR (400 MHz, CDCl3)
OH
O
Me
Ph
Me
4.2
1.00
1.04
1.11
2.25
3.28
1.09
1.07
1.06
1.03
1.04
1.01
1.03
1.03
3.16
3.11
12.0
11.0
10.0
9.0
8.0
7.0
6.0
5.0
4.0
3.0
2.0
1.0
0.0
f1 (ppm)